

**New Dendrimers and Lipids Based on 2,2'-Bi(glycerol), and Lewis Acid Dependent
Rearrangements of a Protected Pinacol**

by

Kavitha Reddy Pulsani

A dissertation submitted to the Graduate Faculty of
Auburn University
in partial fulfillment of the
requirements for the Degree of
Doctor of Philosophy

Auburn, Alabama
May 07, 2017

Keywords: Dendrimer, Lipid, Insertion, 2,2'-Bi(glycerol) Core

Copyright 2017 by Kavitha Reddy Pulsani

Approved by

Peter D. Livant, Chair, Associate Professor of Chemistry
Edward J. Parish, Professor of Chemistry
Michael E. Squillacote, Associate Professor of Chemistry
Bradley L. Merner, Assistant Professor of Chemistry

Abstract

Chapter 1: 2,2'-Bi(glycerol), or 2,3-bis(hydroxymethyl)butane-1,2,3,4-tetraol is of interest because of its utility as a potential A₆ core for novel dendrimers, and because it may lead to hitherto unknown 2,2'-bi(triglyceride)s and 2,2'-bi(phosphodiglyceride)s. It may also serve as a starting point for the preparation of unnatural sugars. Previous work in our group established a workable synthesis of 2,2'-bi(glycerol), however a shorter route was desirable. We examined alternate routes to 2,2'-bi(glycerol) and found all suffered from unexpected cleavage of the central C-C bond.

Chapter 2: We envisioned new dendrimers based on 2,2'-bi(glycerol) functioning as an A₆ core. A convergent synthetic plan called for Rh₂(OAc)₄ catalyzed insertion of the carbenoid derived from dimethyl 2-diazomalonate into both O-H bonds of malonic acid, giving di-[bis(methoxycarbonyl)methyl] malonate. Diazotization of the central CH₂ would then enable a new insertion into malonic acid. We found that all traditional diazo transfer protocols failed for di-[bis(methoxycarbonyl)methyl] malonate. The reasons for this failure were investigated at length. We found that simple base treatment of the tetraester malonate may have resulted in acylketene formation.

Chapter 3: In the course of synthesis of 2,2'-bi(triglycerides), we studied the acylation of 5,5'-bi(5-hydroxy-2,2-dimethyl-1,3-dioxane) under basic and Lewis acidic conditions. All Lewis acid catalysts investigated in this work caused skeletal rearrangements, leading to 4,4'-bi(4-acetoxymethyl-2,2-dimethyl-1,3-dioxolane), or 4,4,5,5,-tetra(acetoxymethyl)-2,2-dimethyl-1,3-dioxolane. Reaction intermediates, for example 2,2,8,8,13,13-hexamethyl-1,3,7,9,12,14-hexaoxa-dispiro[4.5.4.0]pentadecane, were also identified.

Acknowledgments

I express my sincere gratitude to my advisor, Dr. Peter Livant, for his guidance and encouragement throughout my Ph.D. studies. I have learned so much from him in both on academic and personal front.

I am also grateful for my thesis committee members, Dr. Michael Squillacote, Dr. Edward Parish, Dr. Bradley Merner and outside reader Dr. Jack DeRuiter for serving as my advisory committee.

I would like to thank Dr. Michael Meadows for his assistance in using the NMR facilities, Dr. Melissa Boersma, Dr. Wendell Grainger, Dr. Yonnie Wu for their help in getting mass spectral data and Dr. John Gorden for his expertise in obtaining X-ray crystal structures for my compound. I am equally thankful to my friends and family members.

Last, but not least, I would like to thank my husband Pramod Pulsani for his patience, understanding and support throughout my studies in Auburn. Thanks to entire Auburn University Chemistry & Biochemistry Department.

Table of Contents

Abstract	ii
Acknowledgments.....	iii
List of Tables	vii
List of Schemes.....	viii
List of Figures.....	ix
List of Abbreviations	xii
Chapter 1. 2,2'-bi(glycerol).....	1
1.1. The idea of 2,2'-bi(glycerol)	1
1.2. Synthesis of 2,2'-bi(glycerol).....	3
1.2. Alternative route to 1.1	5
Chapter 2. Attempted Synthesis of an aliphatic polyether polyol dendrimer and a polyester dendrimer	10
2.1. Introduction.....	10
2.1.1. Basic concepts.....	10
2.1.2. Synthesis of dendrimers.....	13
2.1.3. Applications	16
2.1.4. Structural evolution of dendrimers	16
2.1.5. Multivalent dendrimer cores (scaffolds).....	17
2.2. Results and Discussion	19
2.2.1. Target compounds.....	19

2.2.2. Rh ₂ (OAc) ₄ catalyzed O-H insertion reaction of diol 1.12 with DDM.....	21
2.2.3. Attempted deprotection of acetonide group of 2.3	25
2.2.4. Proposed synthesis of dendrimer 2.16	26
2.2.5. Insertion of the carbenoid derived from DDM into both O-H bonds of malonic acid.....	26
2.2.6. Diazo transfer reaction of 2.17	28
2.2.6.1. Initial attempts	28
2.2.6.2. Blank reaction of 2.17	37
2.2.6.3. Blank reaction of ¹³ C labeled 2.17	45
2.2.7. Conclusions.....	51
Chapter 3. Studies on the synthesis of bi(triglyceride)s from 2,2'-bi(glycerol).....	59
3.1. Introduction.....	59
3.1.1. Triglycerides (TG)	59
3.1.2. Phospholipids.....	60
3.1.3. Man-made lipids; deviation from traditional structure	61
3.2. Results and Discussion	64
3.2.1. General consideration	64
3.2.2. Lewis acid catalyzed acylation of pinacol 1.12 with Ac ₂ O	65
3.2.3. Lewis acid catalyzed acylation of 1.12 with trifluoroacetic anhydride	75
3.2.4. Base catalyzed acylation of pinacol 1.12 with acetic anhydride	78
3.2.5. Reactions in the absence of anhydride (blank reactions).....	82
3.2.5.1. Reaction of 3.5 with 5 mol% Ce(OTf) ₃ over long times	82
3.2.5.2. Reaction of 1.12 with 5 mol% Ce(OTf) ₃ in the absence of anhydride	82

3.2.5.3. Reaction of 1.12 with 5 mol% TMSOTf catalyst in the absence of anhydride	83
3.2.6. Acylation of acetonide pinacol 1.12 using long chain acid derivatives.....	87
3.2.6.1. Stearic anhydride reaction	87
3.2.6.2. Myristic acid reaction	88
3.2.6.3. Lauroyl chloride reaction	88
3.2.6.4. Lauric anhydride reaction	88
Experimental	90
References	123
Appendix	133

List of Tables

Table 2.1. Reaction of diol 1.12 with DDM, 2.9 under various conditions	24
Table 2.2. ^{13}C NMR of Z , formed by treatment of 2.17 with Et_3N	52
Table 3.1. Acylation of diol 1.12 with acetic anhydride, catalyzed by Lewis acids.....	73
Table 3.2. Acylation of diol 1.12 with trifluoroacetic anhydride, catalyzed by Lewis acids	77
Table 3.3. Acetylation of 1.12 with acetic anhydride, under basic conditions.....	80
Table 3.4. ^{13}C NMR Parameters of Isopropylidene Acetals ^a	86
Table 3.5. ^{13}C NMR Parameters of Isopropylidene Acetals ^a	87

List of Schemes

Scheme 1.1. Proposed conversion of 1.1 to an aldohexose	2
Scheme 1.2. Xiaoxun Li's method of synthesis of 1.1	4
Scheme 1.3. Retrosynthesis of 1.1 by second route	5
Scheme 2.1. Proposed divergent synthesis of dendrimer 2.1	20
Scheme 2.2. Proposed convergent synthesis of polyester dendrimer 2.16	27
Scheme 2.3. Plausible mechanism of diazo transfer reaction using ADMC	30
Scheme 3.1. Possible mechanism for the formation of 3.5 with Lewis acid catalyst	69
Scheme 3.2. Mechanism leading to 3.6	70
Scheme 3.3. Rationale for formation of 3.11	81

List of Figures

Figure 1.1. Possible applications of 1.1	2
Figure 2.1. Second generation PAMAM dendrimer	11
Figure 2.2. Both <i>a</i>) and <i>b</i>) may be termed dendrons. Case <i>b</i>) is also referred to as a dendritic wedge.....	12
Figure 2.3. Diagram of a five generation dendrimer. Of the four identical dendritic wedges attached to the core, only one is shown	12
Figure 2.4. Dendrimer synthesis by divergent strategy	14
Figure 2.5. Convergent method of dendrimer synthesis	15
Figure 2.6. Structural evolution of dendrimers. The horizontal axis is a rough time axis	17
Figure 2.7. Overview of the multivalent scaffolds(cores) used in the synthesis of dendrimers ...	18
Figure 2.8. a) Aliphatic polyether polyol second generation dendrimer 1. b) A ₈ core. c) A ₆ core	19
Figure 2.9. 400 MHz ¹ H NMR spectrum (C ₆ D ₆ solvent) of the first attempt at the Rh ₂ (OAc) ₄ catalyzed O-H insertion reaction of DDM with diol 1.12 . Partial assignments are shown: red circle – 2.3 ; triangle – 2.10 ; star – 2.11 ; diamond – other byproducts 2.13 , 2.14 , and 2.8	23
Figure 2.10. Representative diazo transfer reagents	29
Figure 2.11. 600 MHz ¹ H NMR of the product obtained by treatment of 2.17 with <i>p</i> -ABSA and Et ₃ N (2.17 : <i>p</i> -ABSA:Et ₃ N = 1.0:1.09:2.0) in acetonitrile at rt for 16 h. The product was obtained by means of the workup procedure described in the text. CDCl ₃ solvent	31
Figure 2.12. 150 MHz ¹³ C NMR spectrum of the compound used for Figure 2.11. CDCl ₃	32
Figure 2.13. a) IR spectrum of dimethyl diazomalonate. b) IR spectrum of product of reaction of 2.17 with <i>p</i> -ABSA and Et ₃ N.....	33

Figure 2.14. 600 MHz ^1H NMR spectrum (CDCl_3 solvent) of the product of treating 2.17 with Et_3N and TsN_3 (2.17 : Et_3N : TsN_3 = 1.0:2.0:1.0) at rt for 16 h in CD_3CN	36
Figure 2.15. 150 MHz ^{13}C NMR spectrum (CDCl_3) of the compound used for Figure 2.14.....	36
Figure 2.16. 400 MHz ^1H NMR spectra of 2.17 in the presence of 10 mol%, 15 mol%, 20 mol% Et_3N at rt. CDCl_3 solvent. Diamonds denote peaks from 2.14 impurity.....	38
Figure 2.17. 400 MHz ^1H NMR spectra obtained by treatment of 2.17 with 2 eq Et_3N . a) 2.17 (t = 0) b) 5 min c) 2 h d) 16 h at rt. The lefthand column shows the complete spectrum and the righthand column shows the 3.6-4.0 ppm region in detail. CD_3CN solvent.	40
Figure 2.18. 400 MHz ^1H NMR of crude blank reaction (5.2-3.6 ppm) obtained by a) treatment of 2.17 with Et_3N (2.17 : Et_3N = 1.0:2.0) in CD_3CN . b) 2.17 : Et_3N : CF_3COOH = 1.0:2.0:2.0, CD_3CN solvent	41
Figure 2.19. ^1H NMR spectrum of 2.17 after treatment with 2 equiv Et_3N (larger scale). CDCl_3 solvent. The peaks at 4.89 ppm and 3.75 ppm are due to impurity 2.14	42
Figure 2.20. ^{13}C NMR spectrum of the sample used in Figure 2.19. CDCl_3 solvent. Expanded regions are included beneath the main spectrum. The peaks at 169.0 ppm, 77.2 ppm, and 53.3 ppm are due to impurity 2.14 . The peaks at 46.3 ppm and 8.6 ppm are due to Et_3N	43
Figure 2.21. 600 MHz ^1H NMR spectrum of dimethyl 2-hydroxymalonate product after column chromatography. Signals at 4.93 ppm and 3.78 ppm correspond to 2.14 . (CDCl_3)	44
Figure 2.22. 150 MHz ^{13}C NMR spectrum of the compound used for Figure 2.21. CDCl_3	45
Figure 2.23. 600 MHz ^1H NMR spectrum of 2-^{13}C 2.17 . CDCl_3 solvent.	46
Figure 2.24. 150 MHz ^{13}C NMR of 2-^{13}C 2.17 . CDCl_3 solvent.....	46
Figure 2.25. 400 MHz ^1H NMR spectrum of the product obtained by treatment of 2-^{13}C 2.17 with Et_3N (2.17 : Et_3N = 1.0:2.0) in CDCl_3 at rt for 5 minutes	48
Figure 2.26. 100 MHz ^{13}C NMR of the product obtained by treatment of ^{13}C labeled 2.17 with Et_3N (2.17 : Et_3N = 1.0:2.0) in CDCl_3 at rt for 5 minutes	49
Figure 2.27. 600 MHz ^{13}C NMR of the ^{13}C labeled blank reaction of 2.17 by treatment with Et_3N (2.17 : Et_3N = 1.0:2.0) in acetonitrile at rt for 5 minutes. The product was obtained after column chromatography	50
Figure 2.28. An inexact proposal for the structure of Z	53

Figure 2.29. Dianon proposal for the structure of Z . Proton assignments are in italics	53
Figure 2.30. Ketene formation; another proposal	55
Figure 2.31. Tentative peak assignment for ketene + dimethyl tartronate. All chemical shifts are given in ppm	55
Figure 2.32. Ketene proposal. All chemical shifts are in units of ppm.....	56
Figure 2.33. Cyclic β -keto ester proposal.....	58
Figure 3.1. Some fatty acids	60
Figure 3.2. Cross-section of a liposome. ⁶⁵ White spheres represent polar groups. Yellow lines represent fatty acid chains. A liposome is a spherical structure.....	61
Figure 3.3. Sterically hindered triacylglycerols.....	62
Figure 3.4. Generic structures of conformationally restricted phospholipids A and flexible analogues B	62
Figure 3.5. X-ray crystal structure of “top spot” from Ce(OTf) ₃ catalyzed reaction of acetic anhydride with diol 1.12 . Thermal ellipsoids are at the 50% level	66
Figure 3.6. X-ray crystal structure of “bottom spot” from Ce(OTf) ₃ catalyzed reaction of acetic anhydride with diol 1.12 . Thermal ellipsoids are at the 50% level	67
Figure 3.7. 600 MHz ¹ H NMR of a mixture of diastereomers of 3.5 . CDCl ₃ solvent	68
Figure 3.8. Partial 400 MHz ¹ H NMR spectra of diastereomeric form of 3.5 . a) <i>dl</i> diastereomer b) <i>meso</i> diastereomer	68
Figure 3.9. 400 MHz, ¹ H NMR spectra of TMSOTf catalyzed blank reaction after column, mixture of compounds 3.13 , 3.14 , and unidentified compound X	84
Figure 3.10. 100 MHz ¹³ C NMR spectrum of compound used for Figure 3.9	85
Figure 3.11. 400 MHz ¹ H NMR partial spectrum of 3.14 after column chromatography.....	85
Figure 3.12. 150 MHz, ¹³ C NMR of 3.14 after column chromatography. CDCl ₃ solvent	86

List of Abbreviations

ADMC	2-Azido-1,3-dimethylimidazolium chloride
AIBN	Azobis(isobutyronitrile)
A _x	dendrimer core with x branching points
bp	boiling point
br	broad
d	doublet
dr	diastereomeric ratio
DBU	1,8-Diazabicyclo[5.4.0]undec-7-ene
DDM	Dimethyl diazomalonate
DMAP	4-(Dimethylamino)pyridine
DMA	N,N-Dimethylacetamide
eq	equation
equiv	equivalent
Et	ethyl
EtOAc	Ethyl acetate
Et ₃ N	Triethyl amine
G1, G2, <i>etc.</i>	generation 1, generation 2, <i>etc.</i>
h	hour
HRMS	high resolution mass spectrometry

Hz	Hertz
IR	Infrared spectroscopy
<i>J</i>	coupling constant
LAH	Lithium aluminum hydride
lit.	literature
m	multiplet
Me	methyl
MHz	megahertz
min	minute
mp	melting point
NMR	Nuclear magnetic resonance
<i>p</i> -ABSA	<i>para</i> -Acetamidobenzenesulfonyl azide
ppm	parts per million
q	quartet
quat	quaternary
R_f	Retention factor
rt	room temperature
s	second
t	triplet, or time
TLC	Thin layer chromatography
THF	Tetrahydrofuran
TIPS	triisopropylsilyl
TMS	trimethylsilyl, or tetramethylsilane

TMSOTf	Trimethylsilyl trifluoromethanesulfonate
TsN ₃	<i>p</i> -Toluenesulfonyl azide
TFAA	Trifluoroacetic anhydride
1°, 2°, 3°	primary, secondary, tertiary
°C	degrees Celsius

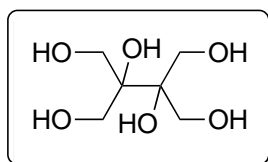
CHAPTER 1

2,2'-BI(GLYCEROL)

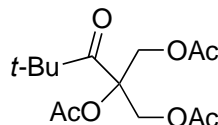
1.1. The idea of 2,2'-bi(glycerol)

One of the previous graduate students from the Livant group, Dr. Yuanping Jie,¹ focused on the synthesis of various hypervalent compounds. When she performed a reductive amination on 1,3-dihydroxyacetone (NaBH₃CN, NH₄Cl, MeOH, HOAc), a good yield of bis(1,3-dihydroxy-2-propyl)amine was obtained, along with a byproduct that she tentatively identified as hexaalcohol

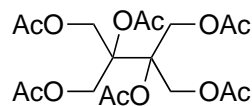
1.1. Compound **1.1** may be named systematically as 2,3-bis(hydroxymethyl)-1,2,3,4-butanetetraol, or more simply as 2,2'-bi(glycerol).



1.1



1.2



1.3

She searched the chemical literature for NMR chemical shift information on **1.1**, to confirm the identity of the byproduct. However, she found that **1.1** had never before been synthesized. A thorough literature search revealed only that (i) FAB ionization of glycerol produced peaks in the resulting mass spectrum that might have come from **1.1** and its isomers,² and (ii) **1.3** was reported to have been formed by photolysis of **1.2** in an esr cavity.³

Subsequent work showed that the byproduct in the reductive amination reaction was not **1.1**, but rather glycerol. However, our interest in **1.1** was born.

Some of the possible applications of **1.1** are shown in Figure 1.1. One application is to use **1.1** as a core (or scaffold) in dendrimer synthesis. Since it is a hexa-alcohol, there are six points of attachment, and it would be termed an A_6 core. As such, it would be a so-called dense core.⁴ Our work toward constructing dendrimers based on **1.1** will be described in Chapter 2 of this dissertation.

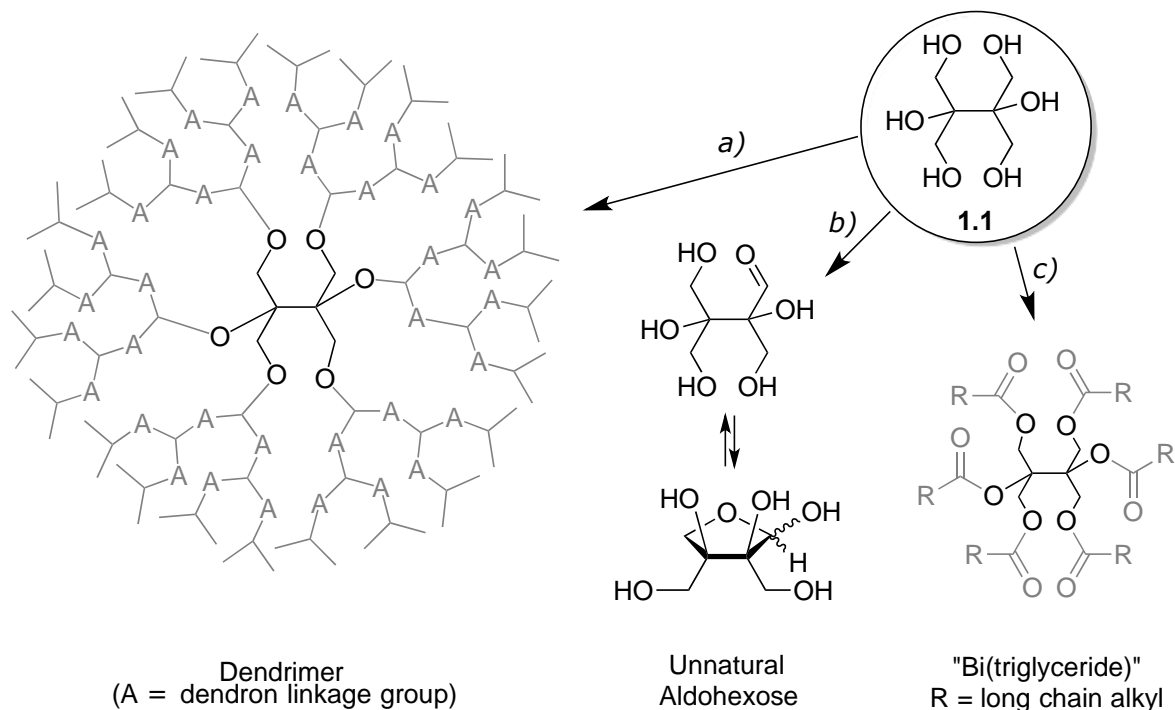
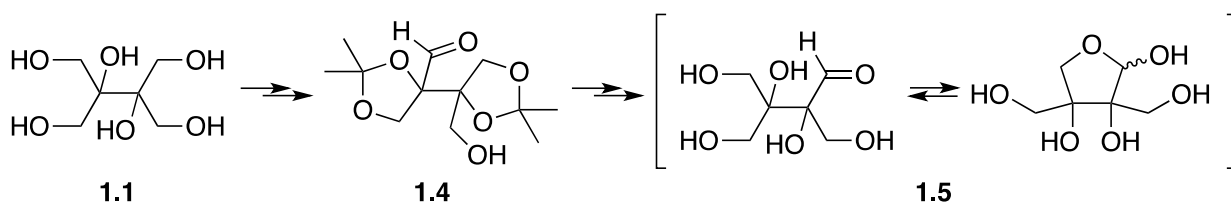


Figure 1.1. Possible applications of 1.1.

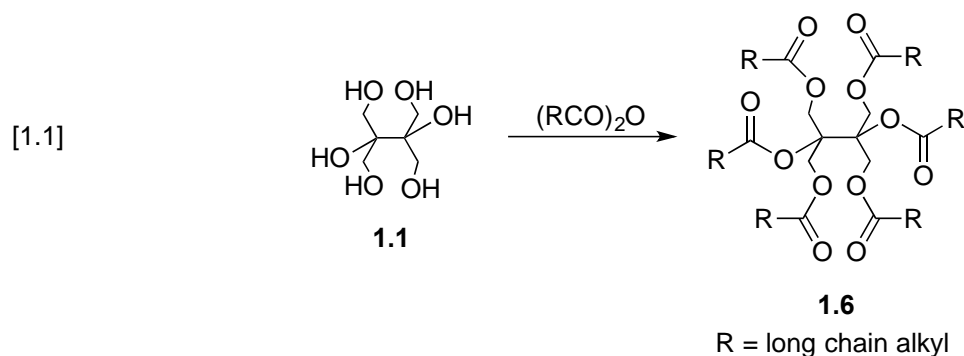
A second application is to use **1.1** to synthesize unnatural sugars. Compound **1.1** is isomeric with alditols (*e.g.* sorbitol, mannitol, *etc.*), and oxidation of one 1° hydroxyl to an aldehyde would produce a new aldohexose, **1.5** (Scheme 1.1).

Scheme 1.1. Proposed conversion of 1.1 to an aldohexose



It is likely that **1.5** would cyclize as shown to a furanose form, which might be used in construction of unnatural ribonucleosides. This application is not discussed in this dissertation.

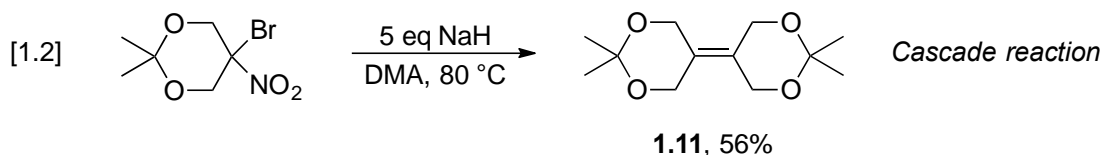
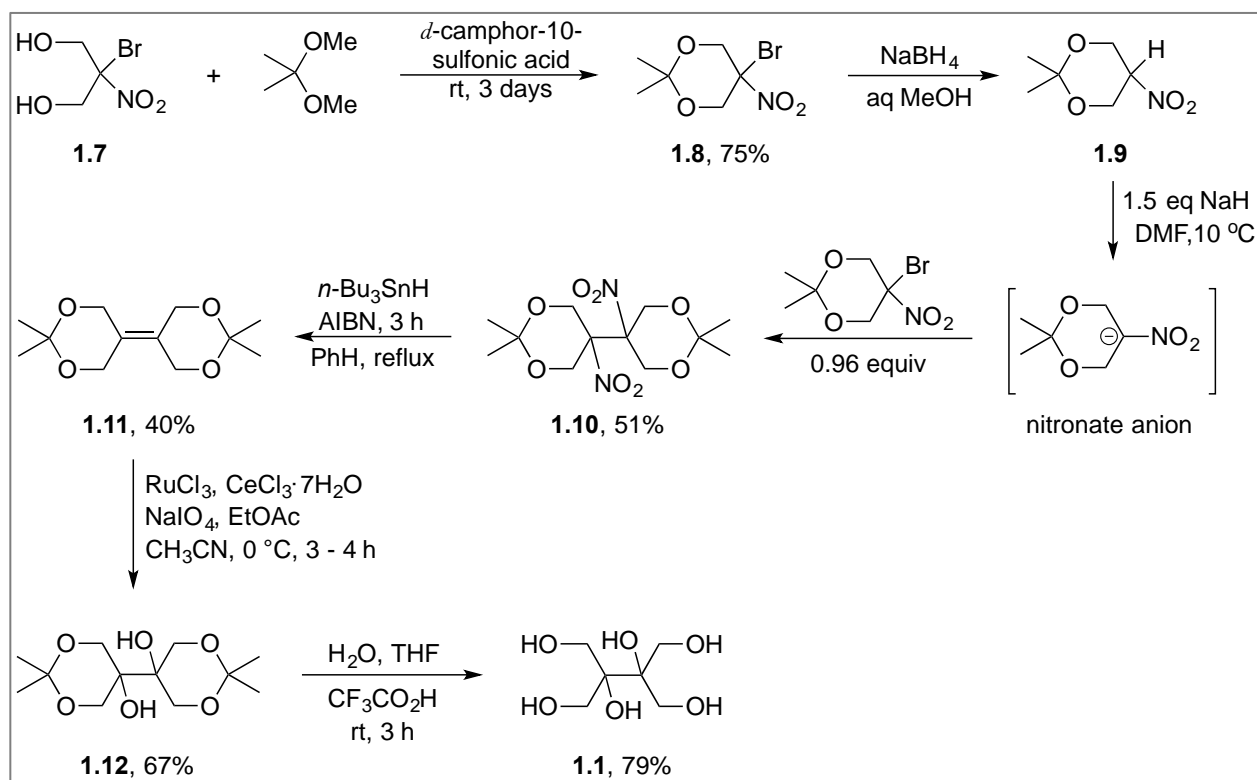
A third application is to use **1.1** to construct a bi(triglyceride). The six –OH groups in **1.1** would be converted to ester groups by esterification using carboxylic acids or derivatives of carboxylic acids as shown in eq [1.1]. The carboxylic acids would be C₁₂ – C₂₀ straight-chain saturated acids (*e.g.* lauric, stearic) or unsaturated acids such as oleic or linoleic that are found in naturally occurring triglycerides. Work on this possible application is described in Chapter 3 of this dissertation.



1.2. Synthesis of 2,2'-bi(glycerol), **1.1**

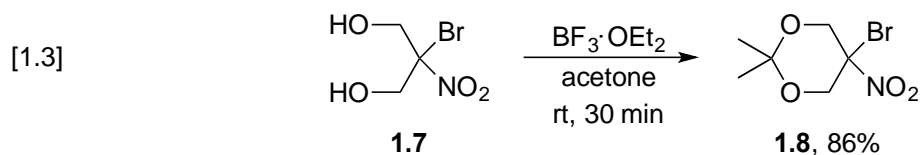
A synthetic route to **1.1** was developed by Dr. Xiaoxun Li, a former graduate student in the Livant group.⁵ This route is shown in Scheme 1.2. Dr. Li later noted that when **1.9** was treated with 2.5 equiv of NaH prior to treatment with **1.8**, some alkene **1.11** accompanied the expected dinitro compound **1.10**. He demonstrated that NaH can reduce dinitro compound **1.10** to **1.11**. Eventually, he found NaH also reduced **1.8** to **1.9**. Therefore, he was able to treat **1.8** with 5 equiv NaH and convert it in one pot to **1.11**. This “cascade” reaction (see eq [1.2]) streamlined the synthesis of **1.1** considerably.

Scheme 1.2. Xiaoxun Li's method of synthesis of 1.1



We used different solvents to investigate the cascade reaction (eq [1.2]). N,N-dimethylacetamide (DMA) was the best choice because the reaction time was 1 h and acceptable yields, ~56%, were obtained. Tetrahydrofuran (THF) as solvent gave 46% yield and required 3 days. Tetramethylurea (TMU) as solvent gave 47% yield and reaction time was 1 h.

Owen Garrett, one of the undergraduate students in our lab, improved the first step of Scheme 1.2 *i.e.*, hydroxyl group protection of **1.7**. Using Lewis acid $\text{BF}_3 \cdot \text{OEt}_2$ in dry acetone at rt for 30 min gave bromonitro acetonide **1.8** in 86% yield (eq [1.3]).⁶ This replaced the 3-day procedure that had been used.

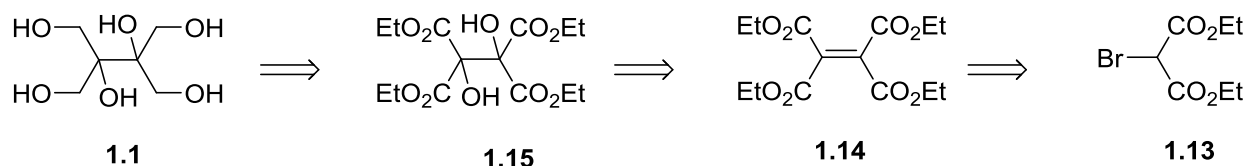


Although the Li synthesis of **1.1** with the cascade reaction and the improved protection was certainly adequate, he also explored alternative approaches that might be shorter and might result in higher overall yield.

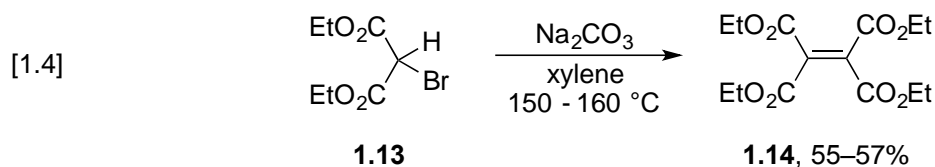
1.3. Alternate route to 1.1

Scheme 1.3 shows a retrosynthetic plan for **1.1**. The hydroxymethyl groups of **1.1** could be obtained from ester group reduction of **1.15**. Dihydroxylation of the alkene group of **1.14** would give **1.15**. Alkene tetraester **1.14** could be prepared by dimerization of commercially available diethyl 2-bromomalonate **1.13**.

Scheme 1.3. Retrosynthesis of 1.1 by second route

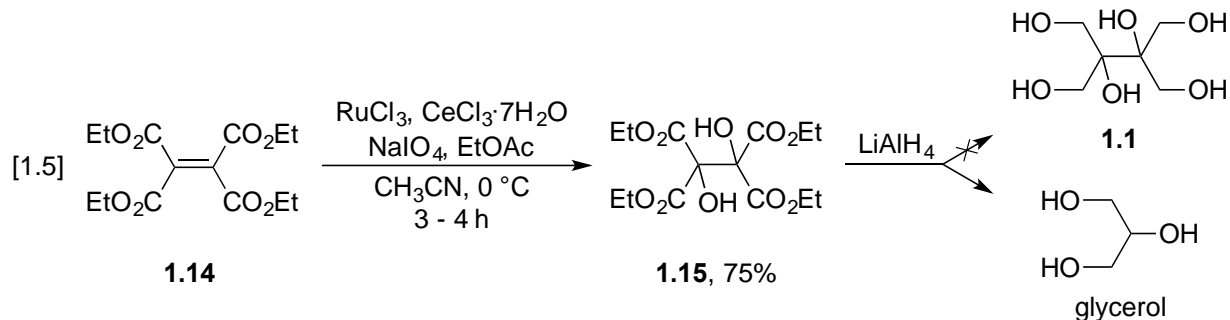


Corson *et al.* reported dimerization of **1.13** under basic conditions at 150–160 °C to give tetraester olefin **1.14** in 55–57% yield (eq [1.4]).⁷ Following the published protocol, Li obtained **1.14** in 40% yield.

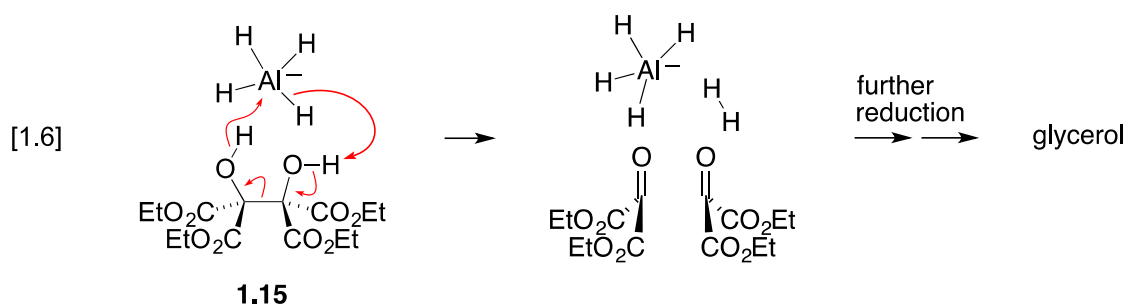


With **1.14** in hand, Xiaoxun Li performed RuCl₃-catalyzed dihydroxylation to give tetraester diol **1.15** as shown in eq [1.5].⁸ When he did reduction of **1.15** using LiAlH₄, surprisingly he got

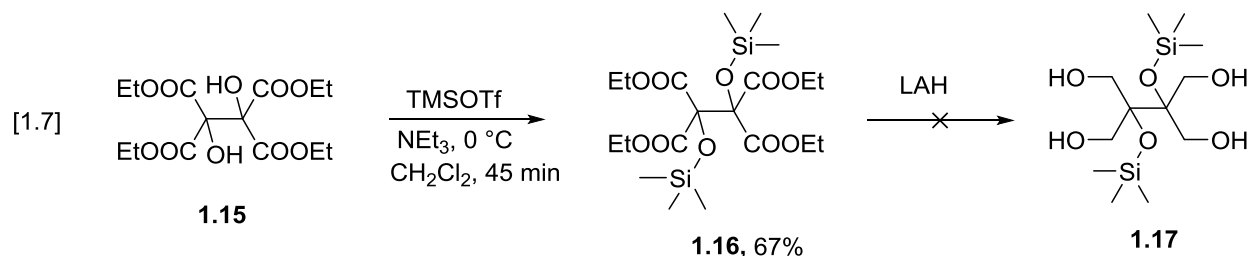
glycerol instead of the expected hexaalcohol **1.1**.



A possible mechanism for getting glycerol is shown in eq [1.6].



So we decided to protect the free OH groups of **1.15** to avoid problems in the reduction step.



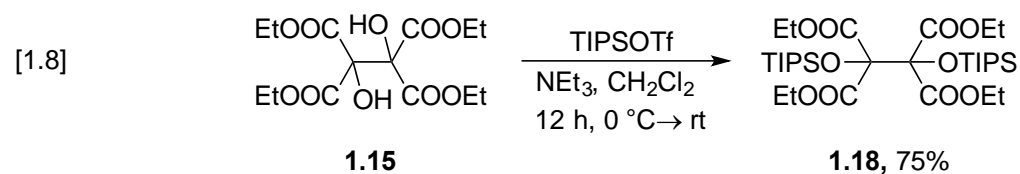
As shown in eq [1.7] we protected the hydroxyl group of **1.15** as trimethylsilyl ether **1.16** using TMSOTf and base at 0 °C, giving an isolated yield of 67%. With trimethylsilyl ether **1.16** in hand, we went for the next step *i.e.*, reduction using LAH. After the addition of LAH to **1.16**, a TLC was taken immediately, which revealed that starting material **1.16** was consumed, and showed only one spot sitting at the origin. We tried various eluent systems to move it, but it didn't move. Workup was difficult because the separation of organic product from the metal salts was very hard. After workup, NMR didn't provide results similar to those expected for **1.17**.

Gevorgyan *et al.*,^{9a} reported that reduction of PhMe₂SiOMe using LiAlH₄ gave the corresponding hydride, PhMe₂SiH. Sommer *et al.*,^{9b} also reported conversion of methyl silyl ethers to the corresponding hydrido compounds by using diisobutylaluminum hydride (DIBALH). Tour *et al.*^{9c} also reported using DIBAL-H to reduce various ethoxysilanes (R₃SiOEt) to the corresponding silanes (R₃SiH). Another article by Midgley *et al.*,^{9d} reported that trimethylsiloxy group was unexpectedly displaced when subjected to aliphatic Grignard reagents, and that malonate anion could displace siloxy groups from benzyl silyl ethers.

From these literature examples we realized that in **1.16**, the trimethylsilyl ether groups are sensitive to metal reduction and the molecule is decomposing.

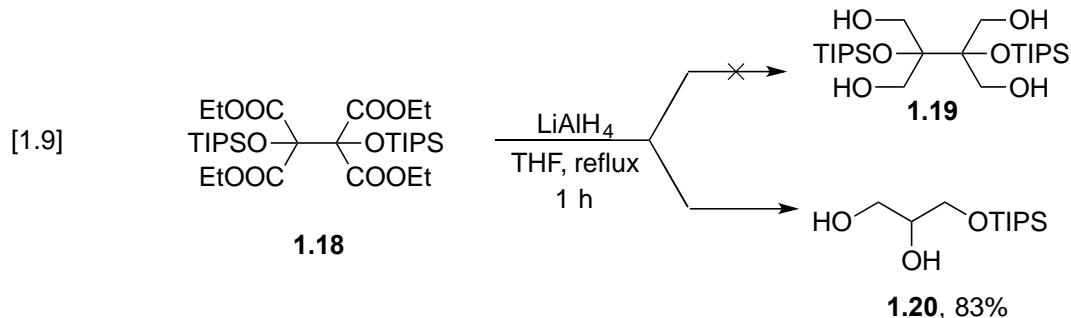
In our next attempts we decided to protect alcohols of **1.15** as triisopropylsilyl ether (TIPS) instead of trimethylsilyl ether (TMS) because TIPS ether is more stable in basic and acidic conditions when compared to TMS ether.¹⁰ (We thank Professor B. Merner of our Department for this suggestion).

Compound **1.15** was treated with triisopropylsilyl triflate (TIPSOTf) and Et₃N for 12 h with stirring to give triisopropylsilylether protected **24** in 75% as shown in eq [1.10].



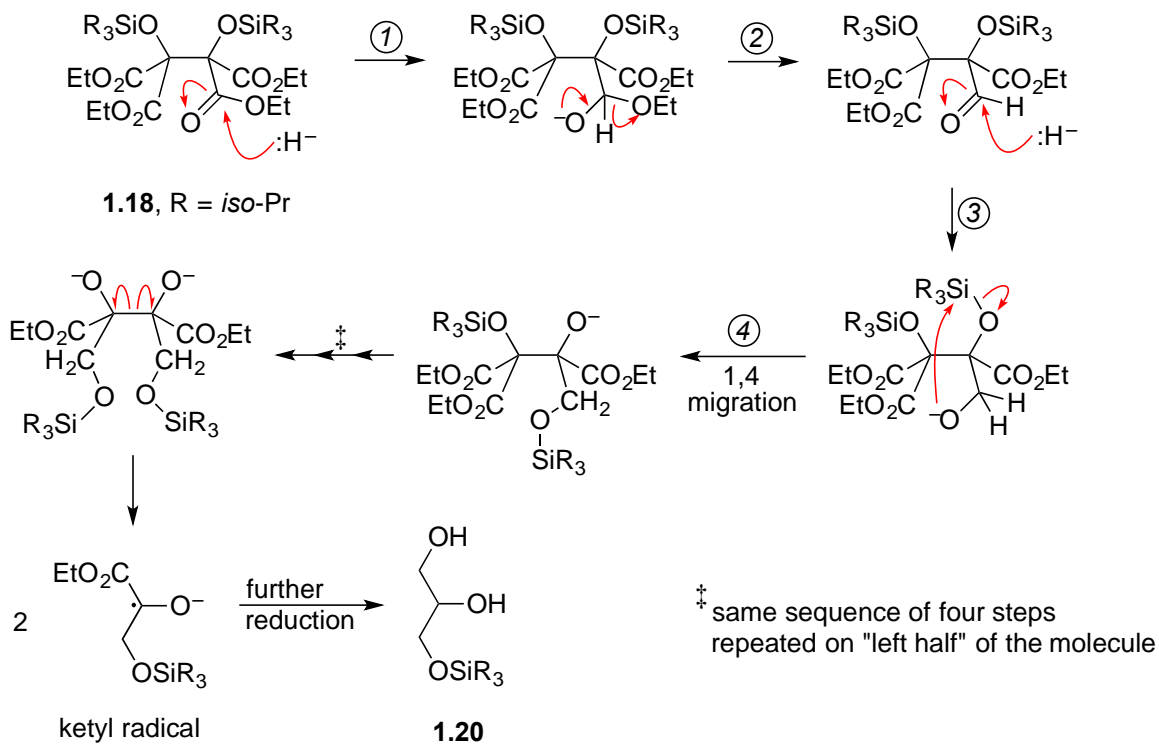
TIPS ether **1.18** was treated with LAH in THF at reflux for 1 h. Surprisingly we got glycerol protected TIPS ether **1.20** in 83% yield instead of desired compound **1.19** (eq [1.9]). Glycerol

TIPS protected compound **1.20** was confirmed by ^1H NMR, ^{13}C NMR, and mass spectrometry.

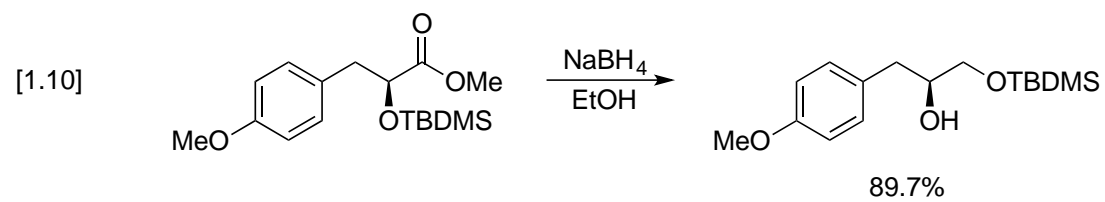


In this reaction, the silyl group migrates from a 3° to a 1° position, and the central C-C bond is cleaved. A highly speculative mechanism to rationalize the formation of **1.20** is presented in Scheme 1.3.

Scheme 1.3. Possible mechanism of formation of 1.20



A precedent for silyl group migration during reduction is shown in eq [1.10].¹¹



Despite our attempts to devise a better route to **1.1**, the Xiaoxun Li synthesis with the improved diol protection step and, significantly, the cascade reaction, remains the best way to access 2,2'-bi(glycerol), **1.1**.

CHAPTER 2

ATTEMPTED SYNTHESIS OF AN ALIPHATIC POLYETHER POLYOL DENDRIMER AND A POLYESTER DENDRIMER

2.1. Introduction

2.1.1 Basic concepts

Figure 2.1 shows one of the earliest dendrimers reported, called PAMAM (for poly(amidoamine)).¹² It will serve here to illustrate some basic concepts and nomenclature of dendrimer chemistry.¹³

Highlighted in green at the center is the dendrimer *core*, sometimes also referred to as the dendrimer *scaffold*. In this example, four chains emanate from the core, with each chain having several branches. A *dendron* is a molecular unit that at one end is attached to either the core or to a dendron closer to the core than itself, and at the other end has a branching point. The term *monomer* is also sometimes used. In a dendrimer, each branch of a dendron bears another dendron; those dendrons bear further dendrons, and so on. The term dendron has a second meaning. A molecule containing multiple dendrons (in the first sense of the word) and having one remaining core-facing functional group is also called a dendron. This is shown in Figure 2.2.

In Figure 2.1, the core bears four dendrons, and thus would be denoted an A₄ core. The concept of dendrimer *generations* is illustrated in Figure 2.3. (Although the dendrimer in the Figure has an A₄ core, only one of the four attached structures is drawn). The four dendrons, *i.e.* branching units, attached directly to the core comprise generation 1, or G1. The eight dendrons

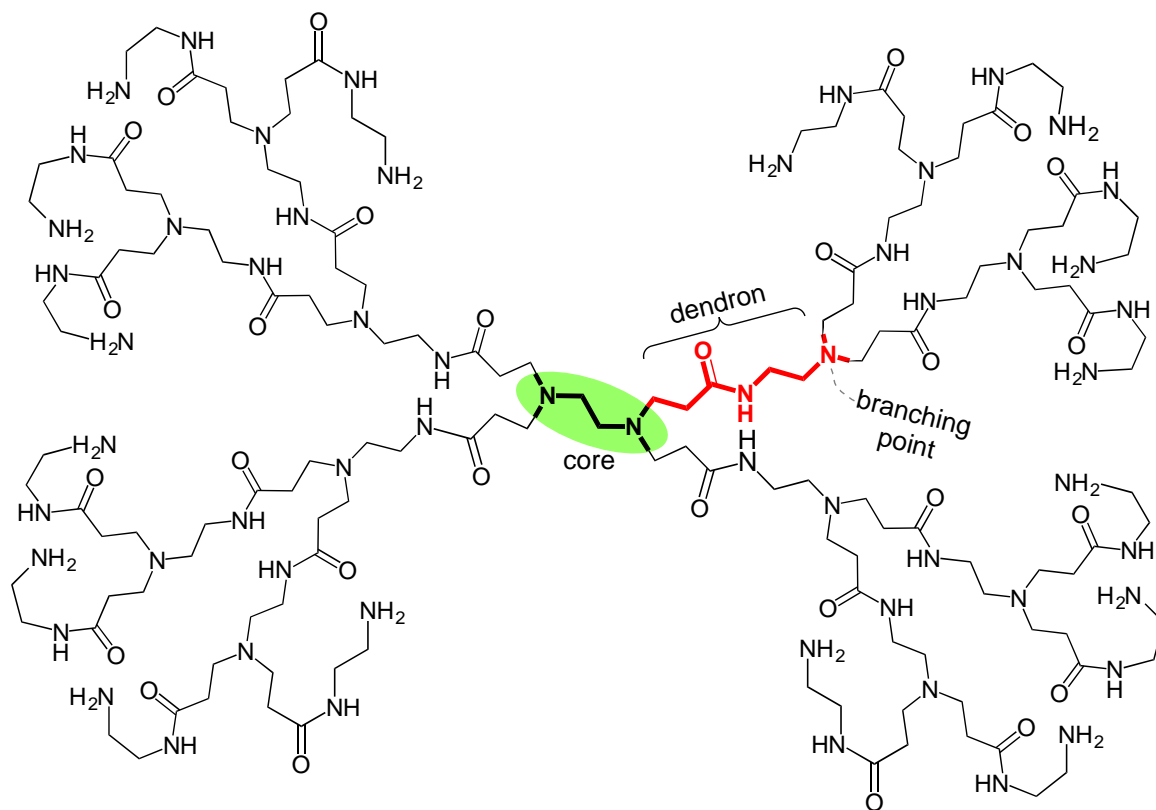


Figure 2.1. Second generation PAMAM dendrimer.

attached to G1 dendrons comprise generation 2, G₂; the sixteen attached to G₂ are G₃, *etc.*

Figure 2.3 shows a G₅ dendrimer. The pendant functional groups of the final generation are called *surface* functional groups, or *peripheral* functional groups, or sometimes *end groups*. In the dendrimer of Figure 2.3, there are 128 surface groups. The chemist may choose these groups, which is an important design feature.

The first “hyperbranched” molecule was discovered in the early 1980’s by Tomalia and coworkers, who named them dendrimers.¹² The term dendrimer derives from Greek words (*dendron* = tree, *meros* = part).¹² Newkome’s group¹⁴ reported the synthesis of similar macromolecules and named them **arborols** from the Latin word *arbor*, also meaning a tree. The term **cascade molecule** is also used, but “dendrimer” is the most well known term. The difference between linear polymers and dendrimers is that a linear polymer molecule consists of

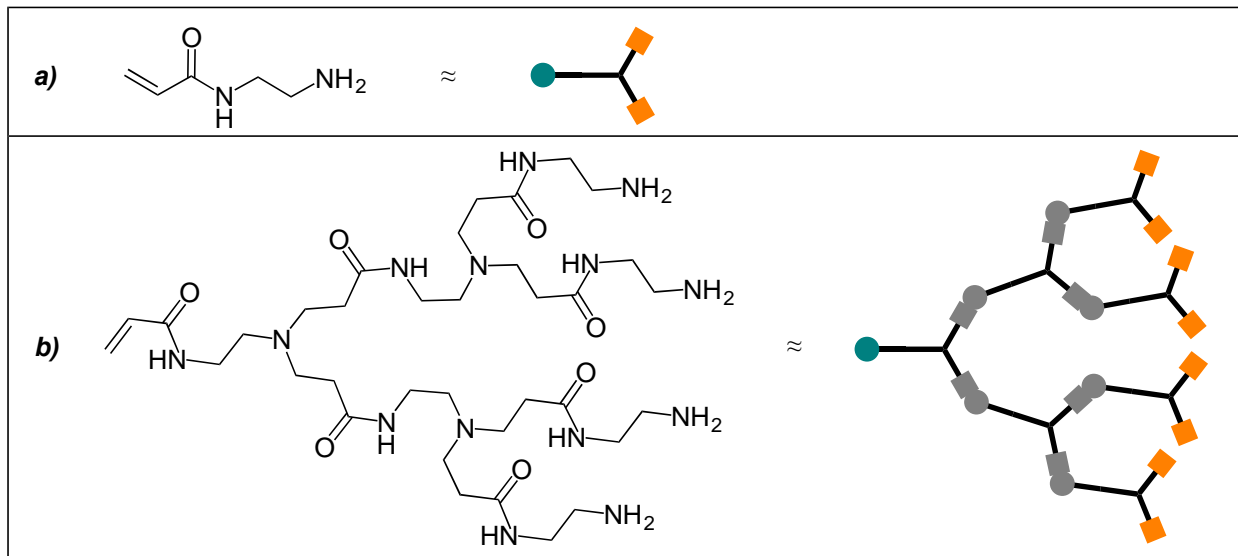


Figure 2.2. Both *a)* and *b)* may be termed dendrons. Case *b)* is also referred to as a dendritic wedge.

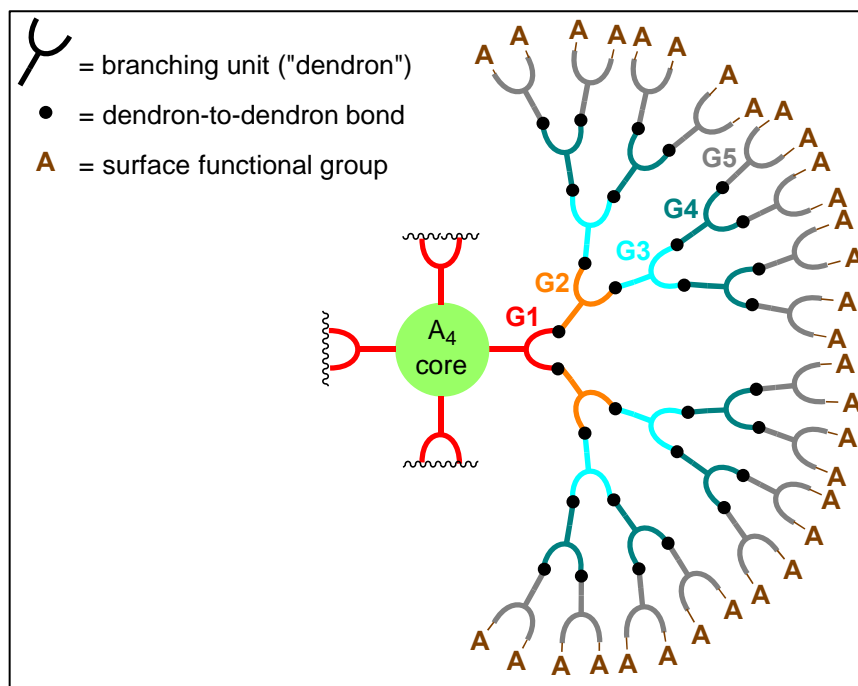


Figure 2.3. Diagram of a five generation dendrimer. Of the four identical dendritic wedges attached to the core, only one is shown.

a long chain of repeating units. Branching, if it occurs, is undesirable typically. Individual polymer molecules in a bulk material are highly entangled. In contrast, a dendrimer consists of several branched chains connected to a common center. Branching is intentional and occurs at regular intervals along the chain. While the “shape” of small dendrimers is the subject of continued investigation, large dendrimers are thought to assume a spherical or globular shape. In that case, entanglements of dendrimer molecules with each other are greatly reduced.

2.1.2. Synthesis of dendrimers

Dendrimers are generally prepared using one of two basic strategies *viz.*, *divergent* (inside out) and *convergent* (outside in) syntheses. There is a fundamental difference between these two construction concepts.¹⁵

The divergent method was proposed by Tomalia *et al.* for the synthesis of PAMAM dendrimers.¹² In this method, the construction of a dendrimer starts from the core and builds out to the periphery, as shown in Figure 2.4. The core molecule reacts with a monomer molecule (or dendron) containing one reactive and two or more dormant groups giving the first generation dendrimer. Then the dormant groups on the periphery of the molecule are activated or transformed to create a new reactive surface functionality. These are used to react with monomer molecules to give generation 2. The process is repeated several times and a dendrimer is built layer after layer.

There are some disadvantages of the divergent approach.¹⁶ The rapid increase in the number of reactive groups at the periphery in every generation leads to a number of potential problems as growth is pursued: (1) any incomplete reaction of these terminal groups would lead to imperfections or structural defects. (2) To prevent side reactions and to force reactions to

completion, extremely large excess amounts of reagents are required in latter stages of growth. This causes some difficulties in purification of the product.

There are some advantages of this approach: (1) It's very easy to modify the full surface of the dendrimer in a single step. Since the properties of dendrimers are mainly determined by the

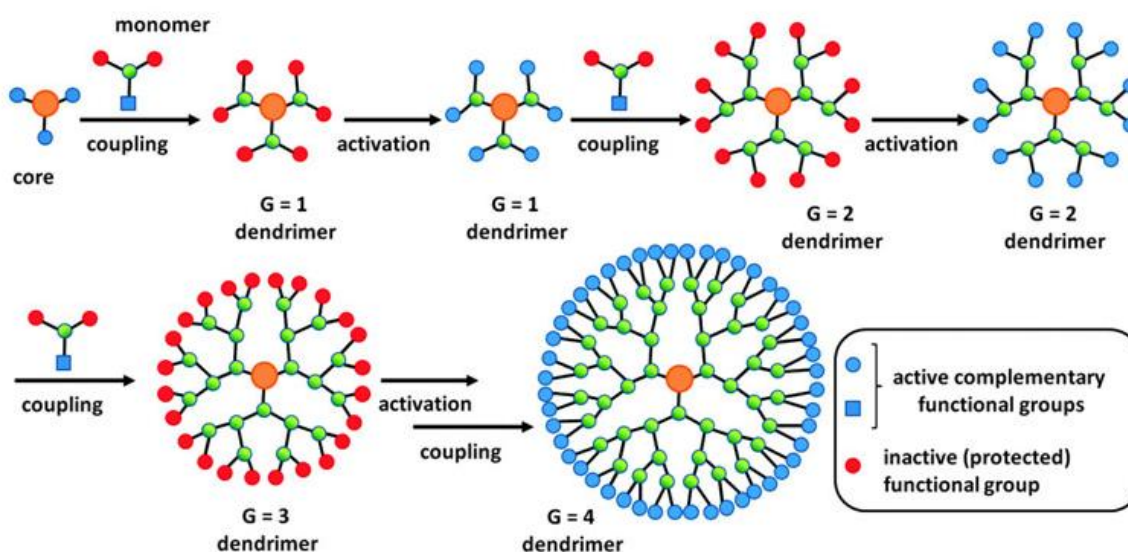


Figure 2.4. Dendrimer synthesis by divergent strategy.¹⁷

type of terminal functional groups, dendrimers with the same internal structure can be used in different fields (*e.g.*, as catalyst, drug delivery, *etc.*). (2) The possibility of stopping the reaction at any step as well as the possibility of automating the repetitive steps, makes a library of various generation dendrimers easier to create. For this reason, the synthesis of all commercially available dendrimers, such as polyamidoamine (PAMAM) or poly(propylene imine) (PPI)¹⁸ are still synthesized using the divergent strategy.

The second method, the convergent method, was first reported by Hawker and Fréchet for the preparation of poly(arylether) dendrimers.¹⁹ In this strategy, the dendrimer is constructed starting from end groups, progressing inward as illustrated in Figure 2.5. Individual dendritic wedges (*i.e.* dendrons) are synthesized first and then coupled with a multifunctional core.

This method has several advantages over the divergent method: (1) Structural defects are fewer in this approach because of the limited number of reactions performed on the same molecule from one generation to the next; and intermediates are more easily purified at successive stages of the synthesis. (2) It's relatively easy to purify the desired product because the reagents are used in equimolar or slight excess amounts for the reaction to progress. (3) Forming a library of dendrimers that differ in the nature of core and that can be organic or inorganic is easy in this approach because the addition of same dendritic wedges to different cores immediately gives a new dendrimer in one reaction step.

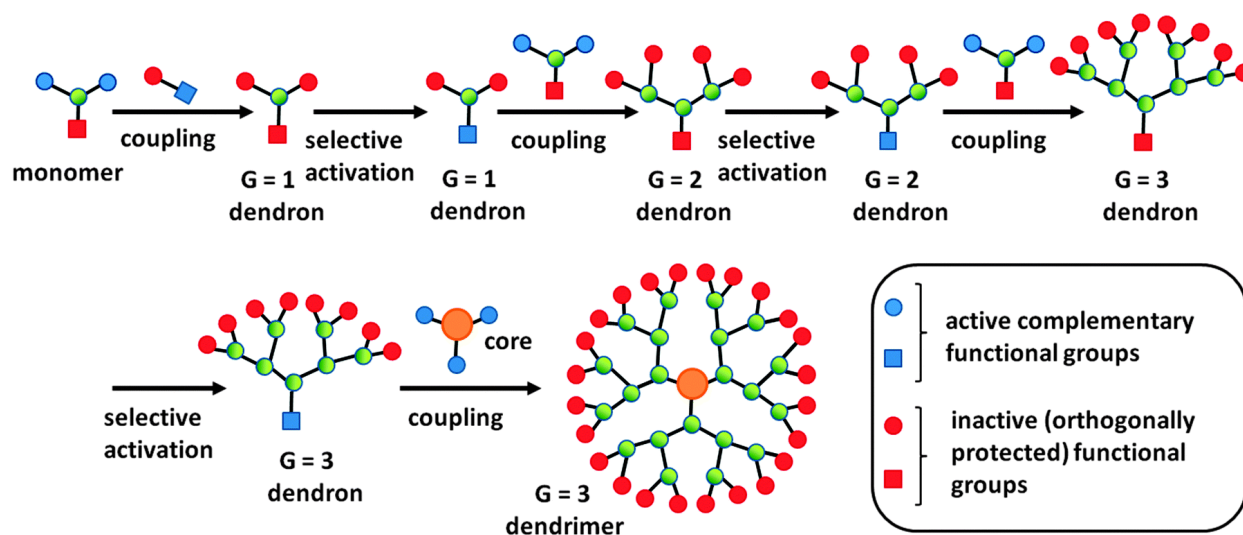


Figure 2.5. Convergent method of dendrimer synthesis.¹⁷

A disadvantage of this method is that it doesn't allow the formation of higher generation dendrimers due to steric problems when coupling large dendritic wedges (*i.e.* dendrons) with the core molecule. The reactive group at the "point" of the wedge is called the "focal point." As the size of the dendron increases, steric hindrance at the focal point increases.

2.1.3. Applications

Dendrimers have unique structural features, and consequently they have been used in various applications in a wide variety of fields. Some noteworthy applications are:

- Drug delivery systems,²⁰
- Catalysis,²¹
- Gene therapy and chemical sensors,²²
- Contrast agents for magnetic resonance imaging (MRI),²³
- Solubility enhancers²⁴
- Boron neutron capture therapy (BNCT).²⁵

2.1.4. Structural evolution of dendrimers

Due to their potential applications, new types of dendrimers were designed, *i.e.* types that possessed different functional groups, building blocks, multifunctional surfaces and metal functionalized cores in contrast to the traditional dendrimers as shown in Figure 2.6. Fréchet's group in the early 90's synthesized block dendrimers or codendrimers.²⁶ Many dendrimers of this type were synthesized and can be classified according to their structural characteristics as layer-block, segment-block and surface-block dendrimers.²⁷ The first bifunctional dendrimers with alternating²⁸ or random²⁹ distributions of terminal groups were prepared in late 90's. The bifunctional dendrimers are often named "Janus³⁰ dendrimers" and they possess at least two different types of terminal functional groups. Dendrimers with multifunctional surfaces can find multiple applications because several properties are combined in one molecule. Nearly a decade later, dendrimers with at least three types of terminal functionalities that resemble a fruit salad tree were synthesized by Steffensen and Simanek.³¹ The first decade of 21st century gave

tremendous progress in dendrimers with functionalized cores or functionalized interiors, where functional groups can be localized in every generation³² or only in certain generations.³²

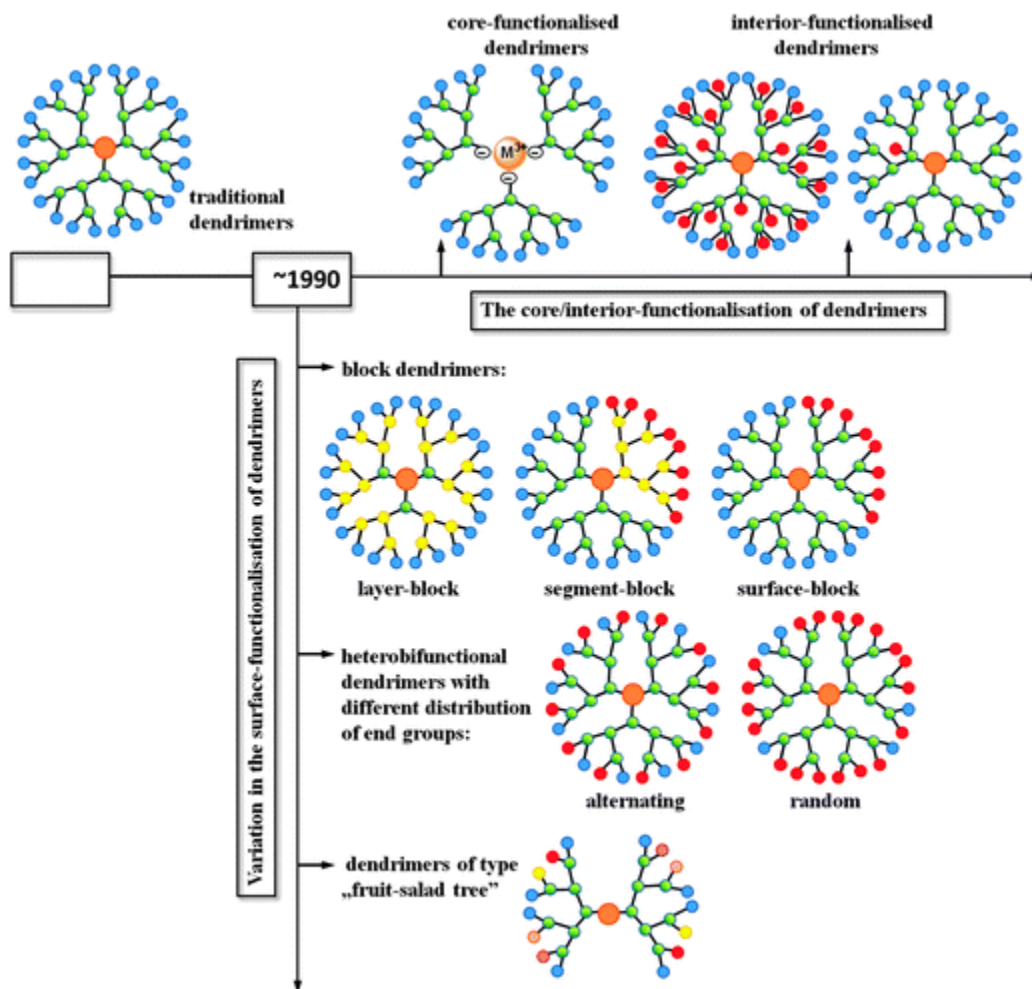


Figure 2.6. Structural evolution of dendrimers.¹⁸ The horizontal axis is a rough time axis.

2.1.5. Multivalent dendrimer cores (scaffolds)

Dendrimers are efficiently prepared by either convergent or divergent method. The number of surface groups accessible by both methods by following the number of surface groups at each generation and number of functional groups or branching points of the core molecule (scaffold).

So core also plays major role.³³ Figure 2.7 illustrates some of the most common multivalent scaffolds that have been used in dendrimer synthesis.³⁴

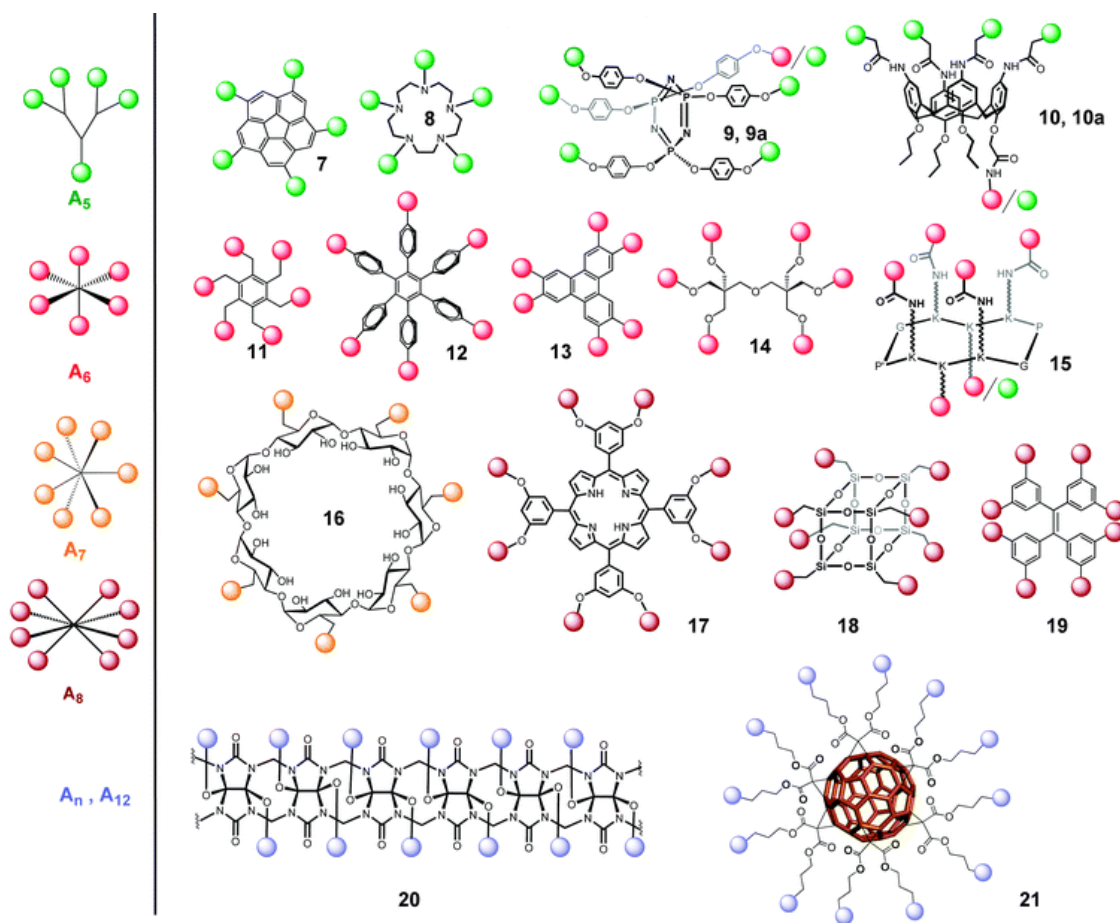


Figure 2.7. Overview of the multivalent scaffolds (cores) used in the synthesis of dendrimers.³⁴

Sugars and naturally occurring polyols such as glycerol, pentaerythritol, dipentaerythritol and even alditols like mannitol, glucitol, xylitol, etc. constitute valuable building blocks and scaffolds as they readily modified to other functional groups.

Our laboratory focused on dendrimer synthesis with new scaffold **2.2** which has eight primary alcohols (Figure 2.8 b).

2.2 Results and Discussion

2.2.1 Target compounds

In recent years aliphatic polyether-polyol dendrimers have been the most intensely studied class of dendritic polymers.³⁵ They gained importance because their high number of hydroxyl end groups offers various further functionalization opportunities. In contrast to hyperbranched polyesters, they are much more stable against acidic or basic hydrolysis.³⁶ In addition, they are valuable compounds for polymer therapeutics because of their excellent solubility in water and biocompatibility³⁷ Keeping these qualities in mind, our laboratory focused on synthesizing dendrimer **1** which has an A_8 core highlighted in red and blue (Figure 2.8). The red structure is an A_6 core, consisting of two tertiary alcohols and four primary alcohols. Our goal is to convert the tertiary alcohols of the A_6 core to primary alcohols to make the A_8 core.

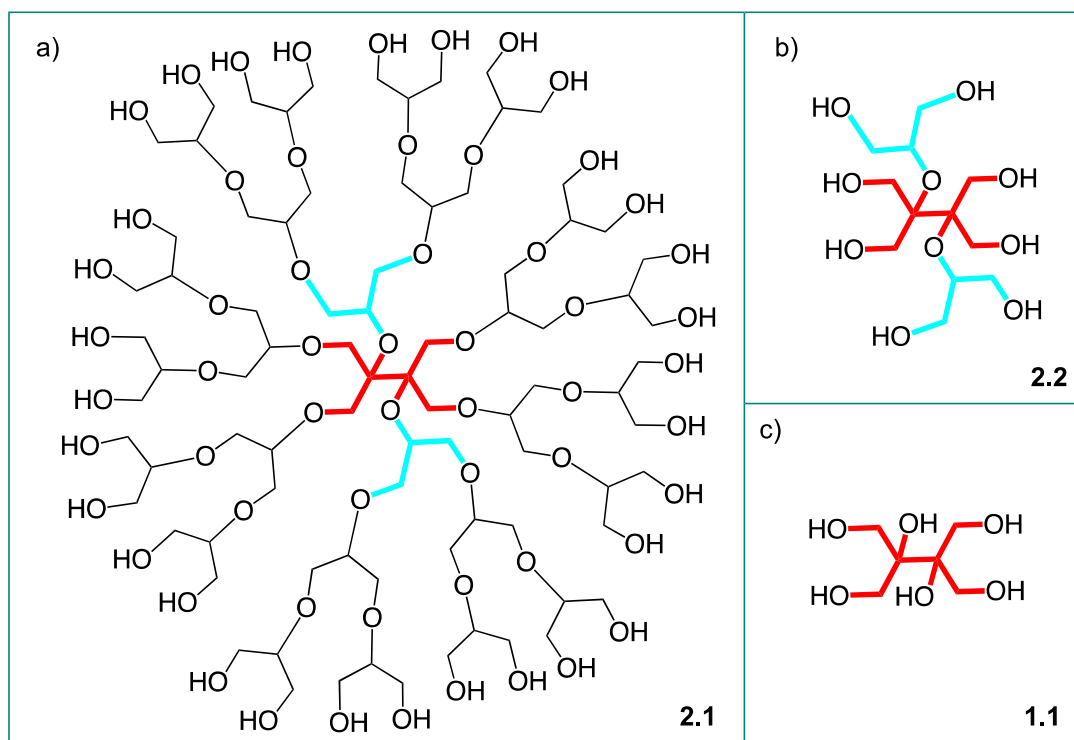
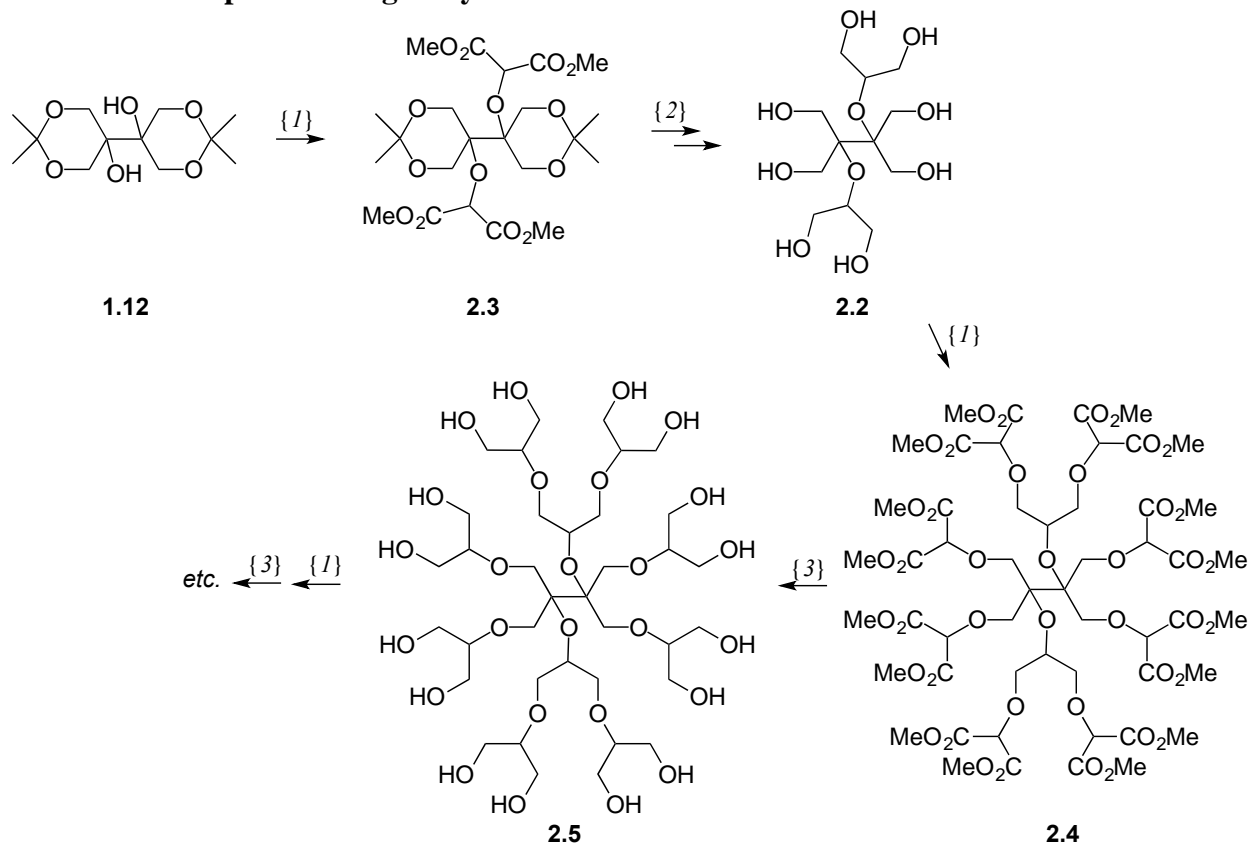


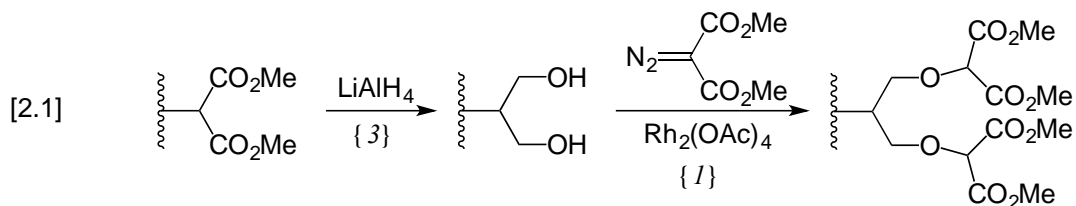
Figure 2.8: a) Aliphatic polyether polyol second generation dendrimer **2.1**. b) A_8 core. c) A_6 core.

Once the A₈ core is in hand, we propose that the dendrimer **2.1** may be made by the divergent dendrimer synthesis shown in Scheme 2.1.

Scheme 2.1. Proposed divergent synthesis of dendrimer 2.1

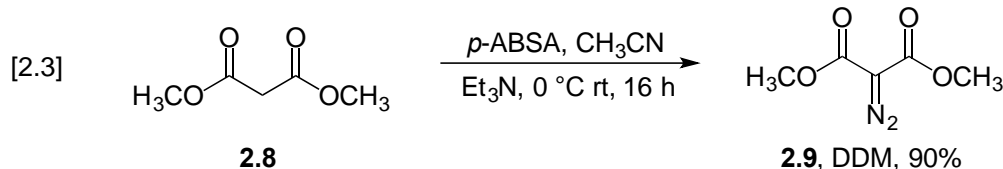
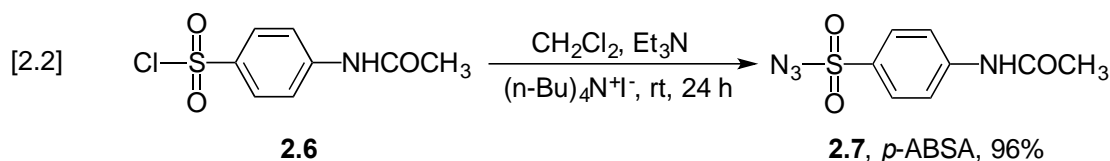


The scheme consists of two main parts. One part is the method of adding generations to the dendrimer *i.e.*, processes {1} and {3} in Scheme 2.1 that convert **2.2** to **2.5**. This is shown in eq [2.1]. A polyester is reduced to a polyalcohol, followed by the insertion of the carbenoid derived from dimethyl diazomalonate (DDM) into the O-H bonds of the polyalcohol, which generates a new polyester. This two-step sequence may be repeated to “grow” the dendrimer.



The other part of the scheme is preparation of the A₈ core. Process {1} converts diol **1.12** to tetraester **2.3**. To get to octaolcohol **2.2** (process {2}), two routes are possible: reduction of the ester groups, followed by cleavage of the acetonide protecting groups, or cleavage followed by ester reduction.

The main challenge that we foresaw in this plan was the carbenoid insertion into the tertiary O-H groups of diol **1.12** using DDM. In various reactions, tertiary alcohols are less reactive than primary or secondary alcohols.³⁸ The starting compounds for the synthesis are diol **1.12** (the preparation of which was described in Chapter 1), and DDM, **2.9**. DDM was easily prepared in two steps, as shown in eq [2.2] and eq [2.3].³⁹

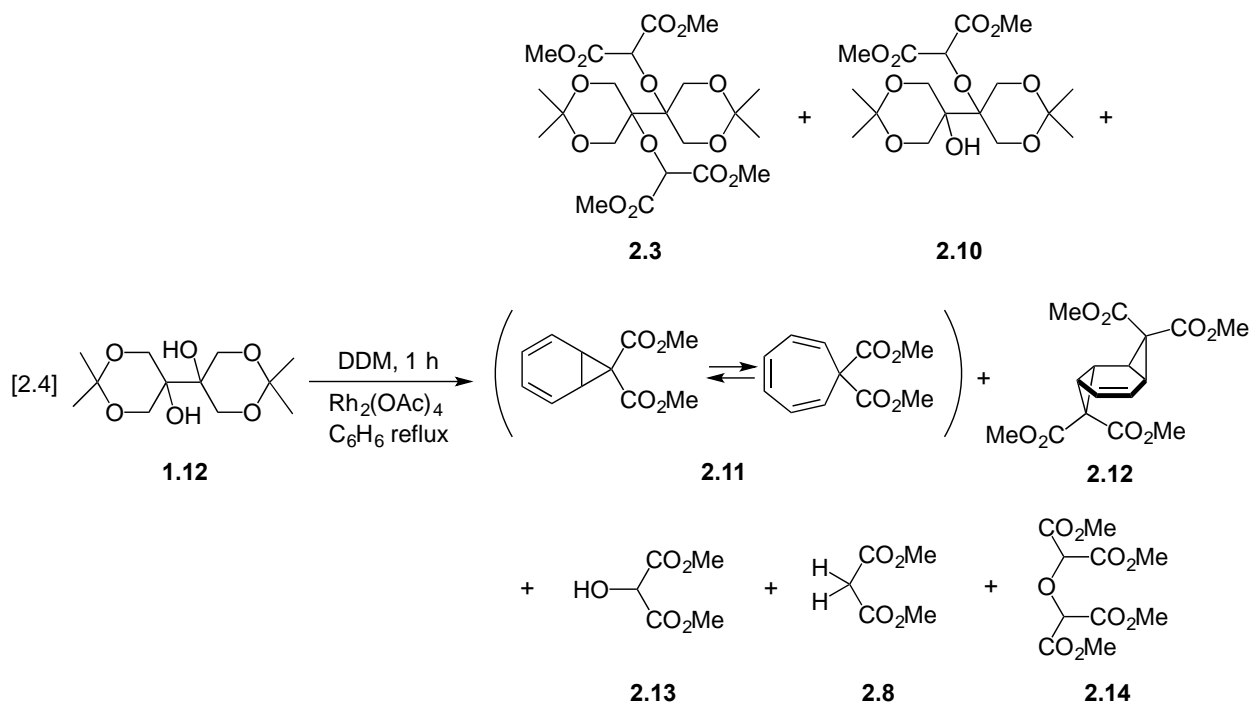


2.2.2. Rh₂(OAc)₄ catalyzed O-H insertion reaction of diol **1.12** with DDM

With DDM **2.9** in hand, we started out on the first step of the synthesis of dendrimer **2.1**, which is the Rh₂(OAc)₄ catalyzed carbene O-H insertion, eq [2.4].

When we performed for the first time the Rh₂(OAc)₄ catalyzed reaction of diol **1.12** with DDM in dry benzene as solvent (eq [2.4]), we obtained a mixture of several compounds, as evidenced by the complex NMR spectrum (see Figure 2.9), and several close spots on TLC (difficult to separate chromatographically). Upon further investigation, we identified the desired di-insertion product **2.3**, and mono-insertion product **2.10**. Products **2.11** and **2.12** resulted from

reaction of the carbenoid with the solvent, benzene. Other ester byproducts **2.13**, **2.14**, and **2.8**, and some unidentified products were also found.



Identification of the benzene-derived products was based on previous assignments by Yang, Webb, and Livant.⁴⁰ Identification of other byproducts was reported by a previous graduate student in our lab, Dr. David Sujee Makhanu, who studied carbenoid N-H insertion reactions with DDM, and observed **2.13**, **2.14**, and **2.8** as byproducts in that reaction.⁴¹

To reduce the byproduct formation in the O-H insertion reaction of diol **1.12** with DDM, we tried different ratios of DDM to **1.12**, various reaction times and different solvents (see Table 2.1). The product distributions reported in Table 2.1 result from integration of areas of ^1H NMR peaks. Overlap of peaks rendered some numbers approximate. However the peaks at 6.34 ppm and 6.25 ppm are relatively unencumbered, and these peaks belong to di-insertion product **2.3** and mono insertion product **2.10**, respectively. (See inset in Figure 2.2) Therefore the ratio of **2.3** to **2.10** is a more trustworthy measurement than others in Table 2.1. The column in Table 2.1 that contains those data is highlighted.

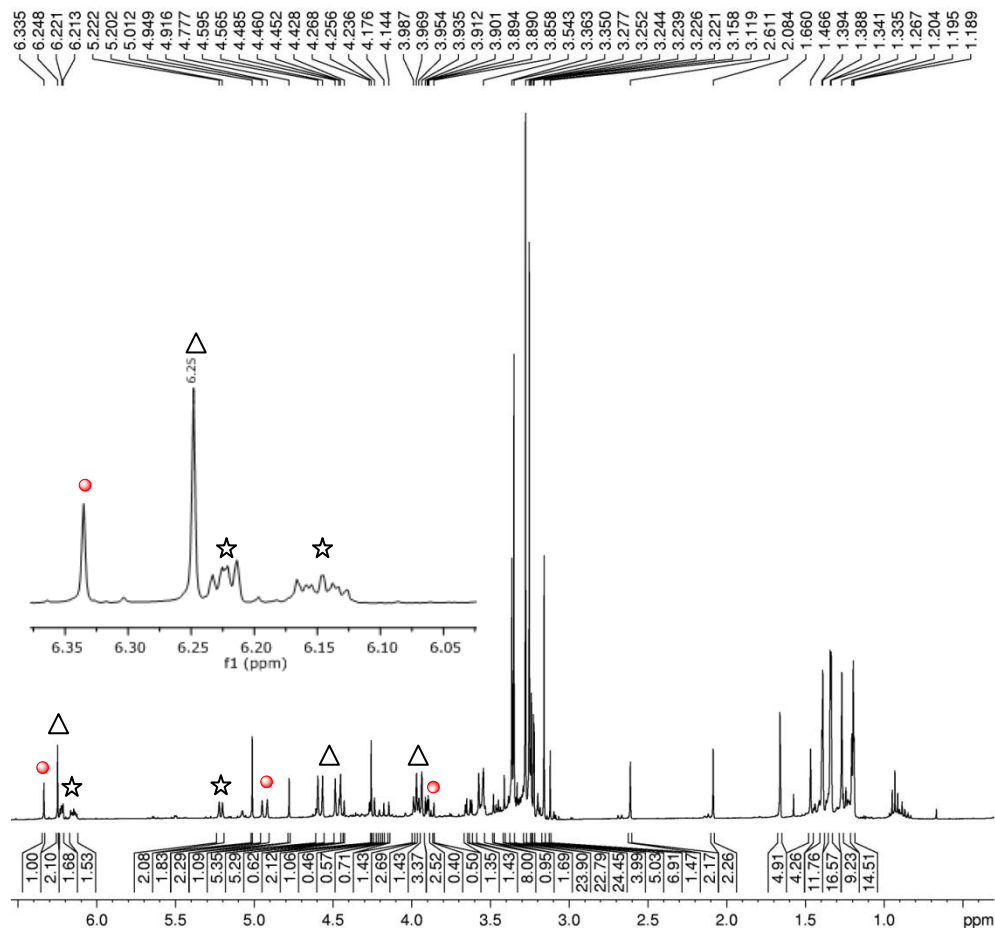


Figure 2.9. 400 MHz ^1H NMR spectrum (C_6D_6 solvent) of the first attempt at the $\text{Rh}_2(\text{OAc})_4$ catalyzed O-H insertion reaction of DDM with diol 1.12. Partial assignments are shown: red circle – 2.3; triangle – 2.10; star – 2.11, 2.12; diamond – other byproducts 2.13, 2.14, and 2.8.

Table 2.1. Reaction of diol 1.12 with DDM, 2.9, under various conditions^a

Entry	DDM diol	Rh ₂ (OAc) ₄ diol	solvent	time (h)	Product distribution (%)				2.3/2.10
					2.3	2.10	solvent- derived ^b	other ^c	
1	2.24	0.02	C ₆ H ₆	7	12	53	21	14	0.23
2	4	0.04	C ₆ H ₆	1	34	19	35	12	1.8
3 ^d	4	0.04	none	2	10	7	–	9	1.4
4 ^d	4	0.04	C ₆ H ₆ ^e	1	25	12	–	10	2.1
5	4	0.04	C ₆ F ₆	1	34	45	–	21	0.76
6	4	0.04	C ₆ D ₆	1	15	51	–	34	0.29
7	4	0.04	CH ₂ Cl ₂	8	–	–	–	–	–
8	5.6	0.056	C ₆ H ₆	1	37	11	40	12	3.4
9	7	0.07	C ₆ H ₆	1	58	9	28	5	6.4
10 ^f	9	0.09	C ₆ H ₆	1	45	8	36	12	5.6
11 ^f	10	0.10	C ₆ H ₆	1	49	4	26	21	12

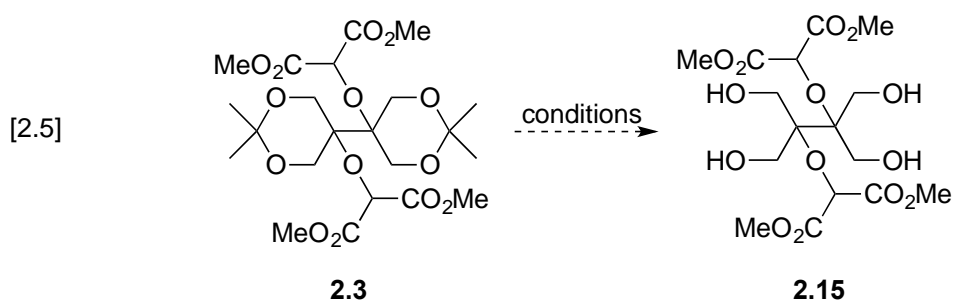
^aExcept where indicated, *ca.* 50 mg of diol **1.12**, and 2.0 mL of solvent were used. ^b**2.11** and **2.12**. ^c**2.8**, **2.13**, and **2.14**. ^d> 65% diol **1.12** remaining after reaction. ^e20 μL ^fDDM remaining after reaction.

When 2.24 equivalent of DDM was used (entry 1), 53% of **2.10** was formed. To promote **2.3** formation, DDM was increased to 4.0 equivalents (entry 2), but in that case benzene-derived and other ester products also increased compared to entry 1. To avoid benzene-derived products, we tried doing the reaction with no solvent (entry 3) or 20 μL of solvent (entry 4), but the results were not satisfying because the reaction mixture could not be uniformly stirred so a lot of starting diol **1.12** remained by the end of the reaction. Instead of benzene, hexafluorobenzene and benzene-d₆ were used (entries 5 and 6). Solvent-derived products could not be observed by ¹H NMR since the solvents had no H atoms, however the **2.3/2.10** ratio was poor for both cases. Dichloromethane as solvent didn't give the desired result. A previous graduate student in our lab,

Xing Wang, studied the rhodium catalyzed N-H insertion reactions of 2-diazo-1,3-cyclohexanedione (DCD) with diarylamines, and found that when dichloromethane was the solvent, it reacted with DCD, producing the enol form of 2-chloro-1,3-cyclohexanedione as product.⁴² In our case, we assume DDM is reacting with dichloromethane analogously, producing chlorinated dimethyl malonate, but we couldn't isolate the chlorinated product.

When we used 9.00 and 10.0 equivalents of DDM (entries 10 and 11), the diol was consumed but excess DDM remained at the end of the reaction. In these cases, purification of the products was difficult because the R_f of DDM was very close to that of the products. Out of all these attempts we finally decided to use 7.00 equivalents DDM (entry 9). The reason for this is when we used 7.00 equiv DDM, some of the excess DDM reacts with benzene and adventitious water in the reaction and the remainder of the DDM reacts with diol **1.12**, so no unreacted DDM is observed after the completion of reaction. Therefore, purification of the product was easy compared to entries 10 and 11. Isolated yields after three successive columns were 7.1% of **2.3** with slight **2.14** as impurity, and 5.4% of **2.10**.

2.2.3. Attempted deprotection of acetonide groups of **2.3**



Compound **2.3**, carrying slight impurity **2.14**, went for the next step of synthesis *i.e.*, acetonide deprotection (eq [2.5]). According to the literature, deprotection of acetonides is commonly done using acids (e.g., Lewis acids, HCl, TFA)⁴³ or other catalytic methods such as 1% I₂/MeOH.⁴⁴ Deprotection of acetonides was attempted under various conditions and reagents

(TMSOTf^{44c} and 1% I₂/MeOH), but ¹H NMR spectra were inconsistent with the expected product, and we had no success in isolating the tetraalcohol tetraester **2.15**, shown in eq [2.5]. Therefore, we decided to close this route, and began work on a new strategy for building a different dendrimer on our A₆ core.

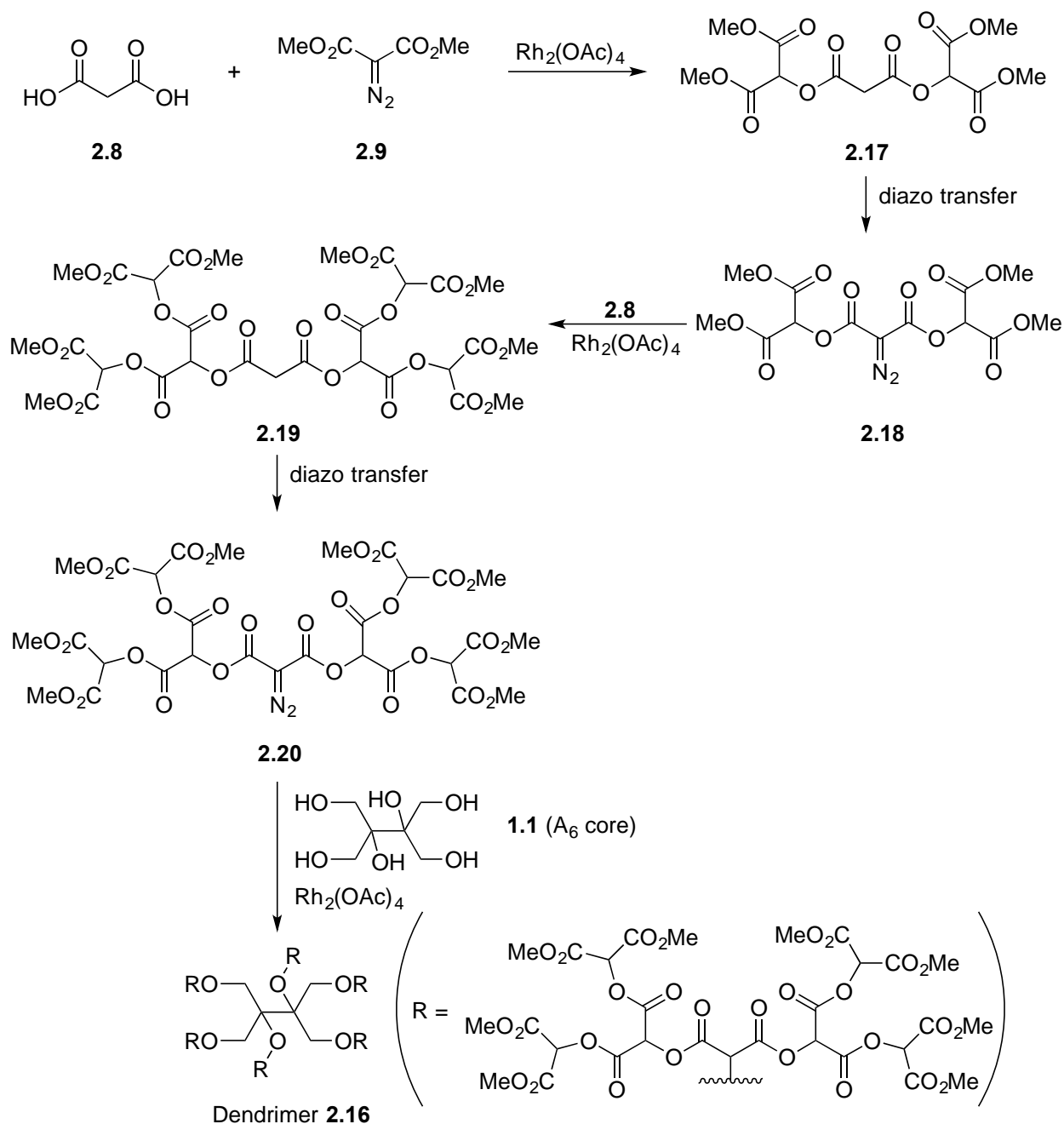
2.2.4. Proposed synthesis of dendrimer 2.16

We decided to prepare new polyester dendrimer **2.16**, which is shown in Scheme 2.2. The major advantage of ester dendrimers as frameworks for biological applications is that they have been found to have low toxicity.⁴⁵ We decided to prepare this polyester dendrimer using a convergent method.⁴⁶ Dendrons (dendrimeric “wedges”) would be built up by repetition of *i*) Rh-catalyzed insertion of a carbenoid into the O-H bonds of malonic acid, **2.17**, and *ii*) diazotization of the malonate ester formed in step *i*). Once the “growing” dendrons (*e.g.*, **2.20**) had reached desired size, they would be attached to the multifunctional core molecule.

2.2.5. Insertion of the carbenoid derived from DDM into both O-H bonds of malonic acid

The starting point for the synthesis of polyester dendrimer **2.16** is insertion of the Rh-carbenoid derived from DDM into the O-H bonds of malonic acid. A refluxing benzene solution of malonic acid and Rh₂(OAc)₄ was treated with 2.2 equiv DDM. This eventually yielded a mixture of compounds **2.17**, **2.21**, and the common contaminant **2.14** (2,2'-oxybis(dimethyl malonate)), eq [2.6]. Since we suspected that **2.14** arose from double insertion of the carbenoid into water, to reduce **2.14** formation in the reaction, we added activated molecular sieves, (type 4 °A, 1–2 mm beads) to the initial reaction mixture and refluxed. Gratifyingly, the amount of **2.14** decreased.

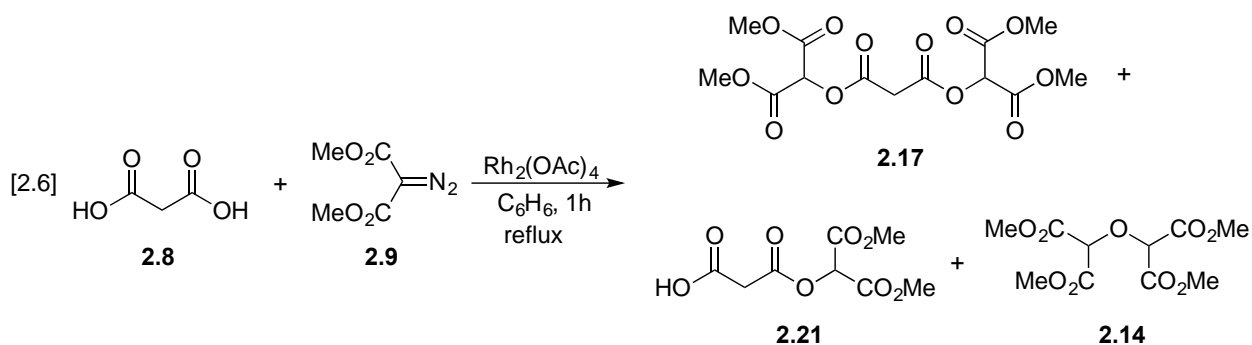
Scheme 2.2. Proposed convergent synthesis of polyester dendrimer 2.16



When we loaded 2.5 equiv DDM to promote **2.17** formation, interestingly monoinsertion product **2.21** formation was not seen, but a slight amount of benzene derived products was observed.

When 2.75 equiv DDM was used in the reaction, benzene derived products were more plentiful, as evidenced by TLC and NMR. Of all the attempts, we decided 2.2 equiv was the best. This is

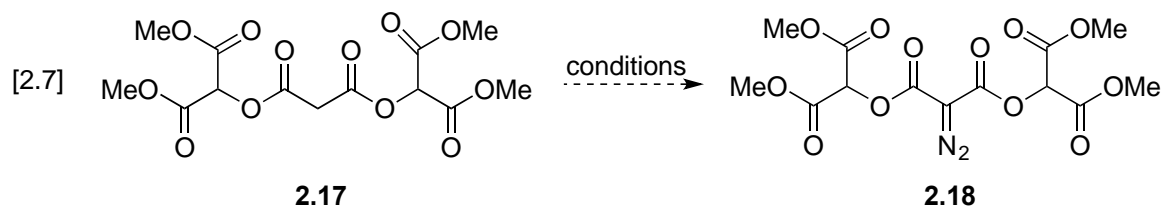
because the R_f values of **2.17** and **2.21** are very well separated, so purification of **2.17** is very easy and the yield was also good, but it has 5% of **2.14** according to ^1H NMR area integration. We tried various mobile phases to separate **2.17** and **2.14**; the best of our attempts was THF/hexanes combinations in ratio of 1:2 (v/v), switching slowly to 1:1 (v/v). Unfortunately we didn't get the clean pure product **2.17**; it still has 5% of **2.14** according to ^1H NMR. In 2.5 equiv DDM and 2.75 equiv DDM cases, product purification was difficult because benzene-derived products have R_f values in TLC that are very close to that of **2.17**. Therefore, for the next step of the synthesis using **2.17**, a slight **2.14** contaminant was present.



2.2.6. Diazo transfer reaction of **2.17**

2.2.6.1 Initial attempts

Second step for polyester dendrimer **2.16** preparation is diazo transfer to **2.17**, eq [2.7]. In general, diazo transfer to the α -methylene position of a carbonyl compound requires the presence of base with sufficient strength to deprotonate at that position, and an azide-bearing diazo transfer reagent.⁴⁷



We used several diazo transfer reagents (see Figure 2.10) such as *p*-toluenesulfonyl azide (tosyl azide, TsN₃),^{48e} *p*-acetamidobenzenesulfonyl azide (*p*-ABSA, **2.7**),⁴⁹ and 2-azido-1,3-dimethylimidazolium chloride (ADMC)⁴⁸ with various bases such as triethylamine, potassium carbonate^{54d} and 1,8-diazabicyclo[5.4.0]undec-7-ene (DBU),^{49c} but we had no success in isolating diazo compound **2.18**.

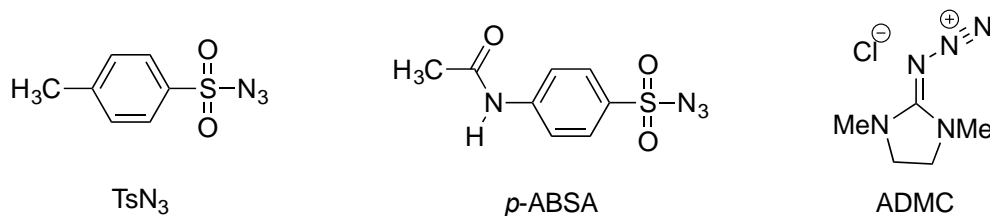
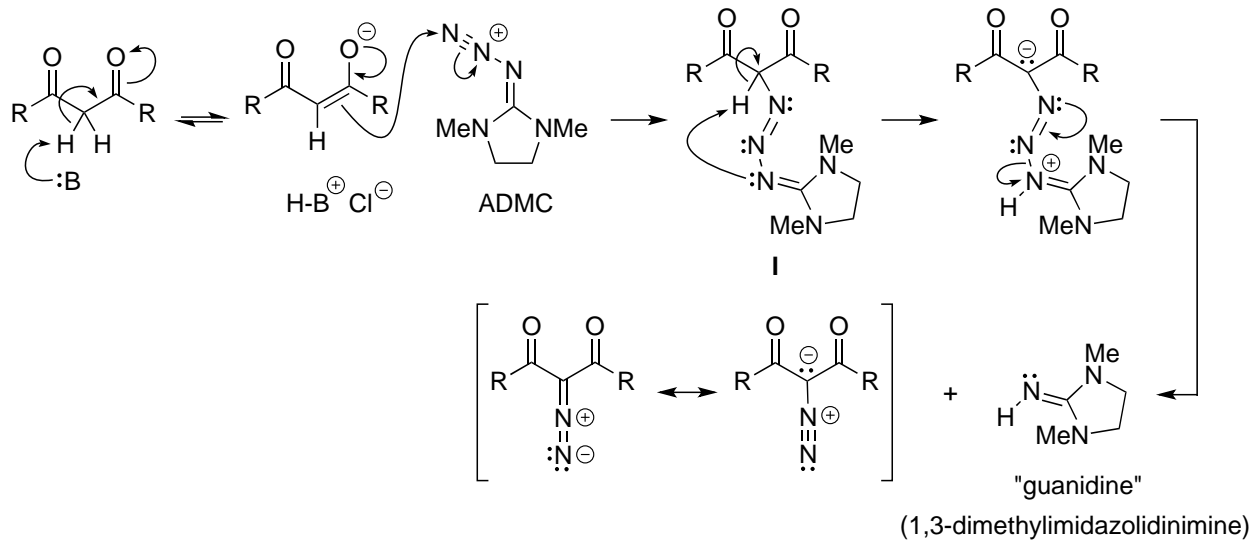


Figure 2.10. Representative diazo transfer reagents.

Scheme 2.3 shows a plausible reaction mechanism of diazotization with ADMC⁴⁸ as diazo transfer reagent in presence of base. In this pathway, the enolate formed from proton abstraction from the 1,3-dicarbonyl compound attacks the terminal azide nitrogen in ADMC to form intermediate **I**. Intramolecular proton abstraction in **I** then occurs to afford the corresponding diazo compound and cyclic guanidine byproduct. An analogous mechanism can describe diazo transfer with the sulfonylazide reagents.

Scheme 2.3. Plausible mechanism of diazo transfer reaction using ADMC^{48a}



In our first attempt to execute the synthesis presented in eq [2.7], we utilized the diazo transfer conditions used which have proven successful by many previous workers in our lab to synthesize DDM: *p*-ABSA and Et₃N in acetonitrile.⁴⁹ Unfortunately, we didn't obtain the desired **2.18**. Workup of the reaction was very difficult; typically, an orange colored gummy substance was obtained. In the DDM case, no such gummy material was encountered. In the DDM preparation, NMR of the crude product mixture after extraction and washing showed no sulfonamide present. By contrast, in the case of **2.17**, NMR of the product mixture showed *p*-acetamidobenzenesulfonamide byproduct. In brief, the workup was as follows. The reaction mixture was filtered, the solvent was removed from the filtrate by evaporation under reduced pressure, and an orange gummy material was obtained. To this CH₂Cl₂ was added, the material dissolved, and the solution was stirred. After 5 minutes, a precipitate formed. It was filtered and the filtrate was evaporated on the rotary evaporator, giving rise to the gummy substance again. Silica gel column chromatography (MeCN:CH₂Cl₂ (1:4 (v/v))) was intended to remove any sulfonamide byproduct. A second chromatography column with EtOAc:hexanes (1:2 (v/v)) switching to EtOAc:hexanes (1:1 (v/v)) gave a substance which had the NMR spectra shown in

Figures 2.11 and 2.12. The overall yield was very low: 6.5%, assuming the product was **2.18**. In the ^1H NMR, singlets at 4.73 ppm and 3.83 ppm in the approximate area ratio of 1:6 appeared to be consistent with the structure of **2.18**, if one ignored the broad peak at 3.4 ppm. The ^{13}C NMR at signals at 169.1 ppm, 71.5 ppm, and 53.6 ppm (see Figure 2.5) were nearly consistent with **2.18**. Compound **2.18** has two types of carbonyls but in Figure 2.5 only one type of carbonyl carbon signal at *ca.* 169 ppm is apparent. In compound **2.17**, ^{13}C NMR carbonyl peaks are very close *viz.*, 164.3 ppm, and 164.2 ppm. Keeping this in mind, we speculated that in **2.18**, two carbonyl signals may be overlapping and showing as one peak.

KRP-1-80'.1.fid — diazo transfer stain visible desired prdt

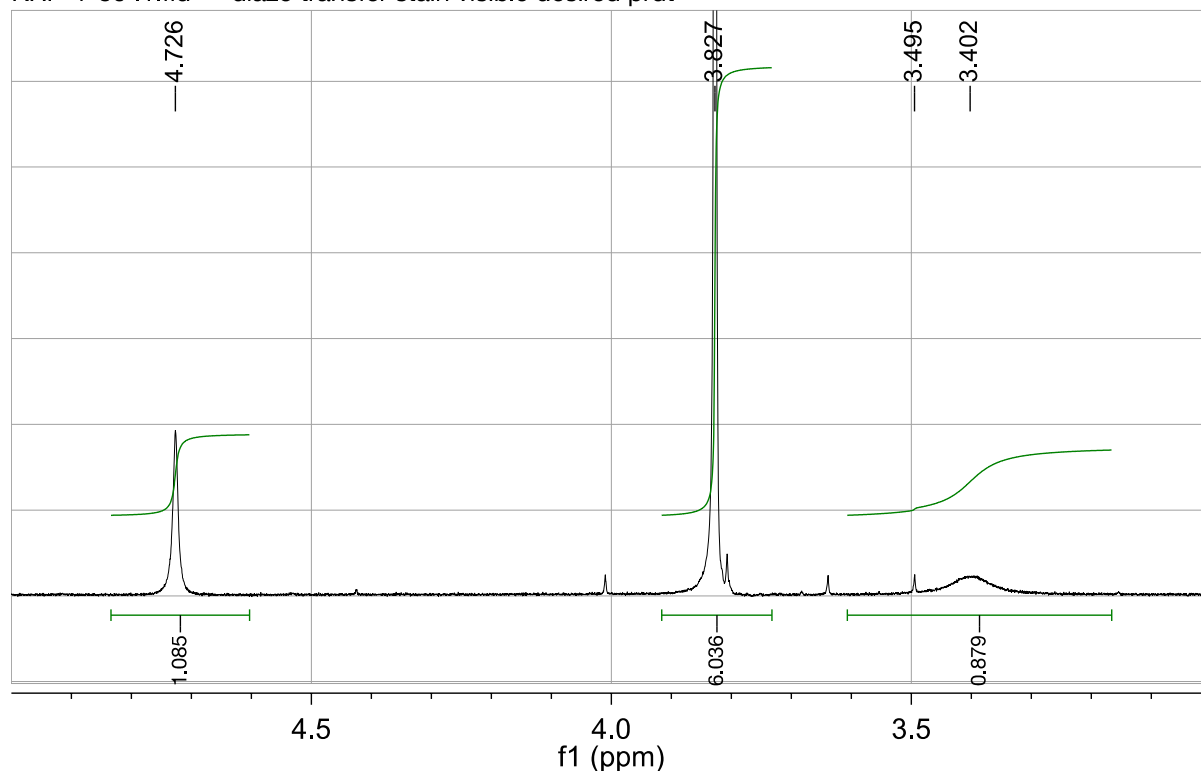


Figure 2.11. 600 MHz ^1H NMR of the product obtained by treatment of **2.17** with *p*-ABSA and Et_3N (**2.17**:*p*-ABSA: Et_3N = 1.0:1.09:2.0) in acetonitrile at rt for 16 h. The product was obtained by means of the workup procedure described in the text. CDCl_3 solvent.

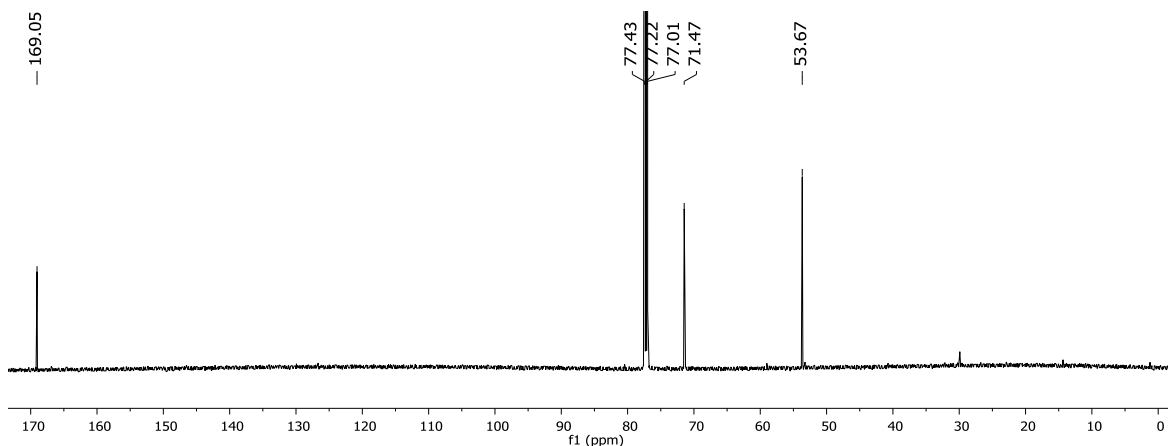
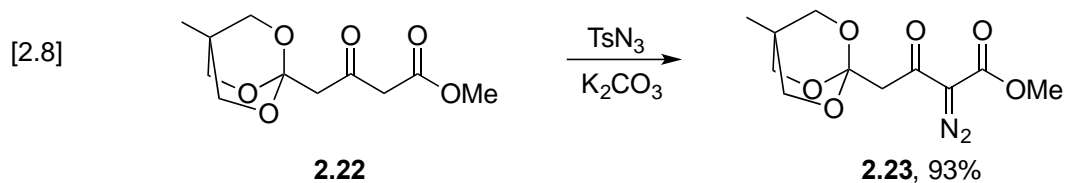
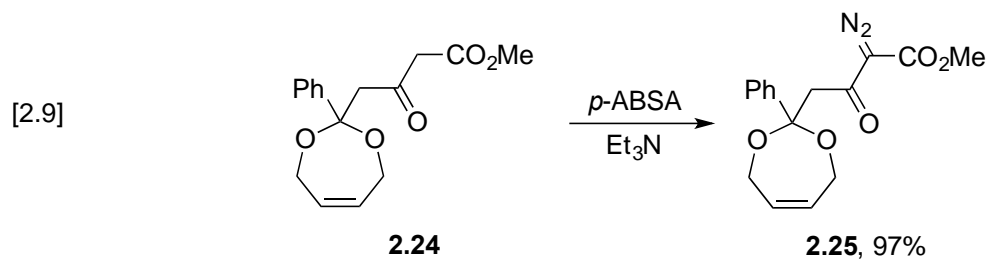


Figure 2.12. 150 MHz ^{13}C NMR spectrum of the compound used for Figure 2.11. CDCl_3 solvent.

But we were not convinced that this material was **2.18**, due to ^1H NMR peak at 4.73 ppm (CH). We reasoned it should be more downfield than the analogous signal in compound **2.17** at 5.56 ppm (CH). Oku *et al.* reported diazo transfer reaction using TsN_3 as shown in eq [2.8].⁵⁰ In this case, after diazo transfer methyl ester protons (CH_3) of **2.23** had shifted to 3.82 ppm compared to **2.22** methyl ester protons at 3.71 ppm. The CH_2 protons between the carbonyl group and the bicyclic system shifted downfield to 3.34 ppm in **2.23**, compared to **2.22** CH_2 protons at 2.88 ppm.



Hodgson *et al.* reported diazo transfer reaction using *p*-ABSA as diazo transfer reagent as shown in eq [2.9].⁵¹ Compound **2.25** CH_2 protons (adjacent to the seven-membered ring) shifted to 3.65 ppm, compared with **2.24** CH_2 protons at 3.25 ppm.



DDM has been synthesized in our lab using dimethyl malonate, *p*-ABSA and Et₃N. Chemical shift of CH₃ in dimethyl malonate was 3.71 ppm; after the diazo transfer reaction, it shifted to 3.81 ppm.

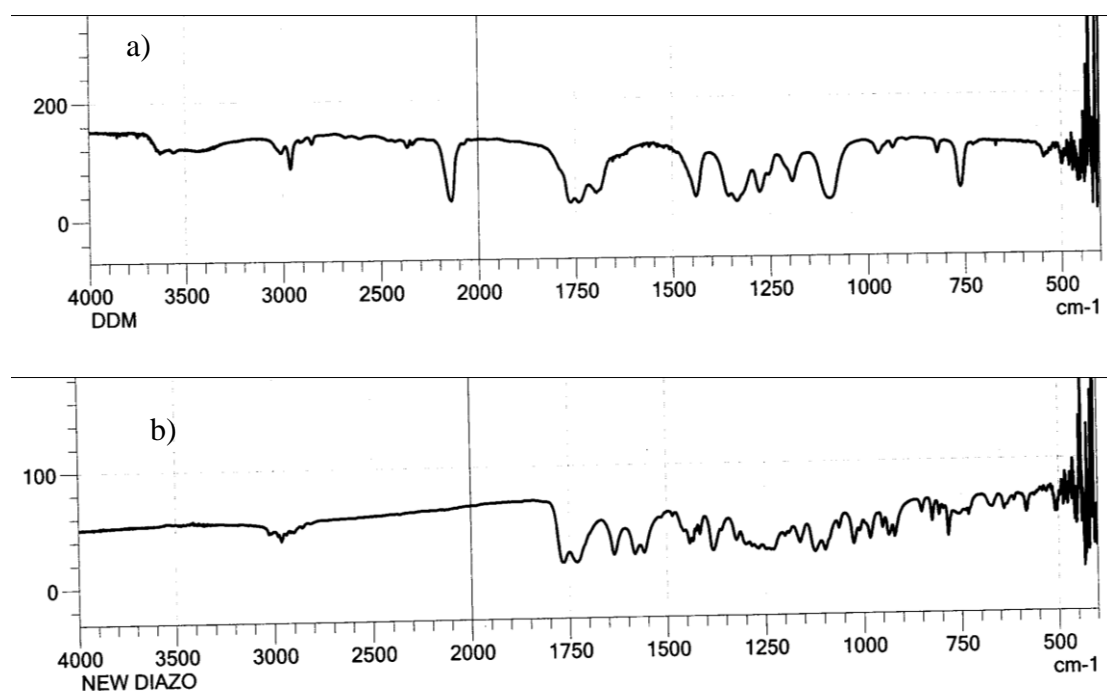


Figure 2.13. a) IR spectrum of dimethyl diazomalonate. b) IR spectrum of product of reaction of 2.17 with *p*-ABSA and Et₃N.

It was therefore strange for the CH peak at 5.56 ppm in **2.17** to move *upfield* to 4.73 ppm in the ¹H NMR spectrum of the product of diazo transfer, **2.18**. Figure 2.13 compares the IR spectrum of authentic dimethyl diazomalonate with the product of the reaction of **2.17** with *p*-

ABSA and Et₃N. The lack of the diazo band at 2120 cm⁻¹ in the product spectrum is obvious. We therefore believed that **2.18** was not the product of this reaction.

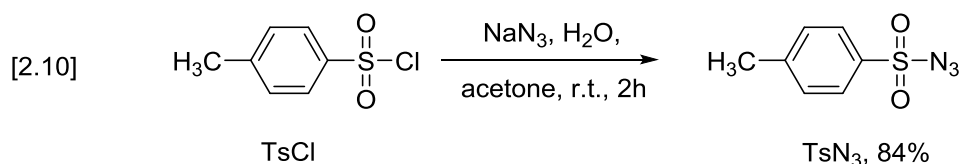
When we used 5 equiv of Et₃N instead of 2 equiv, we got the same results as in the 2 equiv case. At this point, we decided to use a different base: DBU (p*K*_a = 23.9 or 24.3 in MeCN).^{52,53} By comparison the p*K*_a of Et₃N is 18.8 in MeCN.⁵³

Using DBU^{49c} as base and *p*-ABSA as diazo transfer reagent produced the same results as using Et₃N as base. In the DBU case, workup was easier but yields were lower than in the Et₃N case.

The *repeated* inability to produce the diazo compound **2.18** was baffling, especially in light of the excellent yields we and many others in our laboratory obtained in preparing DDM from dimethyl malonate, and those reported for the *p*-ABSA reagent in the literature, *e.g.* eq [2.9].⁵⁴

The diazo transfer reaction was a key step to build our desired dendrimer, so we did not want to give up easily. We next investigated diazo transfer reagents other than *p*-ABSA.

Our next attempt utilized *p*-toluenesulfonyl azide (TsN₃) as diazo transfer reagent. The preparation of tosyl azide is shown in eq [2.10]. Tosyl azide as a diazo transfer reagent is said to be the most efficient approach on laboratory scale despite its potential hazard (explosive decomposition of TsN₃ at temperatures above 120 °C), and purification problems to remove the *p*-tosylamide co-product.⁵⁵ Some serious accidents with tosyl azide have been reported.

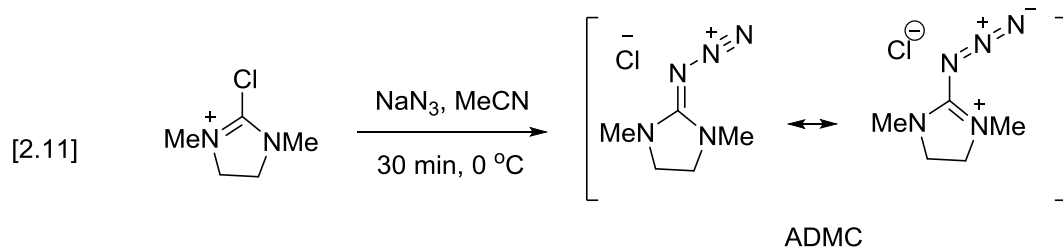


The diazo transfer reaction using tosyl azide and potassium carbonate also gave same results as obtained with *p*-ABSA under several sets of conditions: peaks at 4.73 ppm and 3.83 ppm in ¹H NMR (similar to Figure 2.11) and 169.1 ppm, 71.5 ppm and 53.6 ppm in ¹³C NMR (similar to

Figure 2.12). The same problems occurred, with workup giving an orange gummy compound and byproduct sulfonamide separation being very difficult compared to *p*-ABSA byproduct.

Recent literature of new diazo transfer reagents revealed 2-azido-1,3-dimethylimidazolium chloride (ADMC) as an effective diazo transfer reagent for activated methylene compounds.^{48b} This new reagent is not sulfonyl azide based, thus avoiding the purification problems associated with the formation of the corresponding sulfonamide byproduct. We decided to use ADMC as the diazo transfer reagent in our reaction. Caution must be taken; it is potentially explosive, although we never had any trouble with azidoimidazolium salt (ADMC). The synthesis of ADMC is depicted in eq [2.11]. The reagent must be prepared *in situ* immediately before use, because of its hygroscopic character.^{48e}

Because of the sensitivity of ADMC to moisture, Et₃N and 1,3-dicarbonyl compound in THF were added immediately to the ADMC salt. The byproduct guanidine derivative (see Scheme 2.3) was separated from diazo compound by washing the organic extracts with water.



With the ADMC reagent, after the completion of reaction and workup, we still obtained a gummy orange compound as seen in sulfonyl azides methods. Although washing with water was intended to remove the cyclic guanidine byproduct, a slight amount of this byproduct was observed in NMR spectra of the crude reaction mixture after washing with water. After purification we obtained two compounds; one resembled with Figures 2.11 and another one resembles fig 2.12. The other compound was new. Its ¹H NMR and ¹³C NMR spectra are shown in Figures 2.14 and 2.15.

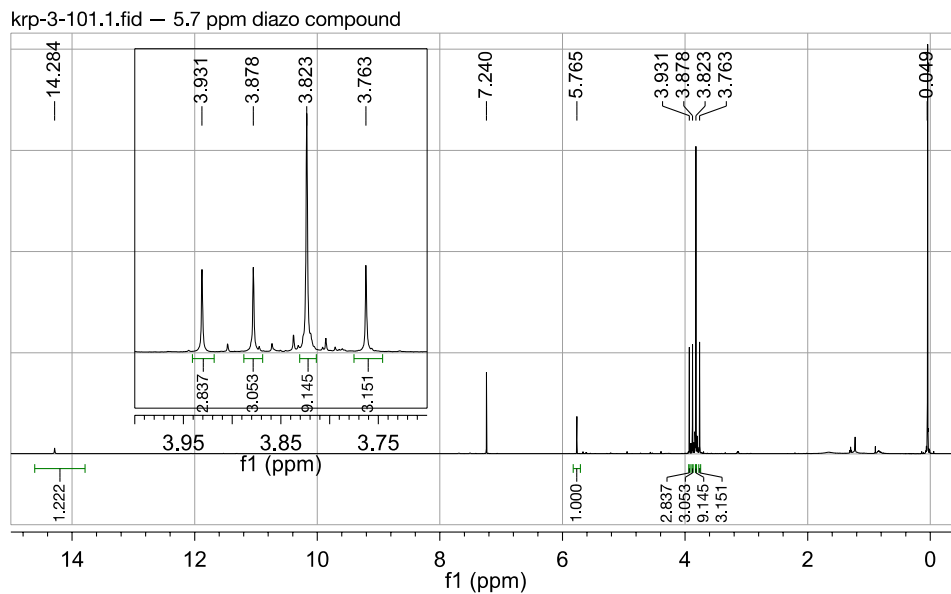


Figure 2.14. 600 MHz ^1H NMR spectrum (CDCl_3 solvent) of the product of treating **2.17** with Et_3N and TsN_3 ($\text{2.17}:\text{Et}_3\text{N}:\text{TsN}_3 = 1.0:2.0:1.0$) at rt for 16 h in acetonitrile.

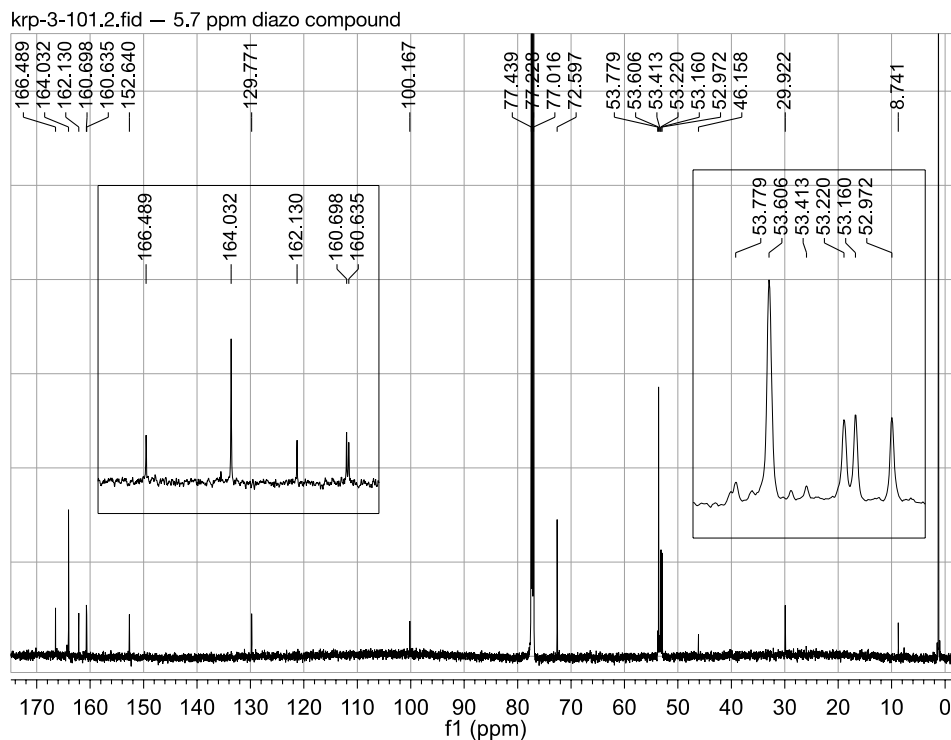


Figure 2.15. 150 MHz ^{13}C NMR spectrum (CDCl_3) of the compound used for Figure 2.14.

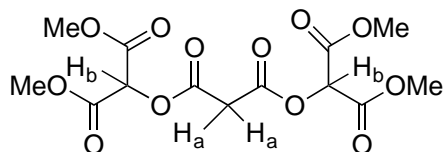
The signal at 5.77 ppm seemed more reasonable, as discussed previously, but protons of methyl ester region (3.5 – 4.0 ppm) appeared as four singlets, three small ones and one large one, mystifying us. It occurred to us that the spectrum might correspond to a mixture of two or more compounds. However, a variety of TLC eluent systems were tried and the compound always appeared as a single spot.

The ^{13}C NMR spectrum of this product is shown in Figure 2.15. A DEPT-135 spectrum (not shown) determined that the 72.6 ppm peak and all peaks in the 50 – 55 ppm region are CH or CH_3 carbon signals. It is likely that the 72.6 ppm peak is a CH carbon and the rest are CH_3 carbons. All peaks between 80 ppm and 170 ppm are quaternary.

A high resolution time-of-flight mass spectrum of the sample gave a peak consistent with the molecular formula of compound **2.18** (plus Na): calcd for $\text{C}_{13}\text{H}_{14}\text{N}_2\text{O}_{12}\text{Na}$, 413.0444; found 413.0436. However, ^1H NMR seems to correspond to 19 hydrogens: one at 5.8 ppm and 18 methyl hydrogens. This is difficult to accommodate with a molecular formula having 14 hydrogens.

We have been unable to crystallize this compound. The compound was also produced in the reaction of **2.17** with TsN_3 and Et_3N . The yield of this compound in either case was very small.

We decided to run a “blank” reaction with triethylamine as base and *without* diazo transfer reagent, to find how our molecule **2.17** reacts with base. Compound **2.17** has three acidic sites: an active methylene (H_a , see below) and two equivalent active methines (H_b).



2.17

2.2.6.2. Blank reactions of 2.17

We performed three experiments with Et₃N as base in the absence of diazo transfer reagent.

2.2.6.2 (1) *Serial addition of sub-stoichiometric amounts of base.* In an NMR tube, microliter amounts of Et₃N were added to **2.17** in CDCl₃, and NMR spectra were taken after each addition. Figure 2.16 shows ¹H NMR spectra after addition of 10 mol%, 15 mol%, and 20 mol% Et₃N.

In the 4.0 ppm – 5.5 ppm region, the peak at 5.5 (-CH(CO₂Me)₂) of **2.17**) decreases, and singlets at ~4.7 ppm and ~4.1 ppm grow in. The singlet at 4.85 ppm is due to **2.14**, and its intensity remains constant. In the 3.6 ppm – 3.9 ppm region, **2.14** (-CH(CO₂CH₃)₂) appears at 3.72 ppm. In the 15 mol% and 20 mol% spectra, two singlets at ~3.70 ppm and ~3.66 ppm grow in together relative to **2.14**. The group of new peaks produced by treatment with Et₃N consists of singlets at ~4.7 ppm, ~4.1 ppm, ~3.70 ppm, and ~3.66 ppm, with relative areas of 1:1:6:6.

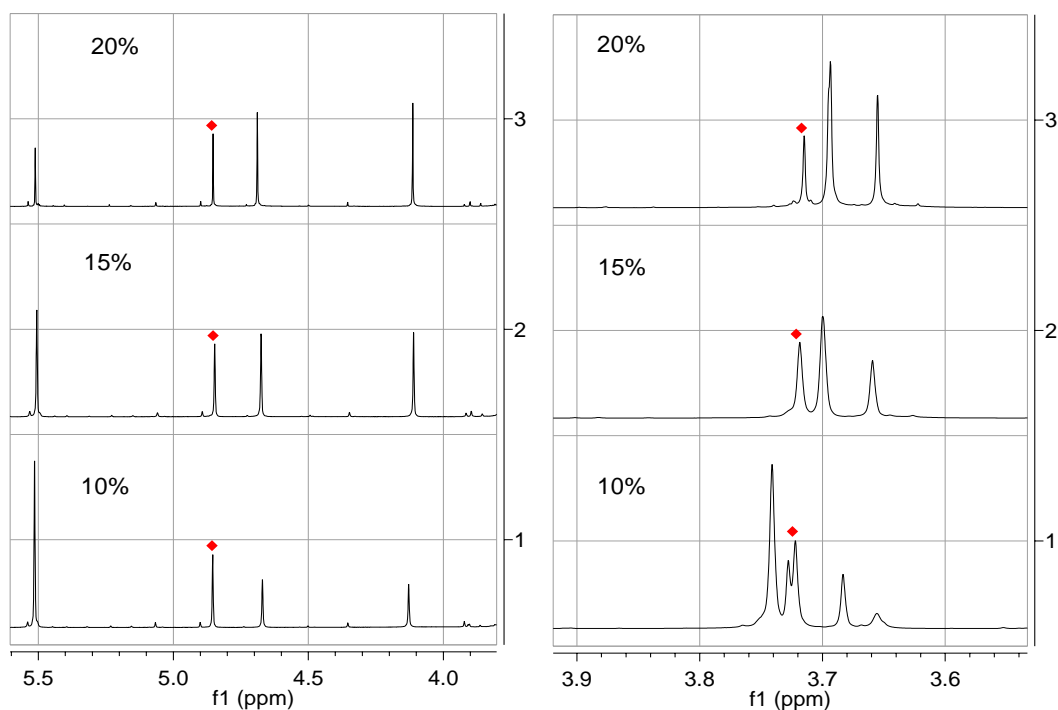
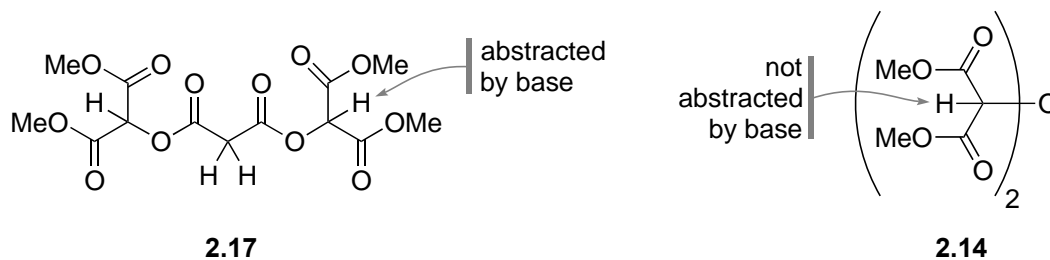


Figure 2.16. 400 MHz ¹H NMR spectra of **2.17** in the presence of 10 mol%, 15 mol%, 20 mol% Et₃N at rt. CDCl₃ solvent. Diamonds denote peaks from **2.14** impurity.

To help us put these results in context, we recorded dimethyl malonate NMR spectra (CDCl_3 solvent) before and after addition of 2 equiv of Et_3N . There was *no discernible change* observed in ^1H NMR and ^{13}C NMR, in contrast to the dramatic changes exhibited by compound **2.17**.

It is worth noting that the methine proton signal of **2.14** is apparently unaffected by base, and thus behaves like the CH_2 signal of dimethyl malonate. However, the methine proton of **2.17** (at 5.5 ppm), structurally similar to that of **2.14**, is clearly affected by base.



2.2.6.2. (2) *Time course study of blank reaction in CD_3CN solvent.* To compound **2.17**, 2 equiv Et_3N were added. NMR spectra were taken after 5 minutes, 2 h and 16 h at rt. See Figure 2.17.

From this time course experiment, we found that reaction is completed in 5 min or less. New peaks apparent at $t \sim 5$ minutes were ~ 7.2 ppm, ~ 4.7 ppm, ~ 4.0 ppm, ~ 3.72 ppm, and ~ 3.71 ppm. These correspond to the “increasing” peaks in the serial addition experiment. Chemical shifts differ because the time course experiment used CD_3CN as solvent, while the serial addition experiment used CDCl_3 . These peaks were joined over time by a few new peaks, some partially obscured and some clearly visible. A visible signal was the doublet at ~ 3.62 ppm, $J = 3.6$ Hz, also possibly two singlets.

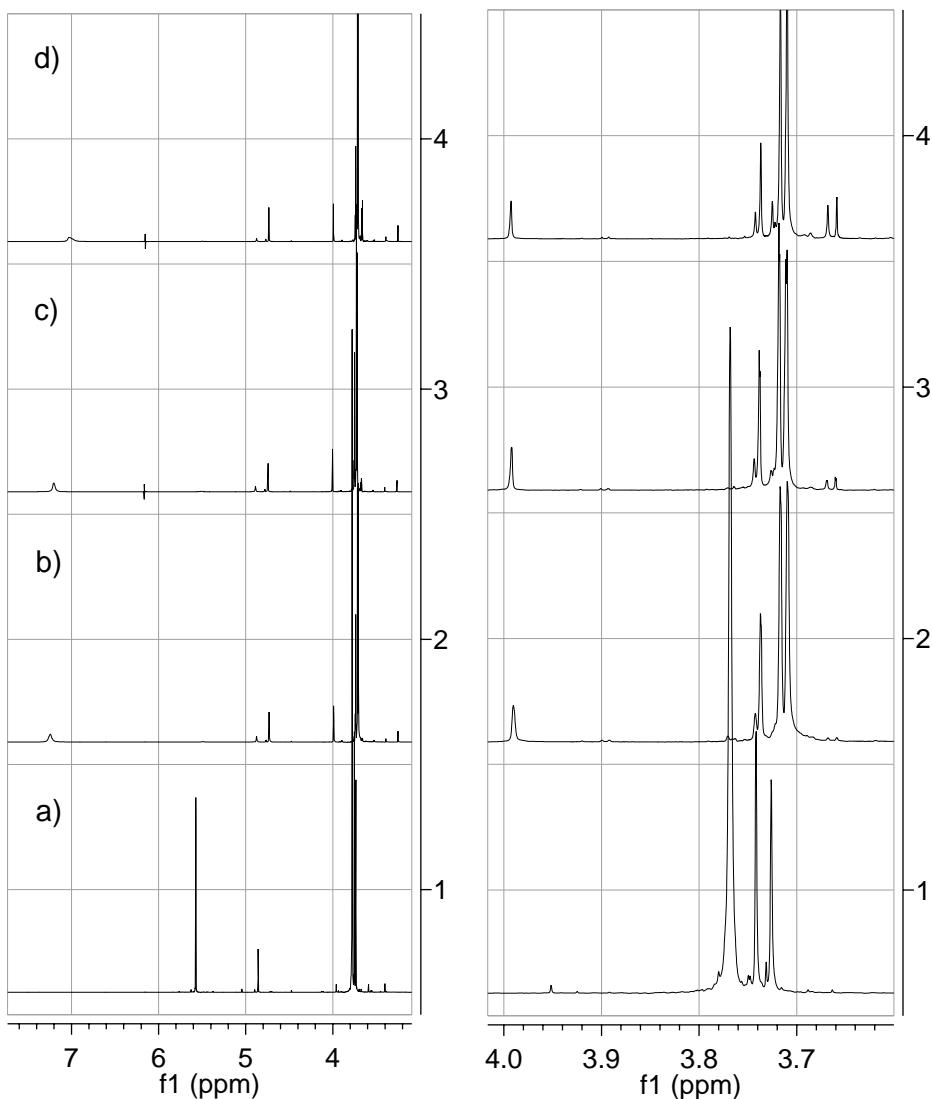


Figure 2.17. 400 MHz ^1H NMR spectra obtained by treatment of **2.17** with 2 eq Et_3N . a) **2.17** ($t = 0$) b) 5 min c) 2 h d) 16 h at rt. The lefthand column shows the complete spectrum and the righthand column shows the 3.6 ppm – 4.0 ppm region in detail. CD_3CN solvent.

2.2.6.2. (3) *Deprotonation-reprotonation test.* In this experiment, we first recorded **2.17** NMR spectra. Next, 2 equiv of Et_3N was added to **2.17** in the NMR tube and NMR spectra were recorded. Finally, 2 equiv CF_3COOH was added to see whether **2.17** could be regenerated by neutralizing the Et_3N . These results are presented in Figure 2.18.

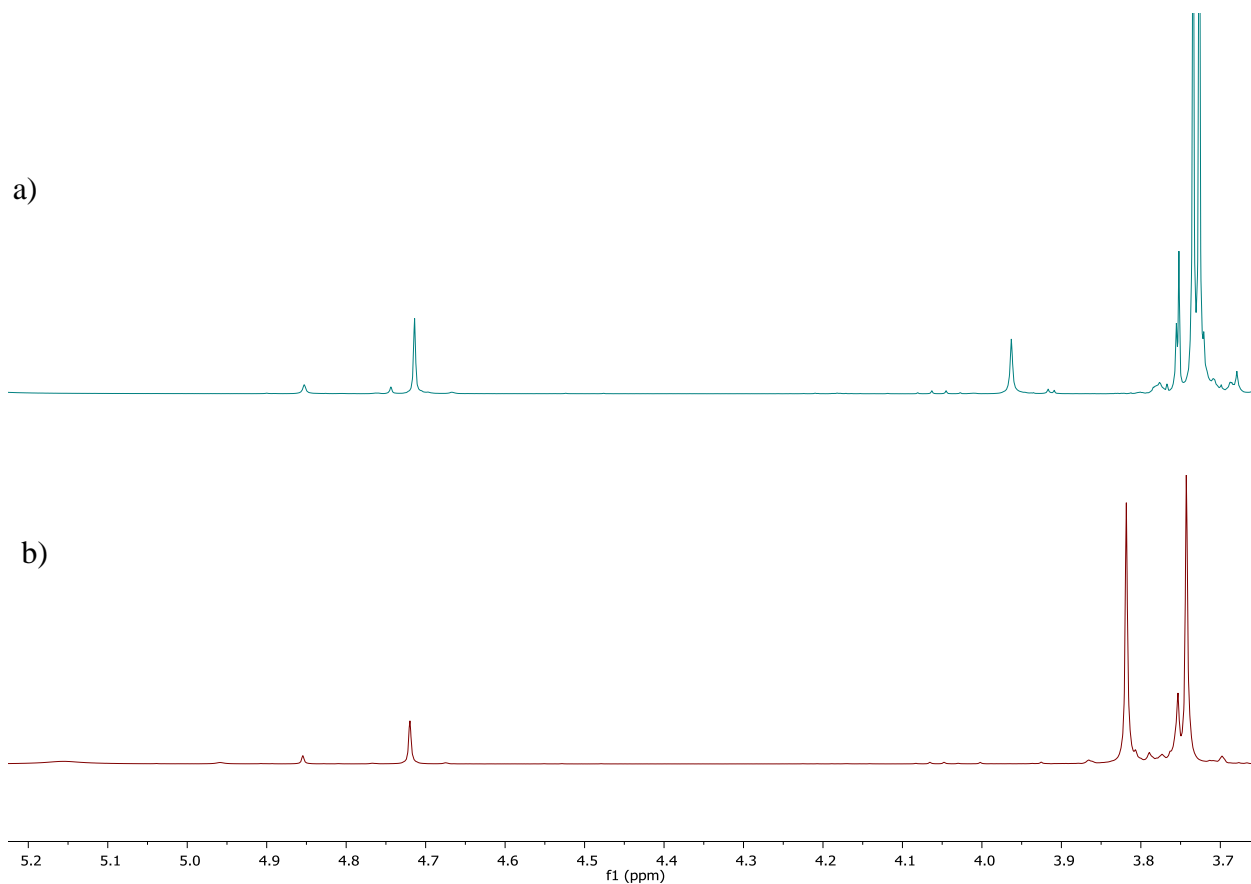


Figure 2.18. 400 MHz ^1H NMR of crude blank reaction (5.2- 3.6 ppm) obtained by a) treatment of **2.17 with Et_3N ($2.17:\text{Et}_3\text{N} = 1.0:2.0$) in CD_3CN . b) $2.17:\text{Et}_3\text{N}:\text{CF}_3\text{COOH} = 1.0:2.0:2.0$, CD_3CN solvent.**

From ^1H NMR experiment we observed that the 3.96 ppm signal in CD_3CN (4.16 ppm in CDCl_3) was shifted *upfield* by addition of acid to 3.75 ppm (generally **2.17** methylene CH_2 protons region) and 4.71 ppm signal didn't change. The 5.5 ppm peak of **2.17** was not regenerated.

In an effort to isolate the compound produced by base treatment of **2.17**, we scaled up the blank reaction, still using 2 equivalents of base. Figure 2.19 shows the ^1H -NMR spectrum

obtained by removing the reaction solvent acetonitrile under reduced pressure and redissolving an aliquot in CDCl_3 . Figure 2.20 shows the corresponding ^{13}C NMR spectrum.

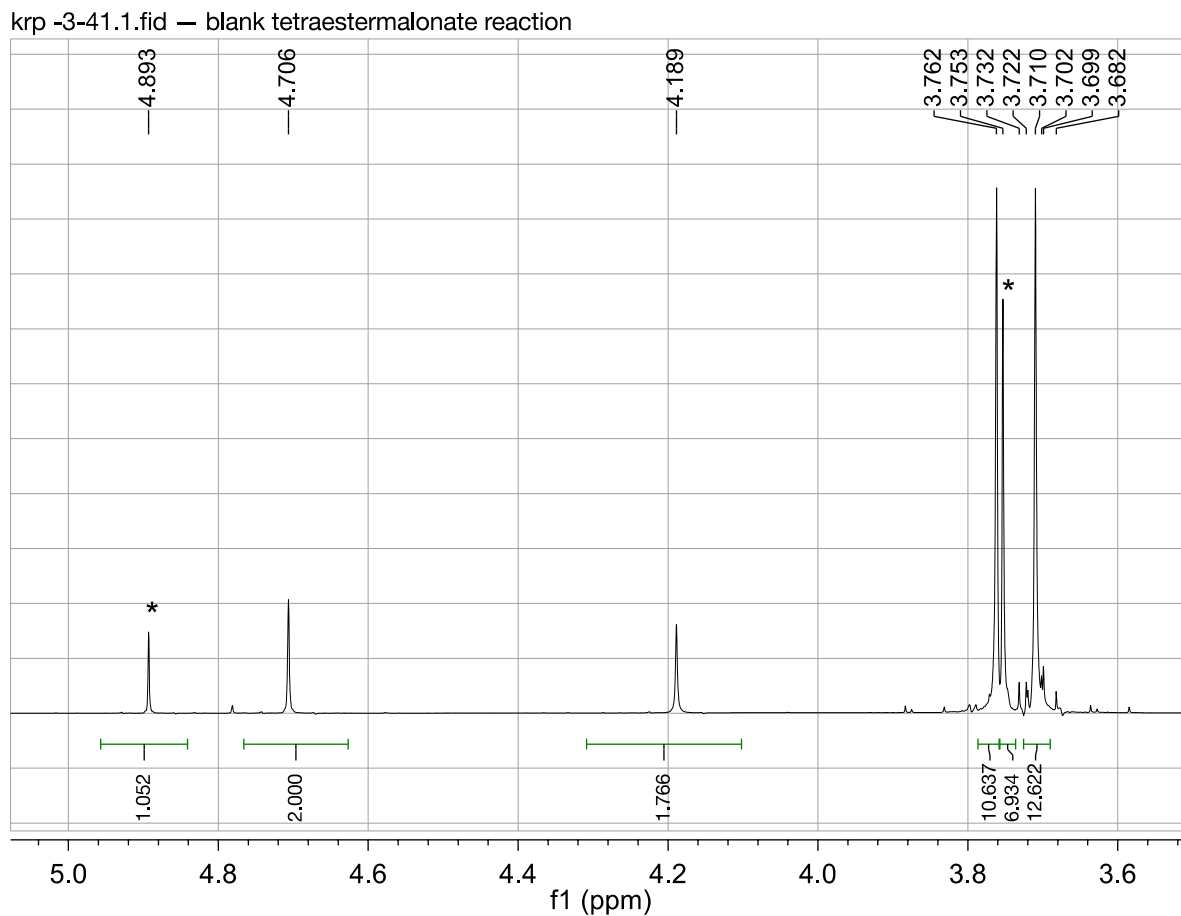


Figure 2.19. ^1H NMR spectrum of 2.17 after treatment with 2 equiv Et_3N (larger scale).

CDCl_3 solvent. The peaks at 4.89 ppm and 3.75 ppm are due to impurity 2.14.

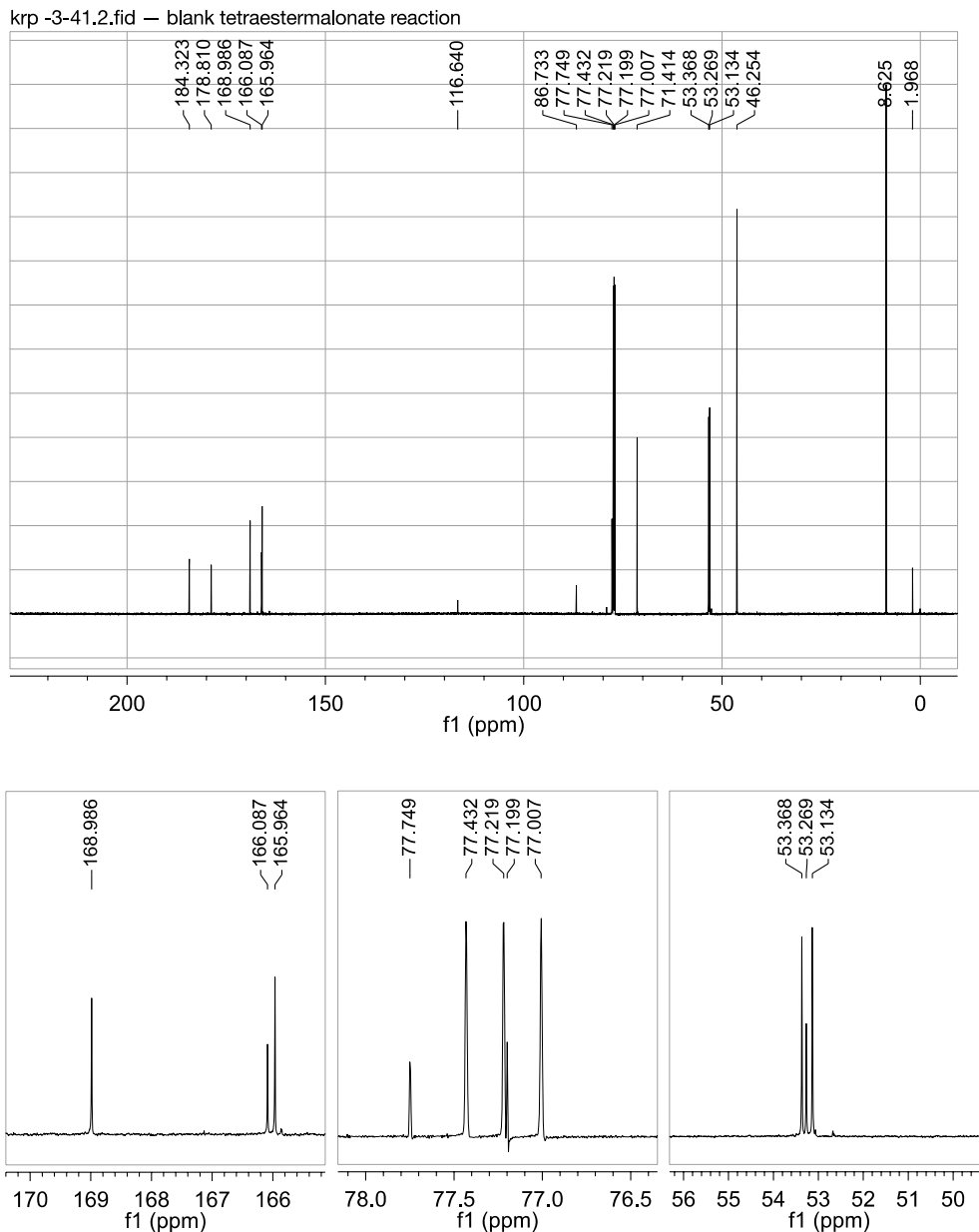


Figure 2.20. ^{13}C NMR spectrum of the sample used in Figure 2.19. CDCl_3 solvent.

Expanded regions are included beneath the main spectrum. The peaks at 169.0 ppm, 77.2 ppm, and 53.3 ppm are due to impurity **2.14**. The peaks at 46.3 ppm and 8.6 ppm are due to Et_3N .

After the addition of base to **2.17**, TLC showed only 2 spots (one spot at the origin and another spot at $R_f = 0.58$ (CH_2Cl_2 :acetonitrile 4:1(v/v))). (On another occasion, several mobile

phases were tried to attempt to move origin spot, but with no luck). Immediately after TLC analysis the reaction was stopped, the solvent was evaporated and silica gel column chromatography was done. The $R_f = 0.58$ peak was collected and NMR spectra were taken. The compound was identified as dimethyl 2-hydroxymalonate **2.13** (dimethyl tartronate). Also present was **2.14**, the impurity carried from starting material **2.17** (see Figures 2.21 and 2.22).

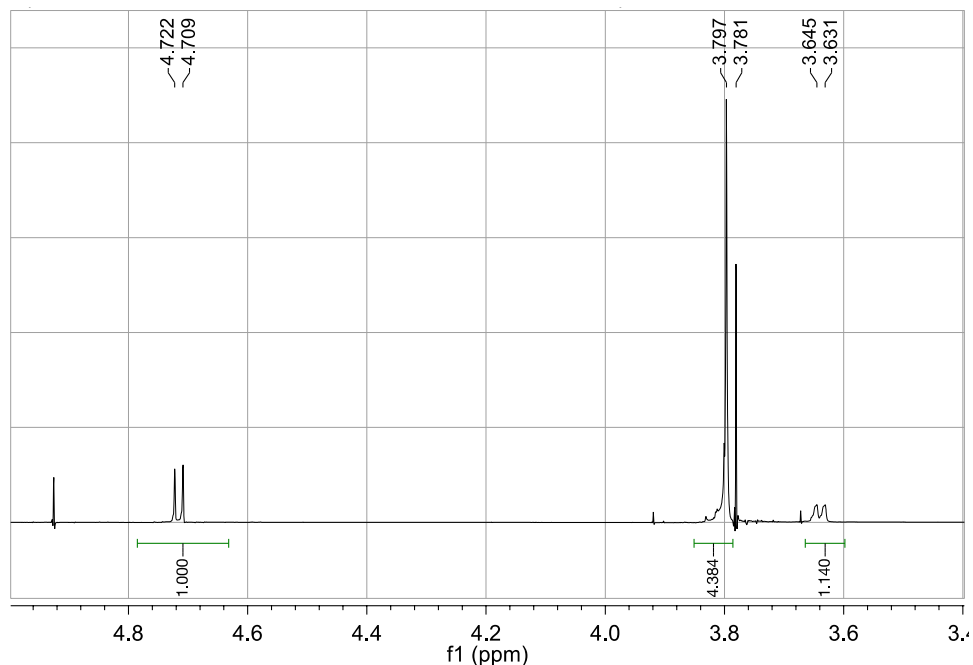


Figure 2.21. 600 MHz ^1H NMR spectrum of dimethyl 2-hydroxymalonate product after column chromatography. Signals at 4.93 ppm and 3.78 ppm correspond to **2.14**. (CDCl_3).

Nikolaev *et al.* reported Rh catalyzed reactions of diazocarbonyl compounds with dicarboximides and identified dimethyl-2-hydroxymalonate **2.13** as a byproduct.⁵⁶ The reported chemical shifts of **2.13** matched those of our product which we isolated after column. Also, the appearance of coupling between the OH proton and the adjacent methine proton is unusual, but characteristic of this particular compound.

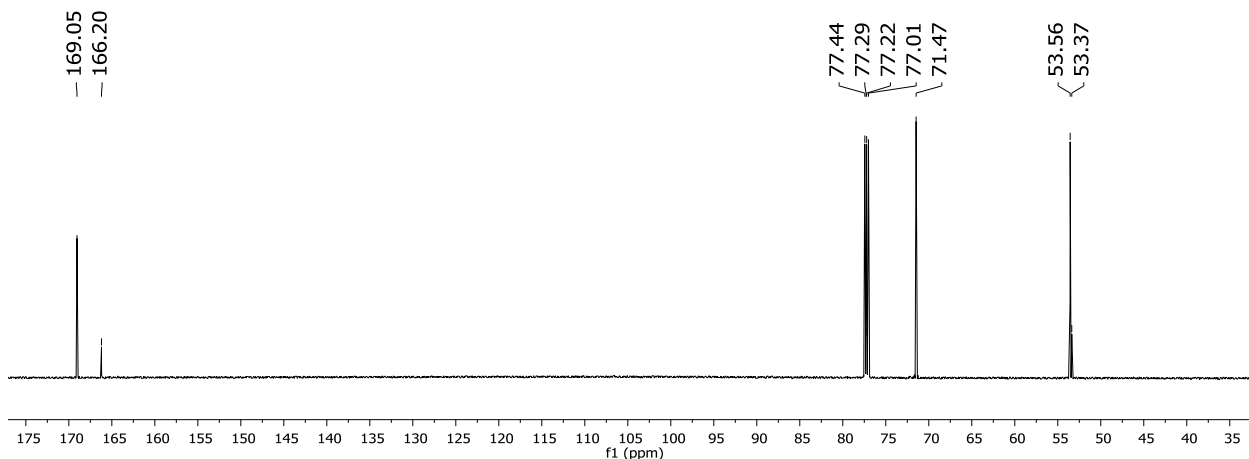
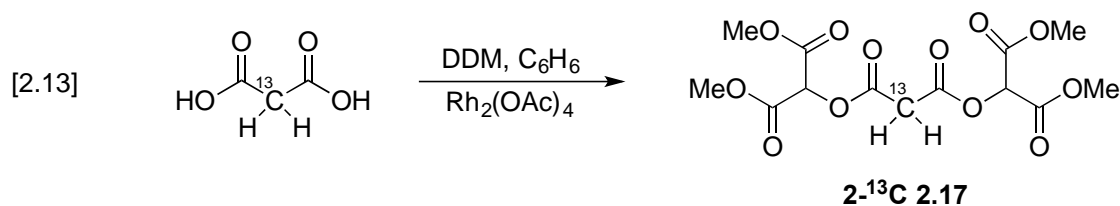


Figure 2.22. 150 MHz ^{13}C NMR spectrum of the compound used for Figure 2.21. CDCl_3 solvent.

Therefore, treatment of **2.17** with 2 equiv Et_3N generates a long lived compound or compounds having the spectra in Figures 2.19 and 2.20. But subsequent chromatography yields considerably different NMR spectra, corresponding to dimethyl 2-hydroxymalonate.

To study further, we decided to prepared **2.17** labeled at C2 with ^{13}C .

2.2.6.2. Blank reactions of ^{13}C labeled **2.17**



As shown in equation [2.13], we prepared ^{13}C labeled **2.17** ($2\text{-}^{13}\text{C}$ **2.17**) starting from $2\text{-}^{13}\text{C}$ malonic acid (isotopic enrichment 99%), using the same conditions developed for synthesis of unlabeled **2.17** (eq [2.6]). The ^1H NMR spectrum of $2\text{-}^{13}\text{C}$ **2.17** is shown in Figure 2.23. The CH_2 signal appears as a doublet $J^{\text{C-H}} = 133$ Hz, centered at 3.76 ppm. The ^{13}C NMR spectrum of $2\text{-}^{13}\text{C}$ **2.17** is shown in Figure 2.17. The gigantic peak at 40.1 ppm unmistakably corresponds to the ^{13}C labeled methylene carbon (C2). The neighboring carbonyl carbon signal appears as a doublet, $J^{\text{C-C}} = 60$ Hz.

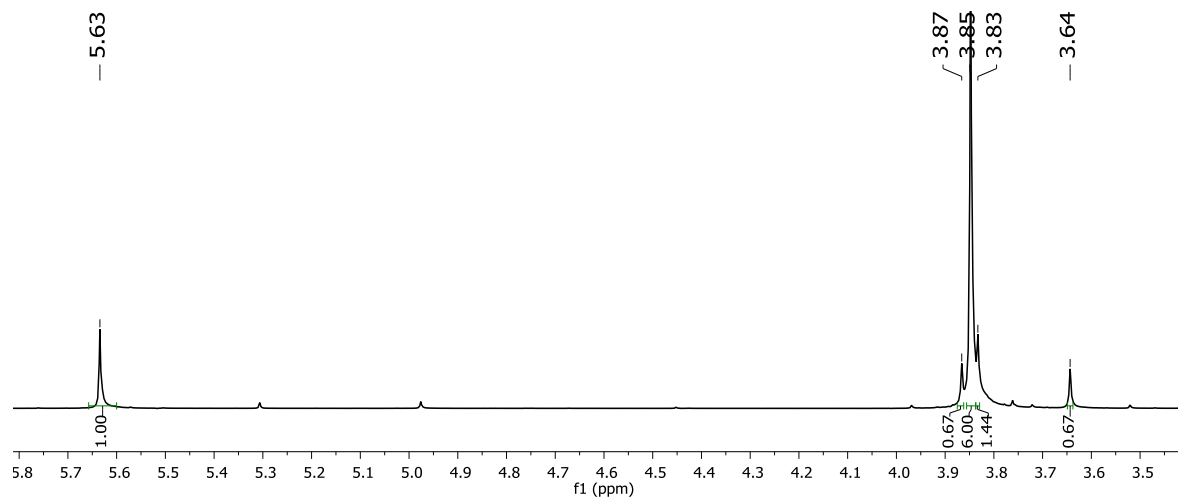


Figure 2.23. 600 MHz ^1H NMR of 2- ^{13}C 2.17. CDCl_3 solvent.

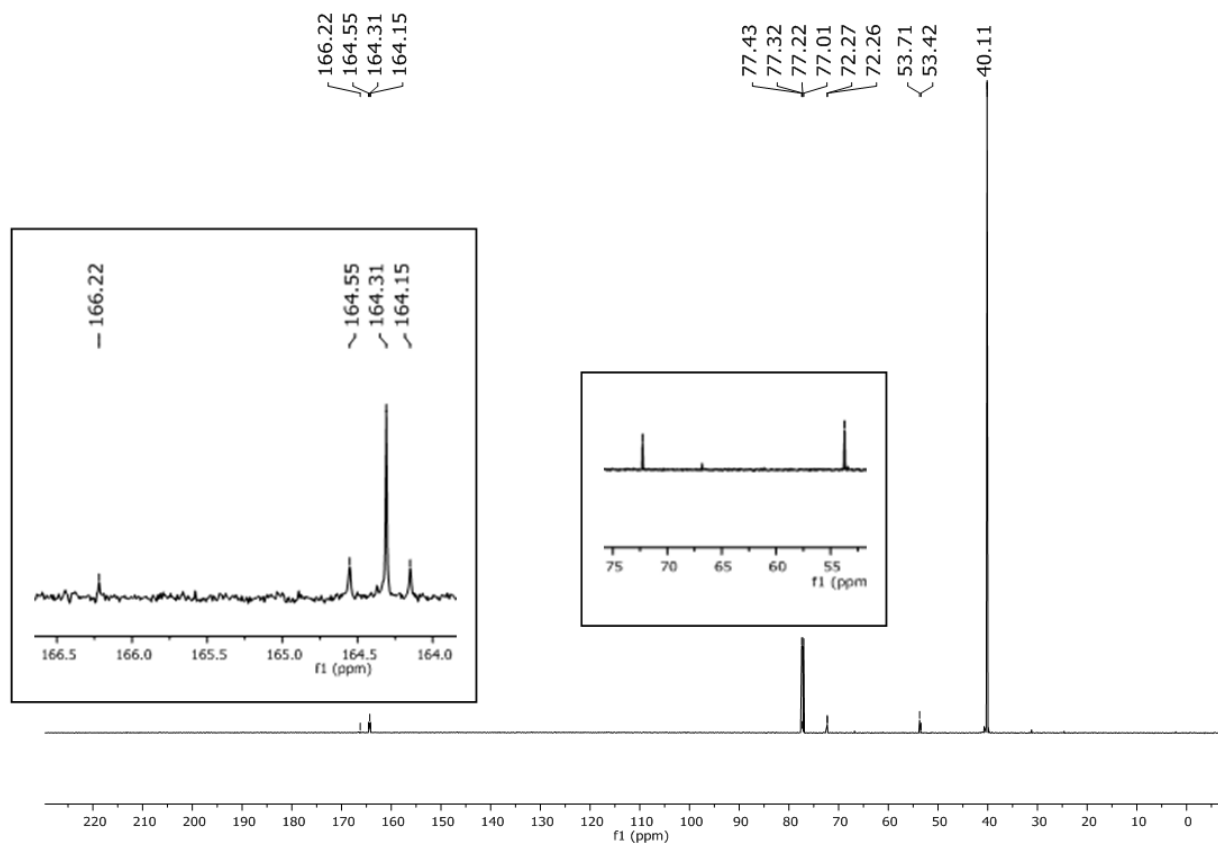


Figure 2.24. 150 MHz ^{13}C NMR of 2- ^{13}C 2.17. CDCl_3 solvent.

With 2- ^{13}C 2.17 in hand, we performed the blank reaction using 2 equivalents of Et_3N as base and reaction progress was monitored by NMR. Some observations were noted during NMR experiments.

With unlabeled **2.17**, the blank reaction produced ^1H NMR signals at δ 4.7, δ 4.2, δ 3.76, and δ 3.70 (*viz.* Figure 2.19). In the case of 2- ^{13}C **2.17**, Figure 2.25, all the signals are similar; the only difference is that the signal at 4.2 ppm was split into two *i.e.* δ 4.41 and δ 3.97 (average of both signals gives δ 4.19). The separation of the peaks in Hz is 176 Hz. To confirm that the splitting was due to the labeled carbon, a ^{13}C NMR spectrum was taken with no proton decoupling. The ^{13}C labeled carbon appeared as a doublet, $J = 176$ Hz, centered at 77.5 ppm.

^{13}C NMR of the blank reaction using 2- ^{13}C **2.17**, Figure 2.26, revealed signals at 184.5 ppm and 179.1 ppm. These were each a doublet with $J^{\text{C-C}} = 74$ Hz and 81 Hz. From this we can say the carbons giving rise to the 184.5 ppm and 179.1 ppm peaks must be attached to the ^{13}C labeled carbon. The ^{13}C labeled carbon has one H attached, evidenced by gigantic peak at δ 77.5 ppm. In order to attempt to isolate the compound giving rise to the spectra in Figure 2.25 and 2.26, we decided to scale up the reaction.

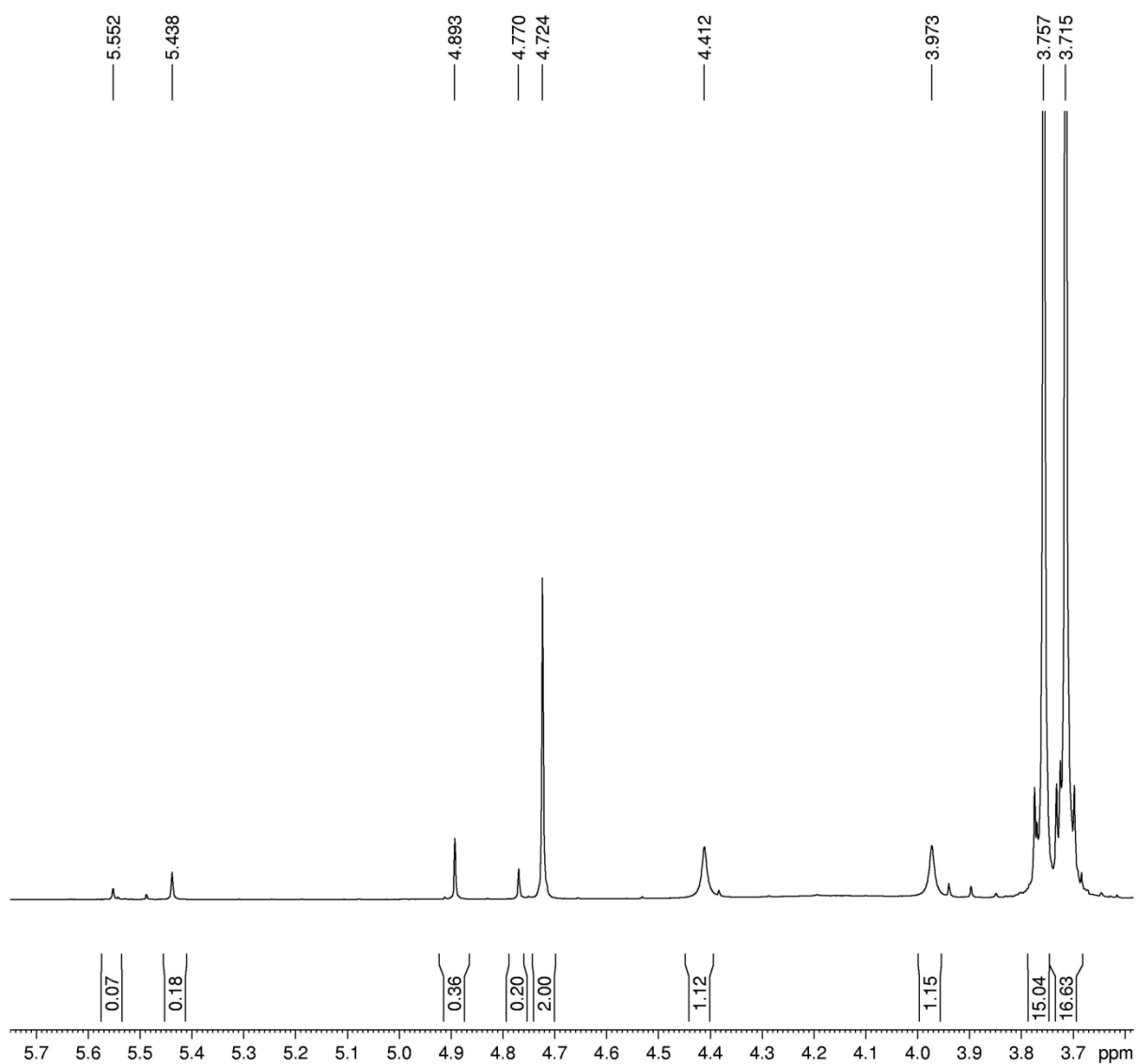


Figure 2.25. 400 MHz ^1H NMR of the product obtained by treatment of 2- ^{13}C 2.17 with Et_3N (2.17: Et_3N = 1.0:2.0) in CDCl_3 at rt for 5 minutes.

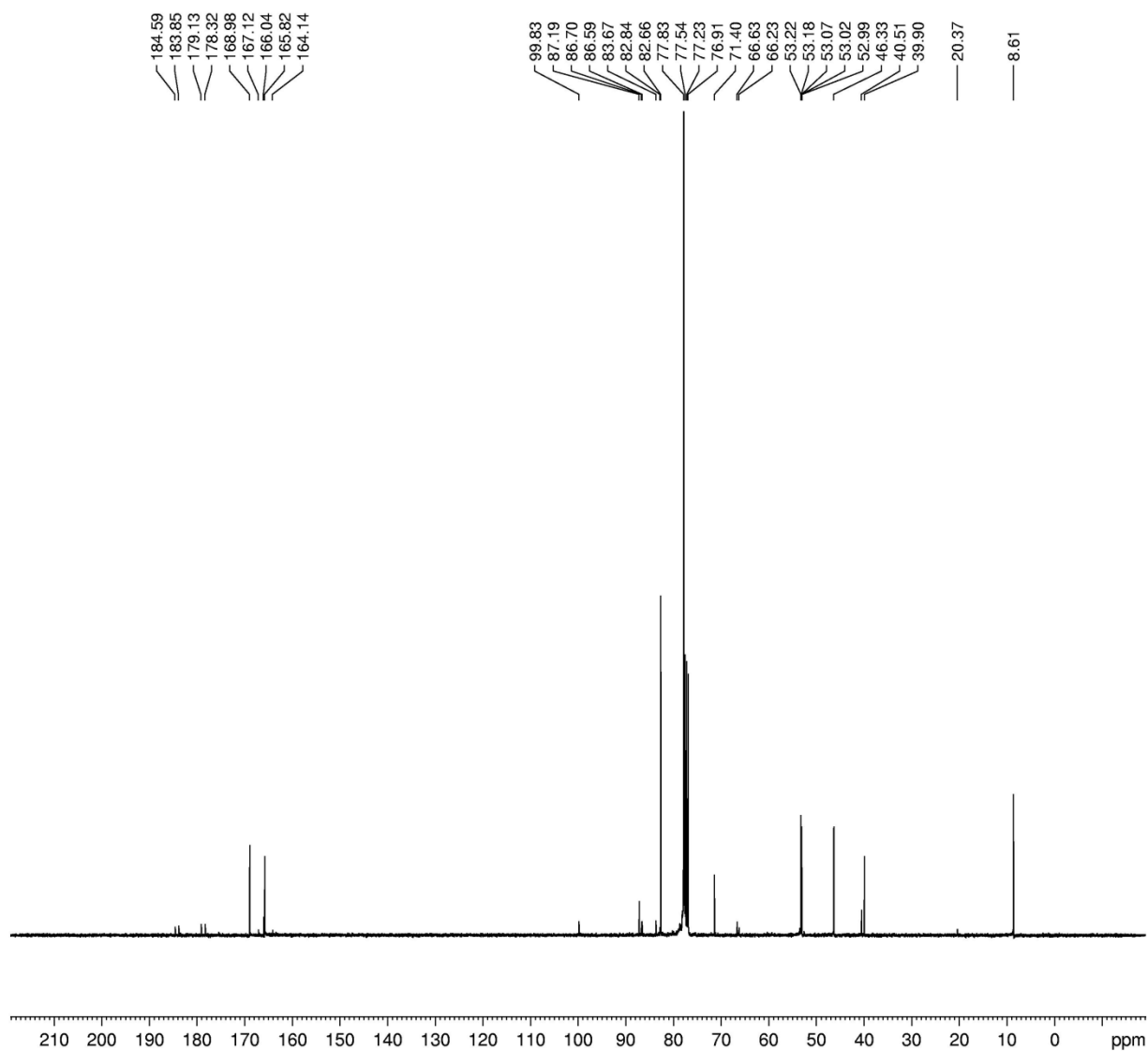


Figure 2.26. 100 MHz ^{13}C NMR of the product obtained by treatment of ^{13}C labeled **2.17 with Et_3N (**2.17**: Et_3N = 1:2.0) in CDCl_3 at rt for 5 minutes.**

The scaled up blank reaction with 2- ^{13}C **2.17** afforded 2 spots in TLC, similar to unlabeled **2.17**. After column chromatography we obtained dimethyl 2-hydroxymalonate **2.13**. The ^1H NMR spectrum perfectly matched **2.13** produced from unlabeled **2.17**. The ^{13}C NMR spectrum, Figure 2.27, was also essentially the same as unlabeled **2.13**: [chemical shift (ppm) in Figure 2.27 followed in parentheses by corresponding peak in ^{13}C NMR spectrum of **2.13** produced

from unlabeled **2.17**] 169.06 (169.05), 77.32 (77.29), 71.48 (71.47), 53.61 (53.56). However Figure 2.27 also exhibits a peak at 66.8 ppm and a large peak at 40.1 ppm. The latter corresponds to the methylene carbon of **2.17**, which in this case would be ^{13}C enriched. It is therefore probably due to a very small amount of unreacted 2- ^{13}C **2.17** that contaminated the chromatographic fraction. The 66.8 ppm peak is a mystery.

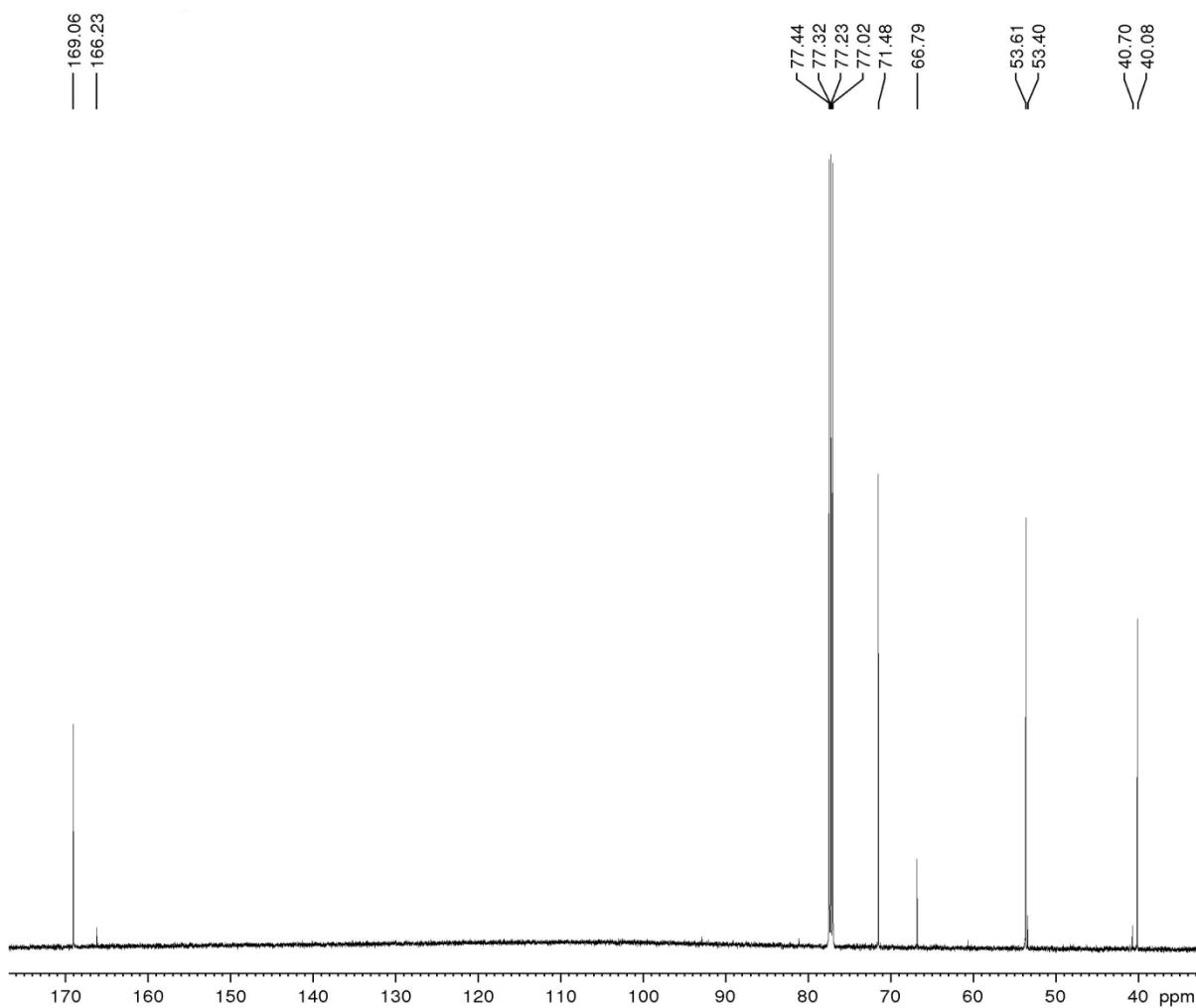


Figure 2.27 MHz ^{13}C NMR of the ^{13}C labeled blank reaction of **2.17** by treatment Et_3N (**2.18**: Et_3N = 1:2.0) in acetonitrile at rt for 5 minutes The product was obtained after column chromatography.

2.27. Conclusions

What explanation or explanations can be offered for these experimental results? The success of the diazo transfer reaction (Et_3N , *p*-ABSA, CH_3CN solvent) when applied to dimethyl malonate, and its utter failure when identically applied to **2.17** suggests that some aspect or behavior of **2.17** prevents successful diazo transfer in this case.

Treating **2.17** with 2 equiv of Et_3N produces a new species, which we will refer to as species **Z**. In the ^1H NMR (CD_3CN solvent), the three singlets of **2.17** at 5.57 ppm ($-\text{CH}(\text{CO}_2\text{Me})_2$), 3.78 ppm ($-\text{CH}(\text{CO}_2\text{Me})_2$), and 3.72 ppm ($\text{O}_2\text{CCH}_2\text{CO}_2$) are replaced by four singlets at 4.71 ppm, 3.96 ppm, 3.734 ppm and 3.726 ppm, with relative areas of approximately 1:1:6:6. In the ^{13}C NMR, the two carbonyl signals of **2.17** at 165.9 ppm ($\text{C}=\text{O}$'s attached to central CH_2) and 165.6 ppm (the methyl ester carbonyls at the periphery; the 165.6 ppm signal roughly twice as tall as the 165.9 ppm signal) become four carbonyl signals at 185.8 ppm, 178.8 ppm, 170.4 ppm, and 167.6 ppm, with the first two much smaller than the latter two. In **2.17**, all CH_3 carbons appear as one signal at 54.4 ppm. After addition of 2 equiv Et_3N , there are two CH_3 signals at 53.9 ppm and 53.8 ppm. The CH_2 and CH carbon signals of **2.17** appear at 41.1 ppm and 73.7 ppm. After base addition, there is a methine (CH) carbon at 77.3 ppm, a methine carbon at 72.9 ppm, and a quaternary carbon signal at 87.9 ppm. These data are summarized in Table 2.2.

Table 2.2. ^{13}C NMR of **Z**, formed by treatment of **2.17** with Et_3N

Peak	Chemical shift (ppm) CD_3CN solvent	Chemical shift (ppm) CDCl_3 solvent	type
1	185.8	184.4	quaternary
2	178.9	178.8	quaternary
3	170.6	166.1	quaternary
4	167.6	166.0	quaternary
5	87.9	86.7	quaternary
6	77.5	77.6	CH
7	72.9	71.6	CH
8	53.9	53.09	CH_3
9	53.7	53.07	CH_3

The use of **2.17** ^{13}C labeled at the central CH_2 position helps to clarify the ^{13}C spectrum. In ^{13}C labeled **Z**, the labeled carbon appears at 77.5 ppm ($J^{\text{C-H}} = 176$ Hz). The splitting is visible in the ^1H NMR spectrum of **Z**, where the signal at ~ 4.2 ppm appears as a doublet with $J = 176$ Hz. It is well known that C–H coupling constants are strongly influenced by the s -character of carbon (125 Hz for sp^3 , 160 Hz for sp^2 , 250 Hz for sp).⁵⁷ Therefore, one may speculate that the labeled carbon is sp^2 -like. Further, peaks at 185 ppm and 179 ppm in unlabeled **Z** appear in labeled **Z** as doublets due to coupling to the enriched ^{13}C . The coupling constants are $J^{\text{C-C}} = 74$ Hz, and $J^{\text{C-C}} = 81$ Hz respectively, which are consistent with one-bond sp^2 - sp^2 carbon-carbon couplings.

The other carbonyl carbon signals (171 ppm and 168 ppm) have not shifted much from the corresponding peak in **2.17** (166 ppm). However, there are *two* of these signals in **Z** instead of one in **2.17**. This indicates that the “left half” of **Z** has become different than the “right half.” Indeed each C=O signal of **2.17** appears as *two* signals in **Z**, and the one methyl carbon signal of **2.17** becomes two signals in **Z**.

This is summarized graphically in Figure 2.28. At this point we do not know whether the chemical shifts are correctly assigned – for example the 171 ppm peak might or might not originate from the same “side” of the structure as the 53.9 peak – but the Figure is meant to convey a preliminary concept of **Z**.

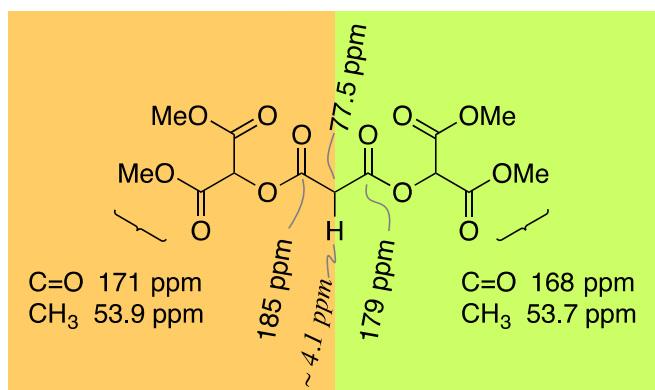


Figure 2.28. An inexact proposal for the structure of **Z.**

The Figure does not address the remaining ¹³C signals: peaks 5 and 7 in Table 2.2, at ~88 ppm (quaternary) and ~73 ppm (methine). If we specify one hydrogen as shown in Figure 2.29, we obtain a dianion structure that is consistent with the spectroscopic data for **Z**.

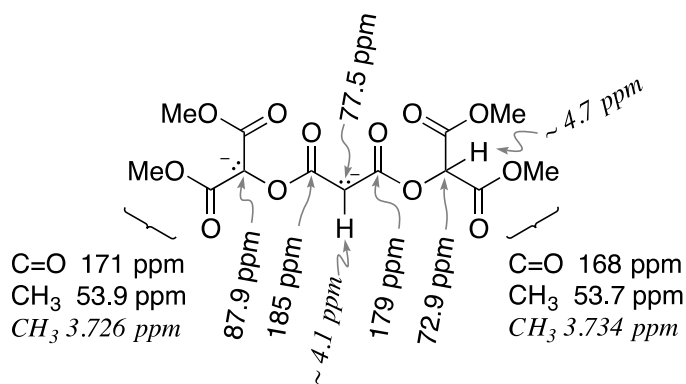
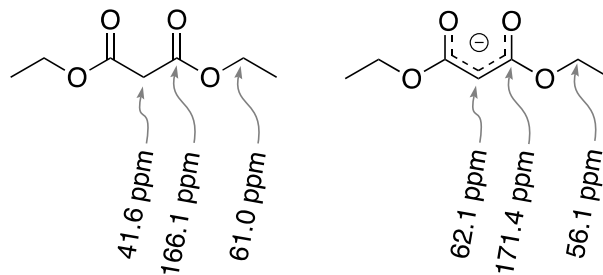


Figure 2.29. Dianion proposal for the structure of **Z. Proton assignments are in italics.**

House, *et al.* reported ¹³C NMR spectra of various enolate anions.⁵⁸ Their data for diethyl malonate is shown below. Deprotonation causes the active methylene carbon signal and the carbonyl signal to move downfield.



Although our proposal is reasonable on spectroscopic grounds, other objections may be raised. When substoichiometric amounts of Et_3N (*i.e.* 10 mol%, 20 mol% *etc.*) are added to **2.17**, **Z** appears to be the only species formed. If **Z** is a dianion, as proposed, why is there no spectroscopic evidence for a monoanion? Also, equilibration between **2.17** and **Z** appears to be absent on the NMR timescale, judging from the sharpness of proton signals and the constancy of their chemical shifts during this NMR titration.

If **Z** is a conjugate base of **2.17** as proposed, it should be possible to acidify **Z** and regenerate **2.17**. We found we could not do this. Once **2.17** is treated with Et_3N , its ^1H NMR signal at 5.6 ppm ($-\text{O}-\underline{\text{C}}\text{H}(\text{CO}_2\text{Me})_2$) disappears, and treatment with CF_3COOH never causes it to reappear. Likewise, the **2.17** ^{13}C NMR signal at 40.1 ppm ($-\underline{\text{C}}\text{H}_2-$) is removed by treatment with Et_3N and never returns when CF_3COOH is added. In fact, the behavior of the system suggests that abstraction of a proton (or protons) from **2.17** enables a rapid irreversible rearrangement or chemical change of some sort.

When isolation of **Z** is attempted by column chromatography, the only compound isolated is dimethyl 2-hydroxymalonate, **2.13**. Therefore **Z** must be capable of generating **2.13**. With this in mind, we speculated that deprotonation of **2.17** might lead to a ketene, as shown in Figure 2.30.

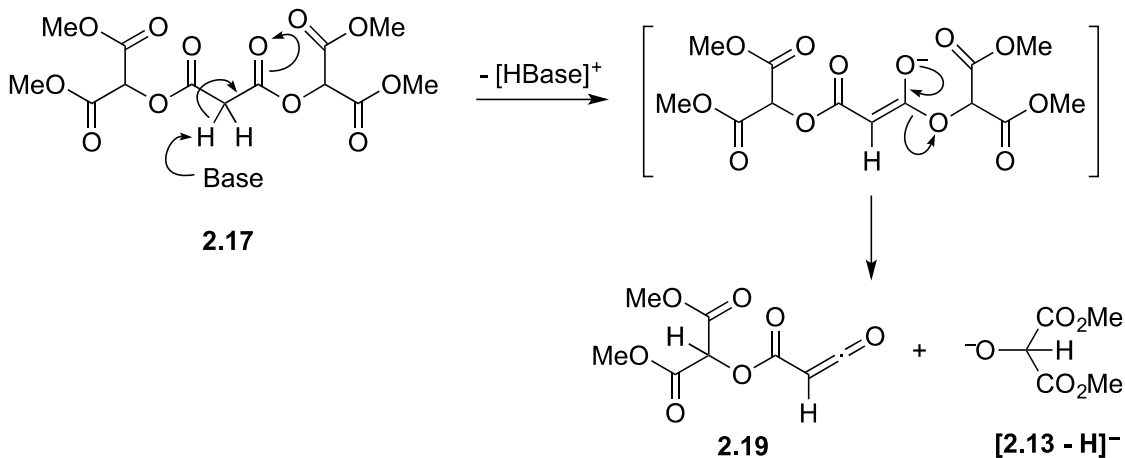


Figure 2.30. Ketene formation; another proposal.

NMR peak assignments are shown in Figure 2.31. Again, peaks 5 and 7 present a problem.

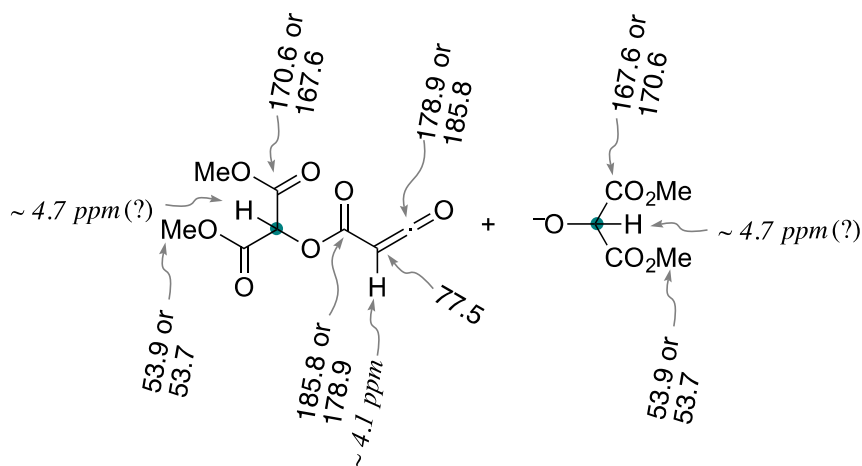


Figure 2.31. Tentative peak assignments for ketene + dimethyl tartronate. All chemical shifts are given in ppm.

Peaks 5 and 7 are a quaternary carbon at 87.9 ppm and a methine carbon at 72.9 ppm.

However the two unassigned carbons in Figure 2.31, highlighted with a green dot, are both methine. A way to “fix” this shown in Figure 2.32, where dimethyl tartronate has been reworked.

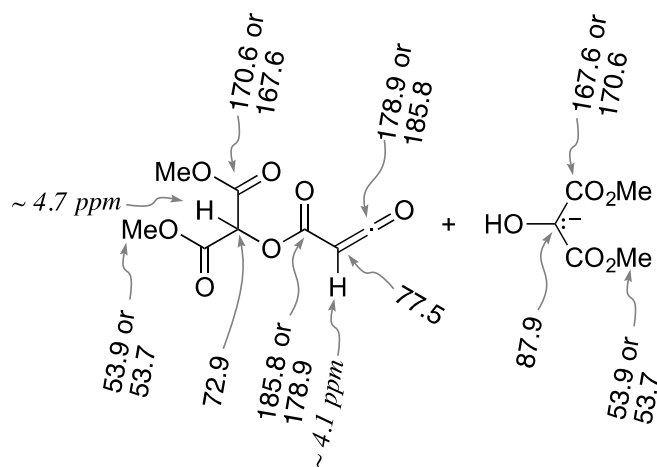


Figure 2.32. Ketene proposal. All chemical shifts are in units of ppm.

Here again, the number and types of carbon atoms match the experimental spectra. The chemical shifts are worrisome. Table 2.3 summarizes the literature on ^{13}C NMR spectroscopy of ketenes. The Table's " C_a " would refer to our 77.5 ppm peak. However, the majority of C_a entries are below 50 ppm. Also, while our C_b appears at 178.9 ppm or 185.8 ppm, most C_b entries are over 200 ppm.

We know that **Z** lasts 16 h at rt with a small amount of decomposition. Ketenes however are known to dimerize, *e.g.* eq [2.12] reports a dimerization of an acylketene, the type of ketene we are proposing.⁵⁹ They also react with alcohols,⁶⁰ and tertiary amines,⁶¹ and may undergo 2+2 or 4+2 cycloadditions.⁶² One wonders, then, whether the proposed acylketene would survive for 16 h.

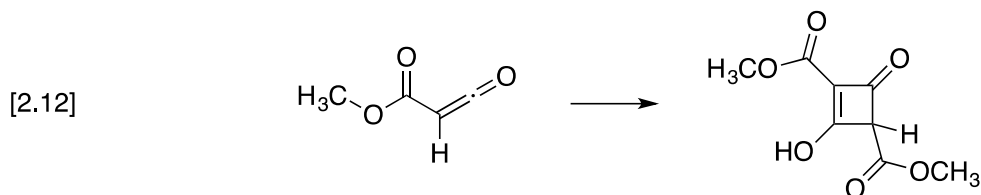
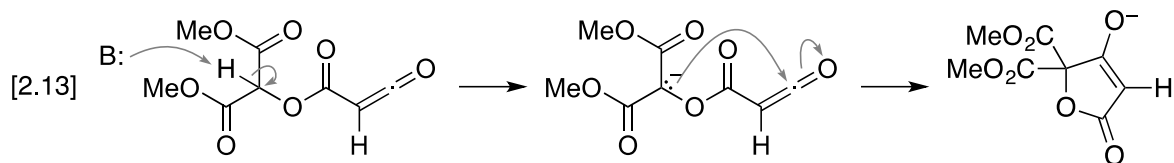


Table 2.3. ^{13}C NMR parameters for ketenes $\text{R}_1\text{R}_2\text{C}_a=\text{C}_b=\text{O}$

R_1	R_2	δC_a (ppm)	δC_b (ppm)	$J^{\text{C-H}}$ (Hz)	ref.
H	H	2.5	194.0	171.5	<i>a</i>
Me	H	10.9	200.0	–	<i>b</i>
Et	H	18.6	200.0	–	<i>b</i>
Et	Me	26.9	206.1	–	<i>b</i>
Ph	Me	33.8	205.6	–	<i>b</i>
Ph	Et	42.1	205.6	–	<i>b</i>
Ph	Ph	47.0	201.3	–	<i>b</i>
CF_3S	CF_3S	18.9	171.8	–	<i>c</i>
PhS	PhS	13.6	172.6	–	<i>c</i>
CF_3SO_2	CF_3SO_2	13.5	181.0	–	<i>c</i>
CF_3Se	CF_3Se	124.9	169.3	–	<i>c</i>
Br	Br	98.5	178.6	–	<i>c</i>
Me	Me	24.2	204.9	–	<i>c</i>
Ph	Ph	46.9	201.1	–	<i>c</i>

^a ref 63 ^b ref 64 ^c ref 65

A plausible reaction of our hypothetical ketene is an internal nucleophilic attack, as shown in eq [2.13].



The resulting cyclic β -keto ester enolate could fit the experimental spectra, Figure 2.33.

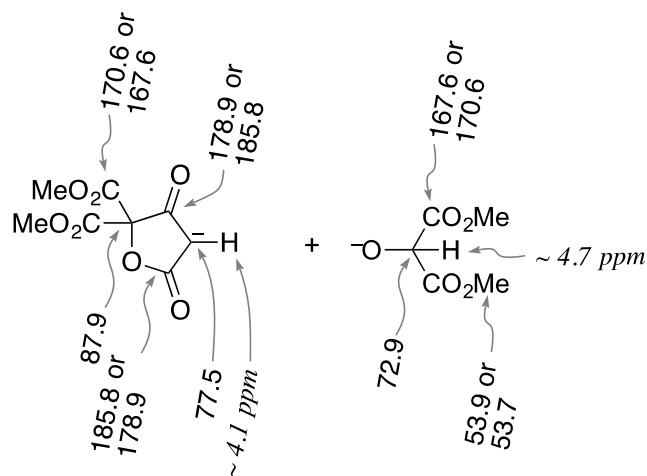
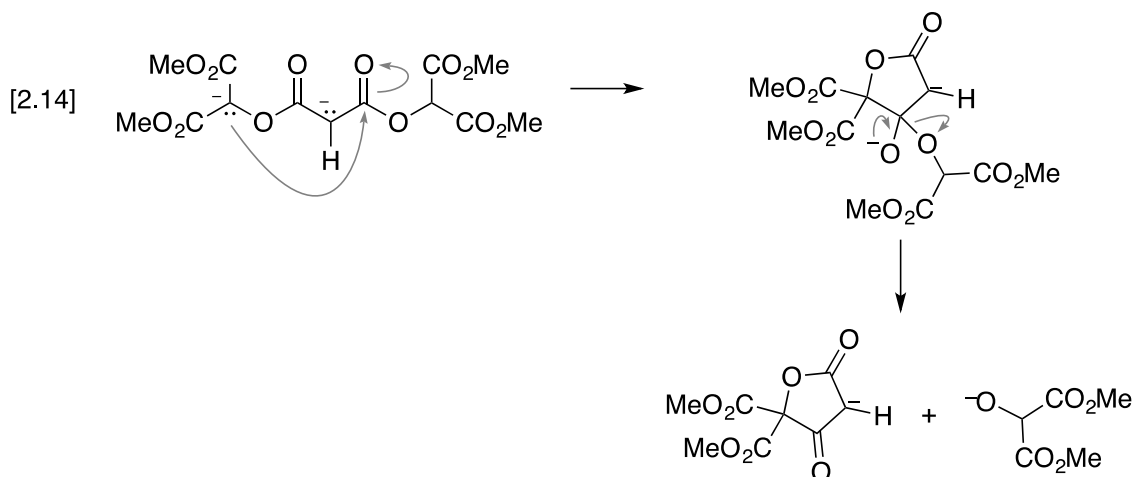


Figure 2.33. Cyclic β -keto ester proposal.

The same two products may be produced from the dianion without the intermediacy of a ketene, eq [2.14].



Aside from chemical shift questions, a problem with this proposal and the dianion proposal is that either the dianion or the cyclic β -keto ester enolate should be able to participate successfully in the diazo transfer reaction. So while those proposals may account for the spectroscopic evidence (with varying degrees of success), neither would unequivocally explain why the diazo transfer reactions failed.

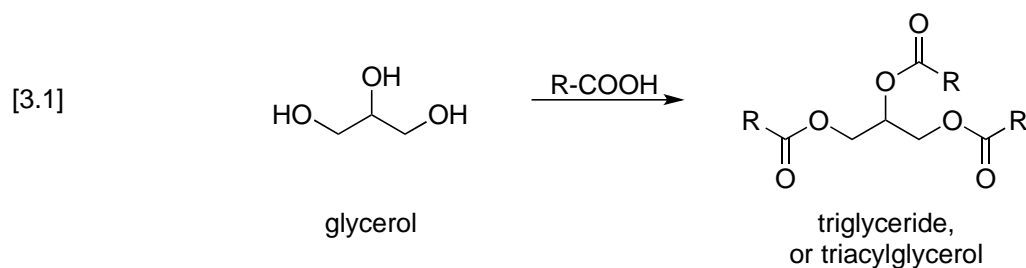
CHAPTER 3
STUDIES ON THE SYNTHESIS OF BI(TRIGLYCERIDE)S FROM
2,2'-BI(GLYCEROL)

3.1. Introduction

Lipids are an unusual category of organic molecules because they are not defined by functional group. Instead, they may be defined as compounds isolated from a natural source, having easy solubility in non-polar solvents.^{66,67} Lipids are classified into two major groups. *Complex lipids* are lipids that readily undergo hydrolysis in basic or acidic conditions. Waxes, triglycerides, and phospholipids are examples of this category. *Simple lipids* are not hydrolyzable. Steroids, prostaglandins and terpenes are called simple lipids.

3.1.1. Triglycerides (TG)

Triglycerides are triesters formed from glycerol and three long chain carboxylic acids, or so-called fatty acids, as shown in eq [3.1]. The three fatty acids need not be identical. Triglycerides play a role in adverse health conditions such as heart disease, peripheral vascular disease, stroke, diabetes mellitus, metabolic syndrome, and cancer, which are common causes of death.⁶⁸



Examples of fatty acids are shown in Figure 3.1.

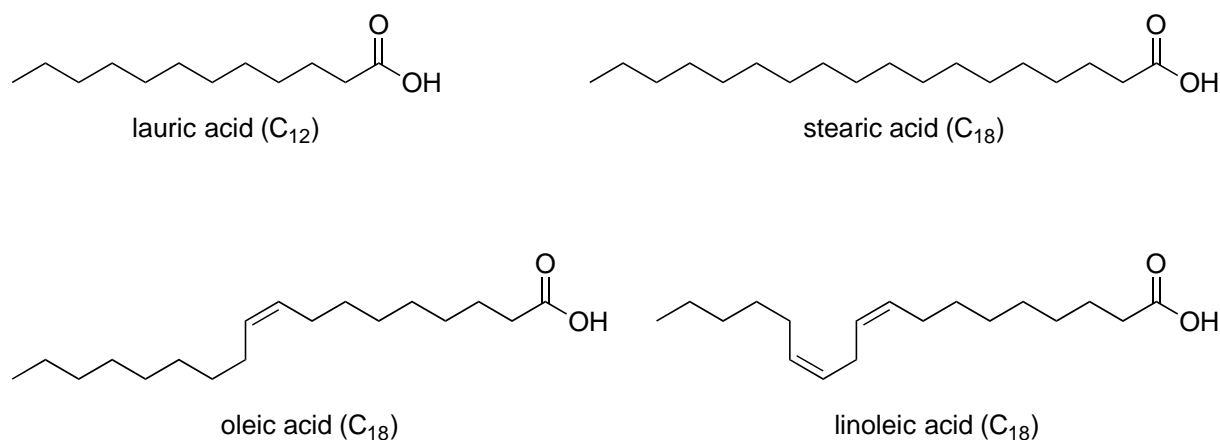
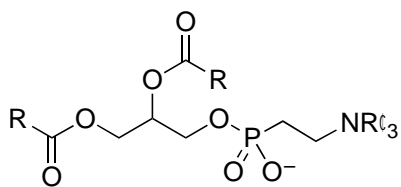


Figure 3.1. Some fatty acids.

3.1.2. Phospholipids

Phospholipids, or more correctly, glycerophospholipids, are molecules in which one hydrophilic head group and two hydrophobic acyl chains are linked to glycerol, as shown below. The variations in head groups, aliphatic chains and alcohols lead to wide variety of phospholipids.⁶⁹



R = long chain fatty acid
R' = Me, H

A typical phospholipid

Phospholipids have excellent biocompatibility because of their amphiphilic structures. For example, phospholipids have a propensity to form liposomes (see Figure 3.2), which can be employed as the drug carriers.⁷⁰ These lipids have good emulsifying properties which can stabilize emulsions.⁷¹ In addition to this property, phospholipids can be used as surface-active wetting agents which can coat the surface of crystals to enhance the hydrophilicity of hydrophobic drugs.⁷²

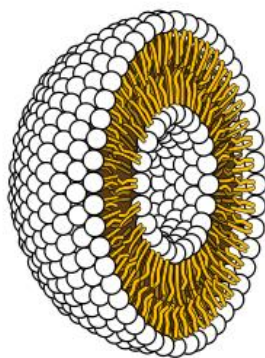
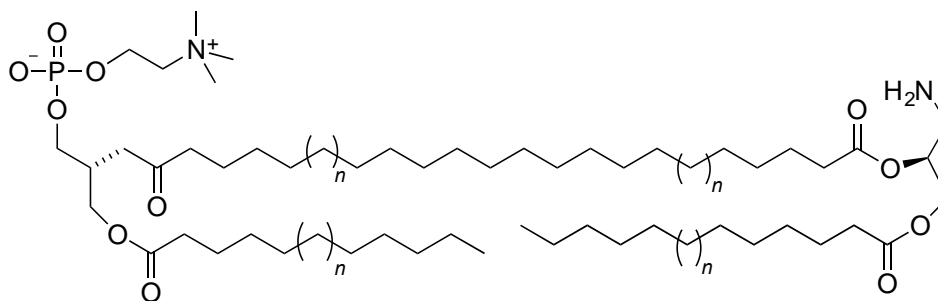


Figure 3.2. Cross-section of a liposome.⁷³ White spheres represent polar groups. Yellow lines represent fatty acid chains. A liposome is a spherical structure.

3.1.3. Man-made lipids; deviations from traditional structure

Kai *et al.* reported the design and synthesis of asymmetric acyclic phospholipid bolaamphiphiles **3.1**.⁷⁴ The authors anticipated that asymmetric lipid bolaamphiphiles would provide facile building blocks for engineering a variety of unique membrane-mimetic structures.

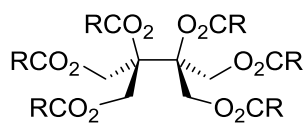


3.1 a: $n = 6$
b: $n = 1$

Constantinou-Kokotou *et al.* reported sterically hindered triacylglycerol analogues as potent inhibitors of human digestive lipases (see Figure 3.3).⁷⁵ The steric hindrance was achieved by adding an alkyl group at the C2 position.

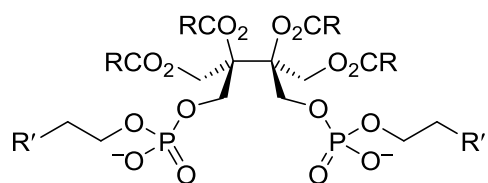
phosphoethanolamine are less permeable than vesicles composed of the more flexible analogue, so the former can pack more closely in a bilayer membrane.

In our laboratory we decided to synthesize novel lipid (bi(triglyceride) **1.6** and/or bi(phospholipid) **3.2**).



R = fatty acid chain

1.6



R = fatty acid chain

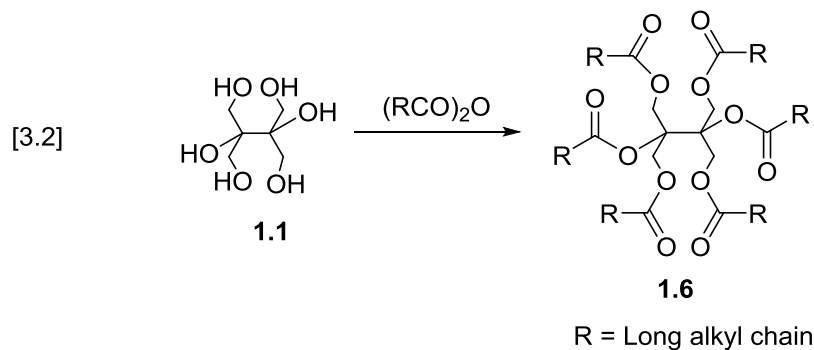
R' = ⁺NH₃, ⁺NMe₃

3.2

3.2 Results and Discussion

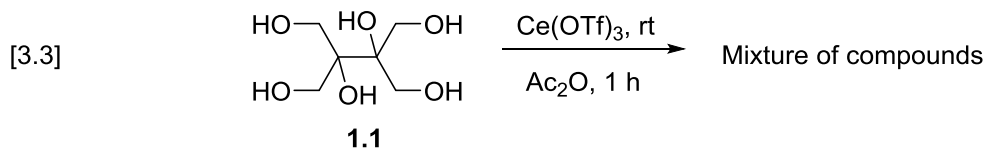
3.2.1. General considerations

Another application of 2,2'-bi(glycerol) or 2,3-di(hydroxymethyl)-1,2,3,4-butanetetraol **1.1**, was converting to 2,2'-bi(triglyceride) **3.2** as shown in eq [3.2].

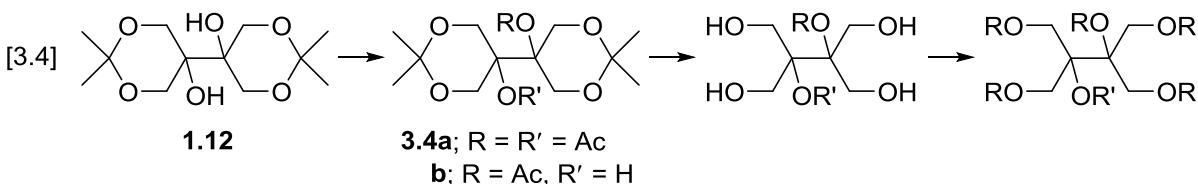


In order to do that, we need to convert alcohol functional groups to ester functional groups. Typically, acylation of alcohols is carried out with carboxylic acids⁷⁷ and carboxylic acid derivatives such as acid anhydrides⁷⁸ or acid chlorides.⁷⁹ Lewis acidic or convenient basic catalysts are used to promote the reaction. Basic catalysts such as Et₃N or pyridine alone or in presence of 4-(dimethylamino)pyridine (DMAP)⁸⁰, 4-pyrrolidine⁸¹, tertiary phosphines⁸² and magnesium bromide⁸³, DCC⁸⁴ are known to catalyze the reaction. In addition to those, a number of Lewis acids are known to catalyze the acylation of alcohols. Some of the Lewis acids used in this way include TMSCl,⁸⁵ TMSOTf,⁸⁶ Yb(OTf)₃,⁸⁷ Ce(OTf)₃,⁸⁸ Cu(OTf)₂,⁸⁹ BF₃·OEt₂,⁹⁰ and Sc(OTf)₃.⁹¹

Our initial attempt at acylation of **1.1** used acetic anhydride as a convenient model acylating agent. In the presence of catalytic amounts of Ce(OTf)₃ as shown in eq [3.3], a mixture of products was obtained, as evidenced by TLC (several close spots) and NMR spectra. Attempts to separate the products with column chromatography met with no success. Presumably the mixture might have contained mono-acylated through hexa-acylated products; 24 products were possible, counting diastereomers.



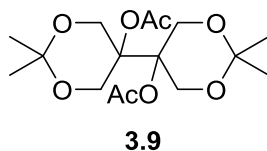
We decided to use a protected form of **1.1**, diol diacetone **1.12**, to simplify the mixture of products. Compound **1.12** is a precursor to **1.1** in the Xiaoxun Li synthesis discussed in Chapter 1. Acylation of **1.12** would be expected to lead to only three possible products *i.e.*, a mono-acylated product, a di-acylated product, and unreacted diol **1.12**, as shown in eq [3.4]. After isolating the di-acylated product, removal of the acetonide groups and esterification of the exposed four primary alcohols as shown in eq [3.4] would lead to the fully acylated product.



3.2.2 Lewis acid catalyzed acylation of pinacol **1.12** with Ac_2O

Our first attempt of acetylation of **1.12** used acetic anhydride and catalytic amounts of Ce(OTf)_3 . Dalpozzo *et al.* reported the highly efficient acetylation of alcohols using Ce(OTf)_3 .^{88b} The catalyst is environmentally friendly, can be recovered after the reaction and can be used without significant loss of activity.^{88c} When we performed acylation of **1.12** with excess acetic anhydride as solvent in presence of catalytic Ce(OTf)_3 , the ^1H NMR spectrum of the product was complex. The ^{13}C NMR spectrum was easier to analyze. We could assign many of the major peaks with little trouble, assuming we had the expected product, **3.9**. However, we observed two CH_2 carbon signals (68.2 ppm and 67.6 ppm) instead of the expected one signal. Except for the acetate peaks (170.4 ppm and 21.1 ppm), every peak was accompanied by a smaller peak not more than 2 ppm away. For example, major *gem* dimethyl peaks appeared at 27.8 ppm and 26.6

ppm; minor peaks appeared at 27.3 ppm and 26.2 ppm. For the carbon bearing the geminal methyls, the major peak appeared at 110.4 ppm, the minor one at 110.7 ppm. The minor peaks were of considerable size. It occurred to us that we might be dealing with rotamers arising from hindered rotation about the central C-C bond. We recorded NMR spectra at elevated temperature and saw no change.



Doing very careful TLC analysis, two partially resolved spots were noted. Careful column chromatography produced two samples, each of which was sufficiently pure to be able to be crystallized. X-ray crystallography of each gave us a (surprising) answer to our puzzle. The crystal structure of the material with the higher R_f - the “top spot” - is shown in Figure 3.5; that of the “bottom spot” is shown in Figure 3.6.

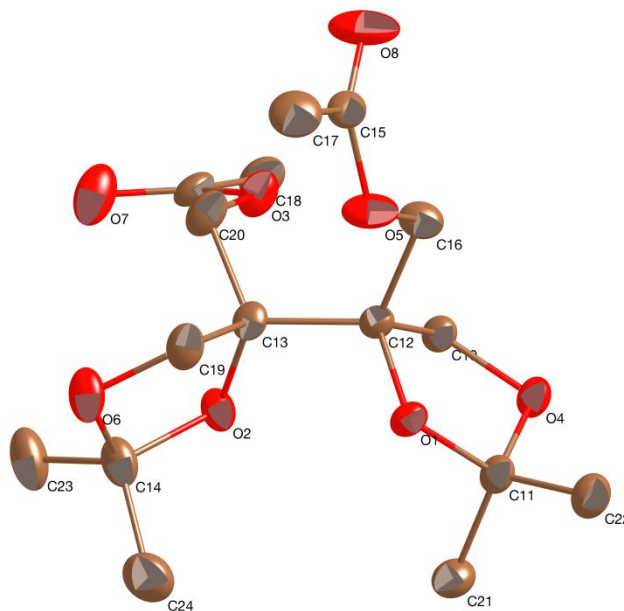


Figure 3.5. X-ray crystal structure of “top spot” from $\text{Ce}(\text{OTf})_3$ catalyzed reaction of acetic anhydride with diol 1.12. Thermal ellipsoids are at the 50% level.

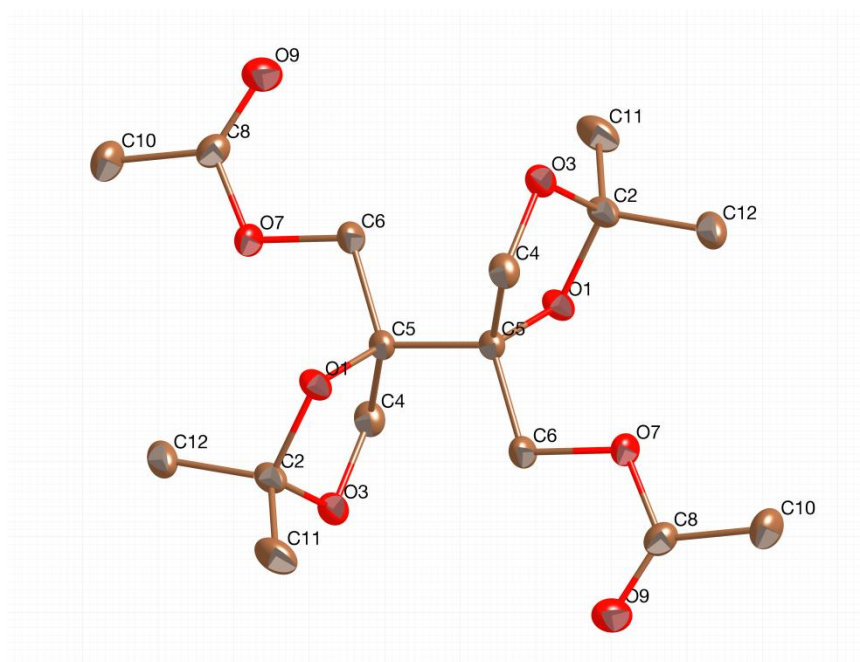
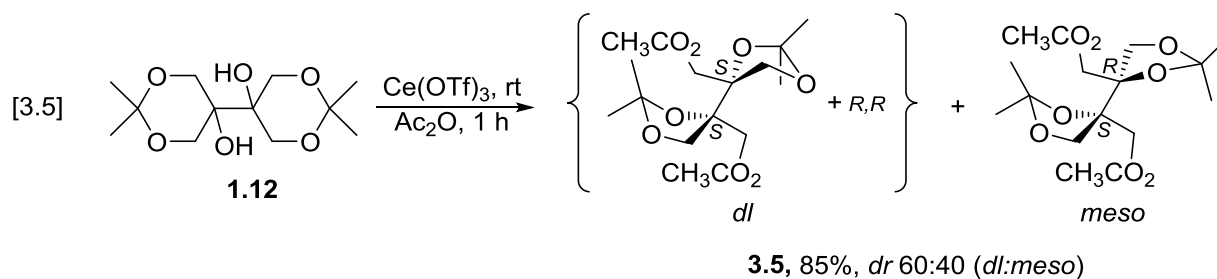


Figure 3.6. X-ray crystal structure of “bottom spot” from $\text{Ce}(\text{OTf})_3$ catalyzed reaction of acetic anhydride with diol **1.12**. Thermal ellipsoids are at the 50% level.

Equation [3.5] shows the outcome of this reaction. Neither product contains a 6-membered ring! The “top spot” material is the *dl* diastereomer of **3.5**, and the “bottom spot” material is the *meso* diastereomer.



The ^1H NMR spectrum of the mixture of diastereomers obtained in this acetylation is shown in Figure 3.7. Figure 3.8 reports the ^1H NMR spectra of the individual diastereomers.

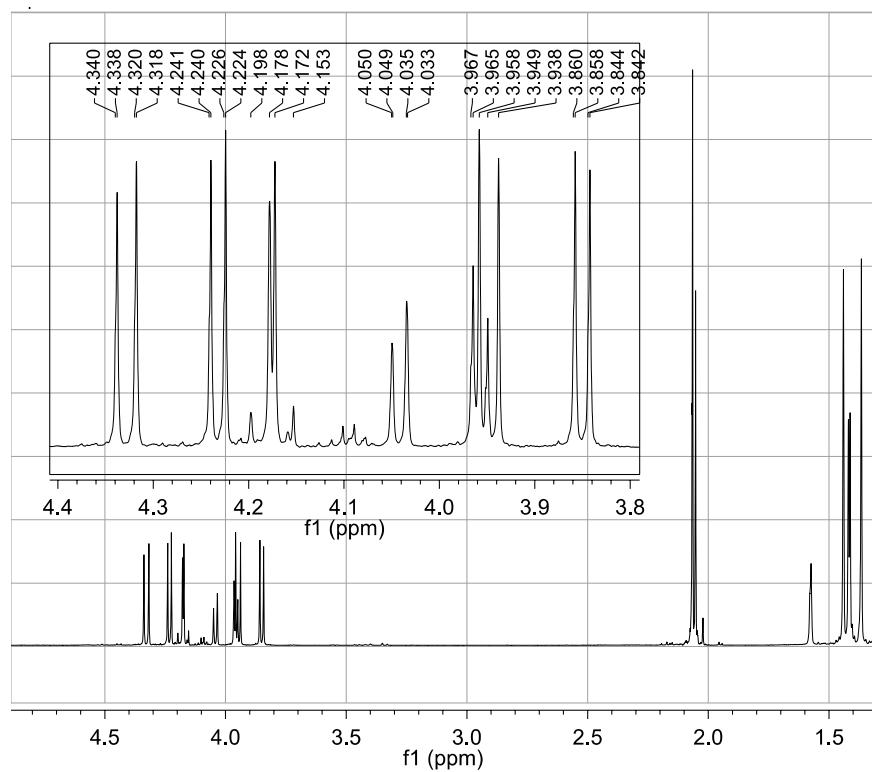


Figure 3.7. 600 MHz ^1H NMR of a mixture of diastereomers of 3.5. CDCl_3 solvent.

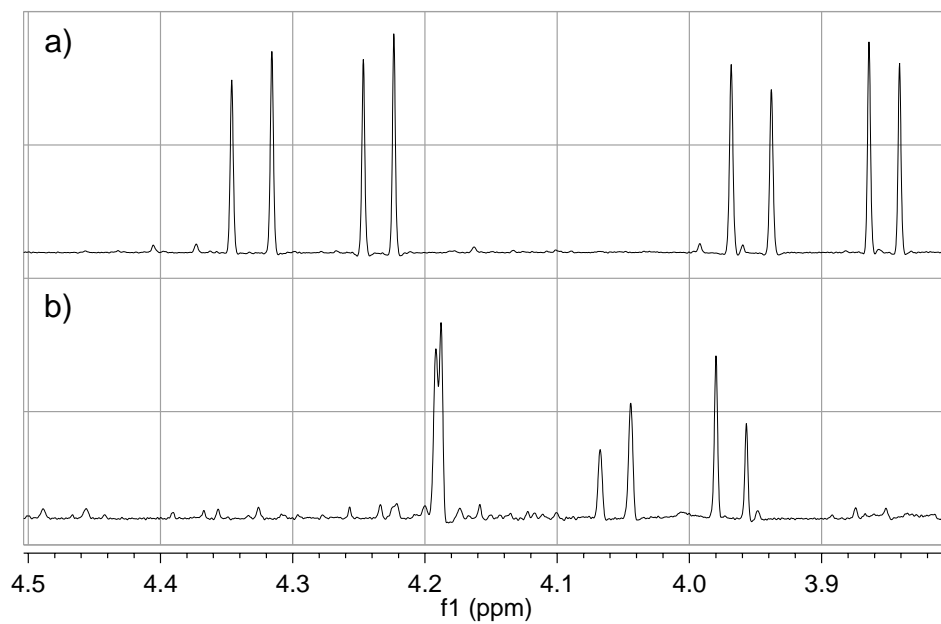
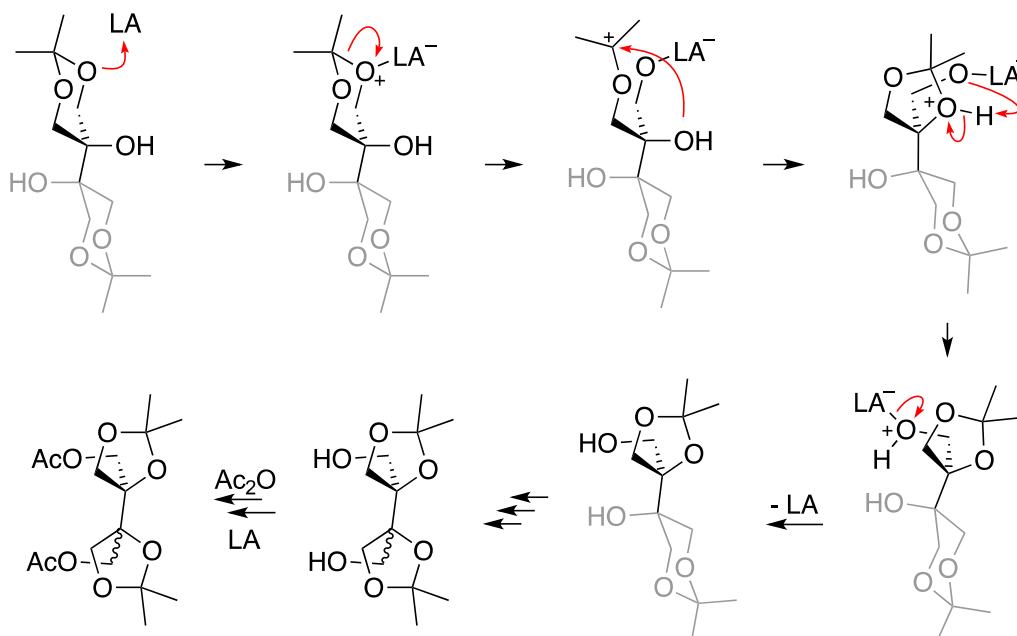


Figure 3.8. Partial 400 MHz ^1H NMR spectra of diastereomeric forms of 3.5. a) *dl* diastereomer b) *meso* diastereomer.

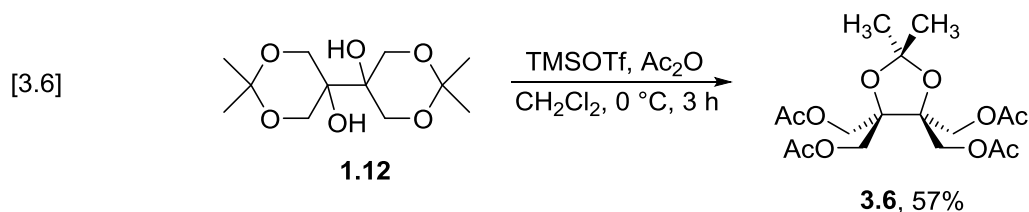
A possible mechanism for the Lewis acid catalyzed reaction of **1.12** with acetic anhydride is shown in Scheme 3.1.

Scheme 3.1. Possible mechanism for the formation of 3.5 with Lewis acid catalyst



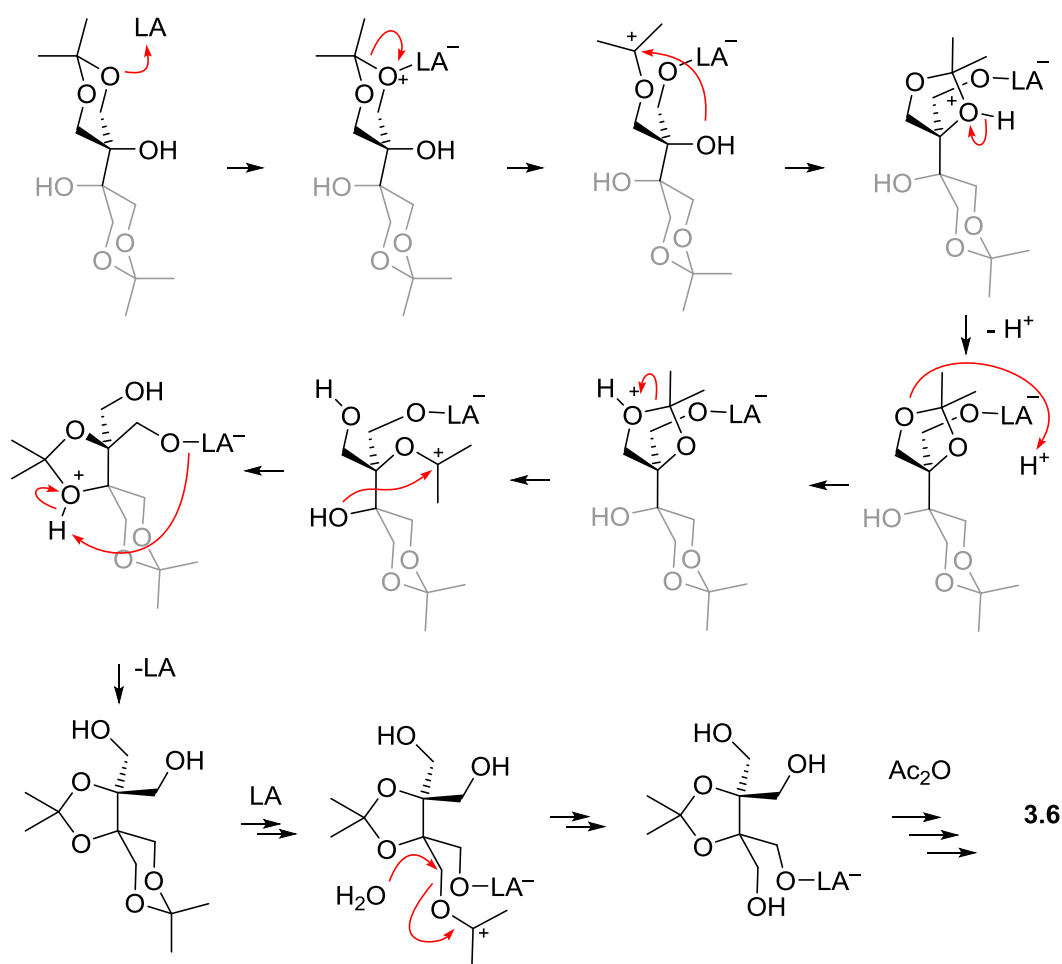
To study further about rearranged products formation, we decided to investigate the reaction of **1.12** with Ac_2O with various Lewis acids such as TMSOTf, $\text{Cu}(\text{OTf})_2$, $\text{BF}_3 \cdot \text{OEt}_2$ and $\text{Sc}(\text{OTf})_3$.

In our next attempt we used trimethylsilyl trifluoromethanesulfonate (TMSOTf) as a Lewis acid catalyst. Procopiu *et al.* reported acylation reactions of alcohols with acid anhydrides catalyzed by TMSOTf without cleaving ketal functional groups.^{86b} When we applied the same reaction conditions to our compound **1.12**, eq [3.6], surprisingly it produced a new rearranged product compared to $\text{Ce}(\text{OTf})_3$ -catalyzed reaction shown in eq [3.13].

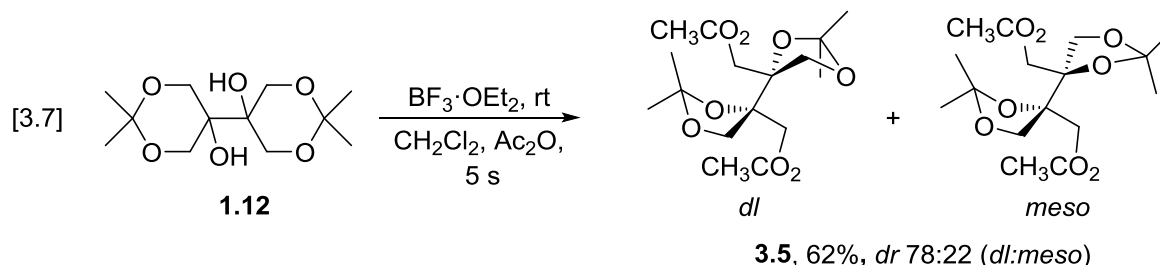


Angibeaud *et al.* reported TMSOTf in the presence of acetic anhydride resulted in the selective cleavage of the endocyclic C1-O bond of methyl β -D-glucopyranoside, in contrast to methyl α -D-glucopyranoside,⁹² which gave exclusive formation of 1,2,3,4,6-penta-*O*-acetyl- α -D-glucopyranose. From this report we realized that in the reaction of **1.12** with Ac₂O-TMSOTf, the ketal group is cleaving and rearrangements are taking place to form **3.6**. A plausible mechanism is shown in Scheme 3.2.

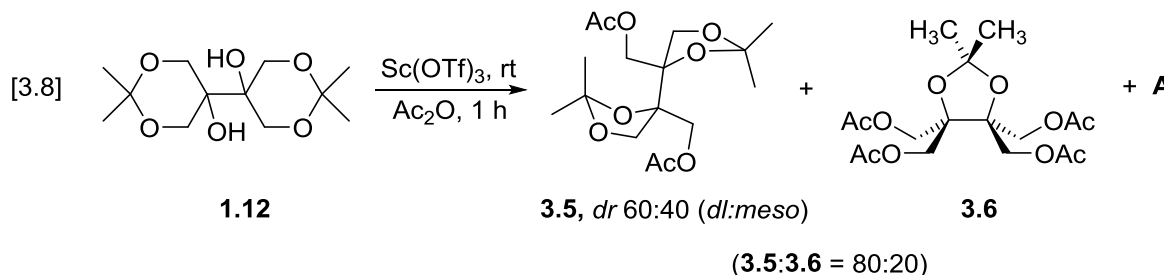
Scheme 3.2. Mechanism leading to 3.6



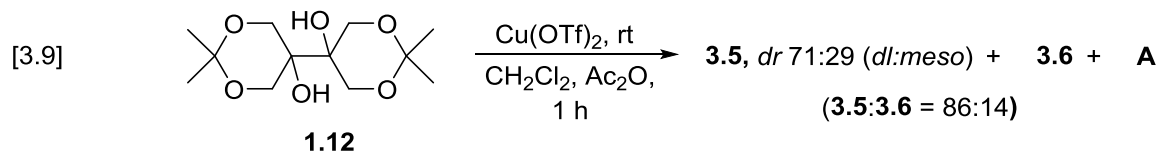
The next Lewis acid we tried was boron trifluoride diethyl etherate ($\text{BF}_3 \cdot \text{OEt}_2$). Acetylation of **1.12** with 2 equiv of $\text{BF}_3 \cdot \text{OEt}_2$ also produced same kind of rearranged products as $\text{Ce}(\text{OTf})_3$ (eq [3.7]).



We tried with $\text{Sc}(\text{OTf})_3$ because it exhibits good stability in air and good solubility in organic or aqueous media.^{91c} Scandium triflate was found to be an extremely effective catalyst for esterification reactions.^{91a} Acetylation of compound **1.12** with excess Ac_2O as solvent and 1 mol% $\text{Sc}(\text{OTf})_3$ produced the same rearranged products **3.5** and **3.6**, and an unidentified product named as **A**, eq [3.8]. The ratio of **3.5**:**3.6** was 80:20 from ^1H NMR integration.



The next Lewis acid catalyst used was $\text{Cu}(\text{OTf})_2$. Saravanan *et al.* reported acylation using catalytic amounts of $\text{Cu}(\text{OTf})_2$.^{89a} When we performed the acetylation of **1.12** with acetic anhydride in presence of catalytic amounts of $\text{Cu}(\text{OTf})_2$, we obtained rearranged products **3.5** and **3.6**, with unidentified compound **A**, same as obtained from $\text{Sc}(\text{OTf})_3$ case, as shown in eq [3.9]. The ratio of **3.5**:**3.6** was 86:14 identified from ^1H NMR integration.



We decided to investigate further about acetylation reactions of **1.12** catalyzed with different Lewis acids by changing reaction conditions such as different reaction times, different mol% of catalyst, and quantity of acetic anhydride.

As illustrated in Table 3.1, acylation of pinacol **1.12** was studied by changing reactions conditions with acetic anhydride as acylating agent. A 1 mol% loading of $\text{Ce}(\text{OTf})_3$ catalyst and acetic anhydride used in excess as solvent produced **3.5** in 85% yield (entry 3.1.1). This reaction gave a clean product which did not require column chromatography for purification. Entries 3.1.2 – 3.1.5 used CH_2Cl_2 as the solvent. With 6 equiv of acetic anhydride and 5 mol% of catalyst $\text{Ce}(\text{OTf})_3$ and a reaction time of 5 sec, we obtained unreacted **1.12** (entry 3.1.2). We repeated the reaction (with 5 instead of 6 equiv of Ac_2O) for 30 minutes, and obtained new compounds, named as **A** and **B** (entry 3.1.3). Their R_f was smaller than the starting diol **1.12**. By contrast, the acetylated products **3.5** and **3.6** both have larger R_f values than **1.12**. Therefore it is reasonable to conclude that **A** and **B** are more polar than the starting diol **1.12**. We repeated the reaction except we extended the reaction time to 3 h (entry 3.1.4). In this case, the progress of the reaction was monitored by TLC. Compounds **A** and **B** were detected early in the reaction and then disappeared as time passed, being replaced by products **3.5** and **3.6**. Finally, using 5 equiv of Ac_2O and a stoichiometric amount of catalyst, 2.1 equiv, over 3 h afforded products **3.5** and **3.6**.

Table 3.1. Acylation of diol 1.12 with acetic anhydride, Ac₂O, catalyzed by Lewis acids

entry ^a	catalyst	[Ac ₂ O]/[5]	catalyst (mol%)	time	Product distribution				yield (%)
					<i>dl</i> -3.5	<i>meso</i> -3.5	3.6	other ^b	
3.1.1	Ce(OTf) ₃	79	1	1 h	60	40	0	0	85
3.1.2	Ce(OTf) ₃	6	5	5 sec	0	0	0	0 ^c	
3.1.3	Ce(OTf) ₃	5	5	0.5 h	0	0	0	A+B	
3.1.4	Ce(OTf) ₃	5	5	3 h	61	26	13	0	
3.1.5	Ce(OTf) ₃	5	200	3 h	56	17	27	0	
3.1.6	Sc(OTf) ₃	83	1	1 h	48	32	20	A	
3.1.7	Sc(OTf) ₃	5	5	1 h	74	26	0	A+B	83
3.1.8	BF ₃ ·OEt ₂	6	210	5 sec	78	22	0	0	62
3.1.9	BF ₃ ·OEt ₂	79	5	5 sec	60	26	14	A	
3.1.10	TMSOTf ^d	5	5	3 h	0	0	100	0	57
3.1.11	TMSOTf ^d	6	5	5 sec	0	0	32	A ^e , C ^f	
3.1.12	TMSOTf ^d	5	200	5 sec	0	0	≥ 95	A ^e	
3.1.13	TMSOTf ^d	5	220	5 h	0	0	100		66
3.1.14	Cu(OTf) ₂	5	5	1 h	61	25	14	A	
3.1.15	Cu(OTf) ₂	79	1	1 h	38	25	37	A	

^a All entries used CH₂Cl₂ as the solvent, except for entries 3.1.1, 3.1.6, 3.1.9, and 3.1.15 where excess Ac₂O functioned as the solvent ^b **A** and **B** are unidentified compounds more polar than **1.12**, **3.5**, or **3.6** as judged by lower *R_f* on silica gel TLC (3:2 hexanes:EtOAc) ^c Only unreacted **1.12** could be detected. ^d All reactions with this catalyst were performed at 0 °C. ^e Very minor spots in TLC. ^f The identity of **C** is discussed later.

Acetylation of **1.12** using 1 mol% of Sc(OTf)₃ and Ac₂O in excess as solvent gave **3.5** and **3.6** (entry 3.1.6). The same catalyst with 5 mol% loading in combination with 5 equiv of Ac₂O in CH₂Cl₂ produced **3.5**, plus unidentified compounds **A** and **B** (entry 3.1.7). After column

chromatographic purification, the yield of **3.5** was 83% so the unidentified products were minor products.

Two experiments were done with $\text{BF}_3 \cdot \text{OEt}_2$ catalyst. In the first case, $\text{BF}_3 \cdot \text{OEt}_2$ was used in stoichiometric rather than catalytic amount, *i.e.* 2.1 equiv. This led to **3.5** as a single product in 62% yield (entry 3.1.8). In the second case, Ac_2O was the solvent. These conditions led to compound **3.6**, and unidentified product **A** (entry 3.1.9).

All TMSOTf reactions were carried out at 0 °C. The use of 5 equiv of Ac_2O , 5 mol% TMSOTf in CH_2Cl_2 and a reaction time of 3 h, produced clean **3.6** and no other rearranged products, with isolated yield of 57% (entry 3.1.10). With the same catalyst and reaction conditions but a reaction time of 5 sec, a new unidentified compound **C** was observed in TLC (larger R_f than **1.12**), along with **3.6** and a very small amount of compound **A**. When we observed by TLC after 5 minutes, **A** had disappeared and only **C** and **3.6** were present. The ratio of **C** to **3.6** was 68:32 from ^1H NMR integration (entry 3.1.11). We identified compound **C** in later stages of our research, and we will discuss that shortly. Next we tried with 2 equiv of TMSOTf catalyst loading with 5 equiv of Ac_2O , CH_2Cl_2 as solvent and a reaction time of 5 sec. This produced exclusively **3.6**, with very minor unidentified **A** (entry 3.1.12). Later on we repeated the same reaction conditions of entry 3.1.12 with a reaction time of 5 h instead of 5 sec. This produced **3.6** with isolated yield of 66% (entry 3.1.13). When we monitored the course of that reaction through TLC, we observed compound **C** forming immediately, and during many hours of reaction, **C** slowly converting to compound **3.6**.

Next attempt was with $\text{Cu}(\text{OTf})_2$ catalyst. When we loaded 5 mol% of $\text{Cu}(\text{OTf})_2$ and 5 equiv of Ac_2O , with CH_2Cl_2 as solvent, and reaction time of 1 h we obtained compound **3.5** (*dr* 71:29 *dl:meso*), **3.6** and unidentified **A** (entry 3.1.14). Another condition was excess Ac_2O as solvent

and 1 mol% of catalyst, and reaction time was 1 h. These conditions produced compound **3.5** (*dr* 60:40 *dl:meso*), **3.6**, and unidentified **A**. The **3.5:3.6** ratio was 63:37 from ¹H NMR integrations (entry 3.1.15).

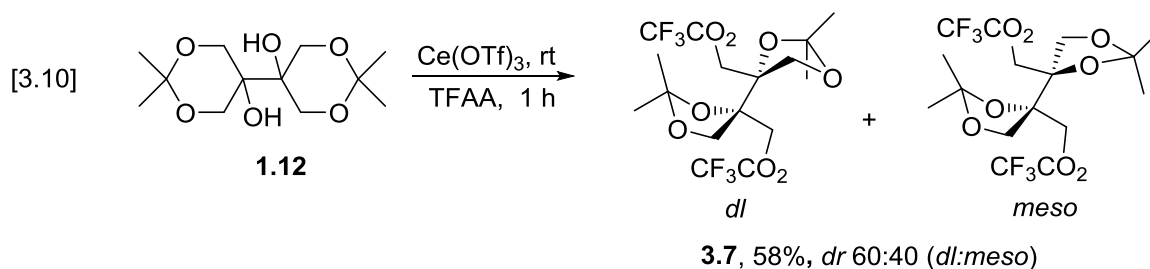
From all the above reaction conditions we can observe:

- Usually there is more *dl*-**3.5** formed than the *meso* diastereomer.
- TMSOTf catalyst is unique. Only that catalyst produces high yields of compound **3.6** with no **3.5** observed.
- New unidentified compound **C** was observed in TMSOTf case. Its *R_f* was higher than that of **1.12**.
- Unidentified intermediate **A** was encountered in some cases. It is more polar than **1.12**.
- Compound **B** (we identified **B** in later stages of research and will discuss shortly) was observed in 30 min –1 h time in 5 equiv Ac₂O and 5 mol% catalyst loading.

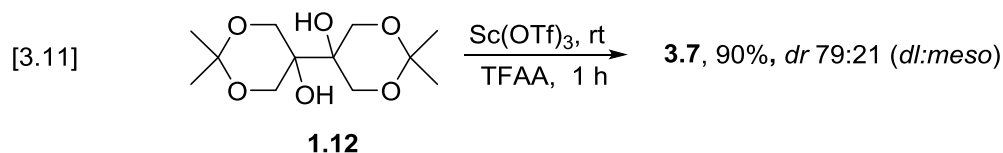
3.2.3 Lewis acid catalyzed acylation of 1.12 with trifluoroacetic anhydride

We undertook an investigation of acylation of **1.12** with trifluoroacetic anhydride (TFAA), using the same Lewis acids employed in our investigation of acetylation. We lacked X-ray structures of the diastereomers analogous to **3.5**, so our assignment of *meso* and *dl* rested on the assumption that the NMR parameters of the trifluoromethyl products were similar to those of **3.5**.

Acylation of **1.12** using excess TFAA as solvent with 1 mol% of Ce(OTf)₃ at rt for 1 h is shown in eq [3.10]. We obtained same type of 5 member acetonide rearranged product as acetylation reaction with 58% isolated yield. Yield was significantly lower than the analogous yield from acetylation (85%).

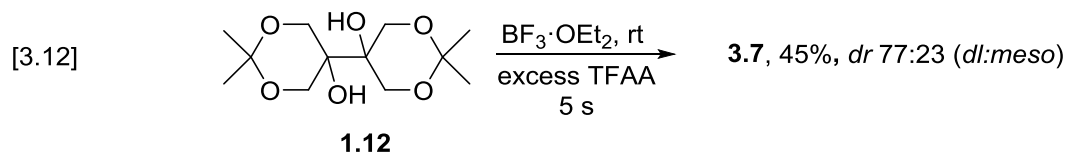


We tried 1 mol% Sc(OTf)₃ with excess TFAA at rt for 1 h and observed the same type of rearranged products **3.7** with 90% isolated yield, eq [3.11].

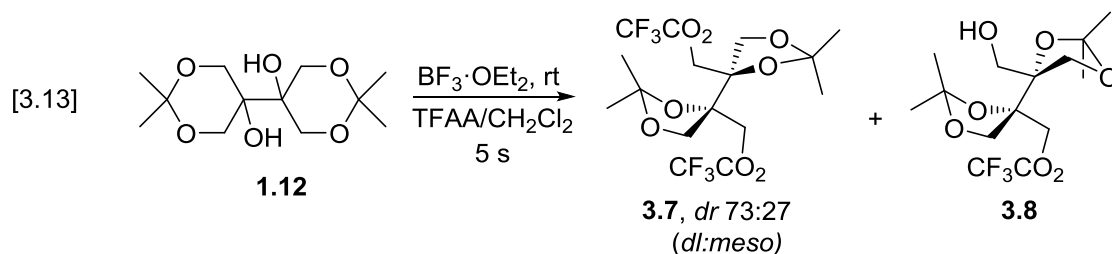


Acylation using 5 equiv TFAA and 5 mol% TMSOTf also produced **3.7** in 39% yield, rather than the trifluoromethyl analog of tetraacetylated **3.6** we got in acetylation. In this case, *dr* was 81:19 (*dl:meso*) for **3.7**.

The BF₃·OEt₂ (1 mol%) catalyzed acylation using excess TFAA as solvent produced **3.7** in 45% yield as shown in eq [3.12].



When we changed reaction conditions, *i.e.* 5 mol% BF₃·OEt₂, 5 equiv of TFAA in CH₂Cl₂ solvent, product **3.7** was accompanied by mono-acetylated acetonide **3.8**, eq [3.13]. Compound **3.8** was not observed in diastereomeric form.



Cu(OTf)₂ (5 mol%) catalyzed acylation with TFAA also gave **3.7** *dr* 73:27(*dl:meso*).

We investigated the trifluoroacetylation by changing reaction conditions such as different mol% catalyst loading, changing quantities of acylation reagent, and various reaction times.

Those reactions are summarized in Table 3.2.

When we used 5 mol% of Ce(OTf)₃ and 5 equivalents of TFAA entry 3.2.2, at rt for 1 h gave diacylated rearranged product **3.7** (*dr* 78:22) with 65% yield. We changed catalyst in next attempt 5 mol% Sc(OTf)₃ and 5 equiv TFAA for 1 h at rt also produced product **3.7** (*dr* 77:23) with 67% yield entry 3.2.4. Next attempt with BF₃·OEt₂ with 2 equivalents and 5 equivalents of anhydride TFAA at room temp for 5 sec produced **3.7** and **3.8** entry 3.2.7. Here we tried changing 5 sec to 10 minutes reaction times but we got same ratio of **3.7** and **3.8**.

Table 3.2. Acylation of diol 1.12 with trifluoroacetic anhydride, TFAA, catalyzed by Lewis acids

entry	catalyst	[TFAA]/[1.12]	[catalyst] (mol%)	time	products ^a	yield (%)
3.2.1	Ce(OTf) ₃	54	1	1 h	3.7 (<i>dr</i> 60:40)	58
3.2.2	Ce(OTf) ₃	5	5	1 h	3.7 (<i>dr</i> 78:22)	65
3.2.3	Sc(OTf) ₃	55	1	1 h	3.7 (<i>dr</i> 79:21)	90
3.2.4	Sc(OTf) ₃	5	5	1 h	3.7 (<i>dr</i> 77:23)	67
3.2.5	BF ₃ ·OEt ₂	52	1	5 sec	3.7 (<i>dr</i> 77:23)	45
3.2.6	BF ₃ ·OEt ₂	5	5	5 sec	3.7 (<i>dr</i> 77:23) + 3.8	-
3.2.7	BF ₃ ·OEt ₂	5	210	5 sec	3.7 (<i>dr</i> 77:23) + 3.8	-
3.2.8	TMSOTf ^b	5	5	1 h	3.7 (<i>dr</i> 81:19)	39
3.2.9	TMSOTf ^b	57	1	1 h	3.7 (<i>dr</i> 83:17)	50
3.2.10	Cu(OTf) ₂	5	5	1 h	3.7 (<i>dr</i> 73:27)	59
3.2.11	Cu(OTf) ₂	54	1	1 h	3.7 (<i>dr</i> 77:23)	64

^a diastereomer ratios obtained by ¹H-NMR peak integration, reported as *dl:meso*.

^b reaction carried out at 0 °C

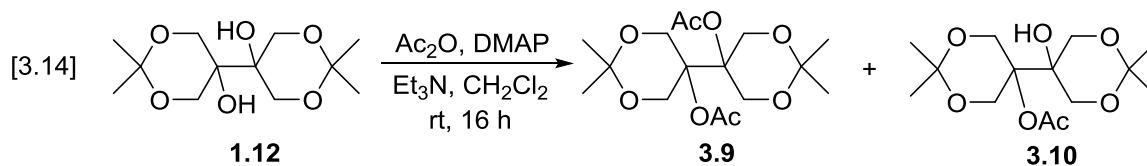
TMSOTf catalyzed reaction with excess anhydride **TFAA** also produced diacylated **3.7** at 0 °C for 1 h entry 3.2.9. Cu(OTf)₂ (1 mol%) catalyzed acylation with excess anhydride **TFAA** produced **3.7** in 1 h at room temperature entry 3.2.11.

From Table 3.2 points to be noted are BF₃·OEt₂ catalyst based reactions with 5 equiv of anhydride **TFAA** producing compound **3.8**. Sc(OTf)₃ catalyzed reaction with excess anhydride **TFAA** gave good yields of **3.7**. Diastereomeric ratio of trifluoroacetylation also *dl* form is major. In the TFAA series, TMSOTf did not produce a compound analogous to tetraacetate **3.6**.

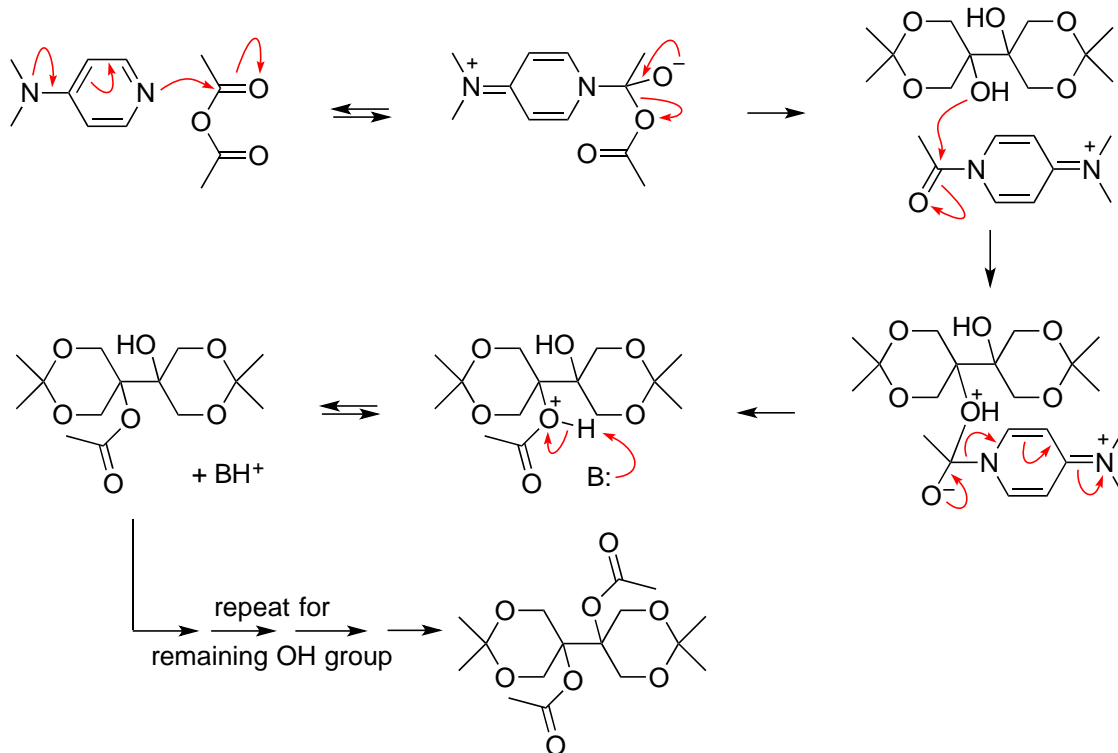
3.2.4 Base catalyzed acylation of **1.12** with acetic anhydride

Next we explored the acetylation of **1.12** under *basic* conditions. The nucleophile 4-(dimethylamino)pyridine (DMAP) is a well known catalyst for the esterification of alcohols by acid anhydrides, in particular for the acylation of sterically hindered secondary and tertiary alcohols.

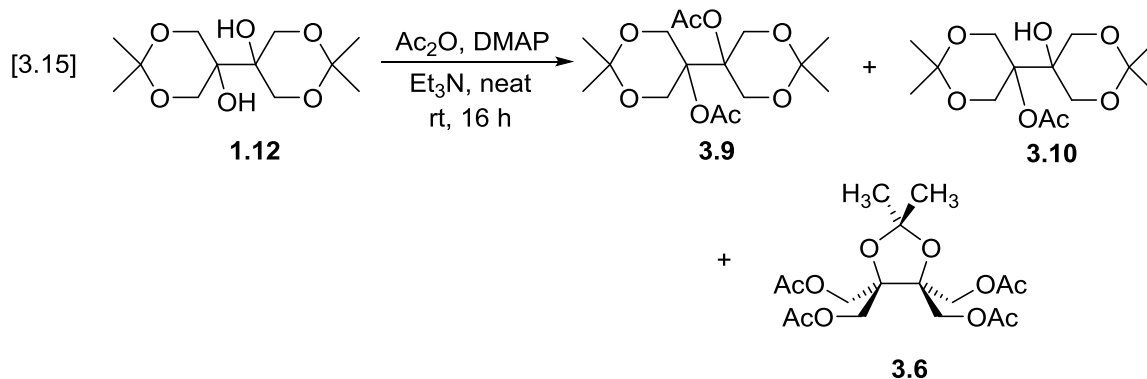
When we reacted **1.12** with 4 equiv of Et₃N, 4 equiv Ac₂O and 20 mol% DMAP catalyst in CH₂Cl₂ solvent at rt for 16 h, we observed no rearranged products. Instead we obtained diacylated compound **3.9** and monoacylated compound **3.10**, eq [3.14]. The ratio of **3.9** to **3.10** was 33:67 according to ¹H NMR integration. When we increased the reaction time to 48 h, no change was observed in the ratio of compounds **3.9** and **3.10** according to ¹H NMR.



Plausible mechanism for DMAP-catalyzed acylation of 1.12 under basic conditions:⁹³



The same reaction conditions but without solvent (neat) gave diacylated compound **3.9**, monoacylated compound **3.10** and tetra-acylated rearranged compound **3.6** (this compound was observed in Lewis acid catalyzed conditions also) see eq [3.15]. Ratio of compounds **3.9**, **3.10** and **3.6** from ¹H NMR integration was 53:42:5.



We tried base catalyzed reactions with varying temperature, presence of solvent and absence of solvent. Those results are summarized in Table 3.3.

Table 3.3. Acetylation of 1.12 with acetic anhydride, Ac₂O, under basic conditions

	Reagents	Conditions (°C, h)	Solvent	Product Distribution ^a			
				3.9	3.10	3.6	3.11
3.3.1	DMAP, Et ₃ N	rt, 16	CH ₂ Cl ₂	33	67	0	0
3.3.2	DMAP, Et ₃ N	rt, 16	neat	53	42	5	0
3.3.3	DMAP, Et ₃ N	40-45, 16	CH ₂ Cl ₂	52	48	0	0
3.3.4	DMAP, Et ₃ N	40-45, 16	neat	57	20	23	0
3.3.5	MgBr ₂ , Et ₃ N	rt, 28	CH ₂ Cl ₂	0	52	0	48

^a Determined by ¹H-NMR peak integration.

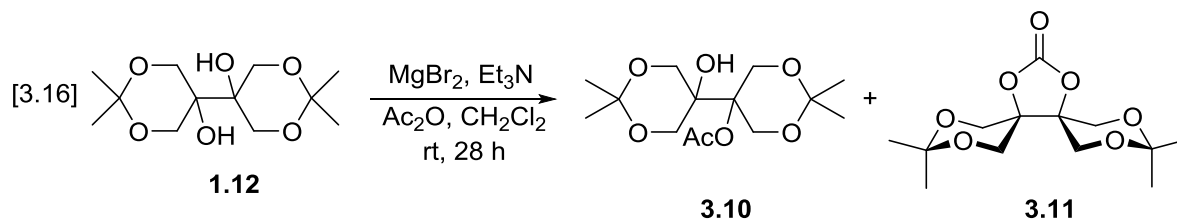
In the next attempt (entry 3.3.3) the temperature was changed from rt to 40–45 °C. Same equivalents of reagents used as earlier with solvent CH₂Cl₂ gave diacylated **3.9** and monoacylated **3.10** in the ratio of 52:48 from ¹H NMR integration. Diacylated product ratio increased when compared to room temperature reaction with solvent.

Another attempt (entry 3.3.4) at 40-45 °C and without solvent (neat) gave diacylated **3.9** and monoacylated **3.10** and compound **3.6**. The ratio of **3.9**, **3.10** and **3.6** was 57:20:23.

From DMAP catalyzed reactions (entry 3.3.1–3.3.4, from Table 3.3) observations that can be noted are with solvent, reactions are clean and solely produced diacylated **3.9** and monoacylated **3.10** compounds. Neat (absence of solvent) reactions gave compound **3.6** with expected **3.9** and **3.10**. Refluxing reaction conditions produced diacylated **3.9** as a larger proportion of the product mixture when compared to room temperature reactions.

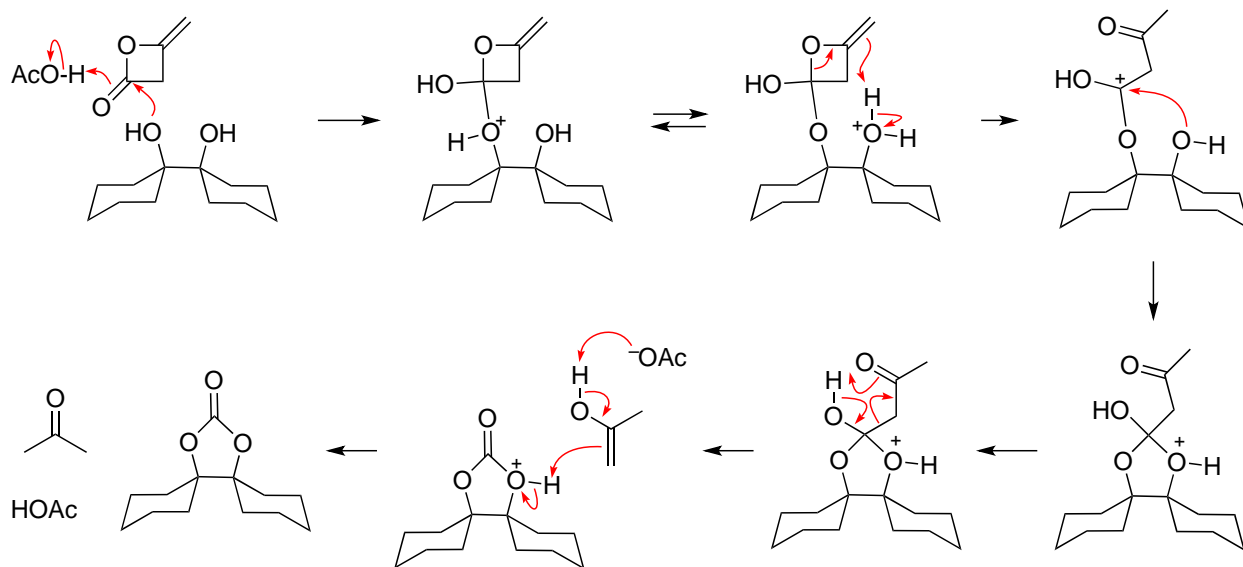
In the course of study of base catalyzed reactions, we attempted using MgBr₂ and triethylamine combination (entry 3.3.5).^{83a} MgBr₂ was prepared freshly using Mg turnings in dry THF with 1,2-dibromoethane at 45 °C for 3 h. According to the authors, the combination of MgBr₂ and Et₃N activates the alcohol and anhydride, and produces remarkable rate acceleration in the anhydride-alcohol reaction.^{83a} Freshly prepared MgBr₂ (4 equiv), triethylamine (6 equiv), and Ac₂O (4 equiv) was used for acylation at rt. Interestingly we got cyclic carbonate **3.11** and

expected mono-acylated **3.10** see eq [3.16]. The ratio of **3.11** to **3.10** was 52:48 according to ^1H NMR.



Bhushan *et al.* reported formation of cyclic carbonates in the reaction of 1,2-ditertiary alcohols with acetic anhydride and DMAP.⁹⁴ Presumably a similar mechanism is at work in our reaction. Their mechanism involves deprotonation of $[\text{N-acetyl DMAP}]^+ \text{OAc}^-$ to give HOAc and ketene, which dimerizes to diketene. The rest of the mechanism is presented in Scheme 3.3. We tried several attempts to reproduce the cyclic carbonate; unfortunately we couldn't reproduce the reaction of eq [3.16].

Scheme 3.3. Rationale for formation of 3.11.



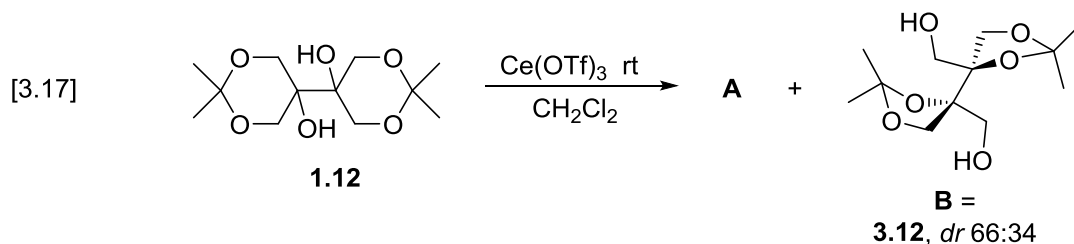
3.2.5. Reactions in the absence of anhydride (“blank reactions”)

3.2.5.1 Reaction of 3.5 with 5 mol% Ce(OTf)₃ over long times

Diacylated rearranged compound **3.5** was treated with 5 mol% of Lewis acid catalyst Ce(OTf)₃ at rt. The reaction was run for 2 weeks with monitoring by TLC. There were no new spots observed in TLC. Therefore no reaction occurred. It should be noted that compound **3.5** has acetonide functional groups but they were not affected by Lewis acidic condition. The *dr* did not change.

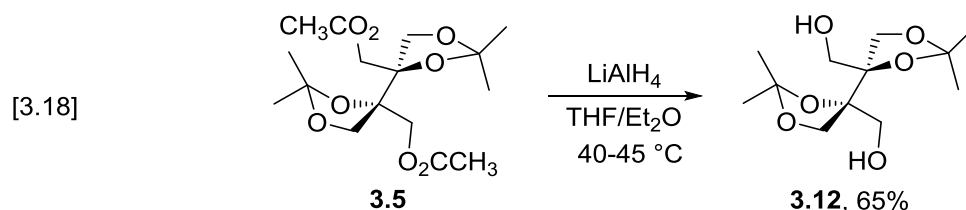
3.2.5.2 Reaction of 1.12 with 5 mol% Ce(OTf)₃ in the absence of anhydride

Compound **1.12** was reacted with 5 mol% Ce(OTf)₃ at rt in CH₂Cl₂ as solvent for 30 minutes with TLC monitoring. This gave rise to compounds **A** and **B**, which were noted in some product mixtures included in Table 3.2. The *R_f* of compounds **A** and **B** were 0.07 and 0.06 (EtOAc:hexanes 2:3 (v/v)). Separation of compound **B** and **A** was done by careful column chromatography with this solvent system. Compound **B** was identified by us as **3.12** and **A** (unidentified intermediate) as shown in eq [3.17]. Compound **B** (**3.12**) and **A** are more polar than acetonide pinacol **5** in TLC. Compound **A** also looked like diastereomer according to TLC, in which two spots ran closely together. Compound **B** and **A** are in the ratio of ~ 76:24 (±1) according to ¹H NMR integration. Diastereomeric ratio of rearranged diol **3.12** was 66:34 (±1) from ¹H NMR integration.



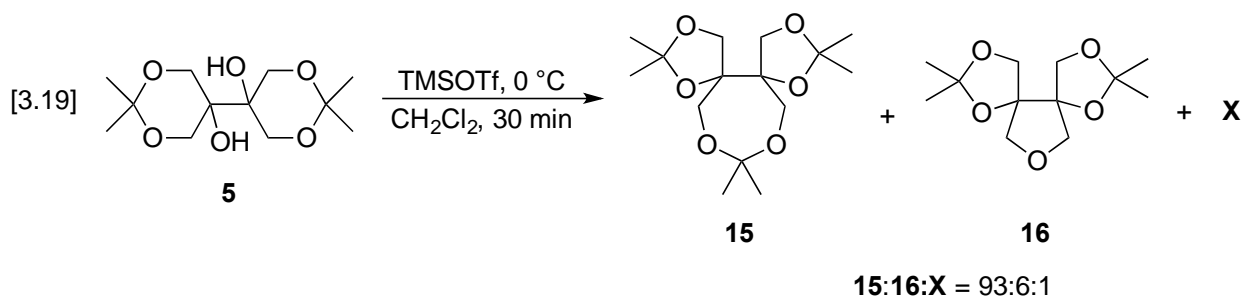
We extended the reaction time from 30 mins to 12 hours, but there was no change in TLC. As discussed earlier, acetylation of pinacol **1.12** in Table 3.1, compound **B** was identified as

rearranged diol **3.12**. To confirm the rearranged diol **3.12** identity, we performed the reduction reaction of rearranged diacylated **3.5** with LiAlH_4 as shown in eq [3.18] to produce diol **3.12**. NMR and mass spectrometric data from the reduction product matched the corresponding data from Lewis acid catalyzed acetylation product.



3.2.5.3. Reaction of **1.12** with 5 mol% TMSOTf catalyst in the absence of anhydride

When we performed the reaction of **1.12** with 5 mol% TMSOTf in CH_2Cl_2 solvent at 0 °C for 30 minutes we obtained three products: 5-7-5 dispiro compound **3.13**, 5-5-5 dispiro compound **3.14** and unidentified compound **X** as shown in eq [3.19].



When we performed the reaction with monitoring by TLC, we observed **3.13**, **3.14**, and **X** as one spot, less polar than **1.12**, and compound **A** and **B** minor spots (as previously discussed, more polar spots in TLC). The ratio of **3.13:3.14:X** was $\sim (\pm 1) 93:6:1$ from ^1H NMR integration. In TLC, with EtOAc/hexane 3:2 (v/v) solvent system, it appeared like single spot. When we recorded the NMR, (Figure 3.9) we observed some minor compound **3.14** ^1H NMR signals (δ 4.29, δ 3.96–3.88), major compound **3.13** ^1H NMR and some unidentified compound (δ 3.70– δ

3.66). ^{13}C NMR was looking like single compound, *i.e.* **3.13** (Figure 3.10). Through careful column chromatography we separated **3.14** compound. The ^1H NMR (Figure 3.11) and ^{13}C NMR (Figure 3.12) spectra are presented below.

Compound **C**, which appears in the early stages of acetylation (Table 3.1) is now identified as **3.14**.

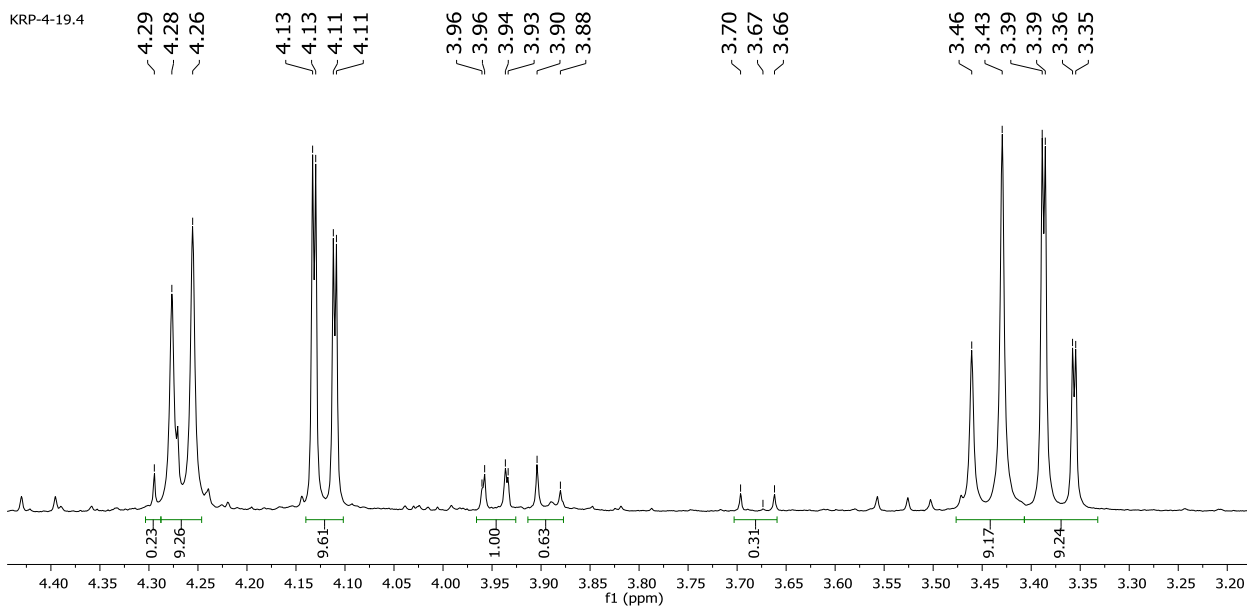


Figure 3.9. 400 MHz ^1H NMR partial spectrum of TMSOTf catalyzed blank reaction after column, mixture of compounds **3.13, **3.14**, and unidentified compound **X**.**

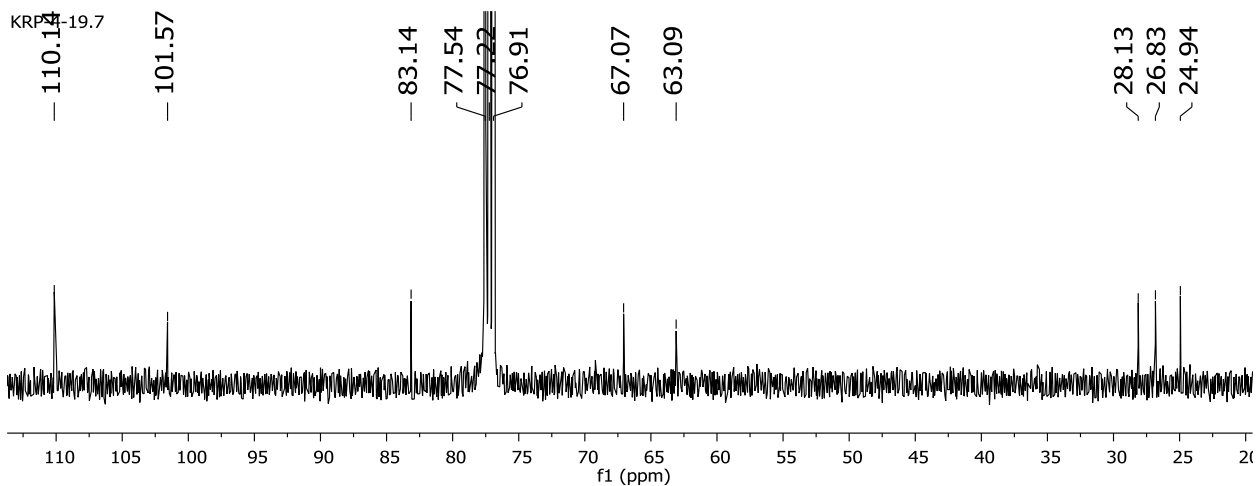


Figure 3.10. 100 MHz ^{13}C NMR spectrum of sample used for Figure 3.9.

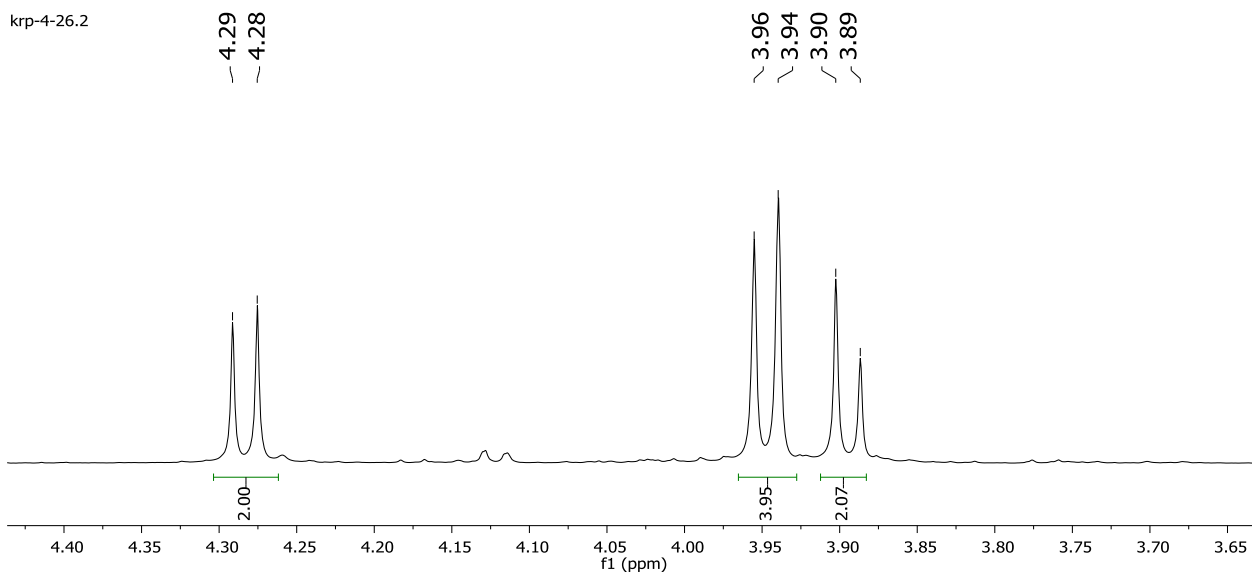


Figure 3.11. 400 MHz ^1H NMR partial spectrum of 3.14 after column chromatography.

CDCl_3 solvent.

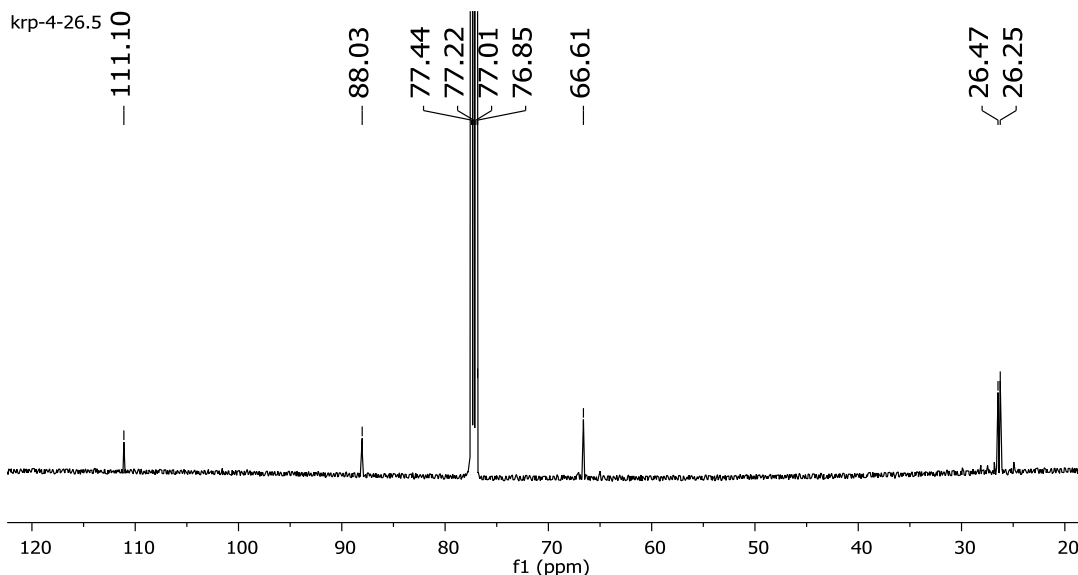


Figure 3.12. 150 MHz ^{13}C NMR of **3.14** after column chromatography. CDCl_3 solvent.

From ^1H NMR, determining the structure of the products **3.13** and **3.14** was difficult. ^{13}C NMR spectroscopy however was very helpful in distinguishing among isopropylidene acetals of various ring sizes, especially 5-membered (2,2-dimethyl-1,3-dioxolane), 6-membered (2,2-dimethyl-1,3-dioxane), and 7-membered (2,2-dimethyl-1,3-dioxepane) acetals. Buchanan, Edgar, and co-workers reported ^{13}C NMR parameters for 14 examples, and in a separate study, 42 examples, which are shown in Tables 3.4⁹⁵ and 3.5,⁹⁶ as well as other work, not summarized below, on the subject of assigning ring size in isopropylidene acetals.^{97,98}

Table 3.4. ^{13}C NMR Parameters of Isopropylidene Acetals^a

Ring size	Acetal carbon	$\Delta\delta$ gem dimethyl
5	108.3, 108.7, 109.0, 109.2, 109.5, 109.6, 109.7, 109.7	0.6, 0.9, 1.0, 1.3, 1.4, 1.4, 1.5, 1.5
6	98.3, 98.4, 98.5, 99.5, 99.9, 99.9	5.2, 8.9, 9.7, 9.8, 9.9, 10.0
7	101.6, 101.8, 101.9, 101.9	0.6, 0.9, 4.6, 4.9

^aRef. 95

Table 3.5. ^{13}C NMR Parameters of Isopropylidene Acetals ^a

Ring size	Acetal carbon	$\Delta\delta$ gem dimethyl
5	107.2, 107.4, 108.1, 108.1, 108.4, 108.5, 108.5, 108.7, 108.9, 108.9, 109.0, 109.2, 109.2, 109.4, 109.4, 109.5, 109.5, 109.6, 109.6, 109.7, 109.9, 110.3, 110.4, 110.5, 111.3, 111.4, 111.8, 112.1, 112.2, 112.3, 112.3, 112.8, 113.3, 114.9	0.5, 0.6, 0.6, 0.7, ≤ 1.2 , 1.3, 1.3, ≤ 1.5 , ≤ 1.5 , ≤ 1.5 , ≤ 1.6 , 1.7, 1.9, ≤ 2.1 , ≤ 2.3 , ≤ 2.4 , ≤ 2.7 , 2.9,
6	97.2, 97.8, 97.9, 98.2, 98.3, 98.4, 98.6, 98.7, 99.2, 99.6, 99.7, 100.0, 100.6, 100.9, 101.0	1.0, 9.7, 9.9, 10.0, 10.2, 10.3, 10.4, 10.5, 10.9
7	100.8, 100.9, 101.6, 101.7,	≤ 4.7 , ≤ 4.8

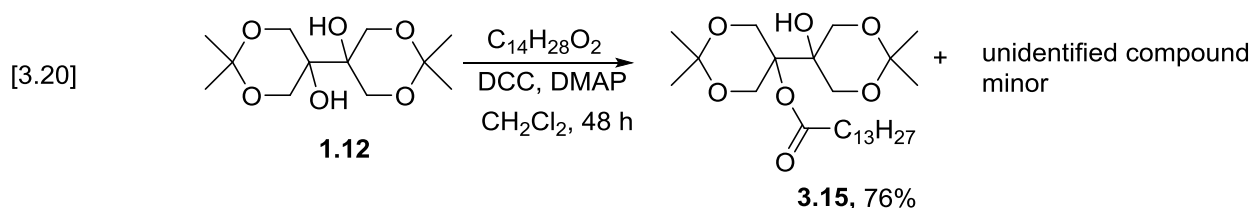
^a ref. 96

From these data, it is clear that no 6-membered cyclic acetals are present in any of the compounds at hand. Figure 3.10 strongly suggests the presence of a seven-membered cyclic acetal, with a peak at 101.6 ppm, and a five-membered cyclic acetal, with a peak at 110.1 ppm.

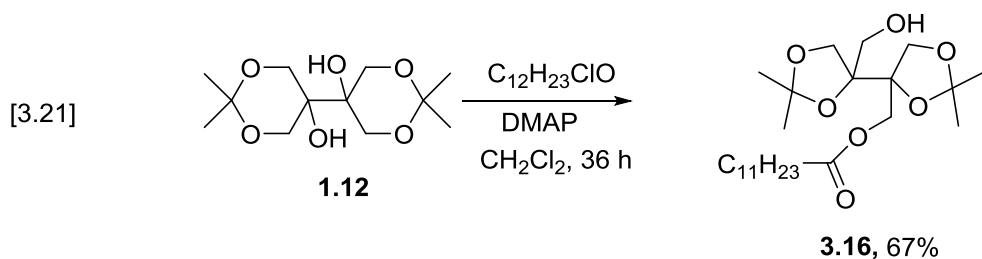
3.2.6. Acylation of acetonide pinacol 1.12 using long chain acid derivatives.

3.2.6.1 Stearic anhydride reaction: Initial attempt acylation of pinacol **1.12** with 5 equivalents of stearic anhydride $[\text{CH}_3(\text{CH}_2)_{16}\text{CO}]_2\text{O}$ and 5 mol% $\text{Ce}(\text{OTf})_3$ catalyzed reaction in dichloromethane at room temperature for 4 h. TLC showed more polar spots **A** and **B** (similar to acetylation) and new spot (expected product). After the starting material consumed by TLC, reaction mixture was quenched in water. It immediately produced a waxy (soap) type of substance. Extraction was very difficult; we couldn't go for further step.

3.2.6.2 Myristic acid reaction: Acylation of pinacol **1.12** with 2.5 equiv myristic acid $C_{14}H_{28}O_2$, DMAP (1 equiv), N,N' -dicyclohexylcarbodiimide (DCC) (3 equiv) in CH_2Cl_2 at rt. The reaction was monitored by TLC; pinacol **1.12** was not completely consumed after 48 hours. Despite that, we stopped the reaction after 48 h, did workup and got monoacylated myristic ester **3.15** with minor inseparable unidentified impurity as shown in eq [3.20].

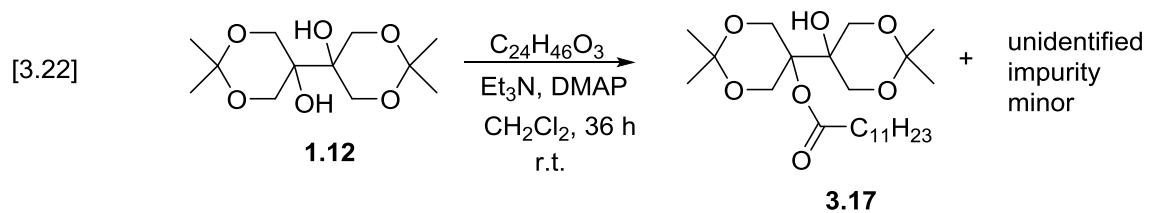


3.5.6.3 Lauroyl chloride reaction: Pinacol **1.12** was treated with 1.5 equiv of lauroyl chloride $CH_3(CH_2)_{10}COCl$ and 1.5 equiv of DMAP in CH_2Cl_2 at rt. The reaction was monitored with TLC; after 36 h of reaction still some starting material pinacol **1.12** was observed. Even though, we stopped reaction after 36 h, did workup and column chromatography, and we obtained rearranged mono acylated lauroyl ester **3.16** with 67% isolated yield see eq [3.21]. According to previous base catalyzed reactions, we should get non rearranged products, but in this case we are getting rearranged product **3.16**; it may be due to the absence of auxiliary base (Et_3N).



3.2.6.4 Lauric anhydride reaction: Pinacol **1.12** was treated with DMAP, Et_3N and lauric anhydride $C_{24}H_{46}O_3$ at room temp in CH_2Cl_2 . The reaction was monitored through TLC; after 36 h still some pinacol **1.12** was observed in TLC. Went for next step *i.e.*, workup.

Workup gave monoacylated lauroyl ester **3.17** with minor inseparable compound as shown in eq [3.22].



Although synthesis of the diacylated product with two fatty acid residues eluded us in the available time, we feel the problem is surmountable in the future by searching for more vigorous reaction conditions.

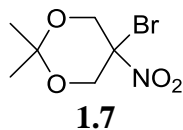
Experimental Section

Reactions were carried out under a nitrogen atmosphere, unless otherwise specified. All reagents and solvents were used as received from commercial sources, unless otherwise stated. Reagent-grade dichloromethane, benzene, and acetonitrile for solvent use was dried at least 24 h over 4 Å molecular sieves before use. ^1H and ^{13}C NMR spectra were obtained, usually at ambient temperature, on a Bruker Avance AV400 (400 MHz for proton 100.6 MHz for carbon) or AV600 (600 MHz for proton and 150.9 MHz for carbon) or AV250 (250 MHz for proton and 62.9 MHz for carbon) spectrometer. TMS was used as an internal chemical shift standard for all solvents except D_2O for ^1H spectra, while the center line of CDCl_3 , C_6D_6 , acetone- d_6 or CD_3CN was used as the chemical shift standard for ^{13}C spectra. NMR chemical shifts are reported as parts per million (ppm or δ), coupling constants are reported in Hz, and multiplicity as s (singlet), d (doublet), t (triplet), q (quartet), br (broad), and m (multiplet).

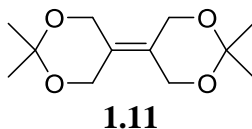
The reactions were monitored by thin layer chromatography (TLC) using 0.25 mm Sorbent Technologies pre-coated silica gel glass plates and visualized using a Mineralight UVGL-25 lamp or by allowing the plates to be covered by a mixture of iodine and silica gel in a closed jar or stained using an aqueous ceric ammonium molybdate (CAM) solution (Hanessian's stain). For the latter method, TLC plates were dipped, glass (back) side of plate wiped well, and heated from the back side of the plate using a hot air gun.

Column chromatography was performed using Scientific Adsorbents, Inc. silica gel. Gravity columns contained 63-200 μm particle size, 60 Å pore size silica gel. Flash columns contained 32-63 μm particle size, 60 Å pore size silica gel using eluents with the indicated solvent systems.

Mass spectral (MS) including high resolution (HRMS) and GC-MC data were obtained using either Waters Micromass GCT premier gc/ms, or Waters Micromass Q-ToF premier.

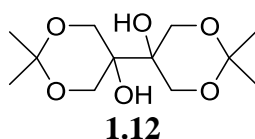


5-Bromo-2,2-dimethyl-5-nitro-1,3-dioxane, 1.7. To a mixture of bronopol (19.9 g, 99.5 mmol) and anhyd acetone (22.0 mL, 0.297 mol), $\text{BF}_3 \cdot \text{OEt}_2$ (12.5 mL, 0.101 mmol) was added dropwise over 10-15 mins at rt. The reaction mixture was stirred for 15 min at rt and quenched with 50 mL of ice-cold satd NaHCO_3 solution and stirred for 30 min. The mixture was filtered, washed with 50 mL of ice-cold water and dried in the air to yield **1.7** (20.3 mg, 85.2%). mp: 79-81 °C (lit mp 76-77 °C ^{6a}). The product was used without further purification. ^1H NMR (250 MHz, CDCl_3) δ 4.78 (d, $J = 13.5$ Hz, 2H), 4.27 (d, $J = 13.5$ Hz, 2H), 1.54 (s, 3H), 1.37 (s, 3H). ^{13}C NMR (63 MHz, CDCl_3) δ 99.6, 66.3, 28.1, 18.6.

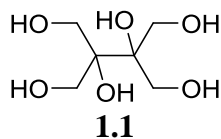


2,2,2',2'-Tetramethyl-[5,5']bi[1,3]dioxanylidene, 1.11. At rt, under N_2 , NaH (60% dispersion in mineral oil, washed repeatedly with hexane to remove mineral oil, filtered, 2.10 g, 87.5 mmol) was added slowly over 10 mins to 10 mL of N,N-dimethylacetamide (DMA). A solution of **1.7** (4.10 g, 17.0 mmol) in 10 mL of DMA was added dropwise over 10-15 mins to the stirred NaH suspension at rt. The reaction mixture was stirred at 80-85 °C (oil bath temperature) with monitoring by TLC (hexanes:EtOAc 4:1 (v/v), Hanessian's stain). After 4 h, reaction mixture was allowed to cool to rt, and quenched in ice-cold water (15 mL), extracted with anhyd diethyl ether (3 \times 25 mL). The combined organic extracts were washed with 30 mL of cold water, dried over anhyd Na_2SO_4 , filtered, and the solvent evaporated under reduced

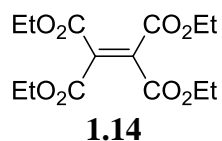
pressure. The residue was purified by silica gel flash chromatography (hexanes:EtOAc 4:1 (v/v)) to yield (1.07 g, 54.8%) of white solid, R_f of **1.11** = 0.26 ((hexanes:EtOAc 4:1 (v/v)). mp 133-135 °C. ^1H NMR (400 MHz, CDCl_3) δ 4.21 (s, 4H), 1.37 (s, 6H). ^{13}C NMR (100 MHz, CDCl_3) δ 125.8, 99.7, 58.9, 24.1.



5,5'-Dihydroxy-5,5'-bi(2,2-dimethyl-1,3-dioxane), 1.12.⁸ To a mixture of NaIO_4 (422 mg, 1.97 mmol) and $\text{CeCl}_3 \cdot 7\text{H}_2\text{O}$ (50.0 mg, 0.134 mmol), 0.45 mL of water was added and gently heated until a bright yellow suspension was formed. The suspension was cooled to 0 °C. EtOAc 1.25 mL and acetonitrile 1.50 mL were added and stirred for 5 min. RuCl_3 (5.2 mg, 25 μmol) was added followed by addition of a solution of **1.11** (300 mg, 1.31 mmol) in 5 mL EtOAc in one portion. The reaction was stirred and monitored by TLC (hexanes:EtOAc 4:1(v/v), Hanessian's stain). After being stirred for 8 h, Na_2SO_4 (500 mg) was added, stirred for 5 min, the solid filtered off, the filtrate washed with 3 mL conc aq Na_2SO_3 solution. The organic layer was dried over Na_2SO_4 , filtered, and solvent was removed under reduced pressure. The residue was purified by silica gel flash chromatography (hexanes:EtOAc 3:2(v/v)) to yield 203 mg (59.2%) of **1.12** as a white solid, R_f of **1.12** = 0.17 (hexanes:EtOAc 3:2(v/v)), mp 188-190 °C. ^1H NMR (600 MHz, CDCl_3) δ 4.19 (d, J = 12.0 Hz, 4H), 3.54 (d, J = 12.0 Hz, 4H), 3.29 (s, 2H), 1.43 (s, 6H), 1.39 (s, 6H). ^{13}C NMR (151 MHz, CDCl_3) δ 98.7, 69.2, 64.5, 27.3, 19.9. HRMS (ESI⁺): m/z Calculated for $\text{C}_{11}\text{H}_{19}\text{O}_6$ ($\text{M}^+ - \text{CH}_3$) 247.1182, found 247.1359.



2,3-Bis(hydroxymethyl)butane-1,2,3,4-tetraol, 1.1. To a solution of **1.12** (255 mg, 0.972 mmol) in 5 mL aq THF (THF:H₂O 4:1(v/v)), trifluoroacetic acid (401 μ L, 59.5 mg, 5.22 mmol) was added at 0 °C. The mixture was stirred at rt for 3 h with monitoring by TLC (hexanes:EtOAc 1:1(v/v)). The solution was evaporated under reduced pressure to yield a colorless oil. The oil solidified after several days, yielding **1.1** (124 mg, 70.1 %). ¹H NMR (400 MHz, D₂O) δ 3.69 (s). ¹³C NMR (100 MHz, D₂O) δ 76.9, 61.8.

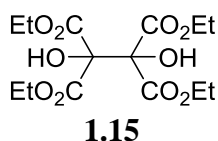


Tetraethyl ethene-1,1,2,2-tetracarboxylate, 1.14. *Method 1:*^{7a} A mixture of Na₂CO₃ (20.0 g, 0.188 mol) and ethyl bromomalonate (30.1 g, 0.125 mol) was heated for 3 h at 150-160 °C. After the heating period, 40 mL of toluene was added while contents of the flask were still hot. The reaction mixture was allowed to reach rt and 50 mL of water was added. The mixture was extracted with EtOAc (3 \times 25 mL). Combined organic layers were washed with brine (20 mL) and dried over Na₂SO₄, filtered, and the filtrate was vacuum distilled. The fore-run up to 170 °C/15 mm Hg was discarded. The product, which was collected at 170-230 °C/15 mm Hg solidified within about 15 min, gave 9.31 g **1.14** (23.5% yield), mp 52-54 °C (lit mp 52.5-53.5 °C). The compound was recrystallized from 95% absolute ethanol. *R_f* = 0.65 (hexanes:EtOAc 3:2(v/v)). ¹H NMR (400 MHz, CDCl₃) δ 4.29 (q, *J* = 7.2 Hz, 8H), 1.29 (t, *J* = 7.2 Hz, 12H). ¹³C NMR (100 MHz, CDCl₃) δ 162.6, 135.6, 62.3, 14.0.

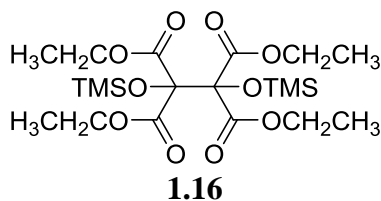
Method 2:^{7b} A mixture of diethyl bromomalonate (2.41 g, 10.1 mmol) and NaOH (0.410 g, 10.3 mmol) was taken in vial and rotated back and forth for 2 h using a motor from a Kugelrohr apparatus at 130 °C. After 2 h, the residue was washed with 10 mL of water and extracted with

EtOAc (3 × 10 mL), the solvent evaporated *in vacuo*, and the residue purified with column chromatography (hexanes:EtOAc 3:2(v/v)) to yield **1.14** (0.140 g, 4.38%). mp 49-52 °C

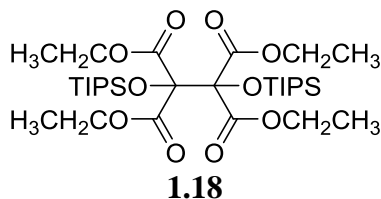
Method 3:^{7c} To a stirred solution of diethylmalonate (168 mg, 1.04 mmol) in anhydrous THF (10 mL) under a nitrogen atmosphere, t-BuOK (561 mg, 4.99 mmol) was added. To this mixture, a solution of NBS (889 mg, 4.99 mmol) in anhydrous THF (15 mL) was added dropwise over 10-15 min. The reaction mixture was stirred overnight at rt. The solvent was removed on the rotary evaporator, the residue quenched in 40 mL of water, extracted with CH₂Cl₂ (3 × 10 mL), and the solvent evaporated *in vacuo*. The residue was purified by column chromatography (hexanes:EtOAc 3:2 (v/v)) to yield **1.14** (1.5 mg, 4.5%).



Tetraethyl 1,2-dihydroxyethane-1,1,2,2-tetracarboxylate, 1.15.⁸ To a mixture of NaIO₄ (588 mg, 2.74 mmol) and CeCl₃·7H₂O (65.4 mg, 176 μmol), 0.45 mL of water was added and gently heated until a bright yellow suspension was formed. The suspension was cooled to 0 °C, EtOAc (1.75 mL) and acetonitrile (2 mL) were added and stirred for 5 min. RuCl₃ (21.7 mg, 101 μmol) was added followed by addition of olefin **1.14** (550 mg, 1.74 mmol) in 5 mL EtOAc in one portion. The reaction was monitored by TLC (hexanes:EtOAc 3:2(v/v)). After being stirred for 12 h, Na₂SO₄ (500 mg) was added, stirred for 5 min, the solid filtered, and the filtrate washed with 4 mL of conc aq Na₂SO₃ solution. The organic layer was dried over Na₂SO₄, filtered, and solvent removed under reduced pressure. The residue was purified with silica gel flash chromatography (hexanes:EtOAc 3:2(v/v)) to yield **1.15** (366 mg, 60.1%) as a colorless oil. *R_f* = 0.32 (hexanes:EtOAc 3:2(v/v)). ¹H NMR (400 MHz, CDCl₃) δ 4.78 (s, 2H), 4.25 (q, *J* = 7.2 Hz, 8H), 1.25 (t, *J* = 7.2 Hz, 12H). ¹³C NMR (100 MHz, CDCl₃) δ 167.8, 80.7, 63.3, 13.9.

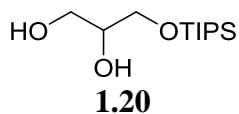


Tetraethyl 1,2-bis(trimethylsilyloxy)ethane-1,1,2,2-tetracarboxylate, 1.16. Under N₂, triethylamine (5.0 mL, 36 mmol) was added to a stirred solution of diol **1.15** (350 mg, 0.999 mmol) in CH₂Cl₂ (5 mL). The reaction mixture was cooled to 0 °C in an ice bath and TMSOTf (0.73 mL, 4.0 mmol) was added over 30 s via syringe, with reaction monitoring by TLC (hexanes:EtOAc 4:1(v/v)). After being stirred at 0 °C for 45 min, the reaction was quenched with 5 mL conc NaHCO₃ solution and extracted with CH₂Cl₂ (3 × 25 mL). The organic phase was washed with brine (20 mL), dried over MgSO₄, filtered, concentrated *in vacuo*, and subjected to flash chromatography on silica gel (hexanes:EtOAc 4:1(v/v)) to yield **1.16** (332 mg, 67.2%) as a colorless oil. *R_f* = 0.74 (hexanes:EtOAc 4:1(v/v)). ¹H NMR (600 MHz, CDCl₃) δ 4.21- 4.10 (m, 8H), 1.25 (t, *J* = 7.2 Hz, 12H), 0.09 (s, 18H). ¹³C NMR (151 MHz, CDCl₃) δ 168.0, 85.4, 61.9, 14.0, 1.53.

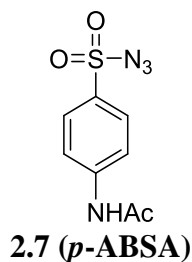


Tetraethyl 1,2-di(triisopropylsilyloxy)ethane-1,1,2,2-tetracarboxylate, 1.18. Triethylamine (5.50 mL, 39.4 mmol) was added to a stirred solution of diol **1.15** (350 mg, 0.999 mmol) in CH₂Cl₂ (5 mL). The reaction mixture cooled to 0 °C in an ice bath and TIPSOTf (1.0 mL, 3.9 mmol) was added over 1 min via syringe. The reaction was monitored by TLC (hexanes:EtOAc 4:1(v/v)). The reaction was left overnight (12 h), quenched with 5 mL conc NaHCO₃ solution, and extracted with CH₂Cl₂ (3 × 25 mL). The organic phase was washed with brine (20 mL),

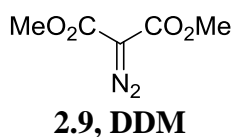
dried over MgSO_4 , filtered, concentrated *in vacuo*. The residue was subjected to flash chromatography on silica gel (hexanes:EtOAc 4:1(v/v)) to yield **1.18** (492 mg, 74.5%) as light golden oil. $R_f = 0.63$ (hexanes:EtOAc 4:1(v/v)). ^1H NMR (400 MHz, CDCl_3) δ 4.26 - 4.17 (m, 8H), 1.25 (t, $J = 7.2$ Hz, 12H), 1.04 - 1.02 (m, 42H, $\text{CH}_3\text{-CSi}$ and CH-Si). ^{13}C NMR (100 MHz, CDCl_3) δ 168.2, 73.7, 61.9, 17.8, 14.2, 12.2. HRMS (ESI+): m/z Calculated for $\text{C}_{32}\text{H}_{63}\text{O}_{10}\text{Si}_2$ ($\text{M}^+ + \text{H}$) 663.0080, found 663.0083.



3-Triisopropylsiloxypropane-1,2-diol, 1.20. LiAlH_4 (22.8 mg, 600 μmol) was slowly added to anhydrous THF (2 mL) in a round bottom flask. To this was added **1.18** (50 mg, 75 μmol) in 2 mL of anhydrous THF over 5 min. After the addition was completed, the mixture was heated to reflux for 1 h with monitoring by TLC (hexanes:EtOAc 4:1(v/v)). After 1 h, the mixture was cooled to 0 $^\circ\text{C}$ in an ice bath, and quenched by cautious sequential addition of 22 mL of water, 22 mL of 15% NaOH, and 66 mL of water. Reaction mixture stirred for 30 min at 0 $^\circ\text{C}$ then allowed to reach to rt. The resulting white solid was vacuum filtered and washed on the filter using total 45 mL ether in 10 mL portions. The filtrate was concentrated under reduced pressure. The residue was purified by column chromatography (hexanes:EtOAc 3:2(v/v)) to yield 15.6 mg **1.20**, 83.4% yield, as a light gold oil. $R_f = 0.15$ (hexanes:EtOAc 3:2(v/v)) with KMnO_4 stain. ^1H NMR (600 MHz, CDCl_3) δ 3.79 - 3.60 (m, 5H), 2.66 (br, 1H), 2.14 (br, 1H), 1.12 - 1.03 (m, 21H, $\text{CH}_3\text{-CSi}$ and CH-Si). ^{13}C NMR (151 MHz, CDCl_3) δ 73.7, 65.3, 64.3, 18.2, 12.0. HRMS (ESI+): m/z Calculated for $\text{C}_{12}\text{H}_{29}\text{O}_3$ ($\text{M}^+ + \text{H}$) 249.1886, found 249.1887.

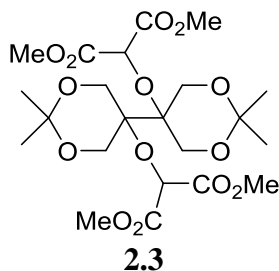


***p*-Acetamidobenzenesulfonyl azide, 2.7.** To a suspension of *p*-acetamidobenzenesulfonyl chloride (24.5 g, 0.11 mol) in CH₂Cl₂ (250 mL) containing tetrabutylammonium iodide (0.29 g, 0.79 mmol) at 0 °C, a solution of sodium azide (7.99 g, 0.122 mol), in water (25 mL) was added dropwise and stirred for 24 h at rt. The organic layer was separated, washed with water (2 × 50 mL), brine (50 mL) and dried over anhydrous Na₂SO₄. Solvent was removed on the rotary evaporator to yield colorless crystalline solid **2.7** (24.0 g, 96.1%) mp 108-109 °C (Lit. mp 106 - 108 °C).³⁹

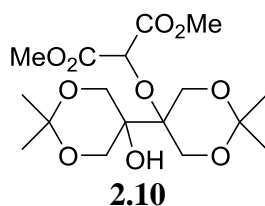


Dimethyl diazomalonate (DDM), 2.9. Under N₂, triethylamine (11.0 g, 0.108 mol) was added dropwise over 20-30 min to a stirred solution of dimethyl malonate (7.20 g, 54.5 mmol) and *p*-acetamidobenzenesulfonyl azide (15.0 g, 62.4 mmol) in acetonitrile (300 mL) at 0 °C. The mixture was allowed to reach rt and stirred for 16 h. The mixture was filtered and solvent was evaporated under reduced pressure. The residue was washed with hexanes:EtOAc (1:1(v/v)), filtered, and the solvent removed on the rotary evaporator to yield golden yellow oily crude product. This was purified with silica gel flash column chromatography (hexanes:EtOAc 4:1(v/v)). This gave a light yellow oil **2.9** (7.3 g, 85%). *R_f* = 0.30 (hexanes:EtOAc 4:1 (v/v)). Stored in a freezer, **2.9** solidified but at rt, it melted. ¹H NMR (400 MHz, CDCl₃) δ_H 3.85 (s). ¹³C

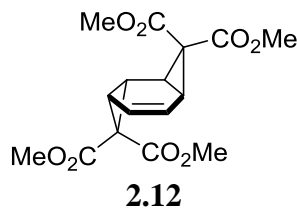
NMR (100 MHz, CDCl₃) δ_C 52.2 (CH₃), 65.5, 161.2. HRMS (ESI⁺): m/z Calculated for C₅H₆N₂O₄ (M⁺ + H) 159.0506, found 159.0388.



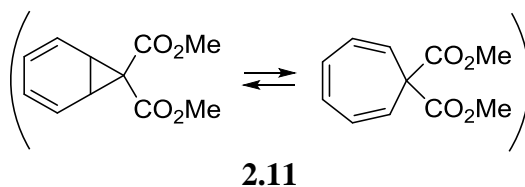
5,5'-Bis(di(methoxycarbonyl)methoxy)-bi(2,2-dimethyl-1,3-dioxane), 2.3. To an oven-dried round bottomed flask under N₂, a mixture of diol **1.12** (27.1 mg, 0.103 mmol), DDM **2.9** (113 mg, 0.714 mmol, 6.9 equiv), Rh₂(OAc)₄ (3.2 mg, 7.2 μ mol) and 3 mL of dry benzene was added and refluxed 1 h. The reaction was monitored by TLC (hexanes:EtOAc 4:1(v/v)). After TLC indicated DDM consumption, the reaction mixture was allowed to reach rt and filtered. The filtrate was evaporated *in vacuo*, and the residue was purified three times by silica gel column chromatography. The first column (hexanes:EtOAc 4:1(v/v)) was to remove products **2.12** and **2.11**. $R_f = 0.55$ (hexanes:EtOAc 4:1(v/v)). These products are UV visible on TLC. The second column with CH₂Cl₂:acetonitrile 9:1(v/v) gave a mixture of **2.3**, unidentified impurity and **2.13** with same R_f values in TLC: $R_f = 0.65$ (CH₂Cl₂/ acetonitrile 9:1(v/v)), and **2.10** (2.2 mg, 5.4%), ($R_f = 0.55$ (CH₂Cl₂/ acetonitrile 9:1(v/v))). The third column used hexanes:EtOAc 1:1(v/v) to yield pure **2.3** (7.1 mg, 12%). ¹H NMR (600 MHz, C₆D₆) δ_H 6.36 (s, 2H), 4.95 (d, $J = 13.2$ Hz, 4H), 3.97 (d, $J = 13.2$ Hz, 4H), 3.33 (s, 12H), 1.46 (s, 6H), 1.40 (s, 6H). ¹³C NMR (151 MHz, C₆D₆) δ_C 168.4, 98.8, 76.2, 75.2, 63.4, 52.5, 28.8, 19.3.



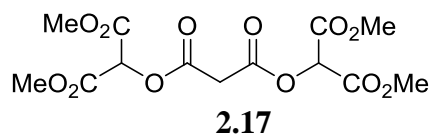
2,2-Dimethyl-5-(dimethoxycarbonyl)methoxy)-5-(2,2-dimethyl-5-hydroxy-1,3-dioxan-5-yl)-1,3-dioxane, 2.10. ^1H NMR (400 MHz, C_6D_6) δ_{H} 6.26 (s, 1H), 4.58 (d, $J = 12.0$ Hz, 2H), 4.46 (d, $J = 13.2$ Hz, 2H), 3.95 (d, $J = 13.2$ Hz, 2H), 3.55 (d, $J = 12.0$ Hz, 2H), 3.45 (s, 1H), 3.33 (s, 6H), 1.39 (s, 3H), 1.33 (s, 3H), 1.32 (s, 3H), 1.25 (s, 3H). ^{13}C NMR (100 MHz, C_6D_6) δ_{C} 168.5, 98.8, 98.6, 75.8, 75.4, 70.4, 64.5, 63.4, 52.4, 28.5, 27.7, 20.0, 19.3.



NMR parameters agree with previously reported data.⁴⁰ ^1H NMR (250 MHz, CDCl_3) δ 5.71 (m, 2H), 3.75 (s, 6H), 3.74 (s, 6H), 2.50 (d, $J = 9.5$ Hz, 2H), 2.02 (d, $J = 9.5$ Hz, 2H). ^{13}C NMR (62.9 MHz, CDCl_3) δ 169.2, 166.0, 122.8, 52.9, 52.6, 42.3, 25.6, 24.9.

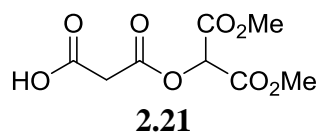


NMR parameters agree with previously reported data.⁴⁰ ^1H NMR (400 MHz, C_6D_6) δ 6.22 (m, 2H), 6.21 (m, 2H), 5.21 (d, $J = 8.0$ Hz, 2H), 3.35 (s, 6H); ^1H NMR (250 MHz, CDCl_3) δ 6.47 (m, 2H), 6.38 (m, 2H), 5.04 (dd, $J = 7.4, 0.8$ Hz, 2H), 3.69 (s, 6H); ^{13}C NMR (62.9 MHz, CDCl_3) δ 169.3, 128.9, 126.2, 100.04, 51.4, 53.1.

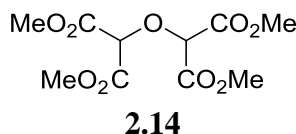


Bis(di(methoxycarbonyl)methyl) malonate, 2.17. To an oven-dried round bottomed flask under N_2 , a mixture of malonic acid (104 mg, 0.999 mmol), DDM **2.9** (348 mg, 2.20 mmol, 2.2 equiv), $\text{Rh}_2(\text{OAc})_4$ (9.0 mg, 22 μmol) and 2 mL dry benzene was added and refluxed for 1 h,

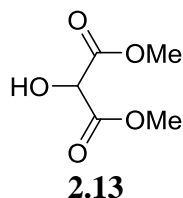
monitoring the reaction via TLC (hexanes:EtOAc 4:1(v/v)). After TLC indicated DDM consumption, the reaction mixture was allowed to reach to rt and filtered. The filtrate was evaporated *in vacuo* to yield a mixture of expected **2.17** and unexpected **2.21** and **2.14** products as a light yellow oil. Separation of products was done by silica gel column chromatography (CH₂Cl₂/acetonitrile 4:1(v/v)), which gave **2.17** and **2.14** as an inseparable mixture (**2.17**:**2.14** was 95:5 by ¹H NMR area integration) as colorless oil 300 mg $R_f = 0.59$ (CH₂Cl₂/acetonitrile 4:1(v/v)) and also **2.21** as oil, 7 mg $R_f = 0.22$ (broad crescent-shaped spot) (CH₂Cl₂/acetonitrile 4:1(v/v)). Purification of **2.17** and **2.14** was difficult, because these compounds have the same R_f values. After several attempts of mobile systems, THF:hexanes combinations worked but gave mediocre separation. Ultimately, purification was achieved by silica gel column chromatography with THF:hexanes 1:2(v/v) (R_f (**2.17**) = 0.06 and R_f (**2.14**) = 0.09) slowly switched to THF/hexanes 1:1 v/v. **2.17**: ¹H NMR (600 MHz, CDCl₃) δ_H 5.56 (s, 2H), 3.78 (s, 12H), 3.34 (s, 2H). ¹H NMR (600 MHz, CD₃CN) δ_H 5.56 (s, 2H), 3.78 (s, 12H), 3.72 (s, 2H). ¹³C NMR (151 MHz, CDCl₃) δ_C 164.3 (CO), 164.2 (CO), 72.2 (CH), 53.6 (CH₃), 39.9 (CH₂). ¹³C NMR (151 MHz, CD₃CN) δ_C 165.1 (CO), 165.3 (CO), 73.4 (CH), 54.1 (CH₃), 40.7 (CH₂). HRMS (ESI+): m/z Calculated for C₁₃H₁₆O₁₂Na (M⁺ +Na) 387.0539, found 387.0538.



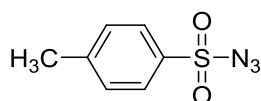
¹H NMR (600 MHz, CDCl₃) δ_H 6.01 (br, 1H), 5.60 (s, 1H), 3.82 (s, 12H), 3.58 (s, 2H). ¹³C NMR (151 MHz, CDCl₃) δ_C 169.9 (CO), 165.2 (CO), 164.4 (CO), 72.3 (CH), 53.7 (CH₃), 40.4 (CH₂); HRMS (ESI+): m/z Calculated for C₈H₁₁O₈ (M⁺ +H) 235.0454, found 235.0461.



Tetramethyl 2,2'-oxybis(malonate), 2.14. ^1H NMR (600 MHz, CDCl_3) δ_{H} 4.90 (s, 2H), 3.76 (s, 12H). ^{13}C NMR (151 MHz, CDCl_3) δ_{C} 166.2 (CO), 77.2 (CH), 53.3 (CH_3) ^1H NMR (600 MHz, CD_3CN) δ_{H} 4.85 (s, 2H), 3.75 (s, 12H). ^{13}C NMR (151 MHz, CD_3CN) δ_{C} 167.1 (CO), 78.5 (CH), 53.7 (CH_3); HRMS (ESI+): m/z Calculated for $\text{C}_{10}\text{H}_{14}\text{O}_9$ ($\text{M}^+ + \text{H}$) 279.0716, found 279.0714.

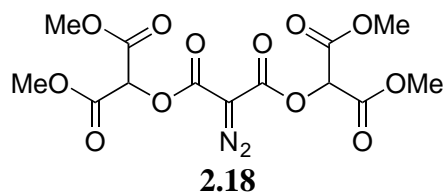


Dimethyl 2-hydroxymalonate, 2.13. ^1H NMR (600 MHz, CDCl_3) δ_{H} 4.70 (d, $J = 7.8$ Hz, 1H), 3.87 (s, 6H), 3.52 (d, $J = 7.8$ Hz, 1H). ^{13}C NMR (151 MHz, CDCl_3) δ_{C} 169.1, 71.6, 53.6. HRMS (ESI+): m/z Calculated for $\text{C}_5\text{H}_8\text{O}_5\text{Na}$ ($\text{M}^+ + \text{Na}$) 171.0269, found 171.0281.



***p*-Toluenesulfonyl azide (TsN_3)**

In an Erlenmeyer flask, to the solution of NaN_3 (0.38 g, 5.83 mmol) in 1 mL water was added 1 mL acetone. *p*-Toluenesulfonyl chloride (1.03 g, 5.40 mmol) dissolved in 5 mL acetone was added to the reaction mixture and stirred for 2 h at rt. Solvent was evaporated on the rotary evaporator, the residue transferred to a separatory funnel containing 5 mL water, and shaken vigorously. The organic layer was dried over Na_2SO_4 , filtered, and placed under high vacuum to afford 0.89 g (83%) TsN_3 as a colorless oil, which was stored in the freezer (solidifies to white solid). ^1H NMR (400 MHz, CDCl_3) δ 7.76 (d, $J = 8.2$ Hz, 2H), 7.40 (d, $J = 8.2$ Hz, 2H), 2.43 (s, 3H). ^{13}C NMR (100 MHz, CDCl_3) δ 146.2, 135.4, 130.2, 127.3, 21.4.



Attempt to synthesize diazo compound 2.18 using *p*-ABSA and Et₃N. Under N₂, to a stirred solution of **2.17** (1.09 g, 2.99 mmol), *p*-ABSA (783 mg, 3.26 mmol) in acetonitrile solvent at 0 °C, triethylamine (0.87 mL, 6.24 mmol) was added dropwise over 15-20 min. The reaction was allowed to reach rt and stirred for 16 h. The mixture was filtered and filtrate was evaporated on the rotary evaporator. An orange gummy substance was obtained. The gummy substance was dissolved in CH₂Cl₂, and the clear solution was stirred. Over 5 min a precipitate formed. It was filtered and the filtrate was evaporated on the rotary evaporator, giving rise to the gummy substance again. Silica gel column chromatography (CH₂Cl₂:acetonitrile 4:1(v/v)) was intended to remove any sulfonamide byproduct. A second chromatography column with EtOAc:hexanes 1:2(v/v) switching to EtOAc:hexanes 1:1(v/v) gave a substance which had the NMR spectra shown in Figures 2.11 and 2.12. The overall yield was very low (7.5 mg, 6.5%). Calculated yield was based on the assumption the product formed was **2.18**.

Attempt to synthesize diazo compound 2.18 using *p*-ABSA and DBU. Under N₂, to a solution of **2.17** (364 mg, 1.00 mmol) and *p*-ABSA (270 mg, 1.12 mmol) in 100 mL dry CH₂Cl₂ was added DBU (0.20 mL, 1.34 mmol) and the reaction mixture stirred at rt for 16 h. TLC (hexanes:EtOAc 1:1(v/v)) showed several close spots. To the reaction mixture water was added and extracted with 3 × 100 mL CH₂Cl₂, the combined organic layer washed with water, dried over MgSO₄, filtered, and the solvent evaporated on the rotary evaporator. Residue was subjected to 3 successive flash chromatography columns: hexanes:EtOAc 2:1(v/v),

hexanes:EtOAc 1:1(v/v), and (CH₂Cl₂:acetonitrile 4:1(v/v)). A yellow solid, 7 mg, was obtained. The NMR spectra of this material are similar to NMR spectra shown in Figures 2.11 and 2.12.

Attempt to synthesize diazo compound 2.18 using TsN₃ and Et₃N. Under N₂, tosyl azide (198 mg, 1.00 mmol) and Et₃N (0.15 mL, 1.1 mmol) was added to a mixture of **2.17** (365 mg, 1.00 mmol) and MeCN at room temperature. The mixture was stirred for 16 h. After being stirred for 16 h, reaction mixture concentrated under rotary evaporator, obtained orange gummy substance. TLC (hexanes:EtOAc 1:1(v/v)) showed several close spots in TLC (EtOAc\hexanes 1:1 v/v). Purification was achieved by four successive flash chromatography columns: 1) hexanes:EtOAc 1:1(v/v), 2) hexanes:EtOAc 1:2(v/v), 3) CH₂Cl₂:acetonitrile 3:2(v/v), and 4) CH₂Cl₂:acetonitrile 4:1(v/v), and yielded 10 mg of a solid material. ¹H NMR (600 MHz, CDCl₃) δ 14.28 (s, 1H), 5.76 (s, 1H), 3.93 (s, 3H), 3.88 (s, 3H), 3.82 (s, 9H), 3.76 (s, 3H). ¹³C NMR (151 MHz, CDCl₃) δ 166.5, 164.0, 162.1, 160.7, 160.6, 152.6, 129.8, 100.2, 72.6, 53.6, 53.22, 53.16, 53.0.

Attempt to synthesize diazo compound 2.18 using TsN₃ and K₂CO₃. Under N₂, **2.17** (368 mg, 1.01 mmol) was dissolved in anhyd acetonitrile, 5 mL, and solid K₂CO₃ (139 mg, 1.00 mmol) was added. TsN₃ (198 mg, 1.00 mmol) in acetonitrile 4 mL was added to the reaction mixture and stirred 16 h at rt. Ether 8 mL was added to precipitate the salts, and the mixture was filtered, filter cake was washed with ether 10 mL, and organic solvents were removed on the rotary evaporator. A gummy orange substance was obtained. It gave several close spots in TLC (EtOAc:hexanes 1:1(v/v)). To the gummy orange substance was added 30-40 mL EtOAc:hexanes 1:1(v/v) extracted thrice, obtained yellow color solution and evaporated the organic solvent under rotary evaporator. Two successive flash chromatography columns 1) hexanes:EtOAc 1:2(v/v) and 2) CH₂Cl₂\acetonitrile 4:1(v/v) gave a golden yellow solid. 10.1

mg. The NMR spectra of this material are similar to NMR spectra shown in Figures 2.11 and 2.12

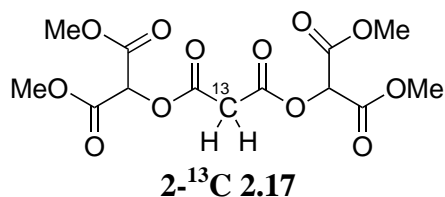
Attempt to synthesize diazo compound 2.18 using ADMC and Et₃N. Under N₂, to a solution of 2-chloro-1,3-dimethylimidazolium chloride (ADMC) (2.02 g, 11.9 mmol) in acetonitrile 10 mL, sodium azide (0.780 g, 11.9 mmol) was added at 0 °C, and the mixture was stirred for 30 mins. Compound **2.17** (3.64 g, 9.99 mmol) and Et₃N (4.16 mL, 29.8 mmol) in 10 mL THF was added to the mixture. The reaction was stirred at rt for 10-15 min with monitoring by TLC (hexanes:EtOAc 1:1(v/v)). Several close spots were observed. The reaction was quenched with 20 mL of water, and organic material was extracted with CH₂Cl₂ (3 × 20 mL), combined extracts were washed with 15 mL brine, 15 mL water, and then dried over Na₂SO₄. The solvent was removed on the rotary evaporator. ¹H NMR of the crude product appeared to be a composite of Figures 2.11 and 2.14. The crude product was subjected to three successive flash chromatography columns 1) hexanes:EtOAc 1:1(v/v), 2) hexanes:EtOAc 2:1(v/v), 3) hexanes:EtOAc 3:2(v/v) which yielded 15.1 mg yellow solid. ¹H NMR of the product was nearly identical to Figure 2.14.

Blank reaction. Serial addition of sub-stoichiometric amounts of base. To **2.17** (30.1 mg, 82.4 μmol) in CDCl₃ solvent in an NMR tube was added at rt Et₃N (0.11 μL, 10 mol%), shaken well and the NMR spectrum recorded. To the same tube Et₃N (0.05 μL, 5 mol%) was added, shaken well and the NMR spectrum recorded. Once again to the same NMR tube Et₃N (0.06 μL, 6 mol%) was charged and the NMR spectrum recorded.

Blank reaction. Time course study. To **2.17** (40.5 mg, 0.111 mmol) in CD₃CN solvent in an NMR tube was added at rt Et₃N (30 μL, 0.22 mmol), shaken well, and the NMR spectrum recorded 5 min, 2 h, and 16 h later.

Blank reaction. Deprotonation-reprotonation test. In an NMR tube, to **2.17** (37.6 mg, 0.103 mmol) in CD₃CN solvent at rt, Et₃N (27 μL, 0.19 mmol) was added, shaken well and the NMR spectrum recorded. To this NMR tube was added CF₃COOH (17 μL, 0.22 mmol), shaken well, and the NMR spectrum recorded.

Blank reaction. Larger scale trial. Under N₂, **2.17** (121 mg, 332 μmol) in acetonitrile 4 mL was cooled to 0 °C. Triethylamine (96 μL, 0.69 mmol) was added dropwise over 3-4 min to the mixture and stirred for 5-10 min with monitoring by TLC (CH₂Cl₂:acetonitrile 4:1(v/v)). After 5 min the solvent was evaporated on the rotary evaporator. Flash chromatography on silica gel (CH₂Cl₂:acetonitrile 4:1(v/v)) gave 40.1 mg (0.270 mmol) of dimethyl 2-hydroxymalonate **2.13**. *R_f* of **2.13** = 0.58 (CH₂Cl₂:acetonitrile 4:1(v/v)). ¹H NMR (600 MHz, CDCl₃) δ_H 4.70 (d, *J* = 7.8 Hz, 1H), 3.87 (s, 6H), 3.52 (d, *J* = 7.8 Hz, 1H). ¹³C NMR (151 MHz, CDCl₃) δ_C 169.1, 71.6, 53.6. HRMS (ESI+): *m/z* Calculated for C₅H₈O₅Na (M⁺ + Na) 171.0269, found 171.0281.



¹³C labeled Bis(di(methoxycarbonyl)methyl) malonate, 2-¹³C 2.17. To an oven-dried round bottomed flask under N₂, a mixture of 2-¹³C malonic acid (156 mg, 1.48 mmol, 99% ¹³C enrichment), DDM **2.9** (520 mg, 3.29 mmol), Rh₂(OAc)₄ (14.6 mg, 33.0 μmol) and 5 mL dry benzene was added and refluxed 1 h, with monitoring by TLC (hexanes:EtOAc 4:1(v/v)). After DDM consumption was indicated by TLC, the reaction mixture was allowed to reach to rt and filtered. Volatiles were removed from the filtrate *in vacuo* to yield a mixture of expected 2-¹³C **2.17** and unexpected 2-¹³C **2.21** and 2-¹³C **2.14** as a light yellow oil. Separation of products done

by silica gel column chromatography (CH₂Cl₂:acetonitrile 4:1(v/v)). This gave 2-¹³C **2.17** and 2-¹³C **2.14** as an inseparable mixture: a colorless oil, 450 mg *R_f* = 0.60 (CH₂Cl₂:acetonitrile 4:1(v/v)). Also obtained was 2-¹³C **2.21** as an oil 12 mg *R_f* = 0.23 (broad crescent shaped spot) (CH₂Cl₂:acetonitrile 4:1(v/v)). ¹H NMR (600 MHz, CDCl₃) δ_H 5.63 (s, 2H), 3.75 (d, *J* = 133 Hz, 2H), 3.85 (s, 12H). ¹³C NMR (151 MHz, CDCl₃) δ_C 164.3, 164.4 (d, *J* = 60 Hz), 72.7, 53.6, 40.1 (gigantic s peak).

Acylation studies (Chapter 3)

Each acylation procedure below is referenced to an entry in Table 3.1, 3.2, or 3.3; *e.g.* “3.2.7” would indicate Table 3.2, entry 7. All reactions were performed under an atmosphere of N₂. All chromatography employed silica gel. Two eluent systems were used: *e1*, hexanes:EtOAc 4:1(v/v); and *e2*, hexanes:EtOAc 3:2(v/v).

The procedures used to obtain the data in Tables 3.1 and 3.2 are repetitive. Each procedure consists of the same series of general steps, namely: *i*) mixing of reagents, *ii*) reaction, *iii*) quench, and *iv*) work-up. Within each type of general step, there were relatively few protocols employed. For example, there were only two ways the reagents were mixed. Therefore those specific protocols are given letters **A** and **B**. The full list of protocols is given below.

<i>Mixing</i>	A: Lewis acid added to a mixture of 1.12 and anhydride; no solvent. B: Anhydride added to solution of 1.12 in CH ₂ Cl ₂ . Lewis acid added last.
<i>Reaction</i>	C: Stir at rt for a length of time, monitor by TLC using eluent <i>e1</i> or <i>e2</i> . D: Stir at 0 °C for a length of time, monitor by TLC using eluent <i>e1</i> or <i>e2</i> .
<i>Quench</i>	E: A volume of H ₂ O at rt added to reaction, stir for a length of time. F: A volume of ice-cold H ₂ O added to reaction, stir for a length of time. G: A volume of satd aq NaHCO ₃ added to reaction, stir for a length of time.
<i>Work-up</i>	H: Extract (number of times × volume) with CH ₂ Cl ₂ . I: Wash with a volume of H ₂ O. J: Dry over solid drying agent, filter, remove solvent under reduced pressure (rotary evaporator) K: Purification by flash chromatography with eluent <i>e1</i> or <i>e2</i> , or “no” if chromatography was not performed.

To condense the descriptions, we use the following system. The entire procedure is described by listing the appropriate letters, *i.e.* the procedures actually used, with actual data included. For example, to report that a reaction was stirred for 1 h with TLC monitoring using eluent system *e2*, one would write | **C:** 1 h, *e2* |. Likewise, a reaction that was quenched by addition of 8 mL ice water followed by stirring for 15 min would appear as | **F:** 8 mL, 15 min |.

Detailed procedures, using the condensed notation where possible, follow. After those, spectral data and other parameters for compounds isolated as pure substances are presented.

Entry 3.1.1. **A:** Ce(OTf)₃ (1.17 mg, 1.99 μmol, 0.997 mol% rel to **1.12**), **1.12** (52.41 mg, 199.8 μmol), Ac₂O (1.50 mL, 15.8 mmol, [Ac₂O]/[**1.12**] = 79.1) | **C:** 1 h, *e2* | **F:** 10 mL, 5 min | **H:** 2 × 10 mL | **I:** 3 mL | **J:** Na₂SO₄ | **K:** no. Product: 58.70 mg white solid, a mixture of *meso*-**3.5** and *dl*-**3.5**, 84.8% yield.

Entry 3.1.2. **B:** **1.12** (10.01 mg, 38.16 μmol) in CH₂Cl₂ (2 mL), Ac₂O (20.0 μL, 0.211 mmol, [Ac₂O]/[**1.12**] = 5.52), Ce(OTf)₃ (1.12 mg, 1.91 μmol, 5.00 mol% rel to **1.12**) | **C:** 5 s | **E:** 2 mL, 5 min | **H:** 2 × 6 mL | **I:** 3 mL | **J:** MgSO₄ | **K:** no. Product: 7.10 mg recovered **1.12**.

Entry 3.1.3. B: 1.12 (26.14 mg, 99.66 μmol) in CH_2Cl_2 (2 mL), Ac_2O (49.4 μL , 0.520 mmol, $[\text{Ac}_2\text{O}]/[\mathbf{1.12}] = 5.22$), $\text{Ce}(\text{OTf})_3$ (2.93 mg, 4.98 μmol , 5.00 mol% rel to **1.12**) | **C**: 0.5 h | **E**: 2 mL, 5 min | **H**: 2×6 mL | **I**: 3 mL | **J**: MgSO_4 | **K**: no. Product: 33.4 mg of a white solid, mixture of two unidentified compounds having R_f values on TLC (*e2*) much smaller than that of **1.12**.

Entry 3.1.4. B: 1.12 (20.10 mg, 76.63 μmol) in CH_2Cl_2 (2 mL), Ac_2O (36.2 μL , 0.381 mmol, $[\text{Ac}_2\text{O}]/[\mathbf{1.12}] = 4.98$), $\text{Ce}(\text{OTf})_3$ (2.25 mg, 3.83 μmol , 5.00 mol% rel to **1.12**) | **C**: 3 h, *e2* | **E**: 2 mL, 5 min | **H**: 2×3 mL | **I**: 3 mL | **J**: MgSO_4 | **K**: *e2*. Product: white solid, a mixture of *meso*-**3.5**, *dl*-**3.5**, and **3.6**.

Entry 3.1.5. B: 1.12 (10.30 mg, 39.26 μmol) in CH_2Cl_2 (2 mL), Ac_2O (21.0 μL , 0.221 mmol, $[\text{Ac}_2\text{O}]/[\mathbf{1.12}] = 5.80$), $\text{Ce}(\text{OTf})_3$ (46.9 mg, 79.9 μmol , 2.04 mol% rel to **1.12**) | **C**: 3 h | **E**: 2 mL, 5 min | **H**: 2×6 mL | **I**: 3 mL | **J**: MgSO_4 | **K**: no. Product: white solid a mixture of *meso*-**3.5**, *dl*-**3.5**, and **3.6**.

Entry 3.1.6. A: Sc(OTf)₃ (0.38 mg, 0.77 μmol , 1.0 mol% rel to **1.12**), **1.12** (20.01 mg, 76.29 μmol), Ac_2O (0.60 mL, 6.3 mmol, $[\text{Ac}_2\text{O}]/[\mathbf{1.12}] = 83$) | **C**: 1 h, *e2* | **G**: $T = 0$ °C, 5 mL | **H**: 2×10 mL | **J**: MgSO_4 | **K**: *e2*. Product: (crude) 30.3 mg white solid, a mixture of *meso*-**3.5**, *dl*-**3.5**, and **3.6**. Total weight 30.9 mg. Flash column chromatography (*e2*) of crude yielded 19.8 mg *meso*-**3.6** and *dl*-**3.5**.

Entry 3.1.7. B: 1.12 (20.91 mg, 79.72 μmol) in 2 mL CH_2Cl_2 , Ac_2O (37.8 μL , 0.398 mmol, $[\text{Ac}_2\text{O}]/[\mathbf{1.12}] = 5.00$), $\text{Sc}(\text{OTf})_3$ (2.01 mg, 4.08 μmol , 5.12 mol%) in 1 mL CH_2Cl_2 | **C**: 1 h, *e2* | **G**: 2 mL | **H**: 2×10 mL | **J**: MgSO_4 | **K**: *e2*. Product: 22.89 mg white solid, a mixture of *meso*-**3.5** and *dl*-**3.5**, 82.9% yield.

Entry 3.1.8. | B: 1.12 (20.0 mg, 76.2 μmol) in 2 mL CH_2Cl_2 , Ac_2O (40 μL , 0.42 mmol, $[\text{Ac}_2\text{O}]/[\mathbf{1.12}] = 5.5$), $\text{BF}_3 \cdot \text{OEt}_2$ (20 μL , 0.16 mmol, $[\text{BF}_3 \cdot \text{OEt}_2]/[\mathbf{1.12}] = 2.1$) | **C**: 5 s | **F**: 4 mL,

15 min | **H**: 2 × 10 mL | **I**: 2 mL satd aq NaHCO₃, then 3 mL H₂O | **J**: Na₂SO₄ | **K**: e2. Product: 16.4 mg of white solid, a mixture of *meso*-**3.5**, and *dl*-**3.5**, 62.1% yield.

Entry 3.1.9. A: BF₃·OEt₂ (0.49 μL, 4.0 μmol, 5.0 mol% rel to **1.12**), **1.12** (20.91 mg, 79.72 μmol), Ac₂O (0.60 mL, 6.3 mmol, [Ac₂O]/[**1.12**] = 79) | **C**: 5 s | **F**: 8 mL, 15 min | **H**: 2 × 6 mL | **I**: 5 mL satd aq NaHCO₃, then 3 mL H₂O | **J**: Na₂SO₄ | **K**: e2. Product: white solid, a mixture of *meso*-**3.5**, *dl*-**3.5**, and **3.6**.

Entry 3.1.10. B: A solution of 2.22 g (9.99 mmol) TMSOTf in 10.0 mL CH₂Cl₂ was prepared. T = 0 °C. **1.12** (20.01 mg, 76.29 μmol) in CH₂Cl₂ (2 mL), Ac₂O (38.12 μL, 0.4016 mmol, [Ac₂O]/[**1.12**] = 5.264), 0.999 M TMSOTf solution (3.82 μL, 3.82 μmol, 5.01 mol% rel to **1.12**) | **D**: 3 h, e2 | **G**: 2 mL | **H**: 2 × 10 mL | **I**: 3 mL | **J**: MgSO₄ | **K**: e2. Product: 17.09 mg white solid **3.6**, 57.39% yield.

Entry 3.1.11. | B: T = 0 °C; **1.12** (9.99 mg, 37.7 μmol) in CH₂Cl₂ (2 mL), Ac₂O (20.1 μL, 0.212 mmol, [Ac₂O]/[**1.12**] = 5.62), 0.99 M TMSOTf (see Entry 2.10) (1.91 μL, 1.91 μmol, 5.0 mol%) | **D**: 3 h, e2 | **G**: 2 mL | **H**: 2 × 10 mL | **I**: 3 mL | **J**: MgSO₄ | **K**: no. Total weight 8.3 mg (**3.6+C**).

Entry 3.1.12. | B: T = 0 °C; **1.12** (10.03 mg, 38.24 μmol) in CH₂Cl₂ (2 mL), Ac₂O (20.0 μL, 0.212 mmol, [Ac₂O]/[**1.12**] = 5.55), TMSOTf (13.8 μL, 76.47 μmol, 200 mol% rel to **1.12**) | **D**: 5 s | **G**: 2 mL | **H**: 2 × 5 mL | **I**: 3 mL | **J**: MgSO₄ | **K**: no. Total weight 9.2 mg (**3.6+ A**)

Entry 3.1.13. | B: T = 0 °C; **1.12** (13.12 mg, 50.02 μmol) CH₂Cl₂ Ac₂O (25 μL, 0.26 mmol, [Ac₂O]/[**1.12**] = 5.3), TMSOTf (20 μL, 0.11 mmol, 220 mol% rel to **1.12**) | **C**: | **D**: 5 h, e2 | **G**: 5 mL | **H**: 2 × 6 mL | **J**: MgSO₄ | **K**: e2. Product: 12.94 mg white solid, **3.6**, 66.27% yield.

Entry 3.1.14. B: 1.12 (20.90 mg, 79.68 μmol) in CH_2Cl_2 (2 mL), Ac_2O (40 μL , 0.42 mmol, $[\text{Ac}_2\text{O}]/[\mathbf{1.12}] = 5.3$), $\text{Cu}(\text{OTf})_2$ (1.5 mg, 4.1 μmol , 5.2 mol% rel to **1.12**) | **C:** 1 h, *e2* | **G:** 2 mL | **H:** 2×3 mL | **I:** 3 mL | **J:** Na_2SO_4 | **K:** *e2*. Product: white solid, mixture of *meso-3.5*, *dl-3.5*, and **3.6**.

Entry 3.1.15. A: 1.12 (20.8 mg, 79.3 μmol), Ac_2O (0.60 mL, 6.3 mmol, $[\text{Ac}_2\text{O}]/[\mathbf{1.12}] = 79$), $\text{Cu}(\text{OTf})_2$ (0.31 mg, 0.86 μmol , 1.1 mol% rel to **1.12**) | **C:** 1 h, *e2* | **E:** 8 mL | **H:** 2×3 mL | **I:** 2 mL satd aq NaHCO_3 , then 3 mL H_2O | **J:** MgSO_4 | **K:** *e2*. Product: 22.10 mg white solid, mixture of *meso-3.5*, *dl-3.5*, 80.1% yield.

Entry 3.2.1. A: $\text{Ce}(\text{OTf})_3$ (0.5 mg, 0.9 μmol , 1 mol% rel to **1.12**), **1.12** (20.04 mg, 76.40 μmol); TFAA (0.58 mL, 4.1 mmol, $[\text{TFAA}]/[\mathbf{1.12}] = 54$) | **C:** 1 h, *e2* | **F:** 10 mL | **H:** 2×10 mL | **I:** 3 mL | **J:** Na_2SO_4 | **K:** no. Product: 20.06 mg white solid, mixture of *meso-3.7* and *dl-3.7*, 57.8% yield.

Entry 3.2.2. B: 1.12 (20.12 mg, 76.71 μmol) in CH_2Cl_2 (2 mL), TFAA (59 μL , 0.42 mmol, $[\text{TFAA}]/[\mathbf{1.12}] = 5.4$), $\text{Ce}(\text{OTf})_3$ (2.10 mg, 3.57 μmol , 4.66 mol% rel to **1.12**) | **C:** 1 h, *e2* | **F:** 2 mL | **H:** 2×6 mL | **I:** 3 mL | **J:** MgSO_4 | **K:** *e1*. Product: 22.5 mg white solid, mixture of *meso-3.7* and *dl-3.7*, 64.6% yield.

Entry 3.2.3. B: 1.12 (20.11 mg, 76.66 μmol), TFAA (0.60 mL, 8.9×10^{-1} g, 4.2 mmol, $[\text{TFAA}]/[\mathbf{1.12}] = 55$), $\text{Sc}(\text{OTf})_3$ (0.40 mg, 0.81 μmol , 1.1 mol%) | **C:** 1 h, *e2* | **G:** 5 mL, added to cooled reaction mixture, dilute with 10 mL H_2O , separate organic layer | **J:** MgSO_4 | **K:** *e1*. Product: 31.3 mg white solid, mixture of *meso-3.7* and *dl-3.7*, 89.8% yield.

Entry 3.2.4. B: 1.12 (20.02 mg, 76.32 μmol), TFAA (53.6 μL , 0.379 mmol, $[\text{TFAA}]/[\mathbf{1.12}] = 4.97$) in CH_2Cl_2 (2 mL), $\text{Sc}(\text{OTf})_3$ (2.02 mg, 4.10 μmol , 5.38 mol%) in CH_2Cl_2 (1 mL) | **C:** 1 h,

e2 | **G**: 2 mL | **H**: 2 × 10 mL | **J**: MgSO₄ | **K**: *el*. Product: 23.10 mg white solid, mixture of *meso*-**3.7** and *dl*-**3.7**, 66.6% yield.

Entry 3.2.5. A: BF₃·OEt₂ (0.1 μL, 0.8 μmol, 1 mol%), **1.12** (20.19 mg, 76.97 μmol), TFAA (0.57 mL, 4.04 mmol, [TFAA]/[**1.12**] = 52) | **C**: 5 s | **F**: 8 mL, 15 min | **H**: 2 × 6 mL | **I**: 5 mL satd aq NaHCO₃, then 3 mL H₂O | **J**: Na₂SO₄ | **K**: *e2*. Product: 15.71 mg white solid, a mixture of *meso*-**3.7** and *dl*-**3.7**, 44.9% yield.

Entry 3.2.6. B: **1.12** (20.11 mg, 76.67 μmol) in 2 mL CH₂Cl₂, TFAA (58 μL, 0.41 mmol, [TFAA]/[**1.12**] = 5.4), BF₃·OEt₂ (0.5 μL, 4 μmol, 5 mol% rel to **1.12**) | **C**: 5 s | **F**: 4 mL, 15 min | **H**: 2 × 10 mL | **I**: 2 mL | **J**: Na₂SO₄ | **K**: *e2* Product: white solid, a mixture of *meso*-**3.7**, *dl*-**3.7**, and **3.8**. Total weight 12.8 mg (**3.7** and **3.8**).

Entry 3.2.7. B: **1.12** (20.13 mg, 76.74 μmol) in 2 mL CH₂Cl₂, TFAA (57 μL, 0.40 mmol, [TFAA]/[**1.12**] = 5.3), BF₃·OEt₂ (20 μL, 0.16 mmol, 2.1 × 10² mol% rel to **1.12**) | **C**: 5 s | **F**: 4 mL, 15 min | **H**: 2 × 10 mL | **I**: 2 mL satd aq NaHCO₃, then 3 mL H₂O | **J**: Na₂SO₄ | **K**: *el*. Product: white solid, a mixture of *meso*-**3.7**, *dl*-**3.7**, and **3.8**. Total weight 13.62 mg ((**3.7** and **3.8**)).

Entry 3.2.8. B: T = 0 °C, **1.12** (20.98 mg, 79.98 μmol) in CH₂Cl₂ (2 mL), TFAA (54.0 μL, 0.382 mmol, [TFAA]/[**1.12**] = 4.78), TMSOTf (0.72 μL, 3.9 μmol, 5.0 mol% rel to **1.12**) | **D**: 1 h, *e2* | **G**: 2 mL | **H**: 2 × 10 mL | **I**: 3 mL | **J**: MgSO₄ | **K**: *el*. Product: 14.17 mg white solid, a mixture of *meso*-**3.7** and *dl*-**3.7**. 39.0% yield.

Entry 3.2.9. A: T = 0 °C **1.12** (20.14 mg, 76.78 μmol), TFAA (57 μL, 0.40 mmol, [TFAA]/[**1.12**] = 5.3), 1.0 M TMSOTf in CH₂Cl₂ (prepared by dissolving 2.22 g TMSOTf (9.99 mmol) in 10 mL CH₂Cl₂) (0.76 μL, 0.76 μmol, 0.99 mol% rel to **1.12**) | **D**: 1 h, *e2* | **G**: 5 mL | **H**:

2 × 6 mL | **J**: MgSO₄ | **K**: *el*. Product: 17.58 mg white solid, a mixture of *meso*-**3.7** and *dl*-**3.7**, 50.40% yield.

Entry 3.2.10. B: **1.12** (20.14 mg, 76.78 μmol) in CH₂Cl₂ (2 mL), TFAA (57 μL, 0.40 mmol, [TFAA]/[**1.12**] = 5.3), Cu(OTf)₂ (1.4 mg, 3.9 μmol, 5.0 mol% rel to **1.12**) | **C**: 1 h, *e2* | **G**: 2 mL | **H**: 2 × 6 mL | **I**: 3 mL | **J**: Na₂SO₄ | **K**: *el*. Product: 20.54 mg white solid, a mixture of *meso*-**3.7** and *dl*-**3.7**, 58.8% yield.

Entry 3.2.11. A: Cu(OTf)₂ (0.31 mg, 0.86 μmol, 1.1 mol% rel to **1.12**), **1.12** (20.15 mg, 76.82 μmol), TFAA (0.59 mL, 4.2 mmol, [TFAA]/[**1.12**] = 54) | **C**: 1 h, *e2* | **F**: 8 mL | **H**: 2 × 6 mL | **I**: 3 mL | **J**: MgSO₄ | **K**: *el*. Product: 22.31 mg white solid, a mixture of *meso*-**3.7** and *dl*-**3.7**, 63.9% yield.

Entry 3.3.1. To a mixture of diol **1.12** (20.91 mg, 79.72 μmol) and CH₂Cl₂ (2 mL) at rt, DMAP (2.10 mg, 17.9 μmol, 22.4 mol%) was added, followed by addition of Et₃N (45 μL, 0.32 mmol) and acetic anhydride (31 μL, 0.33 mmol). The reaction was stirred at rt until the starting material was consumed, monitored through TLC, *e2*. After being stirred for 16 h, reaction mixture filtered through short silica gel column *e2*, evaporated the solvent under reduced pressure to yield **3.9** and **3.10** as white solid in the ratio of 33:67 (from NMR data). *R_f* of **3.9** = 0.71 (*e2*); *R_f* of **3.10** = 0.61 (*e2*).

Entry 3.3.2. To a mixture of **1.12** (27 mg, 0.10 mmol), and DMAP (2.50 mg, 20.5 μmol) at rt, Et₃N (54 μL, 0.38 mmol) was added, followed by acetic anhydride (40 μL, 0.42 mmol). The reaction was stirred at rt until the starting material was consumed, monitored through TLC (*e2*). After being stirred for 16 h, reaction mixture was filtered through a short silica gel column (*e2*), the solvent evaporated under reduced pressure to yield **3.9**, **3.10**, and **3.6** as a white solid in the ratio of 53:42:5 (from NMR data). *R_f* of **3.9** = 0.71; *R_f* of **3.10** = 0.61; and *R_f* of **3.11** = 0.45 (*e2*).

Entry 3.3.3. To a solution of **1.12** (26.20 mg, 0.099 mmol) in CH₂Cl₂ (2 mL) at rt DMAP (2.4 mg, 19.64 μmol) was added, followed by addition of Et₃N (55 μL, 0.39 mmol) and acetic anhydride (41 μL, 0.43 mmol). The reaction mixture was refluxed (40-45 °C) until the starting material was consumed, monitored through TLC (*e2*). After being stirred for 16 h, the reaction mixture was filtered through a short silica gel column (*e2*), the solvent evaporated under reduced pressure to yield a white solid, **3.9** and **3.10** in the ratio of 52:48 (from ¹H NMR data). *R_f* of **3.9** = 0.71; *R_f* of **3.10** = 0.61 (*e2*).

Entry 3.3.4. To **1.12** (14.70 mg, 56.04 μmol) at rt, DMAP (1.38 mg, 11.29 μmol, 20.1 mol%) was added, followed by addition of Et₃N (30 μL, 0.21 mmol) and acetic anhydride (22 μL, 0.23 mmol). The reaction mixture was stirred at 40-45 °C until the starting material was consumed, monitored through TLC (*e2*). After being stirred for 16 h, the reaction mixture was filtered through a short silica gel column (*e2*), the solvent evaporated under reduced pressure to yield a white solid, **3.9**, **3.10**, and **3.6** in the ratio of 57:20:23 (from ¹H NMR data). *R_f* of **3.9** = 0.71, *R_f* of **3.10** = 0.61 and *R_f* of **3.6** = 0.45 (*e2*).

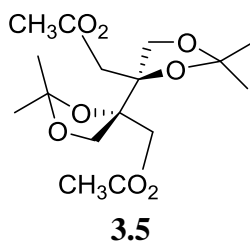
Entry 3.3.5. *Preparation of MgBr₂*:^{83a} Under N₂ atmosphere, 1,2-dibromoethane (1.41 mL, 16.4 mmol) was added dropwise to a suspension of dry THF (60 mL) and magnesium turnings (1.21 g, 49.7 mmol). The reaction mixture was slowly heated to 45 °C in an oil bath. The reaction mixture stirred for 3 h at 45 °C, then allowed to cool to rt. The clear upper solution was transferred to a dry flask via cannula (nitrogen pressure), the precipitate was washed with dry THF, and the THF was transferred into the same flask and the combined solution was diluted to 81.5 mL (0.2 M, assuming quantitative conversion of 1,2-dibromoethane to MgBr₂). The solution was stored under nitrogen; the shelf life of this solution is one month.

Acylation: Under N₂ stream, anhydrous MgBr₂/THF (1.98 mL of 0.2 M solution, 0.39 mmol) was evaporated. To the resulting solid, dry CH₂Cl₂ (1 mL) was added and the solution was cannula transferred into a round bottom flask containing acetic anhydride (37 μL, 0.39 mmol). Triethylamine (84 μL, 0.60 mmol) was added to the reaction mixture followed by addition of diol **1.12** (26.1 mg, 0.999 mmol). The reaction mixture was stirred at rt with monitoring by TLC (*e2*). After being stirred for 28 h, the reaction mixture was quenched with 2 mL water, and extracted with 3 × 4 mL CH₂Cl₂. The organic layer was dried over MgSO₄ and evaporated under reduced pressure. The residue was purified by silica gel flash chromatography (*e2*) to afford a white solid, **3.10** and **3.11** as an inseparable mixture in the ratio of 52:48. *R_f* of **3.10** and **3.11** = 0.61 (*e2*).

Characterization of isolated pure products in acylation studies

R_f of **3.5** = 0.69 and *R_f* of **3.6** = 0.45 (*e2*).

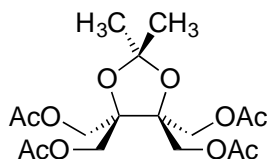
R_f of **3.7** = 0.65 and *R_f* of **3.8** = 0.45 (*e1*).



dl-**4,4'**-Di(acetoxymethyl)-**4,4'**-bi(2,2-dimethyl-1,3-dioxolane), *dl*-**3.5**. This diastereomer of **3.5** has a slightly higher *R_f* than the *meso* diastereomer. ¹H NMR (400 MHz, CDCl₃) δ 4.33 (d, *J* = 12.0 Hz, 2H), 4.23 (d, *J* = 9.2 Hz, 2H), 3.95 (d, *J* = 12.0 Hz, 2H), 3.85 (d, *J* = 9.2 Hz, 2H), 2.06 (s, 6H), 1.44 (s, 6H), 1.36 (s, 6H). ¹³C NMR (150 MHz, CDCl₃) δ 170.5, 110.5, 83.2, 68.2, 66.2, 27.8, 26.6, 21.1. HRMS (ESI⁺): *m/z*. Calculated for C₁₅H₂₃O₈ (M⁺ - CH₃) 331.1393, found

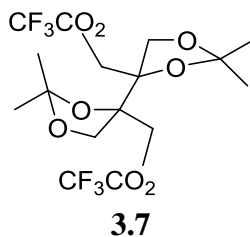
331.1427. A crystal for X-ray crystallography was obtained by recrystallizing with hexanes solvent and sticking fridge for 24 h, obtained sugar type of crystal. The crystal was triclinic $a = 9.3149(3) \text{ \AA}$, $b = 9.4281(3) \text{ \AA}$, $c = 10.3077(4)$, $\alpha = 86.8309(11)^\circ$, $\beta = 79.3853(11)^\circ$, $\gamma = 78.9062(10)^\circ$. $\lambda = 0.71073 \text{ \AA}$, $T = 180 \text{ K}$, $Z = 2$. $P -1$. $R(\text{gt}) = 0.0620$; $wR2(\text{all}) = 0.1190$; goodness of fit 1.144. Full details are in the Appendix.

***meso*-4,4'-Di(acetoxymethyl)-4,4'-bi(2,2-dimethyl-1,3-dioxolane), *meso*-3.5.** ^1H NMR (600 MHz, CDCl_3) δ 4.17 (AB q, $J = 3 \text{ Hz}$, 4H), 4.04 (d, $J = 9 \text{ Hz}$, 2H), 3.95 (d, $J = 9.2 \text{ Hz}$, 2H), 2.05 (s, 6H), 1.42 (s, 6H), 1.41 (s, 6H). ^{13}C NMR (100 MHz, CDCl_3) δ 170.5, 110.7, 83.3, 67.7, 64.6, 27.3, 26.2, 21.1. HRMS (ESI+): m/z Calculated for $\text{C}_{15}\text{H}_{23}\text{O}_8$ ($\text{M}^+ - \text{CH}_3$) 331.1398, found 331.1362. A crystal for X-ray crystallography was obtained by growing crystal with slow evaporation technique in EtOAc solvent, obtained needles. The crystal was triclinic $a = 5.6722(8) \text{ \AA}$, $b = 8.9777(12) \text{ \AA}$, $c = 9.6075(13)$, $\alpha = 113.3108(14)^\circ$, $\beta = 94.5970(15)^\circ$, $\gamma = 102.9913(15)^\circ$. $\lambda = 0.71073 \text{ \AA}$, $T = 180 \text{ K}$, $Z = 1$. Space group $P -1$. $R(\text{gt}) = 0.0425$; $wR2(\text{all}) = 0.1130$; goodness of fit 1.0825. Full details are in the Appendix.



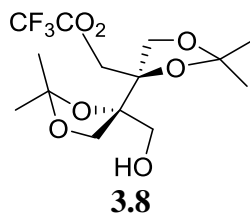
3.6

4,4,5,5-Tetrakis(acetoxymethyl)-2,2-dimethyl-1,3-dioxolane, 3.6. ^1H NMR (600 MHz, CDCl_3) δ 4.27, 4.32 (AB q, $J = 12 \text{ Hz}$, 8H), 2.09 (s, 12H), 1.49 (s, 6H). ^{13}C NMR (151 MHz, CDCl_3) δ 170.4, 110.8, 83.6, 62.0, 30.0, 21.0. HRMS (ESI+): m/z Calculated for $\text{C}_{16}\text{H}_{23}\text{O}_{10}$ ($\text{M}^+ - \text{CH}_3$) 375.1291, found 375.1280.

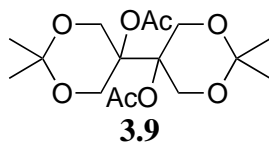


***meso* and *dl*-4,4'-Bis(trifluoroacetoxymethyl)-4,4'-bi(2,2-dimethyl-1,3-dioxolane), 3.7, higher R_f material.** ^1H NMR (600 MHz, CDCl_3) δ 4.67 (d, $J = 12.0$ Hz, 2H), 4.26 (d, $J = 9.6$ Hz, 2H), 4.25 (d, $J = 12.0$ Hz, 2H), 3.90 (d, $J = 9.6$ Hz, 2H), 1.43 (s, 6H), 1.37 (s, 6H). ^{13}C NMR (151 MHz, CDCl_3) NMR δ 156.9 (q), 114.5 (q), 111.4, 82.4, 68.3, 67.7, 27.3, 27.0.

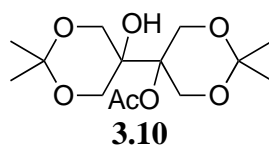
***meso* and *dl*-4,4'-Bis(trifluoroacetoxymethyl)-4,4'-bi(2,2-dimethyl-1,3-dioxolane), 3.7, lower R_f material.** ^1H NMR (600 MHz, CDCl_3) δ 4.47 (d, $J = 11.4$ Hz, 2H), 4.35 (d, $J = 11.4$ Hz, 2H), 4.08 (d, $J = 9.6$ Hz, 2H), 3.97 (d, $J = 9.6$ Hz, 2H), 1.43 (s, 6H), 1.42 (s, 6H). ^{13}C NMR (151 MHz, CDCl_3) δ 156.9 (q), 114.5 (q), 111.4, 82.3, 67.3, 66.8, 26.5, 25.9.



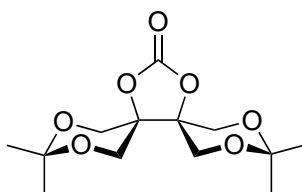
4-Trifluoroacetoxymethyl-4'-hydroxymethyl-4,4'-bi(2,2-dimethyl-1,3-dioxolane), 3.8. ^1H NMR (600 MHz, CDCl_3) δ 4.68 (d, $J = 12.0$ Hz, 2H), 4.33 (d, $J = 12.0$ Hz, 2H), 4.24 (d, $J = 9.6$ Hz, 2H), 4.20 (d, $J = 9$ Hz, 2H), δ 3.93 (d, $J = 9.6$ Hz, 2H), 3.83 (d, $J = 9.6$ Hz, 2H), 3.72 (d, $J = 12.0$ Hz, 2H), 3.61 (br d, $J = 10.2$ Hz, 2H), 1.43 (s, 3H), 1.42 (s, 3H), 1.37 (s, 6H). ^{13}C NMR (151 MHz, CDCl_3) NMR δ 157.1 (q), 114.6 (q), 110.7, 110.3, 82.3, 82.9, 68.8, 68.1, 67.9, 67.6, 27.9, 27.3, 26.6. HRMS (ESI+): m/z Calculated for $\text{C}_{13}\text{H}_{18}\text{O}_7\text{F}_3$ ($\text{M}^+ - \text{CH}_3$) 343.1005, found 343.0962.



5,5'-Diacetoxy-5,5'-bi(2,2-dimethyl-1,3-dioxane), 3.9. ^1H NMR (600 MHz, CDCl_3) δ 4.38 (d, $J = 13.2$ Hz, 4H), 3.96 (d, $J = 13.2$ Hz, 4H), 2.02 (s, 6H), 1.35 (s, 6H), 1.34 (s, 6H). ^{13}C NMR (151 MHz, CDCl_3) δ 170.8, 100.3, 84.7, 62.8, 23.5, 23.21, 22.18; HRMS (ESI $^+$): m/z Calculated for $\text{C}_{16}\text{H}_{26}\text{O}_8\text{Na}$ ($\text{M}^+ + \text{Na}$) 369.1525, found 369.1537.



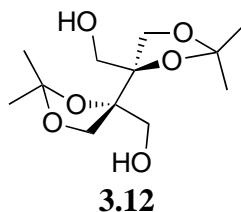
5'-Acetoxy-5-hydroxy-5,5'-bi(2,2-dimethyl-1,3-dioxane), 3.10. ^1H NMR (600 MHz, CDCl_3) δ 4.67 (s, 1H), 4.24 (d, $J = 13.2$ Hz, 2H), 4.04 (d, $J = 13.2$ Hz, 2H), 3.96 (d, $J = 12.60$ Hz, 2H), 3.59 (d, $J = 12.60$ Hz, 2H), 2.15 (s, 3H), 1.41 (s, 3H), 1.38 (s, 3H), 1.37 (s, 3H), 1.35 (s, 3H). ^{13}C NMR (151 MHz, CDCl_3) δ 173.6, 99.5, 99.2, 86.2, 70.8, 65.2, 61.9, 25.6, 24.1, 23.0, 22.1, 21.6. HRMS (ESI $^+$): m/z Calculated for $\text{C}_{14}\text{H}_{24}\text{O}_7\text{Na}$ ($\text{M}^+ + \text{Na}$) 327.1420, found 327.1421.



3,3,13,13-Tetramethyl-2,4,7,9,12,14-hexaoxa-8-oxodispiro[5.3.5.0]pentadecane, 3.11. ^1H NMR (400 MHz, CDCl_3) δ 4.16 (d, $J = 12.6$ Hz, 4H), 3.92 (d, $J = 12.6$ Hz, 4H), 1.46 (s, 6H), 1.43 (s, 6H). ^{13}C NMR (151 MHz, CDCl_3) δ 151.8, 99.6, 79.2, 61.9, 23.7, 23.0; HRMS (ESI $^+$): m/z Calculated for $\text{C}_{13}\text{H}_{21}\text{O}_7$ ($\text{M}^+ + \text{H}$) 289.1287, found 289.1375.

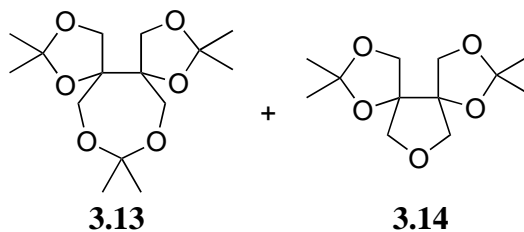
Reactions related to study of acylation

Blank reaction of 3.5 with Ce(OTf)₃ over long times. To a solution of **3.5** (16.10 mg, 61.38 μmol) in CH_2Cl_2 (5 mL), $\text{Ce}(\text{OTf})_3$ (1.36 mg, 2.31 μmol) was added. The reaction mixture was stirred at rt for 2 weeks with monitoring by TLC (hexanes:EtOAc 3:2(v/v)). No reaction was observed; starting material was not consumed at all.

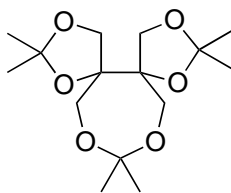


4,4'-Di(hydroxymethyl)-4,4'-bi(2,2-dimethyl-1,3-dioxolane), 3.12. To a solution of **1.12** (57.1 mg, 0.217 mmol) in CH_2Cl_2 (5 mL), $\text{Ce}(\text{OTf})_3$ (6.37 mg, 10.8 μmol) was added. The reaction mixture was stirred at rt for 30 min with monitoring by TLC (hexanes:EtOAc 3:2(v/v)). After 30 min, the reaction mixture was quenched with 5 mL water, and stirred for 5 min. The mixture was extracted with 3 \times 10 mL CH_2Cl_2 , the combined organic phase was washed with 5 mL water, dried over MgSO_4 and the solvent removed on the rotary evaporator, affording 46.9 mg of a mixture of **A** and **B**. The residue underwent flash chromatography with switching slowly from hexanes:EtOAc 4:1(v/v) to hexanes:EtOAc 3:2(v/v) to yield two fractions: one fraction a mixture of **A** and **B**, the other pure **B** (\equiv **3.12**). R_f of **A** = 0.07 and R_f of **B** = 0.06 hexanes:EtOAc 3:2(v/v). **B**: ^1H NMR (600 MHz, CDCl_3) δ 4.21 (d, J = 9.6 Hz, 2H), 4.06 (d, J = 9.6 Hz, 2H), 3.95 (d, J = 9.0 Hz, 2H), 3.93 (d, J = 9.6 Hz, 2H), 3.76 (d, J = 4.8 Hz, 2H), 3.74 (d, J = 4.8 Hz, 2H), 3.71 (dd unresolved, J = 4.2 Hz, 1.2 Hz, 4H) 1.47 (br s, 6H), 1.46 (br s, 6H), 1.42 (s, 12H). ^{13}C NMR (151 MHz, CDCl_3) δ 110.8, 110.1, 84.7, 84.6, 68.5, 68.2, 65.5, 64.9, 27.8, 27.5, 26.7, 26.2. HRMS (ESI⁺): m/z Calculated for $\text{C}_{12}\text{H}_{20}\text{O}_6\text{Na}$ (M^+ + Na) 285.1314, found 285.1313

LAH reduction of 3.5 to 3.12 : LiAlH₄ (8.54 mg, 0.225 mmol) was slowly added to anhydrous THF (2 mL) in a round bottom flask. To this was added **3.5** (25.5 mg, 73.6 μmol) in 2 mL of anhydrous THF over 5 min. After the addition was completed, the mixture was heated to reflux for 1 h with monitoring by TLC (hexanes:EtOAc 3:2(v/v)). After 45 min, the mixture was cooled to 0 °C in an ice bath, and quenched by cautious sequential addition of 9 mL of water, 9 mL of 15% NaOH, and 27 mL of water. Reaction mixture stirred for 30 min at 0 °C then allowed to reach to rt. The resulting white solid was vacuum filtered and washed on the filter using total 20 mL ether in 10 mL portions. The filtrate was concentrated under reduced pressure. The residue was purified by column chromatography (hexanes:EtOAc 3:2(v/v)) to yield 12.5 mg **3.12**, 64.5% yield, as a colorless oil.



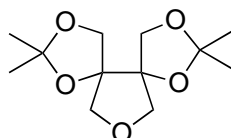
At 0 °C, a solution of **1.12** (40.2 mg, 0.153 mmol) in CH₂Cl₂ (5 mL) was treated with 0.999 M TMSOTf (2.0 μL, 1.9 μmol, 5.0 mol% rel to **1.12**). The reaction was stirred at 0 °C for 30 min, treated with 5 mL satd aq NaHCO₃, and extracted with 3 × 10 mL CH₂Cl₂. The organic extracts were combined, washed once with 5 mL water and dried over MgSO₄, filtered, and solvent was removed under rotary evaporator to yield 30.1 mg of a colorless oil having an *R_f* = 0.68 hexanes:EtOAc 3:2(v/v). NMR showed the oil to be a mixture of two major components: **3.13** and **3.14**, and a minor (~1%) unidentified compound. Separation of **3.14** from **3.13** was done by flash chromatography slowly switching solvent system from hexanes:EtOAc 4:1(v/v) to hexanes:EtOAc 3:2(v/v).



3.13

2,2,8,8,13,13-Hexamethyl-1,3,7,9,12,14-hexaoxadispiro[4.5.4.0]pentadecane, 3.13. ¹H

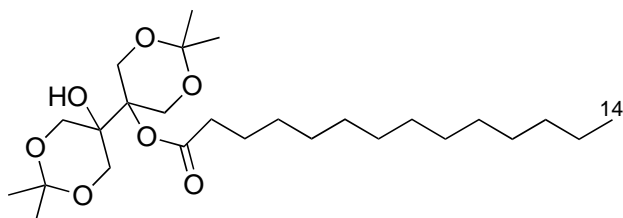
NMR (400 MHz, CDCl₃) 4.24 (d, *J* = 8.8 Hz, 2H), 4.09 (dd, *J* = 8.4 Hz, *J* = 1.2 Hz, 2H), 3.42 (d, *J* = 12.4 Hz, 2H), 3.34 (dd, *J* = 12.4 Hz, *J* = 1.2 Hz, 2H), 1.41 (s, 6H), 1.37 (s, 6H), 1.28 (s, 6H). ¹³C NMR (100 MHz, CDCl₃) δ 110.2, 101.6, 83.2, 67.1, 63.1, 28.1, 26.8, 24.9. HRMS (ESI+): *m/z* Calculated for C₁₅H₂₆O₆Na (M⁺ + Na) 325.1627, found 325.1631.



3.14

2,2,11,11-Tetramethyl-1,3,7,10,12-pentaoxadispiro[4.4.4.0]tridecane, 3.14. ¹H NMR (600

MHz, CDCl₃) δ 4.25 (d, *J* = 9.6 Hz, 2H), 3.92 (d, *J* = 9.6 Hz, 4H), 3.86 (d, *J* = 9.0 Hz, 2H), 1.43 (s, 6H), 1.37 (s, 6H). ¹³C NMR (151 MHz, CDCl₃) δ 110.1, 88.0, 76.9, 66.6, 26.5, 26.3. HRMS (ESI+): *m/z* Calculated for C₁₅H₂₀O₅ (M⁺) 244.1311, found 244.1316.

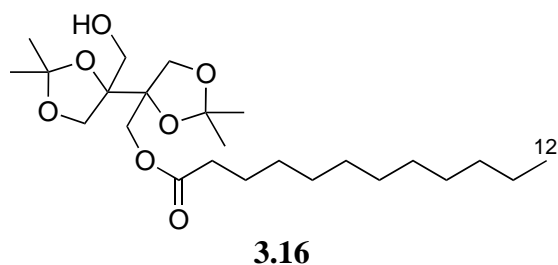


3.15

5-Tetradecanoyloxy-5'-hydroxy-5,5'-bi(2,2-dimethyl-1,3-dioxane), 3.15. A solution of

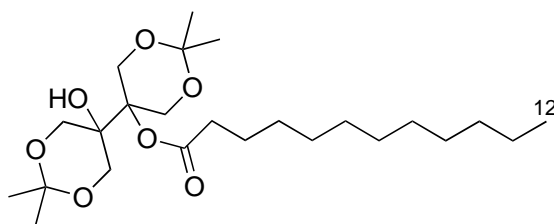
dicyclohexylcarbodiimide (DCC) (92.8 mg, 0.449 mmol) in CH₂Cl₂ (5 mL) was added dropwise over 10-15 min to a solution of diol **1.12** (39.3 mg, 0.149 mmol), DMAP (18.3 mg, 0.149 mmol) and myristic acid (85.6 mg, 0.375 mmol) in CH₂Cl₂ (4 mL) at rt. The reaction mixture was

stirred under N₂ at rt for 48 h with monitoring by TLC (hexanes:EtOAc 3:2(v/v)). Starting material was not completely consumed but the reaction was stopped after 48 h and filtered. The filtrate was concentrated on the rotary evaporator. The residue was purified by flash chromatography with hexanes:EtOAc 4:1(v/v) to give 53.3 mg of a white solid. The solid was a mixture of **3.15** and an unidentified compound. ¹³C NMR (151 MHz, CDCl₃) δ 176.5, 99.4, 99.2, 86.0, 70.7, 65.3, 61.8, 36.2, 35.3, 33.0, 32.1, 31.1, 29.9, 29.8, 29.8, 28.1, 27.6, 26.7, 26.6, 25.7, 25.5, 24.3, 22.9, 14.3.



4-Dodecanoyloxymethyl-4'-hydroxymethyl-4,4'-bi(2,2-dimethyl-1,3-dioxolane), 3.16. To the diol **1.12** (38.9 mg, 0.148 mmol) in CH₂Cl₂ (3 mL) DMAP (27.2 mg, 0.223 mmol) was added and cooled to 0 °C. Lauroyl chloride (51.2 μL, 0.223 mmol) was added dropwise over 5 min. The reaction was stirred for 36 h with monitoring by TLC (hexanes:EtOAc 4:1(v/v)). Although starting material was not completely consumed after 36 h, the solution was filtered under vacuum, and the solvent was removed on the rotary evaporator. The residue was purified by flash chromatography (hexanes:EtOAc 4:1(v/v)) to yield a white solid consisting of a mixture of diastereomers of **3.16** (62.1 mg, 67.6%). *R_f* = 0.55 (hexanes:EtOAc 4:1(v/v)). ¹H NMR (600 MHz, CDCl₃) 4.38(d, *J* = 12 Hz, 2H), 4.23 (d, *J* = 9 Hz, 2H), 4.18 (d, *J* = 9.6 Hz, 2H), 4.04 (d, *J* = 12 Hz, 2H), 3.90 (d, *J* = 9.6 Hz, 2H), 3.81 (d, *J* = 9.6 Hz, 2H), 3.70 (d, *J* = 12 Hz, 2H), 3.57 (d, *J* = 12 Hz, 2H), 2.31 (m, 2H), 1.60 (m, 2H), 1.46 (s, 3H), 1.44 (s, 3H), 1.38 (s, 3H), 1.37 (s, 3H), 1.26-1.23 (m, 16H), 0.85(t, 3H). ¹³C NMR (151 MHz, CDCl₃) δ 173.4, 110.2, 110.1, 84.5, 83.5,

68.6, 68.3, 65.8, 65.7, 34.5, 32.1, 29.8, 29.7, 29.6, 29.5, 29.4, 29.3, 28.1, 27.6, 26.7, 26.6, 25.1, 22.9, 14.3.



3.17

5-Dodecanoyloxy-5'-hydroxy-5,5'-bi(2,2-dimethyl-1,3-dioxane), 3.17. To a solution of diol **1.12** (34.2 mg, 0.130 mmol) in CH₂Cl₂ (3 mL) at rt, DMAP (3.0 mg, 24.5 μmol) was added, followed by addition of Et₃N (73 μL, 0.521 mmol) and lauric anhydride (0.198 g, 0.52 mmol). The reaction was stirred at rt for 36 h, with monitoring by TLC (hexanes:EtOAc 3:2(v/v)), but starting material was not completely consumed. After being stirred for 36 h, the reaction mixture was filtered through a short silica gel column (hexanes:EtOAc 3:2(v/v)), the solvent evaporated on the rotary evaporator, and the residue purified with flash chromatography (hexanes:EtOAc 4:1(v/v)), to yield 72 mg of **3.17** white solid with inseparable unidentified product. ¹³C NMR (151 MHz, CDCl₃) δ 176.4, 99.5, 99.2, 85.9, 70.8, 65.2, 61.9, 34.3, 29.8, 29.7, 29.6, 29.5, 29.4, 29.2, 29.08, 25.7, 25.2, 24.3, 24.4, 24.2, 14.3.

References

1. Jie, Y. “*Tris(1,3-Dihydroxy-2-Propyl)Amine, A Planar Trialkylamine: Synthesis, Structure, and Properties. A Potential Precursor to Hypervalent Nitrogen*” Ph. D. Dissertation, Auburn University, **2006**.
2. Keough, T.; Ezra, F. S.; Russell, A. F.; Pryne, J. D. *Org. Mass Spectrom.* **1987**, *22*, 241–247.
3. Müller, S. N.; Batra, R.; Senn, M.; Giese, B.; Kisel, M.; Shadyro, O. *J. Am. Chem. Soc.* **1997**, *119*, 2795–2803.
4. Roy, R.; Shiao, T. C. *Chem. Soc. Rev.* **2015**, *44*, 3924–3941.
5. Li, X. “*Toward a Breathable Fabric for Protection Against Airborne Toxic Chemicals, and An Olefin-Forming Cascade Reaction En Route to 2,2'-Bi(glycerol)*” Ph. D. Dissertation, Auburn University, **2009**.
6. a) Calvet, G.; Guillot, R.; Blanchard, N.; Kouklovsky, C. *Org. Biomol. Chem.* **2005**, *3*, 4395–4401. b) Linden, G. B.; Gold, M. H. *J. Org. Chem.* **1956**, *21*, 1175–1176.
7. a) Corson, B. B.; Benson, W. L. *Org. Synth. Coll. Vol. 2.* **1943**, 273–275. b) Peng, R. –F.; Wang, G. –W.; Shen, Y. –B.; Li, Y. –J.; Zhang, T. –H.; Liu, Y. –C.; Murata, Y.; Komatsu, K. *Synth. Commun.* **2004**, *34*, 2117–2126. c) Wang, Z.; Yin, G.; Chen, A.; Hu, S.; Wu, A. *Synth. Commun.* **2007**, *37*, 4399–4405.
8. Plietker, B.; Niggemann, M. *J. Org. Chem.* **2005**, *70*, 2402–2405.
9. a) Gevorgyan, V. N.; Ignatovich, L. M.; Lukevics, E. *J. Organometallic Chem.* **1985**, *284*, C31–C32. b) Sommer, L. H.; McLick, J.; Golino, C. M. *J. Am. Chem. Soc.* **1972**, *94*, 669–

670. c) Tour, J. M.; John, J. A.; Stephens, E. B. *J. Organometal. Chem.* **1992**, *429*, 301-310.
- d) Midgley, J. M.; Miller, J. S.; Whalley, W. B. *J. Chem. Soc., Perkin Trans. 1* **1976**, 1384–1385.
10. Greene, T. W.; Wuts, P. G. M. *Protective Groups In Organic Synthesis, 3rd ed*; John Wiley & Sons New York, **1999**, p 134.
11. Madhusudhan, G.; Reddy, G. O.; Ramanatham, J.; Dubey, P. K. *Indian J. Chem.* **2004**, *43B*, 2719–2723.
12. Tomalia, D. A.; Baker, H.; Dewald, J.; Hall, M.; Kallos, G.; Martin, S.; Roeck, J.; Ryder, J.; Smith, P. *Polymer J. (Tokyo, Jpn)* **1985**, *17*, 117-132.
13. a) Bosman, A. W.; Janssen, H. M.; Meijer, E. W. *Chem. Rev.* **1999**, *99*, 1665–1688. b) Moore, J. S. *Acc. Chem. Res.* **1997**, *30*, 402. c) Fréchet, J. M. J.; Tomalia, D. A. *Dendrimers and Other Dendritic Polymers*; Wiley:Chichester, 2001. d) Newkome, G. R.; Moorefield, C. N.; Vögtle, F. *Dendrimers and Dendrons: Concepts, Syntheses, Applications*; Wiley:Weinheim, 2001. e) Majoral, J. P.; Caminade, A.-M. *Chem. Rev.* **1999**, *99*, 845–880. f) Gitsov, I.; Lin, C. *Curr. Org. Chem.* **2005**, *9*, 1025–1051.
14. Newkome, G. R.; Yao, Z.; Baker, G. R.; Gupta, V. K. *J. Org. Chem.* **1985**, *50*, 2003–2004.
15. a) Carlmark, A.; Hawker, C. J.; Hult, A.; Malkoch, M. *Chem. Soc. Rev.* **2009**, *38*, 352–362. b) Twibanire, J-d'A. K.; Grindley, T. B. *Polymers* **2012**, *4*, 794–879.
16. Klajnert, B.; Bryszewska, M. *Acta Biochim. Polon.* **2001**, *48*, 199–208.
17. Sowinska, M.; Urbanczyk-Lipkowska, Z. *New J. Chem.* **2014**, *38*, 2168–2203.
18. Wörner, C.; Mülhaupt, R. *Angew. Chem. Int. Ed. Engl.* **1993**, *32*, 1306–1308.
19. Hawker, C. J.; Fréchet, J. M. J. *J. Am. Chem. Soc.* **1990**, *112*, 7638–7647.

20. a) Zhuo, R. X.; Du, B.; Lu, Z. R. *J. Controlled Release* **1999**, *57*, 249–257. b) Liu, M.; Kono, K.; Fréchet, J. M. J. *J. Controlled Release* **2000**, *65*, 121–131. c) Twyman, L. J.; Beezer, A. E.; Esfand, R.; Hardy, M. J.; Mitchell, J. C. *Tetrahedron Lett.* **1999**, *40*, 1743–1746. d) Caminade, A.-M.; Turrin, C. *J. Mater. Chem. B* **2014**, *2*, 4055–4066.
21. a) Brunner, H. *J. Organomet. Chem.* **1995**, *500*, 39–46. b) Crooks, R. M.; Zhao, M.; Li, S.; Chechik, V.; Yeung, L. K. *Acc. Chem. Res.* **2001**, *34*(3), 181–190.
22. Bielinska, A. U.; Kukowska-Latallo, F. J.; Johnson, J.; Tomalia, D. A.; Baker, J. R. Jr. *Nucleic Acids Res.* **1996**, *24*, 2176–2182. b) Dufès, C.; Uchegbu, I. F.; Schätzlein, A. G. *Adv. Drug. Deliv. Rev.* **2005**, *57*(15), 2177–2202.
23. a) Bryant, L. H.; Brechbiel, M. W.; Wu, C.; Bulte, J. W. M.; Herynek, V.; Frank, J. A. *J. Magn. Reson. Imaging* **1999**, *9*, 348–352. b) Lim, J.; Turkbey, B.; Bernardo, M.; Bryant, L. H.; Garzoni, M.; Pavan, G. M.; Nakajima, T.; Choyke, P. L.; Simanek, E. E.; Kobayashi, H. *Bioconjugate Chem.* **2012**, *23*(11), 2291–2299.
24. Cheng, Y.; Xu, T.; Fu, R. *Eur. J. Med. Chem.* **2005**, *40*, 1390–1393. b) Gupta, U.; Agashe, H. B.; Asthana, A.; Jain, N. K. *Biomacromolecules* **2006**, *7*(3), 649–658.
25. Barth, R. F.; Adams, D. M.; Soloway, A. H.; Alam, F.; Darby, M. V. *Bioconjugate Chem.* **1994**, *5*(1), 58–66. b) Wu, G.; Barth, R. F.; Yang, W.; Chatterjee, M.; Tjarks, W.; Ciesielski, M. J.; Fenstermaker, R. A. *Bioconjugate Chem.* **2004**, *15*(1), 185–194.
26. a) Wooley, K. L.; Hawker, C. J.; Fréchet, J. M. J. *J. Chem. Soc., Perkin Trans. 1*, **1991**, 1059–1076. b) Hawker, C. J.; Fréchet, J. M. J. *J. Am. Chem. Soc.* **1992**, *114*, 8405–8413. c) Wooley, L. K.; Hawker, C. J.; Fréchet, J. M. J. *J. Am. Chem. Soc.* **1993**, *115*, 11496–11505.
27. a) Maraval, V.; Laurent, R.; Donnadiou, B.; Mauzac, M.; Caminade, A.-M.; Majoral, J.-P. *J. Am. Chem. Soc.* **2000**, *122*, 2499–2511.

28. Lartigue, M.-L.; Slany, M.; Caminade, A.-M.; Majoral, J.-P. *Chem. Eur. J.* **1996**, *2*, 1417–1426.
29. Tsuda, K.; Dol, G. C.; Gensch, T.; Hofkens, J.; Latterini, L.; Weener, J. W.; Meijer, E. W.; De Schryver, F. C. *J. Am. Chem. Soc.* **2000**, *122*, 3445–3452.
30. Caminade, A.-M.; Laurent, R.; Delavaux-Nicot, B.; Majoral, P. J. *New J. Chem.* **2012**, *36*, 217–226.
31. Steffensen, M. B.; Simanek, E. E. *Angew. Chem., Int. Ed.* **2004**, *43*, 5178–5180.
32. a) Bo, Z.; Schäfer, A.; Franke, P.; Schlüter, A. D. *Org. Lett.* **2000**, *2*, 1645–1648. b) Kang, T.; Amir, R. J.; Khan, A.; Ohshimizu, K.; Hunt, J. N.; Sivanandan, K.; Montanez, M. I.; Malkoch, M.; Ueda, M.; Hawker, C. J. *Chem. Commun.* **2010**, *46*, 1556–1558.
33. Tomalia, D. A.; Naylor, A. M.; Goddard, W. A. III *Angew. Chem., Int. Ed.* **1990**, *29*, 138–175.
34. Roy, R.; Shiao, T. C. *Chem. Soc. Rev.* **2015**, *44*, 3924–3941.
35. Haag, R.; Sunder, A.; Stumbé, J.-F. *J. Am. Chem. Soc.* **2000**, *122*, 2954–2955.
36. McKee, M. G.; Unal, S.; Wilkes, G. L.; Long, T. *Prog. Polym. Sci.* **2005**, *30*, 507–539.
37. Schomer, M.; Schull, C.; Frey, H. *J. Polym. Sci. Part A.* **2013**, *51*, 995–1019.
38. a) Singh, R.; Kissling, R. M.; Letellier, M. -A.; Nolan, S. P. *J. Org. Chem.* **2004**, *69*, 209–212. b) Nguyen, H. T.; Tran, P. H. *RSC Adv.* **2016**, *6*, 98365–98368.
39. Doyle, M. P.; McKervey, M. A.; Ye, T. *Modern Catalytic Methods for Organic Synthesis with Diazo Compounds*; John Wiley & Sons Inc. **1998**, p 24.
40. Yang, M.; Webb, T. R.; Livant, P. *J. Org. Chem.* **2001**, *66*, 4945–4949.

41. Makhanu, D. S. “*Synthesis of a Congested Heptamine as a Potential Precursor to Hypervalent (10-N-5) Nitrogen, and Effects of Remote Substituents on Planarization of Nitrogen in Trialkylamines*” Ph. D. Dissertation, Auburn University, **2012**.
42. Wang, X. “*New Chemistry of 2-Diazo-1,3-Cyclohexanedione, Including A New Route to Triarylamine*” Ph. D. Dissertation, Auburn University, **2002**, p 16.
43. a) Poon, K. C. W.; Lovell, M. K.; Dresner, K. N.; Datta, A. *J. Org. Chem.* **2008**, *73*, 752–755. b) Li, X. “*Toward a Breathable Fabric for Protection Against Airborne Toxic Chemicals, and An Olefin-Forming Cascade Reaction En Route to 2,2’-Bi(Glycerol)*” Ph. D. Dissertation, Auburn University, **2009**.
44. a) Szarek, W. A.; Zamojski, A.; Tiwari, K. N.; Ison, E. R. *Tetrahedron Lett.* **1986**, *27*, 3827–3830. b) Ramasamy, K. S.; Bandaru, R.; Averett, D. *Synthetic Communications*, **1999**, *29*, 2881-2894. c) Jung, M. E.; Koch, P. *Tetrahedron Lett.* **2011**, *52*, 6051–6054.
45. Morgan, M. T.; Carnahan, M. A.; Immoos, C. E.; Riberio, A. A.; Finkelstein, S.; Lee, J. S.; Grinstaff, W. A. *J. Am. Chem. Soc.* **2003**, *125*, 15485–15489.
46. Hawker, C. J.; Fréchet, J. M. J. *J. Am. Chem. Soc.* **1990**, *112*, 7638–7647.
47. Doyle, M. P.; McKervey, M. A.; Ye, T. *Modern Catalytic Methods for Organic Synthesis with Diazo Compounds*; John Wiley & Sons Inc. **1998**, p 09.
48. a) Kitamura, M.; Tashiro, N.; Miyagawa, S.; Okauchi, T. *Synthesis* **2011**, *7*, 1037–1044. b) Kitamura, M.; Tashiro, N.; Okauchi, T. *Synlett* **2009**, *18*, 2943–2944. c) Kitamura, M.; Takshashi, S.; Okauchi, T. *J. Org. Chem.* **2015**, *80*, 8406–8416. d) Kitamura, M.; Murakami, K. *Org. Synth.* **2015**, *92*, 171–181. e) Passet, M.; Mailhol, D.; Coquerel, Y.; Rodriguez, J. *Synthesis* **2011**, 2549–2552.

49. a) Davies, H. L. M.; Cantrell, R. W.; Romines, R. K.; Baum, S. J. *Org. Synth.* **1992**, *70*, 93–100. b) Padwa, A.; Sheehan, M. S.; Straub, S. C. *J. Org. Chem.* **1999**, *64*, 8648–8659. c) Muthusamy, S.; Gnanaprakasam, B. *Tetrahedron Lett.* **2008**, *49*, 475–480.
50. Oku, A.; Numata, M. *J. Org. Chem.* **2000**, *65*, 1899–1906.
51. Hodgson, D. M.; Man, S.; Powell, K. J.; Perko, Z.; Zeng, M.; Moreno-Clavijo, E.; Thompson, A. L.; Moore, M. D. *J. Org. Chem.* **2014**, *79*, 9728–9734.
52. Kelly-Rowley, A. M.; Lynch, V. M.; Anslyn, E. V. *J. Am. Chem. Soc.* **1995**, *117*, 3438–3447.
53. Glasovac, Z.; Eckert-Maksic, M.; Maksic, Z. B. *New J. Chem.* **2009**, *33*, 588–597.
54. a) Hatch III, C. E.; Baum, J. S.; Takashima, T.; Kondo, K. *J. Org. Chem.* **1980**, *45*, 3281–3285. b) Davies, H. M. L.; Cantrell, W. R.; Romines, K. R.; Baum, J. S. *Org. Synth.* **1992**, *70*, 93. c) Deadman, B. J.; O'Mahony, R. M.; Lynch, D.; Crowley, D. C.; Collins, S. G.; Maguire, A. R. *Org. Biomol. Chem.* **2016**, *14*, 3423–3431.
55. a) Rewicki, D.; Tuchscherer, C. *Angew. Chem., Int. Ed. Engl.* **1972**, *11*, 44–45.
b) Hazen, G. G.; Weinstock, L. M.; Connel, R.; Bollinger, F. W. *Synth. Commun.* **1981**, *11*, 947–956.
56. Nikolaev, V. V.; Heimgartner, H.; Linden, A.; Krylov, S. I.; Nikoleav, A. V. *Eur. J. Org. Chem.* **2006**, *2006*, 4737–4746.
57. Stothers, J. B. *Carbon-13 NMR Spectroscopy*, Academic: New York, 1972, p 332 ff
58. House, H. O.; Prabhu, A. V.; Phillips, W. V. *J. Org. Chem.* **1976**, *41*, 1209–1214.
59. Firl, J.; Runge, W. *Z. Naturforsch. B* **1974**, *29*, 393 – 398.
60. Shelkov, R.; Nahmany, M.; Melman, A. *J. Org. Chem.* **2002**, *67*, 8975–8982.
61. Allen, A. D.; Andraos, J.; Tidwell, T. T.; Vukovic *J. Org. Chem.* **2014**, *79*, 679–685.

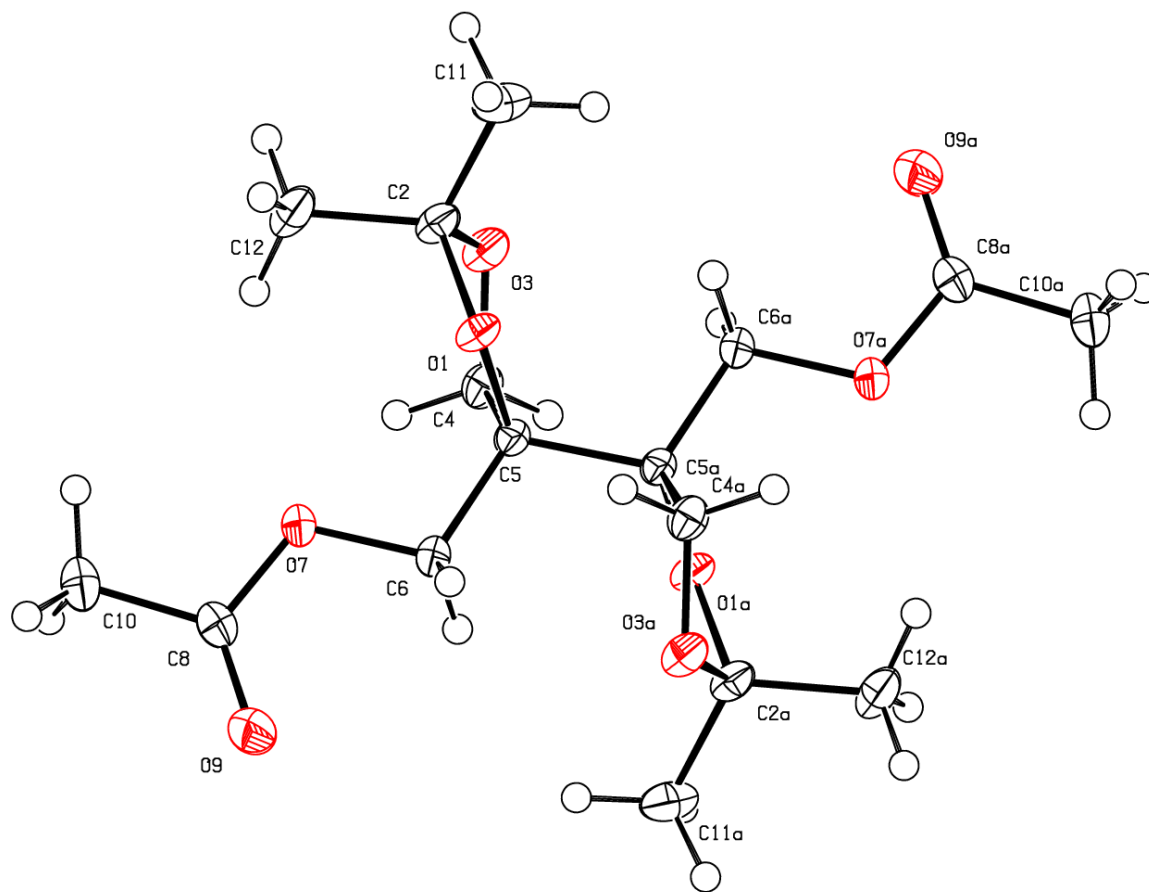
62. Pomerantz, M.; Levanon, M.; Gu, X.; Dias, H. V. R. *Tetrahedron* **1997**, *53*, 10019–10028.
63. Firl, J.; Runge, W. *Angew. Chem. Int. Ed. Engl.* **1973**, *12*, 668 – 669.
64. Duddeck, H.; Praas, H.-W. *Magn. Reson. Chem.* **1993**, *31*, 182 – 184.
65. Jullien, J.; Pechine, J. M.; Perez, F. *Tetrahedron Lett.* **1983**, *24*, 5525–5526.
66. Klein, D. *Organic Chemistry*, 2nd ed.; Wiley: Hoboken, NJ, 2015, p 1240 ff.
67. Fahy, E.; Subramaniam, S.; Murphy, R. C.; Nishijima, M.; Raetz, C. R. H.; Shimizu, T.; Spener, F.; van Meer, G.; Wakelam, M. J. O.; Dennis, E. A. *J. Lipid Res.* **2009**, *50*, S9–S14.
68. Liu, J.; Zeng, F. –F.; Liu, Z. –M.; Zhang, C. –X.; Ling, W. –H.; Chen, Y. –M. *Lipids in Health and Disease*, **2013**, *12*:159; doi:10.1186/1476-511X-12-159.
69. Li, J.; Wang, X.; Zhang, T.; Wang, C.; Huang, Z.; Luo, X.; Deng, Y. *Asian J. Pharm. Sci.* **2015**, *10*, 81–98.
70. Cullis, P. R.; Kruijff, B. D. *Biochim. Biophys. Acta* **1979**, *559*, 399–420.
71. Yang, R.; Zhang, X.; Li, F.; Ding, L.; Li, B.; Sun, H.; Gan, Y. *Colloid Surf A: Physicochem. Eng. Asp.* **2013**, *436*, 434–442.
72. Hyanes DH. Phospholipid-coated microcrystals: injectable formulations of water-insoluble drugs [M]. Google patents 1992.
73. https://commons.wikimedia.org/wiki/File%3ALiposome_cross_section.png
74. Kai, T.; Sun, X.; Faucher, K. M.; Apkarian, R. P.; Chaikof, E. L. *J. Org. Chem.* **2005**, *70*, 2606–2615.
75. Constantinou-Kokotou, V.; Magrioti, V.; Verger, R. *Chem. Eur. J.* **2004**, *10*, 1133–1140.
76. Vares, L.; Koulov, A. V.; Smith, B. D. *J. Org. Chem.* **2003**, *68*, 10073–10078.

77. a) Franklin, C. L.; Li, H.; Martin, S. F. *J. Org. Chem.* **2003**, *68*, 7298–7307. b) Srisiri, W.; Lamparski, H. G.; O'Brien, D. F. *J. Org. Chem.* **1996**, *61*, 5911–5915.
78. a) Orita, A.; Tanahashi, C.; Kakuda, A.; Otera, J. *J. Org. Chem.* **2001**, *66*, 8926–8934. b) Ishihara, K.; Kubota, M.; Kurihara, H.; Yamamoto, H. *J. Org. Chem.* **1996**, *61*, 4560–4567.
79. a) Yadav, V. K.; Babu, K. G. *J. Org. Chem.* **2004**, *69*, 577–580. b) Sugihara, J. M.; Knoblich, J. M.; Yamazaki, T. *J. Org. Chem.* **1971**, *36*, 3407–3411.
80. a) Höfle, G.; Steglich, W.; Vorbrüggen, H. *Angew. Chem., Int. Ed. Engl.* **1978**, *17*, 569–583. b) Scriven, E. F. V. *Chem. Soc. Rev.* **1983**, *12*, 129–161. c) Sakakura, A.; Kawajiri, K.; Ohkubo, T.; Kosugi, Y.; Ishihara, K. *J. Am. Chem. Soc.* **2007**, *129*, 14775–14779. d) Wang, B.; Wu, X.-Y.; Wong, O. A.; Nettles, B.; Zhao, M.-X.; Chen, D.; Shi, Y. *J. Org. Chem.* **2009**, *74*, 3986–3989.
81. Yamanaka, M.; Yoshida, U.; Sato, M.; Shigeta, T.; Yoshida, K.; Furuta, T.; Kawabata, T. *J. Org. Chem.* **2015**, *80*, 3075–3082.
82. Vedejs, E.; Bennett, N. S.; Conn, L. M.; Diver, S. T.; Gingras, M.; Lin, S.; Oliver, P. A.; Peterson, M. J. *J. Org. Chem.* **1993**, *58*, 7286–7288.
83. a) Vedejs, E.; Daugulis, O. *J. Org. Chem.* **1996**, *61*, 5702–5703. b) Vedejs, E.; Chen, X. *J. Am. Chem. Soc.* **1996**, *118*, 1809–1810.
84. a) Neises, B.; Steglich, W. *Angew. Chem. Int. Ed.*, **1978**, *17*, 522–524.
85. Kumareswaran, R.; Gupta, A.; Vankar, Y. D. *Synth. Commun.* **1997**, *27*, 277–282.
86. a) Procopiou, P. A.; Baugh, S. P. D.; Flack, S. S.; Inglis, G. G. A. *J. Org. Chem.* **1998**, *63*, 2342–2347. b) Procopiou, P. A.; Baugh, S. P. D.; Flack, S. S.; Inglis, G. G. A. *Chem. Commun.* **1996**, 2625–2626.

87. Clarke, P. A.; Kayaleh, N. E.; Smith, M. A.; Baker, J. R.; Bird, S. J.; Chan, C. *J. Org. Chem.* **2002**, *67*, 5226–5231.
88. a) Dalpozzo, R.; De Nino, A.; Maiuolo, L.; Procopio, A.; Tagarelli, A.; Sindona, G.; Bartoli, G. *J. Org. Chem.* **2002**, *67*, 9093–9095. (b) Dalpozzo, R.; De Nino, A.; Maiuolo, L.; Procopio, A.; Nardi, M.; Bartoli, G.; Romeo, R. *Tetrahedron Lett.* **2003**, *44*, 5621–5624 (c) Bartoli, G.; Dalpozzo, R.; De Nino, A.; Maiuolo, L.; Nardi, M.; Procopio, A.; Tagarelli, A. *Green Chem.* **2004**, *6*, 191–192.
89. (a) Saravanan, P.; Singh, V. K. *Tetrahedron Lett.* **1999**, *40*, 2611–2614. b) Tai, C.-A.; Kulkarni, S.; Hung, S.-C. *J. Org. Chem.* **2003**, *68*, 8719–8722. (c) Chandra, K. L.; Saravanan, P.; Singh, R. K.; Singh, V. K. *Tetrahedron* **2002**, *58*, 1369–1374. (d) Chen, I.-H.; Kou, K. G. M.; Le, D. N.; Rathbun, C. M.; Dong, V. M. *Chem. Eur. J.* **2014**, *20*, 5013–5018.
90. Martinez-Pascual, R.; Viñas-Bravo, O.; Meza-Reyes, S.; Iglesias-Arteaga, M. A.; Sandoval-Ramírez, J. *Synth. Commun.* **2004**, *34*, 4591–4596.
91. a) Ishihara, K.; Kubota, M.; Kurihara, H.; Yamamoto, H. *J. Org. Chem.* **1996**, *61*, 4560–4567. b) McClure, M. S.; Berry, M. B.; Caine, D.; Crawford, C.; Crump, B. C.; Glover, B. N.; Kedia, S. B.; Millar, A.; Mitchell, M. B.; Nichols, C. J.; Patterson, D. E.; Powers, J. *Eur. J. Org. Chem.* **2012**, 3561–3565. c) Kobayashi, S. *Eur. J. Org. Chem.* **1999**, 15–27.
92. Angibeaud, P.; Utille, J.-P. *J. Chem. Soc., Perkin Trans. 1* **1990**, 1490–1492
93. a) Grondal, C. *Synlett.* **2003**, *10*, 1568–1569. b) Spivey, A. C.; Arseniyadis, S. *Angew. Chem. Int. Ed.* **2004**, *43*, 5436–5441.
94. Bhushan, V.; Chakraborty, T. K.; Chandrasekaran, S. *J. Org. Chem.* **1984**, *49*, 3974–3978.
95. Awal, A.; Boyd, A. S. F.; Buchanan, J. G.; Edgar, A. R. *Carbohydr. Res.* **1990**, *205*, 173–179.

96. Buchanan, J. G.; Edgar, A. R.; Rawson, D. I.; Shahidi, P.; Wightman, R. H. *Carbohydr. Res.* **1982**, *100*, 75–86.
97. Aslani-Shtorbani, G.; Buchanan, J. G.; Edgar, A. R.; Henderson, D.; Shahidi, P. *Tetrahedron Lett.* **1980**, *21*, 1791–1792.
98. Buchanan, J. G.; Chacón-Fuentes, M. E.; Edgar, A. R.; Moorhouse, S. J.; Rawson, D. I.; Wightman, R. H. *Tetrahedron Lett.* **1980**, *21*, 1793–1796.

APPENDICES



```

data_Livant020216_0m
_audit_creation_date      2016-04-15
_audit_creation_method
;
Olex2 1.2
(compiled 2016.02.19 svn.r3266 for OlexSys, GUI svn.r5155)
;
_publ_contact_author_address  ?
_publ_contact_author_email    ?
_publ_contact_author_name     "
_publ_contact_author_phone    ?
_publ_section_references
;
Bourhis, L.J., Dolomanov, O.V., Gildea, R.J., Howard, J.A.K., Puschmann, H.
(2015). Acta Cryst. A71, 59-75.

Dolomanov, O.V., Bourhis, L.J., Gildea, R.J., Howard, J.A.K. & Puschmann, H.
(2009), J. Appl. Cryst. 42, 339-341.
;
_chemical_name_systematic
;
?
;
_chemical_formula_moiety      'C16 H26 O8'
_chemical_formula_sum          'C16 H26 O8'
_chemical_formula_weight      346.38
loop_
_atom_type_symbol
_atom_type_scatter_dispersion_real
_atom_type_scatter_dispersion_imag
_atom_type_scatter_Cromer_Mann_a1
_atom_type_scatter_Cromer_Mann_a2
_atom_type_scatter_Cromer_Mann_a3
_atom_type_scatter_Cromer_Mann_a4
_atom_type_scatter_Cromer_Mann_b1
_atom_type_scatter_Cromer_Mann_b2
_atom_type_scatter_Cromer_Mann_b3
_atom_type_scatter_Cromer_Mann_b4
_atom_type_scatter_Cromer_Mann_c
_atom_type_scatter_source
_atom_type_scatter_dispersion_source
H 0.00000 0.00000 0.49300 0.32291 0.14019 0.04081 10.51090 26.12570 3.14236
57.79970 0.0030380000826
'International Tables Volume C Table 6.1.1.4 (pp. 500-502)'
'Henke, Gullikson and Davis, At. Data and Nucl. Data Tables, 1993, 54, 2'
C 0.00347 0.00161 2.31000 1.02000 1.58860 0.86500 20.84390 10.20750 0.56870
51.65120 0.215599998832
'International Tables Volume C Table 6.1.1.4 (pp. 500-502)'
'Henke, Gullikson and Davis, At. Data and Nucl. Data Tables, 1993, 54, 2'
O 0.01158 0.00611 3.04850 2.28680 1.54630 0.86700 13.27710 5.70110 0.32390
32.90890 0.250800013542
'International Tables Volume C Table 6.1.1.4 (pp. 500-502)'
'Henke, Gullikson and Davis, At. Data and Nucl. Data Tables, 1993, 54, 2'

_space_group_crystal_system  'triclinic'
_space_group_IT_number       2
_space_group_name_H-M_alt    'P -1'
_space_group_name_Hall       '-P 1'
loop_
_space_group_symop_id
_space_group_symop_operation_xyz
1 x,y,z
2 -x,-y,-z

_symmetry_Int_Tables_number  2
_cell_length_a                5.6722(8)
_cell_length_b                8.9777(12)
_cell_length_c                9.6075(13)
_cell_angle_alpha             113.3108(14)
_cell_angle_beta              94.5970(15)

```

```

_cell_angle_gamma      102.9913(15)
_cell_volume           429.92(10)
_cell_formula_units_Z  1
_cell_measurement_reflns_used  2788
_cell_measurement_temperature  180(2)
_cell_measurement_theta_max  28.567
_cell_measurement_theta_min  2.350
_exptl_absorpt_coefficient_mu  0.107
_exptl_absorpt_correction_T_max  0.7458
_exptl_absorpt_correction_T_min  0.6004
_exptl_absorpt_correction_type  multi-scan
_exptl_absorpt_process_details
;
SADABS-2014/2 (Bruker,2014/2) was used for absorption correction.
wR2(int) was 0.0772 before and 0.0412 after correction.
The Ratio of minimum to maximum transmission is 0.8050.
The 1/2 correction factor is 0.00150.
;
_exptl_crystal_density_diffn  1.3378
_exptl_crystal_description  prism
_exptl_crystal_F_000  186.1293
_exptl_crystal_preparation  ?
_exptl_crystal_size_max  0.25
_exptl_crystal_size_mid  0.18
_exptl_crystal_size_min  0.11
_exptl_special_details
;
?
;
_diffn_reflns_av_R_equivalents  0.0342
_diffn_reflns_av_unet/netl  0.0333
_diffn_reflns_limit_h_max  7
_diffn_reflns_limit_h_min  -7
_diffn_reflns_limit_k_max  12
_diffn_reflns_limit_k_min  -12
_diffn_reflns_limit_l_max  12
_diffn_reflns_limit_l_min  -12
_diffn_reflns_number  6867
_diffn_reflns_theta_max  28.70
_diffn_reflns_theta_min  2.35
_diffn_ambient_temperature  180.45
_diffn_measurement_device_type  'Bruker APEX-II CCD'
_diffn_measurement_method  '\f and \w scans'
_diffn_radiation_type  'Mo K\alpha'
_diffn_radiation_wavelength  0.71073
_diffn_standards_number  0
_reflns_Friedel_coverage  0.0
_reflns_limit_h_max  7
_reflns_limit_h_min  -7
_reflns_limit_k_max  10
_reflns_limit_k_min  -12
_reflns_limit_l_max  12
_reflns_limit_l_min  0
_reflns_number_gt  1867
_reflns_number_total  2209
_reflns_threshold_expression  I>=2\sigma(I)
_computing_cell_refinement  'SAINT v8.34A (Bruker, 2013)'
_computing_data_reduction  'SAINT v8.34A (Bruker, 2013)'
_computing_molecular_graphics  'Olex2 (Dolomanov et al., 2009)'
_computing_publication_material  'Olex2 (Dolomanov et al., 2009)'
_computing_structure_refinement  'olex2.refine (Bourhis et al., 2015)'
_computing_structure_solution  'olex2.solve (Bourhis et al., 2015)'
_refine_ls_d_res_high  0.7401
_refine_ls_d_res_low  8.6643
_refine_ls_goodness_of_fit_ref  1.0825
_refine_ls_hydrogen_treatment  mixed
_refine_ls_matrix_type  full
_refine_ls_number_constraints  18
_refine_ls_number_parameters  111
_refine_ls_number_reflns  2209

```

```

_refine_ls_number_restraints      0
_refine_ls_R_factor_all           0.0514
_refine_ls_R_factor_gt            0.0425
_refine_ls_restrained_S_all      1.0825
_refine_ls_shift/su_max           0.0000
_refine_ls_shift/su_mean         0.0000
_refine_ls_structure_factor_coef  Fsqd
_refine_ls_weighting_details
'w=1/[s^2*(Fo^2)+(0.0552P)^2+0.1182P] where P=(Fo^2+2Fc^2)/3'
_refine_ls_weighting_scheme      calc
_refine_ls_wR_factor_gt          0.1079
_refine_ls_wR_factor_ref         0.1130
_olex2_refinement_description
;
1. Fixed Uiso
At 1.2 times of:
  All C(H,H) groups
At 1.5 times of:
  All C(H,H,H) groups
2.a Secondary CH2 refined with riding coordinates:
  C4(H4a,H4b), C6(H6a,H6b)
2.b Idealised Me refined as rotating group:
  C10(H10a,H10b,H10c), C11(H11a,H11b,H11c), C12(H12a,H12b,H12c)
;
_atom_sites_solution_primary      iterative
_atom_sites_special_details
;
The structure was solved using Direct Methods (ShelXS). RE = 0.2, Nqual = -1, Ralpha = 0.025
;
loop_
  _atom_site_label
  _atom_site_type_symbol
  _atom_site_fract_x
  _atom_site_fract_y
  _atom_site_fract_z
  _atom_site_U_iso_or_equiv
  _atom_site_adp_type
  _atom_site_occupancy
  _atom_site_refinement_flags_posn
O7 O 0.18699(17) 0.69890(11) 0.80849(10) 0.0243(2) Uani 1.000000 .
O3 O -0.11241(15) 0.80783(11) 1.15574(10) 0.0218(2) Uani 1.000000 .
O1 O 0.23207(14) 0.95287(10) 1.10832(9) 0.0181(2) Uani 1.000000 .
O9 O 0.2494(2) 0.67185(13) 0.57279(11) 0.0327(3) Uani 1.000000 .
C10 C 0.3144(3) 0.46266(18) 0.65770(17) 0.0316(3) Uani 1.000000 .
H10a H 0.4676(11) 0.4594(7) 0.6176(12) 0.0474(5) Uiso 1.000000 GR
H10b H 0.337(2) 0.4623(7) 0.7598(3) 0.0474(5) Uiso 1.000000 GR
H10c H 0.1813(10) 0.36342(18) 0.5872(10) 0.0474(5) Uiso 1.000000 GR
C5 C 0.0356(2) 0.91651(14) 0.98553(12) 0.0161(2) Uani 1.000000 .
C4 C -0.1717(2) 0.78266(15) 0.99947(14) 0.0201(3) Uani 1.000000 .
H4a H -0.1735(2) 0.66734(15) 0.92705(14) 0.0241(3) Uiso 1.000000 R
H4b H -0.3344(2) 0.80032(15) 0.97820(14) 0.0241(3) Uiso 1.000000 R
C11 C 0.2277(3) 0.97363(19) 1.36622(15) 0.0314(3) Uani 1.000000 .
H11a H 0.1336(15) 1.0570(9) 1.3939(3) 0.0471(5) Uiso 1.000000 GR
H11b H 0.1960(19) 0.9069(3) 1.42589(15) 0.0471(5) Uiso 1.000000 GR
H11c H 0.4039(5) 1.0320(11) 1.3893(3) 0.0471(5) Uiso 1.000000 GR
C8 C 0.2497(2) 0.62017(15) 0.67068(14) 0.0222(3) Uani 1.000000 .
C6 C 0.1191(2) 0.85174(15) 0.83077(14) 0.0230(3) Uani 1.000000 .
H6a H 0.2621(2) 0.93809(15) 0.83013(14) 0.0276(3) Uiso 1.000000 R
H6b H -0.0159(2) 0.82781(15) 0.74630(14) 0.0276(3) Uiso 1.000000 R
C12 C 0.2515(2) 0.70599(18) 1.15213(17) 0.0278(3) Uani 1.000000 .
H12a H 0.1909(15) 0.6413(7) 1.2100(9) 0.0418(4) Uiso 1.000000 GR
H12b H 0.1972(15) 0.6341(7) 1.0412(3) 0.0418(4) Uiso 1.000000 GR
H12c H 0.4319(2) 0.74458(18) 1.1770(11) 0.0418(4) Uiso 1.000000 GR
C2 C 0.1497(2) 0.85796(15) 1.19585(14) 0.0200(3) Uani 1.000000 .
loop_
  _atom_site_aniso_label
  _atom_site_aniso_U_11
  _atom_site_aniso_U_22
  _atom_site_aniso_U_33

```

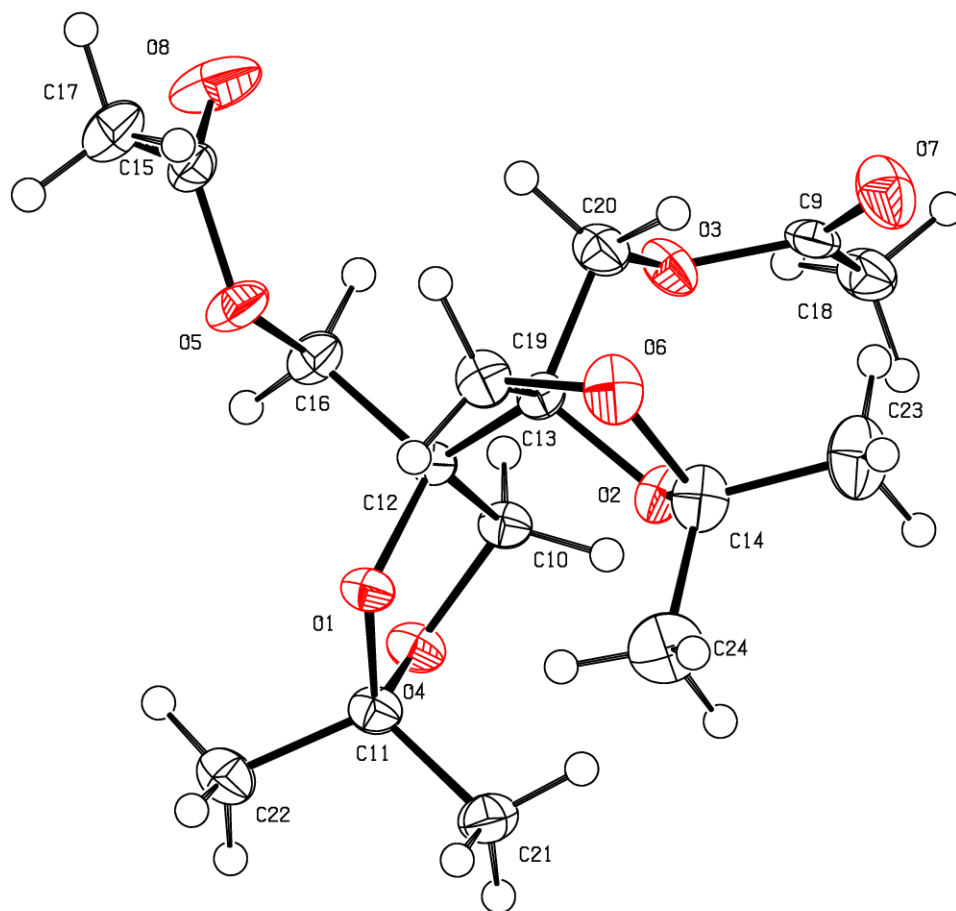
_atom_site_aniso_U_12
 _atom_site_aniso_U_13
 _atom_site_aniso_U_23
 O7 0.0364(5) 0.0239(5) 0.0212(4) 0.0194(4) 0.0117(4) 0.0111(4)
 O3 0.0170(4) 0.0282(5) 0.0277(5) 0.0077(3) 0.0065(3) 0.0184(4)
 O1 0.0148(4) 0.0228(4) 0.0212(4) 0.0047(3) 0.0018(3) 0.0144(3)
 O9 0.0482(6) 0.0321(5) 0.0261(5) 0.0187(5) 0.0162(4) 0.0149(4)
 C10 0.0408(8) 0.0280(7) 0.0319(7) 0.0208(6) 0.0137(6) 0.0115(6)
 C5 0.0162(5) 0.0180(5) 0.0167(5) 0.0072(4) 0.0030(4) 0.0087(4)
 C4 0.0180(5) 0.0183(6) 0.0241(6) 0.0043(4) 0.0021(4) 0.0100(5)
 C11 0.0370(7) 0.0376(8) 0.0230(6) 0.0090(6) 0.0012(5) 0.0180(6)
 C8 0.0227(6) 0.0220(6) 0.0213(6) 0.0087(5) 0.0072(5) 0.0068(5)
 C6 0.0342(7) 0.0220(6) 0.0211(6) 0.0172(5) 0.0103(5) 0.0118(5)
 C12 0.0265(6) 0.0337(7) 0.0395(7) 0.0166(5) 0.0124(5) 0.0263(6)
 C2 0.0176(5) 0.0252(6) 0.0244(6) 0.0074(4) 0.0055(4) 0.0169(5)

loop_
 _geom_bond_atom_site_label_1
 _geom_bond_atom_site_label_2
 _geom_bond_distance
 _geom_bond_site_symmetry_2
 _geom_bond_publ_flag
 O7 C8 1.3516(14) . ?
 O7 C6 1.4474(14) . ?
 O3 C4 1.4265(14) . ?
 O3 C2 1.4253(14) . ?
 O1 C5 1.4358(13) . ?
 O1 C2 1.4501(13) . ?
 O9 C8 1.2021(16) . ?
 C10 H10a 0.9800 . ?
 C10 H10b 0.9800 . ?
 C10 H10c 0.9800 . ?
 C10 C8 1.5004(18) . ?
 C5 C5 1.564(2) 2_577 ?
 C5 C4 1.5368(15) . ?
 C5 C6 1.5252(16) . ?
 C4 H4a 0.9900 . ?
 C4 H4b 0.9900 . ?
 C11 H11a 0.9800 . ?
 C11 H11b 0.9800 . ?
 C11 H11c 0.9800 . ?
 C11 C2 1.5117(18) . ?
 C6 H6a 0.9900 . ?
 C6 H6b 0.9900 . ?
 C12 H12a 0.9800 . ?
 C12 H12b 0.9800 . ?
 C12 H12c 0.9800 . ?
 C12 C2 1.5200(17) . ?

loop_
 _geom_angle_atom_site_label_1
 _geom_angle_atom_site_label_2
 _geom_angle_atom_site_label_3
 _geom_angle
 _geom_angle_site_symmetry_1
 _geom_angle_site_symmetry_3
 _geom_angle_publ_flag
 C6 O7 C8 115.08(9) . . ?
 C2 O3 C4 106.56(8) . . ?
 C2 O1 C5 109.62(8) . . ?
 H10b C10 H10a 109.5 . . ?
 H10c C10 H10a 109.5 . . ?
 H10c C10 H10b 109.5 . . ?
 C8 C10 H10a 109.5 . . ?
 C8 C10 H10b 109.5 . . ?
 C8 C10 H10c 109.5 . . ?
 C5 C5 O1 108.18(10) 2_577 . ?
 C4 C5 O1 103.48(8) . . ?
 C6 C5 O1 110.12(9) . . ?
 C6 C5 C4 112.70(9) . . ?

C5 C4 O3 103.85(9) . . ?
H4a C4 O3 110.99(6) . . ?
H4a C4 C5 110.99(6) . . ?
H4b C4 O3 110.99(6) . . ?
H4b C4 C5 110.99(6) . . ?
H4b C4 H4a 109.0 . . ?
H11b C11 H11a 109.5 . . ?
H11c C11 H11a 109.5 . . ?
H11c C11 H11b 109.5 . . ?
C2 C11 H11a 109.5 . . ?
C2 C11 H11b 109.5 . . ?
C2 C11 H11c 109.5 . . ?
O9 C8 O7 123.04(11) . . ?
C10 C8 O7 111.20(10) . . ?
C10 C8 O9 125.76(11) . . ?
C5 C6 O7 108.28(9) . . ?
H6a C6 O7 110.04(6) . . ?
H6a C6 C5 110.04(6) . . ?
H6b C6 O7 110.04(6) . . ?
H6b C6 C5 110.04(6) . . ?
H6b C6 H6a 108.4 . . ?
H12b C12 H12a 109.5 . . ?
H12c C12 H12a 109.5 . . ?
H12c C12 H12b 109.5 . . ?
C2 C12 H12a 109.5 . . ?
C2 C12 H12b 109.5 . . ?
C2 C12 H12c 109.5 . . ?
O1 C2 O3 104.79(8) . . ?
C11 C2 O3 109.10(10) . . ?
C11 C2 O1 109.08(10) . . ?
C12 C2 O3 111.52(10) . . ?
C12 C2 O1 110.30(9) . . ?
C12 C2 C11 111.79(10) . . ?

_diffn_measured_fraction_theta_max 0.9933
_diffn_reflns_theta_full 26.0000
_diffn_measured_fraction_theta_full 0.9994
_refine_diff_density_max 0.4750
_refine_diff_density_min -0.2272
_refine_diff_density_rms 0.0599



```

data_Livant020816_0m
_audit_creation_date      2016-05-13
_audit_creation_method
;
Olex2 1.2
(compiled 2016.02.19 svn.r3266 for OlexSys, GUI svn.r5155)
;
_shelxl_version_number    2014-3
_publ_contact_author_address ?
_publ_contact_author_email ?
_publ_contact_author_name  "
_publ_contact_author_phone ?
_publ_section_references
;
Bourhis, L.J., Dolomanov, O.V., Gildea, R.J., Howard, J.A.K., Puschmann, H.
(2015). Acta Cryst. A71, 59-75.

Dolomanov, O.V., Bourhis, L.J., Gildea, R.J., Howard, J.A.K. & Puschmann, H.
(2009), J. Appl. Cryst. 42, 339-341.
;
_chemical_name_common      ?
_chemical_name_systematic
;
?
;
_chemical_formula_moiety   'C16 H26 O8'
_chemical_formula_sum      'C16 H26 O8'
_chemical_formula_weight   346.37
_chemical_melting_point    ?
loop_
_atom_type_symbol
_atom_type_description
_atom_type_scatter_dispersion_real
_atom_type_scatter_dispersion_imag
_atom_type_scatter_source
'C' 'C' 0.0033 0.0016 'International Tables Vol C Tables 4.2.6.8 and 6.1.1.4'
'H' 'H' 0.0000 0.0000 'International Tables Vol C Tables 4.2.6.8 and 6.1.1.4'
'O' 'O' 0.0106 0.0060 'International Tables Vol C Tables 4.2.6.8 and 6.1.1.4'

_shelx_space_group_comment
;
The symmetry employed for this shelxl refinement is uniquely defined
by the following loop, which should always be used as a source of
symmetry information in preference to the above space-group names.
They are only intended as comments.
;
_space_group_crystal_system 'triclinic'
_space_group_IT_number      2
_space_group_name_H-M_alt   'P -1'
_space_group_name_Hall      '-P 1'
loop_
_space_group_symop_operation_xyz
'x, y, z'
'-x, -y, -z'

_cell_length_a              9.3149(3)
_cell_length_b              9.4281(3)
_cell_length_c              10.3077(4)
_cell_angle_alpha           86.8309(11)
_cell_angle_beta            79.3853(11)
_cell_angle_gamma           78.9062(10)
_cell_volume                 872.94(5)
_cell_formula_units_Z        2
_cell_measurement_reflns_used 8466
_cell_measurement_temperature 180(2)
_cell_measurement_theta_max 26.76
_cell_measurement_theta_min 2.20
_shelx_estimated_absorpt_T_max 0.995
_shelx_estimated_absorpt_T_min 0.984
_exptl_absorpt_coefficient_mu 0.105

```

```

_exptl_absorpt_correction_T_max 0.7455
_exptl_absorpt_correction_T_min 0.6423
_exptl_absorpt_correction_type empirical
_exptl_absorpt_process_details
'SADABS-2014/2 (Bruker,2014/2) was used for absorption correction. wR2(int) was 0.0718 before and 0.0440 after correction. The
Ratio of minimum to maximum transmission is 0.8616. The 1/2 correction factor is 0.00150.'

```

```

_exptl_crystal_colour colourless
_exptl_crystal_colour_primary colourless
_exptl_crystal_density_diffn 1.318
_exptl_crystal_density_meas ?
_exptl_crystal_density_method ?
_exptl_crystal_description Fragment
_exptl_crystal_F_000 372
_exptl_crystal_size_max 0.15
_exptl_crystal_size_mid 0.1
_exptl_crystal_size_min 0.05
_exptl_special_details
;
?
;
_exptl_transmission_factor_max ?
_exptl_transmission_factor_min ?
_diffn_reflns_av_R_equivalents 0.0438
_diffn_reflns_av_unetl/netl 0.0352
_diffn_reflns_Laue_measured_fraction_full 1.000
_diffn_reflns_Laue_measured_fraction_max 0.994
_diffn_reflns_limit_h_max 11
_diffn_reflns_limit_h_min -11
_diffn_reflns_limit_k_max 12
_diffn_reflns_limit_k_min -12
_diffn_reflns_limit_l_max 13
_diffn_reflns_limit_l_min -13
_diffn_reflns_number 34406
_diffn_reflns_point_group_measured_fraction_full 1.000
_diffn_reflns_point_group_measured_fraction_max 0.994
_diffn_reflns_theta_full 26.000
_diffn_reflns_theta_max 27.142
_diffn_reflns_theta_min 2.011
_diffn_ambient_temperature 180.45
_diffn_detector_area_resol_mean ?
_diffn_measured_fraction_theta_full 1.000
_diffn_measured_fraction_theta_max 0.994
_diffn_measurement_device_type 'Smart Apex'
_diffn_measurement_method 'f and lw scans'
_diffn_radiation_type MoK\alpha
_diffn_radiation_wavelength 0.71073
_diffn_source ?
_diffn_standards_number 0
_reflns_Friedel_coverage 0.000
_reflns_Friedel_fraction_full .
_reflns_Friedel_fraction_max .
_reflns_number_gt 3036
_reflns_number_total 3841
_reflns_special_details
;

```

Reflections were merged by SHELXL according to the crystal class for the calculation of statistics and refinement.

_reflns_Friedel_fraction is defined as the number of unique Friedel pairs measured divided by the number that would be possible theoretically, ignoring centric projections and systematic absences.

```

;
_reflns_threshold_expression 'I > 2\sigma(I)'
_computing_cell_refinement 'SAINT v8.34A (Bruker, 2013)'
_computing_data_collection ?
_computing_data_reduction 'SAINT v8.34A (Bruker, 2013)'
_computing_molecular_graphics 'Olex2 (Dolomanov et al., 2009)'
_computing_publication_material 'Olex2 (Dolomanov et al., 2009)'
_computing_structure_refinement 'olex2.refine (Bourhis et al., 2015)'

```

```

_computing_structure_solution 'olex2.solve (Bourhis et al., 2015)'
_refine_diff_density_max 0.349
_refine_diff_density_min -0.251
_refine_diff_density_rms 0.046
_refine_ls_extinction_coef .
_refine_ls_extinction_method none
_refine_ls_goodness_of_fit_ref 1.144
_refine_ls_hydrogen_treatment constr
_refine_ls_matrix_type full
_refine_ls_number_parameters 223
_refine_ls_number_reflns 3841
_refine_ls_number_restraints 0
_refine_ls_R_factor_all 0.0877
_refine_ls_R_factor_gt 0.0620
_refine_ls_restrained_S_all 1.144
_refine_ls_shift/su_max 0.000
_refine_ls_shift/su_mean 0.000
_refine_ls_structure_factor_coef Fsqd
_refine_ls_weighting_details
'w=1/[\s^2^(Fo^2^)+(0.0412P)^2^+0.5135P] where P=(Fo^2^+2Fc^2^)/3'
_refine_ls_weighting_scheme calc
_refine_ls_wR_factor_gt 0.1105
_refine_ls_wR_factor_ref 0.1190
_refine_special_details
;
?
;
_olex2_refinement_description
;
1. Fixed Uiso
At 1.2 times of:
All C(H,H) groups
At 1.5 times of:
All C(H,H,H) groups
2.a Secondary CH2 refined with riding coordinates:
C10(H10A,H10B), C16(H16A,H16B), C19(H19A,H19B), C20(H20A,H20B)
2.b Idealised Me refined as rotating group:
C17(H17A,H17B,H17C), C18(H18A,H18B,H18C), C21(H21A,H21B,H21C), C22(H22A,H22B,
H22C), C23(H23A,H23B,H23C), C24(H24A,H24B,H24C)
;
_atom_sites_solution_hydrogens geom
_atom_sites_solution_primary iterative
_atom_sites_solution_secondary ?
_atom_sites_special_details
;
The structure was solved using Direct Methods (ShelXS). RE = 0.2, Nqual = -1, Ralpha = 0.034
;
loop_
_atom_site_label
_atom_site_type_symbol
_atom_site_fract_x
_atom_site_fract_y
_atom_site_fract_z
_atom_site_U_iso_or_equiv
_atom_site_adp_type
_atom_site_occupancy
_atom_site_site_symmetry_order
_atom_site_calc_flag
_atom_site_refinement_flags_posn
_atom_site_refinement_flags_adp
_atom_site_refinement_flags_occupancy
_atom_site_disorder_assembly
_atom_site_disorder_group
O1 O 0.24958(13) 0.13350(13) 0.59042(11) 0.0199(3) Uani 1 1 d . . . . .
O2 O 0.41549(13) 0.25443(13) 0.75323(13) 0.0225(3) Uani 1 1 d . . . . .
O3 O 0.22355(15) 0.22098(14) 0.99754(12) 0.0264(3) Uani 1 1 d . . . . .
O4 O 0.03730(14) 0.30059(14) 0.64445(12) 0.0232(3) Uani 1 1 d . . . . .
O5 O 0.22765(16) -0.12513(13) 0.74815(13) 0.0298(3) Uani 1 1 d . . . . .
O6 O 0.61426(15) 0.06846(15) 0.74044(14) 0.0310(3) Uani 1 1 d . . . . .
O7 O 0.38320(17) 0.29149(16) 1.10861(15) 0.0388(4) Uani 1 1 d . . . . .

```

O8 O 0.13374(19) -0.22507(17) 0.93825(16) 0.0484(5) Uani 1 1 d
C9 C 0.2628(2) 0.3090(2) 1.07798(17) 0.0230(4) Uani 1 1 d
C10 C 0.1043(2) 0.27805(19) 0.75956(17) 0.0202(4) Uani 1 1 d
H10A H 0.0293 0.2702 0.8399 0.024 Uiso 1 1 calc R
H10B H 0.1568 0.3574 0.7700 0.024 Uiso 1 1 calc R
C11 C 0.1517(2) 0.2502(2) 0.53647(18) 0.0211(4) Uani 1 1 d
C12 C 0.21406(19) 0.13429(18) 0.73202(17) 0.0172(4) Uani 1 1 d
C13 C 0.3587(2) 0.12390(18) 0.78785(18) 0.0193(4) Uani 1 1 d
C14 C 0.5758(2) 0.2195(2) 0.7146(2) 0.0286(5) Uani 1 1 d
C15 C 0.2167(2) -0.2358(2) 0.83494(19) 0.0241(4) Uani 1 1 d
C16 C 0.1311(2) 0.0119(2) 0.7814(2) 0.0249(4) Uani 1 1 d
H16A H 0.0986 0.0173 0.8783 0.030 Uiso 1 1 calc R
H16B H 0.0417 0.0212 0.7401 0.030 Uiso 1 1 calc R
C17 C 0.3223(3) -0.3694(2) 0.7859(2) 0.0355(5) Uani 1 1 d
H17A H 0.3007 -0.3961 0.7020 0.053 Uiso 1 1 calc GR
H17B H 0.3113 -0.4483 0.8509 0.053 Uiso 1 1 calc GR
H17C H 0.4243 -0.3518 0.7727 0.053 Uiso 1 1 calc GR
C18 C 0.1375(2) 0.4302(2) 1.12163(19) 0.0286(5) Uani 1 1 d
H18A H 0.1446 0.5127 1.0601 0.043 Uiso 1 1 calc GR
H18B H 0.1427 0.4590 1.2103 0.043 Uiso 1 1 calc GR
H18C H 0.0429 0.3988 1.1232 0.043 Uiso 1 1 calc GR
C19 C 0.4890(2) 0.0080(2) 0.7265(2) 0.0255(4) Uani 1 1 d
H19A H 0.4888 -0.0856 0.7750 0.031 Uiso 1 1 calc R
H19B H 0.4865 -0.0060 0.6325 0.031 Uiso 1 1 calc R
C20 C 0.3350(2) 0.1042(2) 0.93776(19) 0.0268(4) Uani 1 1 d
H20A H 0.3029 0.0109 0.9633 0.032 Uiso 1 1 calc R
H20B H 0.4295 0.1030 0.9692 0.032 Uiso 1 1 calc R
C21 C 0.2372(2) 0.3680(2) 0.4814(2) 0.0287(5) Uani 1 1 d
H21A H 0.2830 0.3993 0.5505 0.043 Uiso 1 1 calc GR
H21B H 0.1691 0.4503 0.4510 0.043 Uiso 1 1 calc GR
H21C H 0.3148 0.3306 0.4072 0.043 Uiso 1 1 calc GR
C22 C 0.0826(2) 0.1911(2) 0.4346(2) 0.0296(5) Uani 1 1 d
H22A H 0.1611 0.1463 0.3642 0.044 Uiso 1 1 calc GR
H22B H 0.0166 0.2701 0.3972 0.044 Uiso 1 1 calc GR
H22C H 0.0252 0.1187 0.4764 0.044 Uiso 1 1 calc GR
C23 C 0.6483(2) 0.2979(3) 0.8003(3) 0.0407(6) Uani 1 1 d
H23A H 0.6200 0.4024 0.7860 0.061 Uiso 1 1 calc GR
H23B H 0.7565 0.2691 0.7774 0.061 Uiso 1 1 calc GR
H23C H 0.6155 0.2732 0.8933 0.061 Uiso 1 1 calc GR
C24 C 0.6158(3) 0.2557(3) 0.5696(2) 0.0411(6) Uani 1 1 d
H24A H 0.5698 0.1981 0.5184 0.062 Uiso 1 1 calc GR
H24B H 0.7241 0.2336 0.5422 0.062 Uiso 1 1 calc GR
H24C H 0.5796 0.3587 0.5539 0.062 Uiso 1 1 calc GR

loop_

_atom_site_aniso_label
_atom_site_aniso_U_11
_atom_site_aniso_U_22
_atom_site_aniso_U_33
_atom_site_aniso_U_23
_atom_site_aniso_U_13
_atom_site_aniso_U_12
O1 0.0209(7) 0.0197(7) 0.0162(6) -0.0001(5) -0.0022(5) 0.0022(5)
O2 0.0160(6) 0.0172(6) 0.0332(7) -0.0020(5) -0.0045(5) 0.0001(5)
O3 0.0262(7) 0.0301(8) 0.0216(7) -0.0074(6) -0.0080(6) 0.0039(6)
O4 0.0189(7) 0.0260(7) 0.0220(7) 0.0000(5) -0.0053(5) 0.0038(5)
O5 0.0413(9) 0.0159(7) 0.0265(7) 0.0016(5) 0.0052(6) -0.0030(6)
O6 0.0191(7) 0.0283(8) 0.0438(9) -0.0076(6) -0.0095(6) 0.0059(6)
O7 0.0363(9) 0.0356(9) 0.0472(9) -0.0086(7) -0.0232(7) 0.0037(7)
O8 0.0553(11) 0.0351(9) 0.0414(10) 0.0143(7) 0.0142(8) -0.0016(8)
O9 0.0305(11) 0.0233(10) 0.0148(9) 0.0039(7) -0.0075(8) -0.0018(8)
C10 0.0180(9) 0.0199(9) 0.0202(9) 0.0002(7) -0.0027(7) 0.0018(7)
C11 0.0193(9) 0.0200(9) 0.0221(9) 0.0003(7) -0.0049(7) 0.0021(8)
C12 0.0179(9) 0.0161(9) 0.0157(9) -0.0013(7) -0.0011(7) 0.0003(7)
C13 0.0203(9) 0.0123(8) 0.0237(10) -0.0005(7) -0.0059(7) 0.0024(7)
C14 0.0173(10) 0.0278(11) 0.0390(12) -0.0062(9) -0.0044(8) 0.0013(8)
C15 0.0263(10) 0.0208(10) 0.0282(11) 0.0047(8) -0.0081(9) -0.0100(8)
C16 0.0262(10) 0.0191(9) 0.0269(10) -0.0001(8) 0.0009(8) -0.0036(8)
C17 0.0419(13) 0.0207(10) 0.0430(13) 0.0027(9) -0.0055(10) -0.0066(9)
C18 0.0349(12) 0.0268(11) 0.0219(10) -0.0020(8) -0.0056(9) 0.0008(9)

C19 0.0226(10) 0.0210(10) 0.0307(11) -0.0039(8) -0.0072(8) 0.0046(8)
C20 0.0324(11) 0.0212(10) 0.0250(10) -0.0020(8) -0.0102(9) 0.0047(8)
C21 0.0317(11) 0.0256(11) 0.0285(11) 0.0058(8) -0.0067(9) -0.0054(9)
C22 0.0297(11) 0.0331(11) 0.0267(11) -0.0010(9) -0.0096(9) -0.0030(9)
C23 0.0222(11) 0.0417(13) 0.0605(16) -0.0109(11) -0.0124(10) -0.0038(10)
C24 0.0307(12) 0.0460(14) 0.0421(14) -0.0008(11) 0.0026(10) -0.0046(10)

_geom_special_details

; All esds (except the esd in the dihedral angle between two l.s. planes) are estimated using the full covariance matrix. The cell esds are taken into account individually in the estimation of esds in distances, angles and torsion angles; correlations between esds in cell parameters are only used when they are defined by crystal symmetry. An approximate (isotropic) treatment of cell esds is used for estimating esds involving l.s. planes.

; loop_

_geom_bond_atom_site_label_1
_geom_bond_atom_site_label_2
_geom_bond_distance
_geom_bond_site_symmetry_2
_geom_bond_publ_flag
O1 C11 1.444(2) . ?
O1 C12 1.436(2) . ?
O2 C13 1.433(2) . ?
O2 C14 1.450(2) . ?
O3 C9 1.347(2) . ?
O3 C20 1.438(2) . ?
O4 C10 1.427(2) . ?
O4 C11 1.424(2) . ?
O5 C15 1.343(2) . ?
O5 C16 1.443(2) . ?
O6 C14 1.423(2) . ?
O6 C19 1.426(2) . ?
O7 C9 1.199(2) . ?
O8 C15 1.192(2) . ?
O9 C18 1.490(3) . ?
C10 H10A 0.9900 . ?
C10 H10B 0.9900 . ?
C10 C12 1.538(2) . ?
C11 C21 1.515(3) . ?
C11 C22 1.509(3) . ?
C12 C13 1.544(2) . ?
C12 C16 1.523(2) . ?
C13 C19 1.533(3) . ?
C13 C20 1.526(3) . ?
C14 C23 1.506(3) . ?
C14 C24 1.510(3) . ?
C15 C17 1.490(3) . ?
C16 H16A 0.9900 . ?
C16 H16B 0.9900 . ?
C17 H17A 0.9800 . ?
C17 H17B 0.9800 . ?
C17 H17C 0.9800 . ?
C18 H18A 0.9800 . ?
C18 H18B 0.9800 . ?
C18 H18C 0.9800 . ?
C19 H19A 0.9900 . ?
C19 H19B 0.9900 . ?
C20 H20A 0.9900 . ?
C20 H20B 0.9900 . ?
C21 H21A 0.9800 . ?
C21 H21B 0.9800 . ?
C21 H21C 0.9800 . ?
C22 H22A 0.9800 . ?
C22 H22B 0.9800 . ?
C22 H22C 0.9800 . ?
C23 H23A 0.9800 . ?
C23 H23B 0.9800 . ?
C23 H23C 0.9800 . ?

C24 H24A 0.9800 . ?
C24 H24B 0.9800 . ?
C24 H24C 0.9800 . ?

loop_

_geom_angle_atom_site_label_1
_geom_angle_atom_site_label_2
_geom_angle_atom_site_label_3
_geom_angle
_geom_angle_site_symmetry_1
_geom_angle_site_symmetry_3
_geom_angle_publ_flag
C12 O1 C11 109.61(13) . . ?
C13 O2 C14 109.37(13) . . ?
C9 O3 C20 118.26(15) . . ?
C11 O4 C10 106.26(13) . . ?
C15 O5 C16 117.84(15) . . ?
C14 O6 C19 106.36(14) . . ?
O3 C9 C18 110.82(16) . . ?
O7 C9 O3 123.94(18) . . ?
O7 C9 C18 125.23(18) . . ?
O4 C10 H10A 111.2 . . ?
O4 C10 H10B 111.2 . . ?
O4 C10 C12 102.90(13) . . ?
H10A C10 H10B 109.1 . . ?
C12 C10 H10A 111.2 . . ?
C12 C10 H10B 111.2 . . ?
O1 C11 C21 109.50(15) . . ?
O1 C11 C22 109.17(15) . . ?
O4 C11 O1 105.28(14) . . ?
O4 C11 C21 111.18(15) . . ?
O4 C11 C22 108.44(15) . . ?
C22 C11 C21 112.97(16) . . ?
O1 C12 C10 102.88(13) . . ?
O1 C12 C13 108.98(14) . . ?
O1 C12 C16 109.50(14) . . ?
C10 C12 C13 114.18(14) . . ?
C16 C12 C10 107.91(14) . . ?
C16 C12 C13 112.89(15) . . ?
O2 C13 C12 108.56(13) . . ?
O2 C13 C19 102.18(14) . . ?
O2 C13 C20 108.48(14) . . ?
C19 C13 C12 115.31(14) . . ?
C20 C13 C12 112.78(15) . . ?
C20 C13 C19 108.84(15) . . ?
O2 C14 C23 109.94(16) . . ?
O2 C14 C24 108.53(16) . . ?
O6 C14 O2 105.17(15) . . ?
O6 C14 C23 108.42(17) . . ?
O6 C14 C24 111.45(17) . . ?
C23 C14 C24 113.04(19) . . ?
O5 C15 C17 111.33(17) . . ?
O8 C15 O5 123.16(18) . . ?
O8 C15 C17 125.50(18) . . ?
O5 C16 C12 109.47(15) . . ?
O5 C16 H16A 109.8 . . ?
O5 C16 H16B 109.8 . . ?
C12 C16 H16A 109.8 . . ?
C12 C16 H16B 109.8 . . ?
H16A C16 H16B 108.2 . . ?
C15 C17 H17A 109.5 . . ?
C15 C17 H17B 109.5 . . ?
C15 C17 H17C 109.5 . . ?
H17A C17 H17B 109.5 . . ?
H17A C17 H17C 109.5 . . ?
H17B C17 H17C 109.5 . . ?
C9 C18 H18A 109.5 . . ?
C9 C18 H18B 109.5 . . ?
C9 C18 H18C 109.5 . . ?
H18A C18 H18B 109.5 . . ?

H18A C18 H18C 109.5 . . ?
H18B C18 H18C 109.5 . . ?
O6 C19 C13 102.08(14) . . ?
O6 C19 H19A 111.4 . . ?
O6 C19 H19B 111.4 . . ?
C13 C19 H19A 111.4 . . ?
C13 C19 H19B 111.4 . . ?
H19A C19 H19B 109.2 . . ?
O3 C20 C13 109.55(15) . . ?
O3 C20 H20A 109.8 . . ?
O3 C20 H20B 109.8 . . ?
C13 C20 H20A 109.8 . . ?
C13 C20 H20B 109.8 . . ?
H20A C20 H20B 108.2 . . ?
C11 C21 H21A 109.5 . . ?
C11 C21 H21B 109.5 . . ?
C11 C21 H21C 109.5 . . ?
H21A C21 H21B 109.5 . . ?
H21A C21 H21C 109.5 . . ?
H21B C21 H21C 109.5 . . ?
C11 C22 H22A 109.5 . . ?
C11 C22 H22B 109.5 . . ?
C11 C22 H22C 109.5 . . ?
H22A C22 H22B 109.5 . . ?
H22A C22 H22C 109.5 . . ?
H22B C22 H22C 109.5 . . ?
C14 C23 H23A 109.5 . . ?
C14 C23 H23B 109.5 . . ?
C14 C23 H23C 109.5 . . ?
H23A C23 H23B 109.5 . . ?
H23A C23 H23C 109.5 . . ?
H23B C23 H23C 109.5 . . ?
C14 C24 H24A 109.5 . . ?
C14 C24 H24B 109.5 . . ?
C14 C24 H24C 109.5 . . ?
H24A C24 H24B 109.5 . . ?
H24A C24 H24C 109.5 . . ?
H24B C24 H24C 109.5 . . ?

loop_

_geom_torsion_atom_site_label_1
_geom_torsion_atom_site_label_2
_geom_torsion_atom_site_label_3
_geom_torsion_atom_site_label_4
_geom_torsion
_geom_torsion_site_symmetry_1
_geom_torsion_site_symmetry_2
_geom_torsion_site_symmetry_3
_geom_torsion_site_symmetry_4
_geom_torsion_publ_flag
O1 C12 C13 O2 67.23(17) ?
O1 C12 C13 C19 -46.66(19) ?
O1 C12 C13 C20 -172.53(14) ?
O1 C12 C16 O5 64.41(18) ?
O2 C13 C19 O6 33.58(17) ?
O2 C13 C20 O3 63.63(19) ?
O4 C10 C12 O1 28.02(16) ?
O4 C10 C12 C13 145.94(14) ?
O4 C10 C12 C16 -87.68(16) ?
C9 O3 C20 C13 -118.17(17) ?
C10 O4 C11 O1 31.32(17) ?
C10 O4 C11 C21 -87.17(17) ?
C10 O4 C11 C22 148.05(15) ?
C10 C12 C13 O2 -47.15(19) ?
C10 C12 C13 C19 -161.04(15) ?
C10 C12 C13 C20 73.09(19) ?
C10 C12 C16 O5 175.69(14) ?
C11 O1 C12 C10 -9.65(17) ?
C11 O1 C12 C13 -131.18(14) ?
C11 O1 C12 C16 104.90(16) ?

C11 O4 C10 C12 -36.81(17) ?
C12 O1 C11 O4 -12.41(17) ?
C12 O1 C11 C21 107.20(16) ?
C12 O1 C11 C22 -128.65(15) ?
C12 C13 C19 O6 151.12(15) ?
C12 C13 C20 O3 -56.7(2) ?
C13 O2 C14 O6 -6.04(19) ?
C13 O2 C14 C23 -122.56(18) ?
C13 O2 C14 C24 113.33(17) ?
C13 C12 C16 O5 -57.18(19) ?
C14 O2 C13 C12 -139.22(15) ?
C14 O2 C13 C19 -16.95(18) ?
C14 O2 C13 C20 97.91(17) ?
C14 O6 C19 C13 -38.80(19) ?
C15 O5 C16 C12 143.65(16) ?
C16 O5 C15 O8 -1.5(3) ?
C16 O5 C15 C17 179.48(17) ?
C16 C12 C13 O2 -170.88(14) ?
C16 C12 C13 C19 75.2(2) ?
C16 C12 C13 C20 -50.6(2) ?
C19 O6 C14 O2 28.78(19) ?
C19 O6 C14 C23 146.34(17) ?
C19 O6 C14 C24 -88.63(19) ?
C19 C13 C20 O3 174.05(15) ?
C20 O3 C9 O7 -4.2(3) ?
C20 O3 C9 C18 175.24(16) ?
C20 C13 C19 O6 -81.01(18) ?